Thèse de Doctorat

de
l'Université Paris-Saclay
Préparée à
l'Université Paris-Sud

École Doctorale n°567
Sciences du Végétal : du gène à l'écosystème

Spécialité : Biologie

par

Guillaume Dubeaux

Mécanismes moléculaires contrôlant l'ubiquitination et l'endocytose du transporteur de fer
IRON-REGULATED TRANSPORTER 1 d'*Arabidopsis thaliana*

Thèse présentée et soutenue à Gif-sur-Yvette, le 8 Décembre 2016 :

Composition du Jury :

Mme Anne Krapp	Directeur de Recherche, INRA, Versailles	Présidente du Jury
M. Bruno André	Professeur, Université libre de Bruxelles, Bruxelles	Rapporteur
M. Laurent Nussaume	Directeur de Recherche, CEA, Cadarache	Rapporteur
M. Niko Geldner	Professeur associé, Université de Lausanne, Lausanne	Examinateur
M. Doan-Trung Luu	Chargé de Recherche, CNRS, Montpellier	Examinateur
M. Grégory Vert	Directeur de Recherche, CNRS, Gif-sur-Yvette	Directeur de thèse
M. Enric Zelazny	Chargé de Recherche, CNRS, Gif-sur-Yvette	Invité

Remerciements

Je souhaite avant tout remercier Grégory Vert. Au long de mes quatre années de travail en tant qu'étudiant de Master 2 puis thésard, il m'a communiqué son ouverture scientifique, sa passion pour la recherche et son humour qui ont fait de cette thèse un plaisir au quotidien. Tout ce qui fait l'essence du travail présenté ici, il l'a initié, suivi et développé, avec une passion et une attention sans faille, tant par les méthodes innovantes, l'utilisation intensive de l'imagerie et de la quantification mais surtout par l'importance accordée à la pertinence physiologique des résultats.

Je remercie également Enric Zelazny pour le co-encadrement de cette thèse. Il a notamment su apporter des idées rafraîchissantes et un nouveau point de vue. Sa façon différente d'encadrer m'a aidé à me fonder un avis propre sur de nombreuses thématiques scientifiques.

Je tiens à remercier Bruno André et Laurent Nussaume d'avoir accepté d'être rapporteurs de cette thèse et d'y apporter leur expertise. Merci à Anne Krapp, Doan-Trung Luu et Niko Geldner qui sauront sans le moindre doute enrichir les discussions scientifiques en tant qu'examinateurs de ce travail. C'est un plaisir et un honneur de compter tous ces scientifiques au sein de mon jury de thèse.

Je remercie Yvon Jaillais et Sébastien Thomine d'avoir accepté de faire partie de mon comité de thèse. Nos longues discussions ont permis d'étoffer mes connaissances scientifiques mais surtout l'épanouissement de ce projet.

Je tiens aussi à remercier le reste de l'équipe de Signalisation Cellulaire et Ubiquitination pour son accueil, son soutien et sa présence au quotidien tout au long de cette thèse. Merci à Anne, Sara, Alex, Pauline A., Amanda, Aloy, Natali et Alvaro pour l'ambiance dans le laboratoire, la musique, les rires, les trajets en RER et leurs conseils avisés qui m'ont permis de m'épanouir dans cet environnement scientifique mais aussi de me changer les idées quand il le fallait. Un remerciement particulier à Julie pour les "pauses-café" matinales et en soirée qui ont été siège de nombreuses interactions et surtout de très belles idées scientifiques. Merci également pour toute l'aide et les nouvelles techniques qu'elle a pu apporter à mon projet de thèse mais aussi au reste du laboratoire. Merci à Pauline B. et à Michal d'avoir accepté d'être stagiaire sous ma supervision. Leurs apports, tant au niveau technique qu'au niveau de nos interactions au cours de leurs stages respectifs, ont fait de ces quelques mois d'encadrement un plaisir que j'espère partagé.

Remerciements

Je ne pourrais pas m'arrêter sans remercier les différentes personnes des services administratif et technique pour leur gentillesse et leur sourire au quotidien. Je souhaite aussi remercier Marie-Noëlle et Romain pour leurs formations respectives qui m'ont permis de maîtriser les différentes techniques d'imagerie abordées au cours de cette thèse.

Je ne pourrais parler de microscopie sans mentionner Arthur, autre doctorant, qui, au fil des mois, est devenu un réel ami et avec qui il était plus facile de surmonter les difficultés rencontrées au cours de cette thèse.

Je remercie tous ceux qui n'ont pas été cités plus haut et qui ont appartenu à l'Institut des Sciences du Végétal. Je tiens aussi à remercier toutes les équipes avec lesquels j'ai pu interagir au sein de du nouvel Institut de Biologie Intégrative de la Cellule que notre équipe a rejoint au début de l'année 2016. Merci à tous les "non-permanents" qui se reconnaitront pour les nombreux déjeuners en leur compagnie tant au sein de l'ISV que de l'I2BC.

Je remercie aussi ma famille pour avoir été présente dans les moments positifs mais aussi difficiles de cette thèse. Je remercie tout particulièrement celle qui est devenue ma femme au cours de cette thèse et qui, par son amour, m'a donné la force de continuer dans les moments de doute. C'est la présence de Pauline à mes côtés pour me motiver, me distraire, me choyer ou me rassurer, qui m'a guidé tout au long de ce doctorat et a permis l'aboutissement de ce manuscrit.

Enfin, je remercie *Arabidopsis thaliana* sans qui tous ces résultats n'auraient pas été possibles...

Avant-propos

Les plantes sont des organismes fixés qui doivent à tout prix s'adapter à leur environnement pour survivre. La nutrition métallique est au centre de ces adaptations car, bien que les métaux soient essentiels à la plante, ils peuvent également être toxiques à forte concentration. IRT1 est responsable de l'absorption du fer depuis le sol au niveau des cellules épidermiques situées à l'interface sol-racine et est ainsi un acteur majeur de l'homéostasie du fer chez la plante comme l'atteste la très forte chlorose et la létalité du mutant perte de fonction *irt1-1*. IRT1 est également responsable de l'absorption d'autres métaux divalents potentiellement toxiques pour la plante que sont le zinc, le manganèse, le cobalt et le cadmium. Récemment, en utilisant comme modèle d'étude IRT1, notre équipe a mis en évidence pour la première fois chez les plantes un rôle de l'ubiquitination dans l'endocytose d'une protéine membranaire. L'ubiquitination des protéines est une modification post-traductionnelle jouant un rôle majeur dans le monde du vivant, permettant de contrôler l'activité ou le devenir des protéines. Bien que le rôle de l'ubiquitination dans l'endocytose et la dégradation des protéines membranaires soit bien décrit chez la levure et les animaux, sa fonction chez les plantes reste très peu documentée et IRT1 constitue un modèle majeur d'étude de ce phénomène.

Au niveau cellulaire, la protéine IRT1 est principalement localisée au niveau des endosomes précoces et cycle rapidement avec la membrane plasmique où se produit l'influx de fer et de métaux. Des approches biochimiques ont démontré que la protéine IRT1 est monoubiquitinée au niveau de deux résidus lysine présents dans la grande boucle cytosolique située entre les segments transmembranaires III et IV. De plus, une forme mutée d'IRT1 non-ubiquitinable ($IRT1_{K154,179R}$) est localisée exclusivement à la membrane plasmique, ce qui conduit à une absorption incontrôlée de Zn^{2+}, Mn^{2+} et Co^{2+} dans la plante. Ces données prouvent le rôle fondamental joué par l'ubiquitination dans le contrôle de la localisation subcellulaire d'IRT1 entre la surface cellulaire et les endosomes précoces, et démontrent son caractère essentiel au niveau du maintien de l'homéostasie métallique chez les plantes. Récemment, l'équipe a montré par des approches d'immunolocalisation que lors d'une carence en métaux substrats secondaires d'IRT1, le transporteur se trouvait uniquement localisé à la membrane plasmique et présentait ainsi un profil de localisation subcellulaire similaire aux plantes exprimant IRT1 non-ubiquitinable. Cela m'a conduit à étudier le rôle des métaux substrats secondaires du transporteur dans la dynamique et l'ubiquitination d'IRT1 ce qui a constitué l'objectif principal de cette thèse.

Mon projet scientifique visait à :

i) Mieux comprendre comment l'ubiquitination contrôle la localisation et le destin du transporteur IRT1 en fonction de la nutrition métallique. Pour cela, j'ai caractérisé l'influence des métaux substrats secondaires d'IRT1 (carence, concentrations physiologiques et excès) sur le trafic intracellulaire d'IRT1, et sur le type, le degré et les sites d'ubiquitination de la protéine IRT1.

ii) Étudier un mécanisme potentiel de "sensing" du statut métallique par la protéine IRT1 et son rôle dans l'ubiquitination de ce transporteur.

iii) Identifier des acteurs moléculaires responsables de l'ubiquitination d'IRT1 en relation avec la nutrition métallique.

Jusqu'à présent, notre équipe étudiait le trafic intracellulaire d'IRT1 par immunolocalisation à l'aide d'un anticorps anti-IRT1. Or, cette technique est fastidieuse, onéreuse, et ne permet pas d'étudier la dynamique d'une protéine. Mon premier objectif a donc été de caractériser des lignées transgéniques exprimant des formes étiquetées d'IRT1 avec une protéine fluorescente, la mCitrine. Ces fusions exprimées sous le contrôle du promoteur pIRT1 endogène sont fonctionnelles car elles permettent de complémenter le phénotype du mutant *irt1-1*. L'observation en microscopie confocale, l'utilisation de drogues et de conditions interférant avec le trafic endosomal, ainsi que la co-localisation avec des marqueurs endosomaux a permis de confirmer que la protéine de fusion IRT1-mCitrine se comportait comme la protéine IRT1 endogène observée par immunofluorescence. Disposant d'une lignée exprimant la protéine IRT1-mCitrine fonctionnelle, j'ai pu tester l?influence des métaux autres que le fer et substrats d'IRT1 sur sa dynamique. Pour cela, j'ai cultivé les plantes sur différentes concentrations en zinc, manganèse et cobalt. Contrairement à ce qui est observé lors de conditions contrôles correspondant à un milieu de culture Murashige et Skoog classique où IRT1-mCitrine est présent à la membrane plasmique et dans les endosomes, IRT1-mCitrine est exclusivement observé à la membrane plasmique en conditions d'absence de Zn, Mn et Co (dénommés par la suite métaux substrats secondaires), confirmant ce qui avait été observé par des approches d'immunolocalisation. Cela nous a conduit à tester l'effet d'un excès de métaux sur la dynamique du transporteur. Il se trouve qu'en présence d'un excès de métaux, la protéine de fusion n'est plus localisée à la membrane plasmique mais se retrouve principalement dans des endosomes tardifs. J'ai aussi pu mettre en évidence qu'après transfert en conditions d'excès de métaux substrats secondaires d'IRT1, le transporteur est rapidement envoyé vers la vacuole afin d'y être dégradé. Nous avons donc émis l'hypothèse qu'IRT1 devait être régulé post-traductionnellement par les métaux autres que le fer afin d'ajuster sa localisation subcellulaire et sa dégradation en condition d'excès métallique. Cependant, nous avons aussi mis en évidence que la nutrition en métaux (Zn, Mn et Co) modifiait l?activité du promoteur IRT1 et que lors d'une carence de ces trois métaux, l'expression du gène codant la protéine IRT1-mCitrine était très faible. Ces niveaux variables d'expression de la protéine de fusion IRT1-mCitrine selon le statut métallique peuvent donc poser des problèmes lors de l'analyse de sa dynamique ou lors de l'étude de ses profils d'ubiquitination en réponse aux métaux. Afin de contourner les problèmes liés à la régulation indirecte du promoteur IRT1 par les métaux substrats secondaires

du transporteur, nous avons généré des plantes transgéniques exprimant IRT1-mCitrine de façon constitutive. Des lignées homozygotes et mono-insertionnelles exprimant IRT1-mCitrine constitutivement ont ainsi été isolées au cours de cette thèse. Ces nouvelles lignées ont notamment permis d'étudier les niveaux d'ubiquitination d'IRT1 ainsi que le type d'ubiquitination en relation avec la nutrition métallique. IRT1 se trouve être plus ubiquitiné en réponse à l?excès de métal mais aussi différemment modifié. En effet, des analyses biochimiques ont montré qu'IRT1 porte des chaînes de polyubiquitines liées entre elles par la lysine 63 en réponse à l'excès métallique.

Un des objectifs du projet de thèse concernait l'identification d'une E3 ligase régulant IRT1 mais, au début de mon doctorat, une équipe a montré qu'IRT1 DEGRADATION FACTOR 1 (IDF1), une ubiquitine ligase de la famille RING, était impliqué dans l'endocytose d'IRT1 médiée par l'ubiquitination. Ainsi, une fois la régulation post-traductionnelle d'IRT1 par les métaux caractérisée en détail, je me suis donc attaché à étudier le rôle d'IDF1 dans la régulation post-traductionnelle d'IRT1 en lien avec la nutrition métallique. J'ai notamment testé l'effet des métaux chez un mutant perte de fonction *idf1-1*. De telles plantes s'avèrent être hypersensibles à l'excès métallique et suraccumulent les substrats secondaires d'IRT1. De plus, la protéine IRT1 s'accumule dans ce contexte mutant en excés de métal indiquant le rôle prépondérant d'IDF1 dans la dégradation d'IRT1 en conditions de stress métallique. Pour aller plus loin, l'expression d'IRT1-mCitrine dans ce fond mutant a permis d'apporter des réponses quant à l'implication de cette E3 ligase dans la dynamique et l'ubiquitination d'IRT1 en réponse à l'excès de métaux. En effet, IRT1-mCitrine n'est plus polyubiquitiné en réponse à l'excès de métaux et n'est pas non plus adressé aux endosomes tardifs dans de telles conditions. IDF1 semble être l'E3 ligase responsable de l'adressage à la vacuole d'IRT1 en réponse à l'excès de métaux *via* la polyubiquitination du transporteur.

J'ai aussi pu mettre en évidence au cours de cette thèse qu'IRT1 était modifié par phosphorylation en réponse à l'excès de métaux. Une des hypothèses de travail concernait le rôle de cette modification post-traductionnelle dans la possible interaction entre IRT1 et IDF1 dans un contexte de stress métallique. La phosphorylation pourrait permettre un changement de conformation du transporteur et ainsi rendre accessible les sites d'ubiquitination pour l'E3 ligase IDF1. Il se trouve que dans un système hétérologue, IRT1 et IDF1 interagissent mieux lorsque la phosphorylation du transporteur est mimée. Cela semble indiquer un rôle de la phosphorylation en amont de la polyubiquitination médiée par IDF1. Pour confirmer cela, j'ai analysé le statut de phosphorylation d'IRT1 dans le contexte mutant *idf1-1* et il se trouve que le transporteur est toujours phosphorylé, ceci appuyant l'importance de l'ubiquitination et donc avant l?action d'IDF1 *per se*. Le mécanisme moléculaire de régulation d'IRT1 par ses substrats secondaires semble donc impliquer deux modifications post-traductionnelles mais sans aucune idée de la cascade d'évènements permettant cette réponse. J'ai donc cherché si IRT1 était capable de percevoir les métaux directement. La protéine IRT1 possède ainsi une répétition de résidus histidine (H) au sein de la boucle comprise entre les segments transmembranaires III et IV qui porte les sites d'ubiquitination K154 et K179. Il a été montré dans la littérature que les répétitions H ne sont

pas requises pour l'activité de transport d'IRT1. Cependant, les résidus H ayant la capacité de coordonner les métaux, nous avons émis l'hypothèse qu'IRT1 pourrait percevoir directement la présence de métaux au niveau de cette boucle. Afin de tester cette hypothèse, des formes mutées d'IRT1 pour ces résidus H ont été générées et sont exprimées de façon stable chez *Arabidopsis* afin d'évaluer le rôle de ces résidus en réponse aux métaux. Il est important de noter que de telles plantes sont hypersensibles à un excès de métal comme j'ai pu le montrer pour le mutant perte de fonction *idf1-1*. L'étude de la localisation subcellulaire et des profils d'ubiquitination et de phosphorylation de cette forme mutée en réponse à l'excès de métaux par des approches d'imagerie confocale et biochimique ont permis de montrer que ce motif était primordial pour la réponse du transporteur à l'excès de métaux. Cette répétition semble être à la base de la réponse permettant ainsi directement ou indirectement l'intervention d?une protéine kinase qui phosphorylerait IRT1 ce qui permettrait le recrutement d'IDF1 et la polyubiquitination du transporteur entrainant ainsi sa dégradation. Cette régulation permettrait de modifier les niveaux de la protéine et ainsi directement l'influx de métaux depuis le milieu extérieur selon le contexte métallique. IRT1 étant régulé au niveau transcriptionnel par le fer, l'addition de cette double régulation post-traductionnelle par ses substrats secondaires ajoute un niveau de complexité qui n'a jamais été décrit dans la littérature faisant d'IRT1 un modèle prépondérant pour l'étude des régulations de protéines membranaires chez les plantes.

Toutes ces strates de régulations du transporteur permettraient donc à la plante d'optimiser l'absorption du fer tout en évitant d'accumuler des métaux potentiellement toxiques à sa physiologie et à son développement. Le travail présenté ici ouvre donc une voie majeure à la compréhension de mécanismes conduisant au possible développement de plantes permettant la phytoremédiation ou autre stratégie de dépollution des sols dans le futur.

Cette thèse sur articles comprend plusieurs travaux rédigés initialement en anglais dans les parties III et IV. Dans un désir de cohérence, le reste de ce manuscrit est ainsi présenté en anglais afin d'éviter de perturber le lecteur.

Abbreviations

DNA	desoxyribonucleic acid
cDNA	complementary DNA
ADP	adenosine diphosphate
ATP	adenosine triphosphate
ARF	ADP ribosylation factor
ARF-GEF	ARF GDP/GTP exchange factor
RNA	ribonucleic acid
mRNA	messenger RNA
BFA	brefeldin A
bHLH	basic helix-loop-helix
CCP	clathrin-coated pit
CCV	clathrin-coated vesicle
Cd	cadmium
CHC	clathrin heavy chain
CHX	cycloheximide
CLC	clathrin light chain
Co	cobalt
Col	columbia
ConcA	concanamycin A
DNase	deoxyribonuclease
dNTP	deoxynucleotide triphosphate
DTT	dithiothreitol
E1	Ub-activating enzyme
E2	Ub-conjugating enzyme
E3	Ub ligase
EE	early endosome
ER	endoplasmic reticulum
RE	recycling endosome
ERAD	ER-associated protein degradation
ESCRT	endosomal sorting complex required for transport
Fe	iron
Fe^{2+}	ferrous iron
Fe^{3+}	ferric iron
FIT	Fe-deficiency induced transcription factor
FLS	FLAGELLIN SENSING
FM4-64	N-(3-triethyl-ammoniumpropyl)-4-(p-diethyl-aminophenyl-hexatrienyl)pyridinium dibromide
FYVE	zing finger domain named after FAB1, YOTB, VAC1 and EEA1

GAP	GTPase-activating protein
GDP	guanosine diphosphate
GFP	green fluorescent protein
GTP	guanosine triphosphate
GUS	β-glucuronidase
H	histidine
HECT	homology to E6-AP carboxyl terminus
IRT	IRON-REGULATED TRANSPORTER
K	lysine
kDa	kilodalton
LE	late endosome
mCit	mCitrine
MES	2-(N-morpholino)ethanesulfonic acid
Mn	manganese
MS	Murashige and Skoog medium
MVB	multivesicular body
Ni	nickel
PCR	polymerase chain reaction
PEG	polyethylene glycol
PIP	plasma membrane intrisic protein
PM	plasma membrane
PIP	phosphatidylinositol phosphate
PVC	prevacuolar compartment
PVDF	Polyvinylidene fluoride
qRT-PCR	quantitative RT-PCR
R	arginine
ROS	reactive oxygen species
RT	reverse transcription
SDS	sodium dodecyl sulfate
SNX	SORTIN NEXIN
T	threonine
TE	Tris-EDTA
TGN	*trans*-Golgi network
Tris	2-amino-2-(hydroxymethyl)propane-1,3-diol
TyrA23	tyrphostin A23
UIM	Ub interacting motif
Ub	ubiquitin
VSR	vacuolar sorting receptor
Wm	wortmannin
YFP	yellow fluorescent protein
WS	Wassilewskija
ZIP	ZRT-IRT-like protein
Zn	zinc
ZRT	ZINC REGULATED TRANSPORTER

Contents

Contents

List of Figures

List of Figures

14

Part I

Introduction

Eukaryotic cells are continuously sensing external and internal stimuli in order to survive. As such, the ability to dynamically reorganize the composition of the plasma membrane is a key component for the proper development and survival of a cell. Endocytosis is the process of internalizing patches of plasma membrane (PM) *via* the formation of vesicles called endosomes. On the contrary, exocytosis drives the fusion of intracellular membrane fractions with the plasma membrane (Doherty and McMahon, 2009). In 2013, James Rothman, Randy Schekman, and Thomas Südhof received the Nobel Prize in Physiology or Medicine for their discoveries on membrane trafficking and particularly on exo- and endocytosis, highlighting the importance of this field for the scientific community. The equilibrium between exo- and endocytosis allows a tight control of protein levels at the PM. Thus, endocytosis plays a crucial role in the control of the level or activity of receptors, transporters and other PM proteins (Doherty and McMahon, 2009). While the endocytic system and the mechanisms driving its regulation in yeast and animals has been well characterized during the past few decades, the study of endocytosis in plants has mostly been made through analogies with what has been described in other organisms (Paez Valencia et al., 2016).

The objective of my thesis was to study the molecular mechanisms driving the endocytosis of an integral multipass plasma membrane protein, IRON-REGULATED TRANSPORTER 1 (IRT1), in response to environmental cues in *Arabidopsis thaliana*. Before describing the reasons making of IRT1 one of the model proteins to study intracellular dynamics of PM proteins, I will first review our current knowledge on endocytosis in yeast, mammals and plants. I will then give an overview on the regulation of endocytosis, in particular on the molecular mechanisms described as crucial for internalization, establishment of polarity and lysosomal/vacuolar sorting.

Chapter 1

The endocytic pathways of membrane proteins

1 The endomembrane system

1.1 The secretory system

The secretory system of eukaryotic cells is the membrane network linking the endoplasmic reticulum (ER), the plasma membrane and the lysosome/vacuole (Foresti and Denecke, 2008). The secretory system is involved in the biosynthesis of membrane proteins and on their targeting to various destinations along the endomembrane network (Foresti and Denecke, 2008; Hwang and Robinson, 2009). Interestingly, the secretory system has been described as a dynamic structure that co-exist and is imbricated within the endocytic system (Hwang and Robinson, 2009).

The secretory system allows not only synthesis of membrane and secreted proteins but also their maturation through the ER and the Golgi apparatus (Fig. 1). Indeed, properly folded proteins follow the anterograde pathway from the ER to the Golgi apparatus mediated by coat protein II (COPII)-coated vesicles (Bonifacino and Glick, 2004) (Fig. 1). Conserved di-acidic and di-hydrophobic motifs found in specific transmembrane proteins are required for their selection into COPII-coated vesicles and have been characterized in plants (Sieben et al., 2008; Zelazny et al., 2009; Sorieul et al., 2011). Finally, the recruitment process occurring throughout the formation of such vesicles requires ADP-ribosylation factor (ARF) GTPases such as ARF1 or SAR1 and the ARF GTPase guanine-nucleotide exchange factor (ARF-GEF) GNOM-LIKE 1 (GNL1). These ARF and ARF-GEF are essential for ER-Golgi trafficking processes as well as for protein recycling between endosomes and the plasma membrane (Richter et al., 2007; Teh and Moore, 2007; Nielsen et al., 2008; Du et al., 2013). Similar to ER-Golgi trafficking, vesicle formation and movement, vesicle tethering and fusion are influenced by GTP-binding proteins of the ARF and RAS genes from rat brain (Rab) types (Nielsen et al., 2008). Subcellular localization observations reveal that many Rabs share organelle specificity with yeast and mammalian orthologs (Nielsen et al., 2006). GFP-tagged RabD1 and RabD2 GTPases co-localize at the Golgi
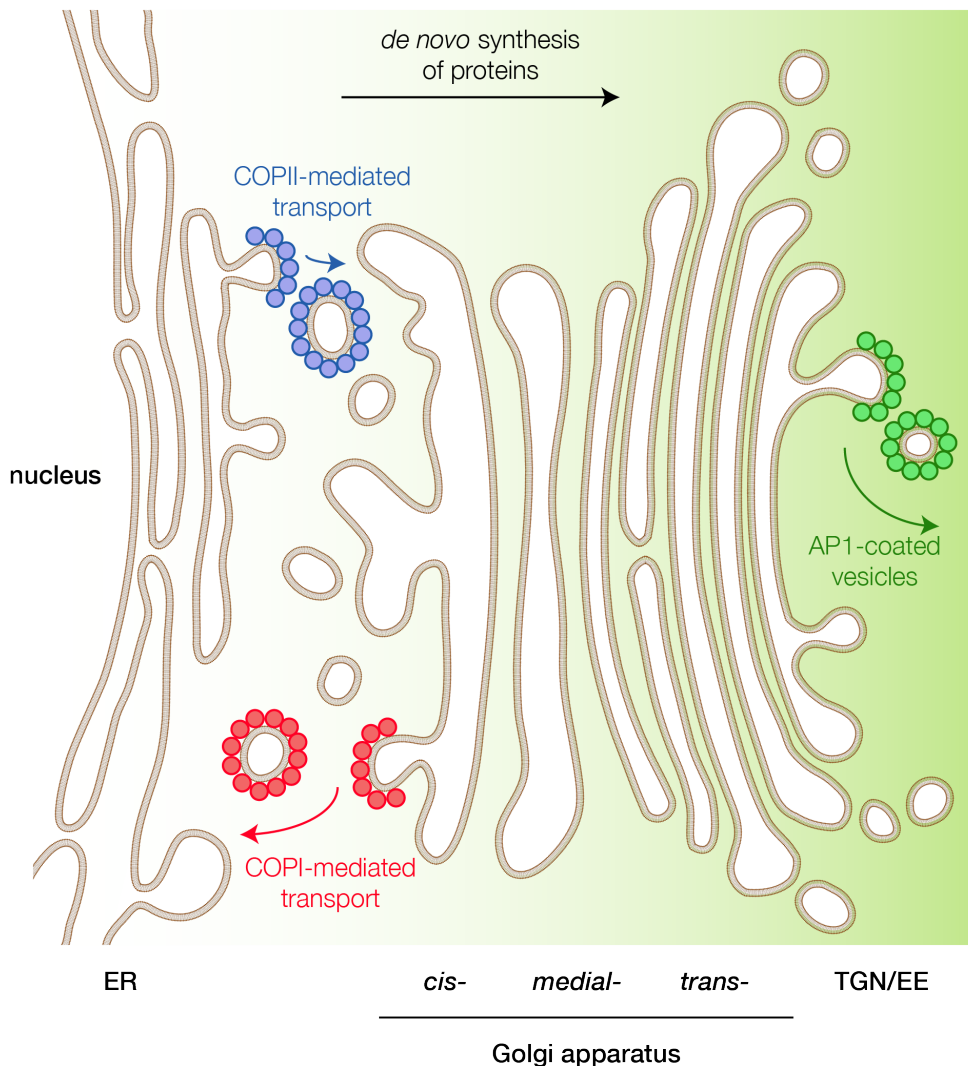
Figure 1 – **The secretory system in plants.** Protein synthesis occurs in the endoplasmic reticulum (ER) where the protein starts its maturation. The protein reaches the Golgi apparatus *via* COPII-coated vesicles (blue). A retrograde transport also exists through COPI-coated vesicles (red). Finally, the protein can be released to the *trans*-Golgi network/early endosomes (TGN/EE) and then transported to the plasma membrane or to other compartments *via* AP1-coated vesicles (green).

apparatus and in the *trans*-Golgi network/early endosomal (TGN/EE) compartments (Pinheiro et al., 2009). Dominant-negative forms of RabD1 (DN-RabD1) inhibit the trafficking from ER to Golgi (Pinheiro et al., 2009). In addition, ER/Golgi apparatus trafficking is inhibited when a dominant negative form of RabD2a is expressed (Pinheiro et al., 2009). Interestingly, DN-RabD1 inhibits *Arabidopsis* growth and cannot be rescued by RabD2a further suggesting that the activity of these two Rab subclasses are linked to distinct sorting events (Pinheiro et al., 2009). As such, RabD1 and RabD2 could potentially act in different secretory pathways or at a different

level of the same pathway. In addition, a retrograde transport exists for ER-Golgi trafficking and it is mediated by COPI-coated vesicles (Hwang and Robinson, 2009) (Fig. 1).

In recent years, a role for the exocyst complex in cargo trafficking has also emerged. Exocyst represents an evolutionarily conserved component of the eukaryotic sorting machinery that functions as a tethering complex for exocytic vesicles upon fusion with the plasma membrane (Fendrych et al., 2013). In yeast and mammals, exocyst was described as a cytosolic complex composed of eight proteins: SEC3, SEC5, SEC6, SEC8, SEC10, SEC15, EXO70, EXO84 (TerBush et al., 1996). Orthologs of these subunits have been identified in plant genomes (Zárský et al., 2013). The analysis of fluorescently-tagged exocyst subunits has shown that they co-localize at the cell surface with the endocytic tracer FM4-64, as would be predicted for a plasma membrane tethering complex (Fendrych et al., 2013).

1.2   The endocytic system

Endosomes can be classified on their kinetic properties (early or late), their structure (tubular or multivesicular) or even their function (recycling or sorting) (Perret et al., 2005; Robinson et al., 2008). However, these different classifications are subjected to overlap but are still useful to define specific compartments and their function in the endocytic pathway (Robinson et al., 2008).

An early endosome (EE) is defined as the first compartment reached by an internalized cargo protein (Fig. 2). In plants, EE is the first compartment highlighted by the styryl lipophilic derivate FM4-64 commonly used as an endocytic tracer (Bolte et al., 2004). After treatment, FM4-64 is inserted within the PM, quickly internalized, and follows the endocytic route towards the vacuole (Bolte et al., 2004; Dettmer et al., 2006) (Fig. 2). However, EE does not correspond to a unique cellular compartment within the cell. This is well illustrated with both auxin influx AUX1 and auxin efflux PIN1 transporters that cycle from the PM through distinct EE (Kleine-Vehn et al., 2006). AUX1 trafficking depends on a Brefeldin A (BFA)-resistant ARF-GEF whereas PIN1 is sensitive to the drug further indicating the existence of several endocytic pathways. Indeed, BFA is a fungal metabolite that specifically inhibits the activity of certain ARF-GTPases interacting with their ARF-GEF (Donaldson and Jackson, 2000). Interestingly, the first compartment marked by the FM4-64 totally overlap with the VHA-a1 TGN marker (Dettmer et al., 2006). As such, EE and TGN are sub-domains of the same compartment where secreted and endocytosed proteins are going through and thus referred as TGN/EE (Viotti et al., 2010; Dettmer et al., 2006) (Fig. 2). RabA2 and RabA3 Rab-GTPases, BEN1 ARF-GEF, as well as VTI12 are also well described TGN/EE markers (Chow et al., 2008; Tanaka et al., 2009; Geldner et al., 2009) (Fig. 2). When plasma membrane proteins are internalized to the TGN/EE, they can be recycled back to the PM *via* recycling endosomes (RE) or sorted to the lysosome/vacuole through maturation of TGN/EE into multivesicular bodies/late endosomes/prevacuolar compartments (MVB/LE/PVC) (Robinson et al., 2008) (Fig. 2). The GNOM ARF-GEF was initially described as a RE marker and mainly characterized for his role in the recycling back of PIN1 to the PM (Geldner et al., 2003). GNOM was shown to co-localize with
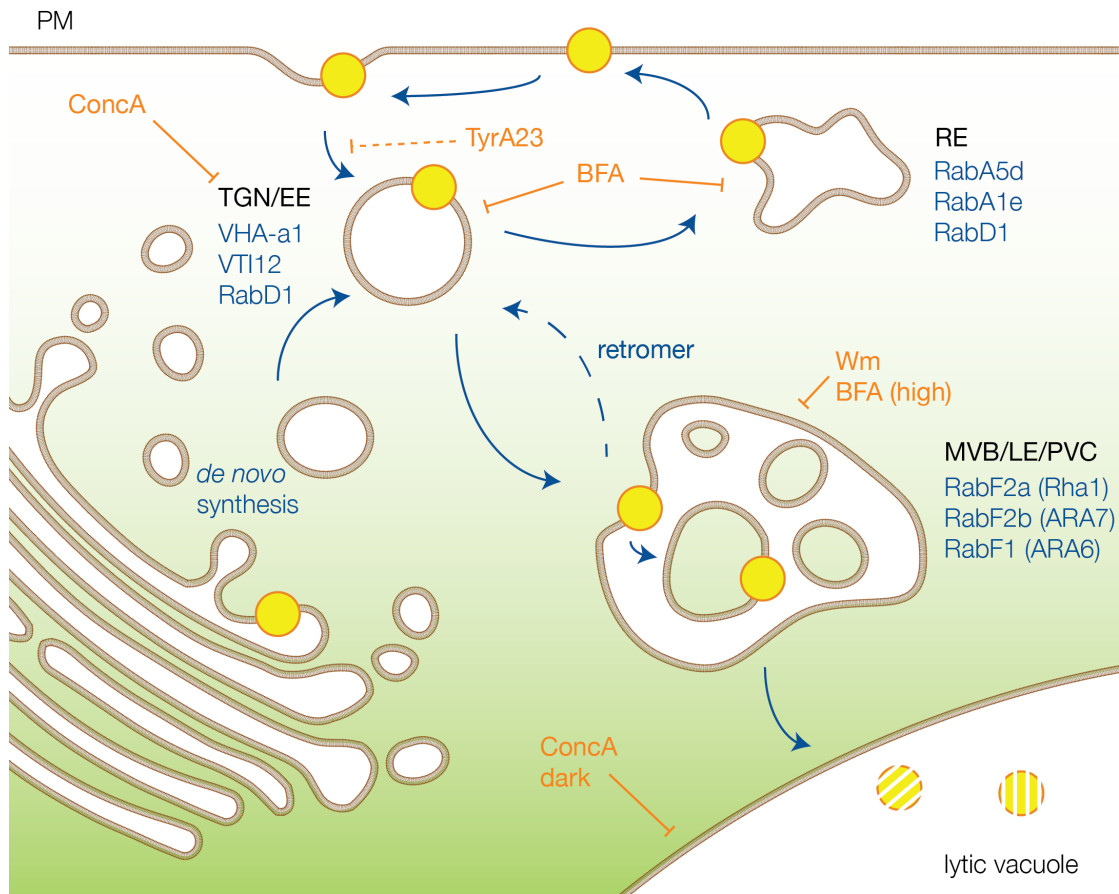
Figure 2 – The endocytic system in plants. Model presenting the different compartments (black), their associated markers (blue) and their susceptibility to drugs (orange). PM, plasma membrane; TGN/EE, *trans*-Golgi network/early endosomes; RE, recycling endosomes, MVB/LE/PVC, multivesicular bodies/late endosomes/prevacuolar compartments; TyrA23, Tyrphostin A23; BFA, Brefeldin A; Wm, Wortmannin; ConcA, Concanamycine A.

the FM4-64 tracer, with no overlapping with TGN/EE or MVB/LE/PVC markers, suggesting that this ARF-GEF defined an endocytic compartment *per se* (Geldner et al., 2003; Chow et al., 2008; Kleine-Vehn et al., 2009). Additional evidences indicate a role of GNOM in the control of endocytosis directly at the PM (Naramoto et al., 2010; Irani et al., 2012). Ultrastructure and super-resolution microscopy approaches were then used to decipher more precisely the localization of GNOM *in planta*. A GNOM-GFP fusion protein was mostly found at the Golgi apparatus in both transmission electron-microscopy and super-resolution microscopy technique (Naramoto et al., 2014). Interestingly, time-lapse imaging and immunolocalization analysis demonstrated that GNOM is stabilized at the Golgi apparatus after short-term BFA treatment. GNOM was more recently shown to gradually translocated from the Golgi cisternae to TGN/EE compart-

ments after prolonged BFA treatments (Naramoto et al., 2014). Altogether, these results reveal the complex localization pattern of GNOM and the limitations of pharmacological approaches to draw solid conclusions on trafficking events.

RabF1 (ARA6), RabF2a (Rha1) and RabF2b (ARA7) were described as markers of MVB/-LE/PVC (Haas et al., 2007; Reichardt et al., 2007; Geldner et al., 2009) (Fig. 2). MVB/LE/PVC are characterized as enriched in phosphatidylinositol-3-phosphate (PI3P) that are recognized by several domains such as pleckstrin-homology (PH) domains, phox homology (PX) domains and Fab1, YOTB, Vac1 and EEA1 (FYVE) domains (Cheever et al., 2001; Ellson et al., 2001; Gillooly et al., 2001). Dimers of FYVE domains fused to YFP co-localize with the FM4-64 and the ARA7 marker in BY2 cells (Vermeer et al., 2006). Similarly, in *Arabidopsis*, a dimer of the FYVE domain from the mammalian HRS protein strongly overlaps with Rha1-positive compartments (Simon et al., 2014). MVB/LE/PVC compartments are also described at the crossroads between secretory and endocytic pathways (Jaillais et al., 2006; Oliviusson et al., 2006; Jaillais et al., 2008). Indeed, a retrograde transport from MVB/LE/PVC to the TGN/EE was described for the recycling of the Vacuolar Sorting Receptors (VSRs) (Oliviusson et al., 2006). VSRs are proteins implicated in the transport of lytic enzymes from the TGN/EE to the vacuole. In *Arabidopsis*, the retromer complex was described as implicated in this retrograde transport (Jaillais et al., 2006; Oliviusson et al., 2006; Jaillais et al., 2008). SORTIN NEXIN 1 (SNX1) was notably described as associated with the retromer complex and co-localizes with the ARA6 and ARA7 MVB/LE/PVC markers at the *Arabidopsis* root tip (Jaillais et al., 2008). However, the core retromer with its three subunits VPS26, 29 and 35, can function independently of SNX1 in *Arabidopsis* (Pourcher et al., 2010; Zelazny et al., 2013). More recently, SNX1 was shown to localize to the TGN/EE in *Arabidopsis* protoplasts (Niemes et al., 2010). Strikingly, in this article, the authors used combination of immunolocalization and electron microscopy approaches to observe the subcellular localization of SNX1, VPS29 and SNX2a cargos. However, the endomembrane system is highly dynamic and the constant maturation of endosomes from TGN/EE to MVB/LE/PVC makes complicated the interpretations of co-localization approaches. Furthermore, confocal microscopy approaches in protoplasts are not sufficient *per se* to rule out the work that was previously done at the root tip. More experiments using correlative microscopy for instance are necessary to shed light on the exact localization of SNX1 in plant cells *in vivo*.

When proteins are targeted to the lysosome/vacuole to be degraded, they need prior invagination in intraluminal vesicles (ILVs) of the MVB/LE/PVC to ensure the proper entry inside the lumen of the lytic compartment. The recognition and targeting of proteins in ILVs from MVB/LE/PVC compartments is mediated *via* ubiquitination and recognition by the endosomal sorting complexes required for transport (ESCRT) as described hereafter (Spitzer et al., 2006; Spitzer et al., 2009; Haas et al., 2007; Schellmann and Pimpl, 2009). Tonoplastic proteins do not traffic through ILVs and can possibly be routed directly from the ER to the vacuolar membrane through provacuolar compartments that are not linked with the autophagy machinery (Viotti et al., 2013). These tonoplastic proteins are degraded using an ubiquitin-dependent mechanism in a process that was recently elucidated in yeast (Li et al., 2015b). These mechanisms involving

ubiquitin will be further described in the section 3.4.2.

2   The internalization from the plasma membrane

2.1   Constitutive and regulated endocytosis

The internalization of a membrane protein from the cell surface controls its localization, its level and its activity. Most membrane proteins are endocytosed in a constitutive manner to allow their turnover *via* a lysosomal/vacuolar degradation. In plants, BRASSINOSTEROID INSENSITIVE 1 (BRI1) is endocytosed, cycled between TGN/EE and the PM, and degraded constitutively in the vacuole (Geldner et al., 2007; Viotti et al., 2010). A stimulus can also induce the internalization and/or further the degradation of a cargo. In response to boron (B) excess, the borate transporter BOR1 is endocytosed and degraded, likely to avoid B overaccumulation in the plant (Takano et al., 2005; Takano et al., 2010). The flagellin receptor FLS2 is also endocytosed and degraded in response to flagellin ligand binding (Robatzek et al., 2006). Flagellin-induced degradation of FLS2 desensitizes cells after ligand binding by controlling the levels of activated receptors at the PM (Robatzek et al., 2006; Smith et al., 2014b). This may serve to desensitize cells to the same stimulus, preventing a continuous signal output upon repetitive ligand stimulation. The auxin efflux transporter PIN2 is also internalized and degraded inside the vacuole in response to changes of light, with less PIN2 proteins at the PM in the dark (Laxmi et al., 2008). Moreover, PIN2 trafficking and degradation has been well described in the case of root gravitropism (Abas et al., 2006; Leitner et al., 2012). Following gravistimulation, PIN2 protein levels are modulated at the upper and lower part of the root further resulting in asymmetric distribution of the auxin-efflux facilitator. Furthermore, stabilization of PIN2 both affected its abundance and distribution leading to defects in auxin distribution and gravitropic responses (Abas et al., 2006).

Internalization also allows the relocalization of proteins and thus finely tune their activity. In animals, signaling from early endosomal compartment has been described for the transforming growth factor (TGFβ) receptor where some of the major molecular players of the TGFβ signaling pathway accumulate in EE compartments (Chen, 2009). In plants, the first evidence of a possible signaling from TGN/EE came from studies of the BRI1 steroid hormone receptor. Sequestration of BRI1 in endosome-derived BFA bodies after treatment with BFA has been associated with increased steroid hormone signaling (Geldner et al., 2007). However, more recently, several reports ruled out the ability of BRI1 to signal from intracellular compartments. Stabilization of BRI1 at the cell surface, using Tyrphostin A23 (TyrA23) treatment and genetic interference with clathrin-mediated endocytosis (CME) using a dominant-negative form of clathrin, AP2 mutants, or ubiquitination-defective BRI1 enhanced BRI1 signaling (Irani et al., 2012; Di Rubbo et al., 2013; Martins et al., 2015). The original observation supporting signaling from endosomes likely result from the inability of the negative regulator BKI1 to accumulate in BFA compartments (Wang and Chory, 2006; Jaillais et al., 2011), therefore allowing BRI1 to fire from these intracellular structures.

Endocytosed proteins are not necessarily meant to be degraded. The potassium channel KAT1 is internalized and sequestered in endosomes in response to abscisic acid (ABA). This sequestration limits the entry of potassium in the guard cell and allows stomata closure in response to ABA (Sutter et al., 2007). This sequestration could allow a rapid relocalization of KAT1 to the PM in absence of ABA therefore triggering a reopening of stomata without any waste of energy needed for an extra synthesis of KAT1 protein. Salt stress are also responsible for the internalization and cycling of PM proteins (Leshem et al., 2007; Boursiac et al., 2008; Luu et al., 2011; Martiniere et al., 2012). The PIP1;2 and PIP2;1 aquaporins are internalized in response to reactive oxygen species (ROS) generated in presence of salicylic acid or salt stress, thus controlling the hydraulic conductance in roots in the case of salt excess conditions (Boursiac et al., 2008). Furthermore, fluorescence recovery after photobleaching (FRAP) experiments indicate a high cycling dynamics of PIP1;2 and PIP2;1 aquaporins in response to salt stress (Luu et al., 2011; Martiniere et al., 2012).

Different types of endocytosis have been described in animals: phagocytosis, pinocytosis, caveolin-dependent, clathrin-dependent, caveolin-independent and clathrin-independent endocytosis (Doherty and McMahon, 2009). CME is the best studied endocytic pathway in mammals and yeast. In plants, CME is the major way of plasma membrane internalization as attested by the stabilization at the PM of the majority of cargos and even FM4-64 when CME is blocked (Dhonukshe et al., 2007; Pérez-Gómez and Moore, 2007).

2.2 Clathrin-dependent or independent endocytosis

Clathrin is an ubiquitous molecule composed of three heavy chains (CHC) and three light chains (CLC) organized in a triskelelion (Fig. 3). The clathrin triskelion has three protrusions that radiate from a central vertex (Kirchhausen, 2000) (Fig. 3). The CHC chain is divided in
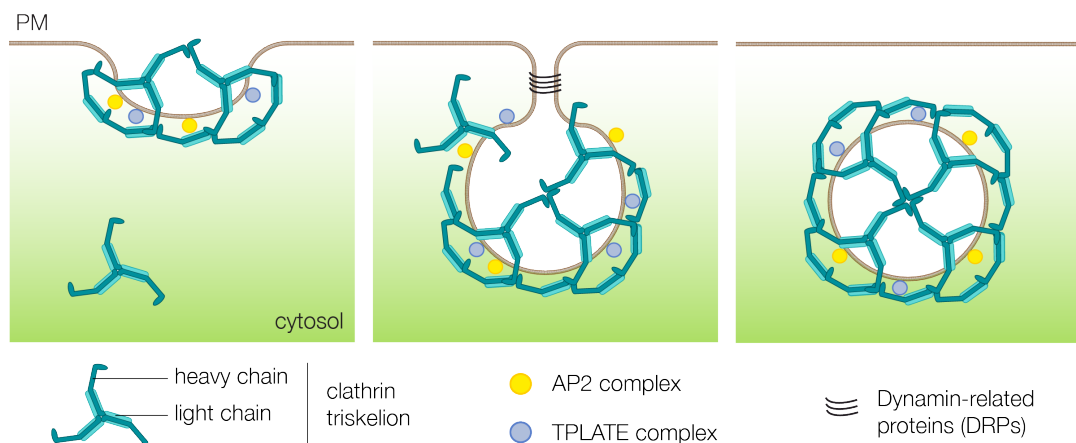
Figure 3 – **Model of the key steps of Clathrin-Mediated Endocytosis (CME) in plants.** CME starts with recognition of AP2 or TPLATE adaptors and recruitment of clathrin for the clathrin-coated pit (CCP). This is followed by membrane curvature for invagination and maturation of the vesicle. Finally, dynamin mediated twisting promotes scission and release of the clathrin-coated vesicle (CCV).

three regions: a proximal region that is close to the vertex where the light chain attaches, a distal region, and the N-terminal domain. This arrangement was first visualized by electron microscopy (EM) observations of isolated triskelia (Ungewickell and Branton, 1981; Kirchhausen and Harrison, 1981). CME is the association process of clathrin triskelia forming a clathrin-coated pit (CCP) and then a clathrin-coated vesicle (CCV) (Fig. 3). AP2 or Epsin adaptors recognize internalization motifs allowing the polymerization of clathrin and other accessory proteins to form a CCP and then a CCV. The vesicles are then uncoated before the fusion with or the maturation into TGN/EE. In plants, the CCP formation is not PM specific. Indeed, it was also described at the level of the Golgi apparatus and the TGN/EE and implicates the adaptor AP1 (Happel et al., 2004; Park et al., 2013; Gershlick et al., 2014) (Fig. 1). Cytological approaches of clathrin-mediated endocytosis revealed CCP and CCV at the plant cell periphery (Holstein, 2002; Dhonukshe et al., 2007; Onelli et al., 2008; Karahara et al., 2009).

Completion of the *Arabidopsis* genome sequencing project revealed the presence of genes homologous to *CHC*, *CLC*, adaptors (AP complexes and Epsins) and dynamin-like GTPase found in animals (Holstein, 2002; Paul and Frigerio, 2007; Hwang and Robinson, 2009). Genetic and pharmacological approaches in *A. thaliana* indicate a conservation of CME (Ortiz-Zapater et al., 2006; Dhonukshe et al., 2007). For example, overexpression of a dominant-negative form of clathrin, corresponding to the C-terminus of CHC (HUB1), blocks the internalization of FM4-64, PINs and other membrane proteins (Dhonukshe et al., 2007). TyrA23 was supposed to prevent recognition between cargo proteins and AP2 complexes thereby inhibiting the formation of CCV, at least in animals (Crump et al., 1998; Banbury et al., 2003). TyrA23 treatment disrupts internalization of membrane proteins in plant cells and it was suggested that it was through inhibition of CME *via* impairment of cargo recognition by AP2 adaptor (Ortiz-Zapater et al., 2006; Dhonukshe et al., 2007; Barberon et al., 2011; Dejonghe et al., 2016). However, a recent paper described this drug-induced block of endocytosis as a role of TyrA23 as a protonophore in plants (Dejonghe et al., 2016). Indeed, acidification of the cytosol by uncoupling mitochondrial oxidative phosphorylation led to a dramatic interference with CME. In plants, we still lack biochemical evidences that TyrA23 affects cargo recognition by AP2 adaptor. As such, the use of TyrA23 should be avoided for CME-specific inhibition in plants, unless a TyrA23 analogue which cannot dissipate proton gradients is developed.

Genetic interference with clathrin in plants results in severe developmental defects, including alterations in root elongation, root and hypocotyl gravitropism, as well as lateral root primordia initiation (Kitakura et al., 2011; Wang et al., 2013). *Arabidopsis* clathrin chains associate with AP2 complex and form punctate foci at the plasma membrane (Fan et al., 2013; Kim et al., 2013; Yamaoka et al., 2013). As such, and similar to clathrin mutants, plants impaired in AP2 subunits show alterations in general endocytosis, as visualized by FM4-64 internalization kinetics, in PIN internalization and/or polarity, and in BRI1 internalization (Di Rubbo et al., 2013; Fan et al., 2013; Kim et al., 2013; Yamaoka et al., 2013). More recently, the activity of the TPLATE adaptor complex, which is plant-specific, has been linked to early events in CME (Gadeyne et al., 2014; Zhang et al., 2015). TPLATE consists of eight core subunits and has been

demonstrated to accumulate at distinct sites at the plasma membrane, preceding the recruitment of further components required for CCV formation (Gadeyne et al., 2014). Interestingly, the authors observed that a minor fraction of CCP only recruited AP2 subunits, further suggesting that the TPLATE complex and AP2 can be independent adaptors of the CME process (Fig. 3). The loss of AP2 adaptor complex function only results in mild phenotypes in plants while a *tplate* mutant appears to display a fully penetrant pollen defect causing male sterility (Van Damme et al., 2011; Gadeyne et al., 2014). This establishes TPLATE as a major adaptor complex that acts during early stages of CCV formation in plant cells (Zhang et al., 2015). However, cargo recognition by plant adaptor complex subunits remains largely underexplored.

Other components of CME, such as the dynamin-related proteins DRP1A and DRP2B were characterized in *A. thaliana* and could be involved in the fission of CCV (Fujimoto et al., 2010). These proteins interact in CCP and are sensitive to TyrA23 (Fujimoto et al., 2010). Recruitment of DRP1A and DRP2B to CCP occurs subsequently to clathrin (Fujimoto et al., 2010), consistent with what has been observed for Dynamins in yeast and mammals (Loerke et al., 2009; McMahon and Boucrot, 2011) (Fig. 3). The biological importance of DRPs for the plant physiology have recently been uncovered. DRP1A/B and C were shown to be essential for boron-induced degradation of BOR1 (Yoshinari et al., 2016). In *Arabidopsis*, a null *drp2b* mutant shows increased sensitivity to *Pseudomonas syringae pv. tomato* (Pto) DC3000 (Smith et al., 2014a). Based on live-cell imaging studies, ligand-triggered internalization of FLS2 was found to be partially dependent on DRP2B but not on DRP2A (Smith et al., 2014a). This article provides genetic evidence for a CME component implicated in ligand-induced endocytosis of FLS2. More recently, a *Phytophthora infestans* effector AVR3a was shown to interact with DRP2 (Chaparro-Garcia et al., 2015). AVR3a further interferes with FLS2 internalization usually triggered by the addition of its ligand (Chaparro-Garcia et al., 2015). Taken together, these results indicate a role of a bacterial effector in the DRP2-mediated ligand-induced endocytosis of FLS2 further providing new interesting roles of dynamin-related proteins in plants. Dynasore is a molecule described in animals as a dynamin inhibitor, blocking the formation of CCV from the PM (Macia et al., 2006; Miyauchi et al., 2009). Furthermore, Dynasore stabilizes LeEIX2 at the PM in transiently transfected tobacco leaves further suggesting the inhibition of dynamin-related activity by this drug in plant cells (Sharfman et al., 2011).

The disassembly of the CCV is mediated by auxilin in animals. This protein is recruited to the clathrin coat once the vesicle is free in the cytosol (McMahon and Boucrot, 2011). Auxilin allows the recruitment of the ATPase heat shock cognate 70 (HSC70) which initiates the clathrin uncoating *per se* (Schlossman et al., 1984; Ungewickell et al., 1995). In *Arabidopsis*, the SH3P1 protein contains an SH3 domain and co-localizes with clathrin at the PM (Lam et al., 2001). Furthermore, SH3P1 interacts with phospholipids such as PI4P and PI(4,5)P$_2$, actin and an auxilin-like protein (Lam et al., 2001). This auxilin-like protein increases clathrin uncoating from plant microsomal fraction in the presence of animal HSC70 (Lam et al., 2001). This strongly argues in favor of a conservation of the clathrin uncoating process in plants. Interestingly, overexpression of *auxilins* have been shown to block internalization of cargos from the

PM (Ortiz-Morea et al., 2016). In *Arabidopsis thaliana*, endogenous elicitor peptides (Peps) are released into the apoplast after cellular damage and can directly bind to the leucine-rich repeat receptor kinases (LRR-RK) PEP RECEPTOR1 (PEPR1) and PEPR2. The interaction between Peps and PEPR1/2 triggers the interaction between these receptors and their coreceptor BRI1-ASSOCIATED KINASE 1 (BAK1) (Mbengue et al., 2016; Tang and Zhou, 2016). Interestingly, overexpression of *auxilin2* inhibits CME of Pep1-PEPR1 (Ortiz-Morea et al., 2016), suggesting that the internalization of the Pep/PEPR complex largely relies on clathrin and that auxilin does play a role in CME in plants.

Besides CME, a number of endocytic pathways originating from membrane microdomains have been linked to cargo internalization. A well-characterized pathway in mammals uses caveolae, but the structural components of caveolae are absent from plants (Kurzchalia and Parton, 1999). Flotillins are structurally related to caveolins and are probably associated with membranes through acylation and the insertion of hydrophobic hairpins into the inner leaflet of the membrane (Bauer and Pelkmans, 2006). In animal cells, flotillin-enriched microdomains are internalized in a clathrin-independent manner and contain specific cargo, such as the glycophosphatidylinositol (GPI)-anchored protein CD59 and the receptor for cholera toxin, the glycosphingolipid GM1 (Glebov et al., 2006; Saslowsky et al., 2010). Plant membranes contain flotillin-based microdomains that are distinct from CCVs, and plant flotillin function has been associated with endocytic events during symbiotic bacterial infection, although no cargo has been clearly identified to date in plants (Haney and Long, 2010). The PIP2;1 aquaporin has been reported to co-localize and co-migrate with the FLOT1 flotillin (Li et al., 2011). Interestingly, both membrane rafts and CME contribute to the internalization of PIP2;1 (Li et al., 2011). In addition, using variable angle total internal reflection fluorescence microscopy (VA-TIRFM), fluorescence correlation spectroscopy (FCS) and fluorescence cross-correlation spectroscopy (FCCS), BRI1 was shown to co-localize with FLOT1 at the PM (Wang et al., 2015). In contrast with CCVs, flotillin endocytic vesicles in plants are three times larger with an approximate diameter of 100nm (Li et al., 2011).

Although little is known about the mechanisms that regulate microdomain-mediated endocytosis in plants, it seems to be highly sensitive to environmental cues. For example, the association of the NADPH oxidase RboHD in microdomains and its CME-independent internalization are enhanced under salt stress (Hao et al., 2014). However, the internalization of RboHD, the ammonium transporter AMT1;3, and PIP2;1 depends on both CME and clathrin-independent membrane microdomains (Li et al., 2011; Wang et al., 2015). Recently, BRI1 was also shown to be endocytosed in a clathrin-independent manner (Wang et al., 2015). BRI1 is found enriched in FLOT1-positive rafts in response to binding of its ligand brassinolide (BL). This suggests a partitioning of BRI1 endocytosis in response to brassinosteroids (BRs) as attested by the attenuation of BR signaling after disruption of membrane microdomains (Wang et al., 2015). This article clearly indicates the co-existence of two endocytic pathways for a given cargo and the existing balance between the two in response to a ligand. This further suggests a putative cooperative role of CME and microdomain-associated endocytosis for cargo internalization.

3 The recycling to the plasma membrane

Proteins recycling from the TGN/EE compartment back to the PM can have different biological functions: constitutive recycling of receptors in the case of BRI1 or FLS2 (Russinova et al., 2004; Robatzek et al., 2006; Geldner et al., 2007), a rapid adaptation to environmental conditions in the case of endosome-sequestered KAT1 that recycles to the PM after a few hours for modulating potassium levels in the cell (Sutter et al., 2007) or a polar localization of a membrane protein like PIN transporters or BOR1 (Geldner et al., 2001; Geldner et al., 2003; Takano et al., 2010; Alassimone et al., 2010; Langowski et al., 2010).

At the molecular level, the GNOM ARF-GEF is involved in recycling events (Geldner et al., 2001; Geldner et al., 2003). ARF-GTPases associate with membranes after exchange of their GDP into GTP. This reaction is catalyzed by an ARF-GEF. The ARF-GTPase-membrane association allows the recruitment of proteins necessary for vesicle formation (Donaldson and Jackson, 2000). Once formed, the vesicles are uncoated after GTP hydrolysis by the GAP (GTPase activating protein) activated GTPases (Donaldson and Jackson, 2000). As mentioned previously, BFA specifically inhibits the activity of certain ARF-GTPases interacting with their ARF-GEF (Donaldson and Jackson, 2000). In the *Arabidopsis* root tip, BFA leads to aggregation of RE and TGN/EE into a so-called BFA body (Fig. 2). As a result, BFA treatment provokes an interruption of endocytosed proteins recycling, as well as the trapping or *de novo* synthesized proteins passing through TGN/EE (Geldner et al., 2001). Sensitivity to BFA has been described for many membrane proteins such as PINs, BOR1, PIP2, FLS2, BRI1 or IRT1 (Geldner et al., 2001; Geldner et al., 2003; Kleine-Vehn et al., 2006; Takano et al., 2005; Robatzek et al., 2006; Dhonukshe et al., 2007; Geldner et al., 2007; Barberon et al., 2011). GNOM is sensitive to BFA (Geldner et al., 2001; Geldner et al., 2003), however there are also BFA-sensitive routes independent of GNOM (Tanaka et al., 2009). The BEN1 ARF-GEF is sensitive to BFA but is distinct from GNOM. BEN1 is localized in the TGN/EE and is involved primarily in the transport from the TGN/EE to the RE compartment (Tanaka et al., 2009).

The close link between recycling and polarity establishment will be further discussed in the section 2.3.2.

4 The lysosomal/vacuolar degradation of membrane proteins

In plants, internalized proteins localized in the TGN/EE can be transported to the lytic vacuole *via* the MVB/LE/PVC in order to be degraded (Robinson et al., 2008). This degradation is carried out by lytic enzymes under acidic conditions *via* the combined activity of vacuolar H^+-ATPase and vacuolar H^+-pyrophosphatase (Tamura et al., 2003; Kriegel et al., 2015). The phospholipids forming the vesicle in which the membrane protein is buried are degraded through the action of phospholipases in the vacuole/lysosome (Kolter and Sandhoff, 2009). Sphingolipids are degraded by the co-action of hydrolases, glucosidases, ceramidases and lipases (Kolter and

Sandhoff, 2009). The glycocalyx layer of the vacuolar/lysosomal protects the membrane from the action of these degrading enzymes (Kolter and Sandhoff, 2009). Concanamycin A (ConcA), which inhibits the activity of the V-ATPase subunit c, blocks the vacuolar degradation and allows the accumulation of proteins in vacuolar compartments (Tamura et al., 2003) (Fig. 2). However, this drug also blocks the endocytic transport of FM4-64 on its way to the tonoplast implicating the accumulation of the dye but also interfering with the formation of BFA bodies (Dettmer et al., 2006) . In addition, BRI1 accumulates in intracellular vesicles in presence of both cycloheximide (CHX) and ConcA further suggesting the impairment of endocytosis on its way to the vacuole by the drug (Dettmer et al., 2006). This strongly suggests that ConcA affects the V-ATPase subunit a located in the TGN/EE, as the identity of this compartment is impacted by drug treatment (Viotti et al., 2010) (Fig. 2). Despite their ease of use, many precautions must be taken into account for pharmacological approaches.

Vacuolar degradation has been demonstrated for BOR1, PIP2, BRI1, PIN2 and IRT1 plant cargos (Takano et al., 2005; Kleine-Vehn et al., 2008; Barberon et al., 2011). Interestingly, dark growth conditions also decrease the lytic activity of vacuoles. These conditions can therefore be used to reveal the vacuolar accumulation of a protein fused to a fluorescent protein (Tamura et al., 2003). Consistently, the fusion PIP2-GFP, BOR1-GFP, BRI1-GFP, BRI1-mCitrine and PIN2-GFP proteins are visualized in the vacuole after a few hours of incubation in the dark (Kleine-Vehn et al., 2008; Kasai et al., 2011; Martins et al., 2015).

Pharmacological approaches have also been implemented to characterize the endocytic pathway from the TGN/EE to the vacuole, and the molecular players involved. Indeed, high concentrations of BFA lead to swelling of MVB/LE/PVC compartments in BFA bodies further indicating the pleiotropic effect of this drug along the endocytic pathways (Tse et al., 2006; Robinson et al., 2008) (Fig. 2). PIN2, BRI1 and FM4-64 sorting to the vacuole is sensitive to BFA treatment but independent of GNOM (Kleine-Vehn et al., 2008). This indicates the intervention of another ARF-GEF sensitive to BFA in this pathway (Kleine-Vehn et al., 2008). Wortmannin (Wm) inhibits the activity of phosphatidylinositol-3-kinase (PI3K) involved in the formation of PI3P. As previously mentioned, PI3P are found in MVB/LE/PVC and are essential phospholipids for the formation of ILVs of such compartments (Robinson et al., 2008). In plants, Wm particularly affects the vacuolar targeting of FLS2, PIN2 and PIP2, revealing a role of PI3P in late events of endocytosis for these cargos (Robatzek et al., 2006; Leshem et al., 2007; Kleine-Vehn et al., 2008). In most cases, Wm treatment leads to an accumulation of cargo proteins at the PM (Robatzek et al., 2006; Kleine-Vehn et al., 2008). This is probably linked with the defective sorting of such cargos in MVB/LE/PVC, leading to their recycling back to the PM. Wm can also inhibit phosphatidylinositol-4-kinase (PI4K) at elevated concentrations thereby affecting endocytosis (Matsuoka et al., 1995). Wm can also lead to endosomal aggregates formation called Wm bodies, with reference to BFA bodies, resulting from homotypic fusions of MVB/LE/PVC (Jaillais et al., 2006) (Fig. 2). Interestingly, genetic interference with PI3K leads to the same result as a Wm treatment (Leshem et al., 2007). SNX1 accumulates in the Wm body and belongs to the retromer complex in plants (Jaillais et al., 2006; Oliviusson et al., 2006; Jaillais et al.,

28

2008). In yeast and animals, the retromer complex is involved in the retrograde transport of MVB/LE/PVC to TGN/EE (McGough and Cullen, 2011). SNX1 was initially identified for its role in the recycling of PIN2 (Jaillais et al., 2006). SNX1 now seems to be preferentially involved in the retrograde transport from the MVB/LE/PVC and also acts as a key player for the vacuolar sorting of endocytosed proteins (Kleine-Vehn et al., 2008). Thus, a *snx1* mutant exhibits increased vacuolar degradation of PIN2 (Kleine-Vehn et al., 2008). Consistently, in response to a gravi-stimulation, where PIN2 was demonstrated to be degraded in the vacuole (Abas et al., 2006; Kleine-Vehn et al., 2008), PIN2 is addressed to a SNX1-endosome (Jaillais et al., 2006). More recently, SNX1 was shown to be important for the trafficking and stability of IRT1 (Ivanov et al., 2014). The *snx1* loss-of-function mutant shows decreased IRT1 protein with no change in mRNA levels, further indicating an enhanced degradation of the transporter when SNX1 is absent. This is correlated with the apparent chlorosis due to lack of iron in aerial parts of *snx1* and *snx* triple mutants (Ivanov et al., 2014).

The endosomal sorting complex required for transport (ESCRT) machinery is involved in the formation of ILVs of MVB/LE/PVC compartment and the sorting of cargos of their way to the vacuole. This complex will be further presented in the section 3.2.

29

Chapter 2

Molecular mechanisms driving the fate of membrane proteins

Proteins are removed from the PM for different reasons. In some instances, endocytosis is required for the degradation of the cargo protein to the lysosome/vacuole. In other cases, endocytosis of cargo proteins underlies the cycling events between the PM and TGN/EE. The internalization of PM proteins is controlled by signals present in their cytosolic parts (Bonifacino and Traub, 2003; Traub, 2009). These signals include tyrosine or di-leucine motifs recognized by the AP2 adaptor complex (Bonifacino and Traub, 2003; Traub, 2009; Kozik et al., 2010). Internalization signals may also be conjugated to cargo proteins by covalent bonds, as in the case of ubiquitin (Hicke and Dunn, 2003; Traub, 2009). Phosphorylation is another signal that can control i) the activity of factors implicated in the endocytic pathways (Schroeder et al., 2012) ii) the proteins themselves by changing their conformation (Reiter and Lefkowitz, 2006) and iii) the polarity of cargos such as PIN proteins (Luschnig and Vert, 2014).

1   Tyrosine motifs

In animals, the role of tyrosine motifs as internalization signals was first illustrated by a study of the hemagglutinin (HA) where the substitution of a cysteine residue into a tyrosine in a cytosolic domain allows the quick internalization of the protein *via* CCPs (Lazarovits and Roth, 1988). Subsequently, tyrosine motifs were involved in the internalization of many membrane proteins (Bonifacino and Traub, 2003). The tyrosine motifs NPXY and YXXΦ are particularly well described (Bonifacino and Traub, 2003; Traub, 2009), while the YXXXLN sequence was identified more recently (Kozik et al., 2010). Structural approaches have shown that the NPXY and YXXΦ motifs can directly interact with the C-terminus of $\mu2$ subunit of the AP2 complex, allowing the formation of a CCV (Owen and Evans, 1998).

In plants, these YXXΦ motives are found in many membrane receptors (Geldner and Robatzek, 2008), and their role was originally characterized for the tomato xylanase receptor

LeEix2 (Ron and Avni, 2004; Bar and Avni, 2009). Substitution of a tyrosine residue into an alanine within an YXXΦ motif of LeEix2 prevents the internalization of the receptor in the presence of the fungal elicitor, which causes a loss of the hypersensitive response (Ron and Avni, 2004; Bar and Avni, 2009). The lateral polarity and the vacuolar degradation of the boron transporter BOR1 in presence of boron excess also involves an internalization *via* an YXXΦ motif (Takano et al., 2010). Indeed, mutation of three tyrosine (Y) residues Y373, Y398 and Y405 into alanines in a predicted cytosolic loop of BOR1 leads to an apolar localization of the transporter in root epidermal cells (Takano et al., 2010). Furthermore, these mutations led to the stabilization of BOR1 in response to high boron (Takano et al., 2010). This indicates that those tyrosine residues are required for both vacuolar and polar trafficking pathways. Interestingly, and as previously mentioned, TyrA23 was described to inhibit the formation of CCVs by interfering with the recognition between YXXΦ motif and the $\mu 2$ subunit of the AP2 complex (Banbury et al., 2003). In plants, this mechanism was thought to be conserved since TyrA23 also inhibits the internalization of many plant membrane proteins (Ortiz-Zapater et al., 2006; Dhonukshe et al., 2007; Barberon et al., 2011). However, recent evidence point to a protonophore role of TyrA23 thereby inhibiting CME by suppression of proton gradient within cells, as already mentioned in section 1.2.2 (Dejonghe et al., 2016).

Recognition of these tyrosine motifs by the AP2 complex is regulated by phosphorylation (Bonifacino and Traub, 2003). Phosphorylation of the $\mu 2$ subunit on residue threonine (T) 156 by the serine (S)/T kinase AAK1 increases the affinity of AP2 complex purified from pigs for the YXXΦ motif (Ricotta et al., 2002)). This phosphorylation step is necessary for the CCP formation and further internalization of hTfr, a cargo know to rely on YXXΦ motif for its internalization (Collawn et al., 1990; Ohno et al., 1995; Olusanya et al., 2001). Thus, the phosphorylation/dephosphorylation state of the $\mu 2$ subunit controls the recruitment of the cargo protein into the CCP (Ricotta et al., 2002; Semerdjieva et al., 2008). The role of phosphorylation in the recognition of the YXXΦ patterns has not been shown yet in plants. The interaction of the AP2 complex with PI(4,5)P$_2$ and PI(3,4,5)P$_3$ phosphoinositides also increases the recognition of the YXXΦ motifs (Bonifacino and Traub, 2003; Semerdjieva et al., 2008). In *A. thaliana*, this type of mechanism is probably conserved as salt stress induces the formation of CCV in combination with PI(4,5)P$_2$ (König et al., 2008).

The tyrosine motifs described above for their role as signal for cargo internalization are also involved in the transport from the TGN/EE to the MVB/LE/PVC (Bonifacino and Traub, 2003). In *A. thaliana*, the YXXΦ motif from VSR proteins interacts with the μ subunit from the AP1 complex and allows the transport of this Golgi receptor to the PM and to the MVB/LE/PVC compartments (Happel et al., 2004; daSilva et al., 2006) (Fig. 1).

2   Di-leucine motifs

Di-leucine motifs were also described as signal for internalization of membrane proteins (Bonifacino and Traub, 2003; Traub, 2009). In humans, the cytosolic domain from the CD3-γ chain

of the antigen receptor of T-cells contains no tyrosine motifs but is still capable of being internalized. This allowed the identification of a di-leucine motif (or isoleucine) [DE]XXXL[LI] (Letourneur and Klausner, 1992). Structural approaches revealed that the [DE]XXXL[LI] motif interacts with the $\sigma 2$ subunit of the AP2 complex (Kelly et al., 2008; Kozik et al., 2010). The interaction between [DE]XXXL[LI] and $\sigma 2$ subunit occurs in a certain conformation. Thus, the [DE]XXXL[LI] motif is localized near the α subunit associated with PI(4,5)P$_2$ (Kelly et al., 2008). The interaction between the di-leucine motif and the AP2 complex allows the formation of CCP and the internalization of cargo protein (Bonifacino and Traub, 2003; Traub, 2009). In plants, the di-leucine motives are found in the protein sequence of many membrane receptors or transporters (Geldner and Robatzek, 2008). To date, only the nicotianamine synthase 2 (NAS2) protein from *Oryza sativa* was shown to be impaired, at least in part, for its internalization when mutated in a di-leucine motif (Nozoye et al., 2014).

3   Phosphorylation

3.1   Generalities

Phosphorylation is the reversible addition of a phosphate group to a serine, threonine or tyrosine residue of a substrate protein. Large scale phosphopeptide sequencing analysis indicates that the majority of the mammalian cellular protein content may be phosphorylated (Olsen et al., 2006). Phosphorylation itself changes the electrostatic properties of proteins. This enables conformational changes that can allosterically regulate the modified protein. Alternatively, phosphorylation can induce protein-protein interaction, as it is sensed by specialized protein domains (Pawson and Scott, 2005). Phosphorylation is performed by 518 protein kinases in human cells, whereas there are fivefold less protein phosphatases able to remove phosphate groups (Manning et al., 2002). In the *Arabidopsis* genome are found over 1000 genes encoding kinases and 112 genes encoding phosphatases (Kerk et al., 2002; Wang et al., 2003).

Phosphorylation is implicated in a myriad of processes and one of its well-described role in endocytosis is the control of PINs polarity.

3.2   Polar recycling

In the case of the plant auxin hormone PIN efflux carrier, the basal or apical localization is controlled by phosphorylation at their cytosolic loop thanks to the antagonistic action of the serine/threonine kinase PINOID (PID) and phosphatase-2A (PP2A) (Friml et al., 2004; Michniewicz et al., 2007; Kleine-Vehn et al., 2009; Zhang et al., 2010). In a *pp2a* loss-of-function mutant or with gain-of-function plant for the PID protein, the polarity of PIN2 in young cortical cells switches to apical instead of basal (Michniewicz et al., 2007). Similarly, PIN4, which is basally localized in proximal initials and daughter cells of the wild-type root meristem, shifted to the apical side in a *pp2a* mutant background (Michniewicz et al., 2007). Interestingly, PIN2 polarity remains unaffected in the epidermis in a *pp2a* mutant background compared to WT (Michniewicz

et al., 2007). Site-directed mutagenesis approaches also indicate that constitutive phosphorylation of PINs is sufficient to cause a polarity inversion (Zhang et al., 2010). More recently, PIN phosphorylation by another protein kinase, the D6 protein kinase (D6PK), was also shown to control auxin transport activity (Zourelidou et al., 2014). Besides its role in polarity inversion, PID kinase also activate PINs activity but to a lesser extent compared with D6PK (Zourelidou et al., 2014; Barbosa et al., 2014). D6PK and PID phosphorylate PINs at different phosphosites (Zourelidou et al., 2014). However, D6PK overexpression does not lead to a change of polarity of PINs (Zourelidou et al., 2014; Barbosa et al., 2014). In epidermal cells of the shoot apical meristem or at the root tip, respectively both PIN1 and PIN2 are at the apical PM whereas D6PK is basally localized further indicating that D6PK and PINs polarity are independent (Friml et al., 2004; Barbosa et al., 2014). Altogether, these results suggest a strong involvement of phosphorylation in PINs localization as well as for their transport activity.

In the endodermis, the Casparian strip (CS) represents a cell wall modification acting as a physical barrier for the apoplastic flow. CS membrane domain is defined by the presence of CASPs proteins (Roppolo et al., 2011). This CASP domain formation is restricted to a median longitudinal position in endodermal cells, requiring tightly-controlled mechanisms to establish such a restricted domain. Recently, the receptor-like cytoplasmic kinase SCHENGEN 1 (SGN1) was shown to be required for CS domain positioning and integrity (Alassimone et al., 2016). SGN1 is localized at the outer polar domain of the PM in endodermal cells. The authors also showed that the kinase activity of SGN1 was important for its localization and function. Indeed, a kinase-dead version of SGN1 is mostly observed in the cytosol and did not display any rescue activity (Alassimone et al., 2016). However, the direct target of SGN1 is not known. SGN3 is a receptor-like kinase and greatly co-localizes with the CASP domain (Pfister et al., 2014). KO mutants of both *SGN3* and *SGN1* genes display very similar phenotypes with the formation of highly discontinuous CASP domain suggesting that both kinases act in close functional relation to each other (Pfister et al., 2014; Alassimone et al., 2016). Furthermore, functional genetic data suggests that both SGN3 and SGN1 individually contribute to CASP domain formation, but that their respective activities could be enhanced at their region of overlap (Pfister et al., 2014; Alassimone et al., 2016). Altogether, these results suggest a role of these kinases for the polar positionning of the CASP domain in the root endodermis.

4 Ubiquitination

4.1 Generalities

Ubiquitin (Ub) is a 76 amino acid-long polypeptide whose structure is highly conserved in all eukaryotes (Craig et al., 2009; Komander, 2009). Ubiquitination is the reaction where an Ub moiety is attached by a covalent bond between a glycine residue of its C-terminus and a -NH2 group of a lysine (K), in most cases, within the target protein. This process leads to the covalent attachment of a single Ub moiety and is named monoubiquitination (Fig. 4A). A target protein can have multiple lysine residues that can be monoubiquitinated, leading to
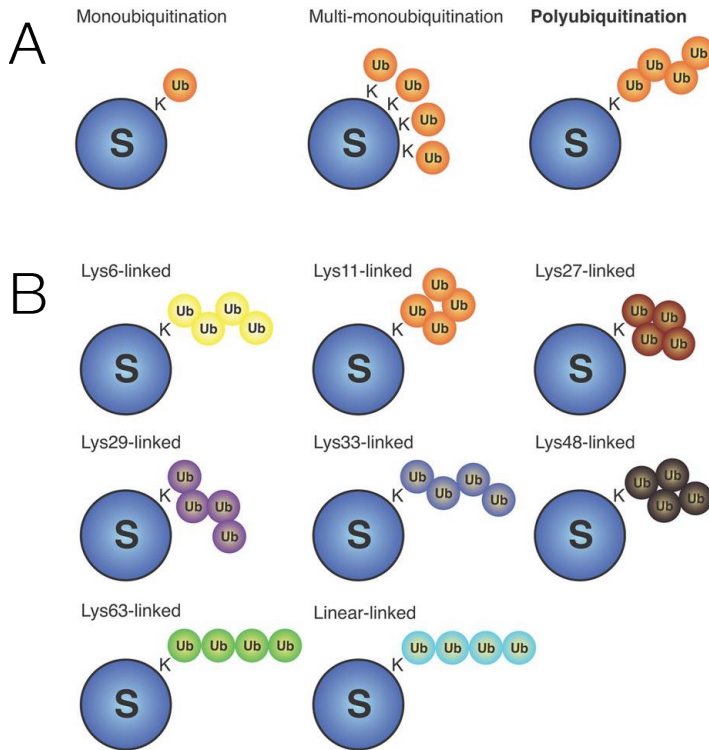
Figure 4 – **Forms of ubiquitination (adapted from (Komander, 2009)).** (A) The ubiquitin modification has three general layouts: mono-ubiquitination, multi-monoubiquitination and polyubiquitination. (B) Forms of polyubiquitination, where each ubiquitin chain contains a single linkage type. Individual linkages may lead to distinct ubiquitin chain structure, and K48- and K63-linked/linear chains have different conformations.

multi-monoubiquitination (Fig. 4A). Ub itself contains seven lysine residues (K6, K11, K27, K29, K33, K48 and K63) that can be self-ubiquitinated, forming polyUb chains with different conformations (Hicke, 2001; Belgareh-Touzé et al., 2008; Komander, 2009) (Fig. 4A and B; Fig. 5). All these different polyUb chains have been detected in plants except for the K27 linkage (Kim et al., 2013) (Fig. 4B). Linear polyUb chains can be made by linking Ub to the N-terminal methionine in a protein (Swatek and Komander, 2016). More complex arrangements of ubiquitin exist such as mixed polyUb carrying alternative linkage types within the same chain (Ben-Saadon et al., 2006), or branched ubiquitin chains where more than one lysine residue from a single ubiquitin is used to make a chain (Kim et al., 2007). Finally, lysine residues from Ub can also be modified by Ub-like molecules such as SUMO or NEDD8 (Hendriks et al., 2014; Singh et al., 2012), and Ub can also be phosphorylated at residue S65 by PINK1 (Koyano et al., 2014). All these different forms of ubiquitin dramatically increase the complexity of Ub-dependent processes and point to our lack of resolution in the analysis of ubiquitinated proteins.

Ubiquitination *per se* needs the sequential action of three enzymes: the Ub-activating enzyme (E1), the Ub-conjugating enzyme (E2) and the Ub ligase (E3) (Hicke and Dunn, 2003) (Fig. 6). The E1 enzyme activates ubiquitin in an ATP-dependent reaction and then transfers ubiquitin

to an E2 (Fig. 6). The E2 enzyme then cooperates with an E3 ligase to catalyze the formation of an isopeptide bond between ubiquitin and substrate (Fig. 6). In most cases, the E2 enzymes are implicated in catalyzing the type of ubiquitination. For instance, the ubiquitin-conjugating enzyme from the UBC13 family is implicated in the formation of K63 polyUb chains (Hofmann and Pickart, 1999; Pickart and Fushman, 2004). On the contrary, E3 ligases play a critical role in the recognition of cargo proteins to be ubiquitinated and therefore provide specificity in the reaction (Léon and Haguenauer-Tsapis, 2009; David et al., 2011). This is further supported by the abundance of E3 ligases (>600 in animals, >1400 in plants) compared with E2s (37 in animals and plants) or E1s (2 in animals and plants) (Komander, 2009; Callis, 2014). In many cases the interaction between a cargo protein and the E3 ligase is finely tuned by adaptors, or activators/inhibitors of post-translational modifications such as phosphorylation (Léon and Haguenauer-Tsapis, 2009). E3 ligases are traditionally categorized into two main types: Really Interesting New Gene (RING) family and Homologous to E6AP C-Terminus (HECT) E3s. The two E3 families differ in the general mechanism of Ub transfer: HECT E3s accept Ub from E2s and then ligate the moiety onto the substrate, while RING ligases facilitate Ub transfer from E2 enzymes to substrate lysine (Fig. 6).
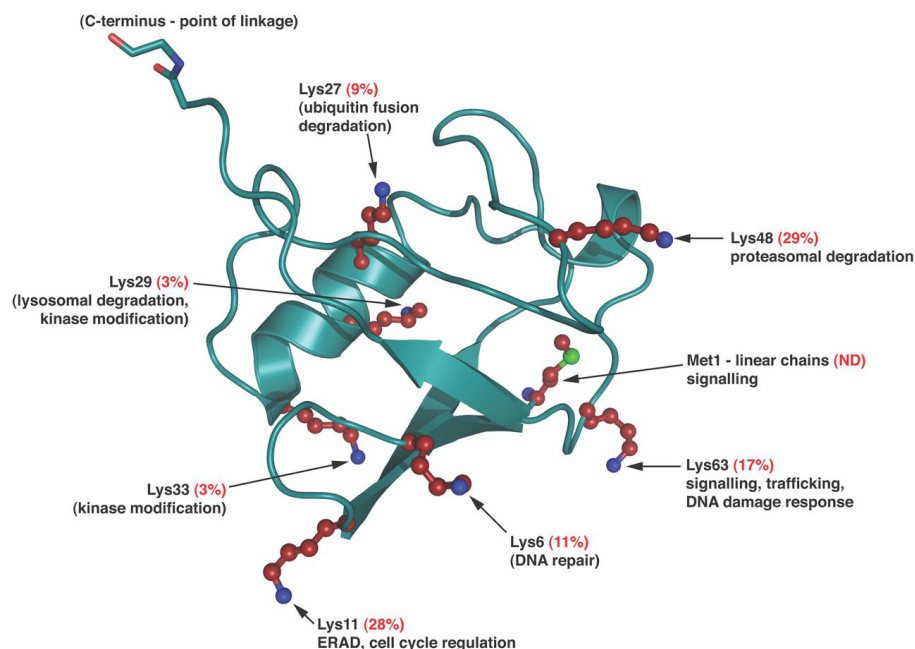
Figure 5 – The ubiquitin structure and its lysine residues (adapted from (Komander, 2009)). Analysis of the Ub structure reveals that all seven lysine residues (red, with blue nitrogen atoms) reside on different surfaces of the molecule. Methione 1 (with a green sulfur atom) is the linkage point in linear chains, and is spatially close to K63. The C-terminal glycine (G)75-G76 motif involved in isopeptide bond formation is indicated (red oxygen atoms, blue nitrogen atoms). Lysine residues are labelled, and red numbers in parentheses refer to the relative abundance of the particular linkage in yeast (Xu et al., 2009). The proteomic study relied on His-tagged ubiquitin, and hence linear chains could not be determined (ND) (Xu et al., 2009). The roles of the particular linkages are indicated.
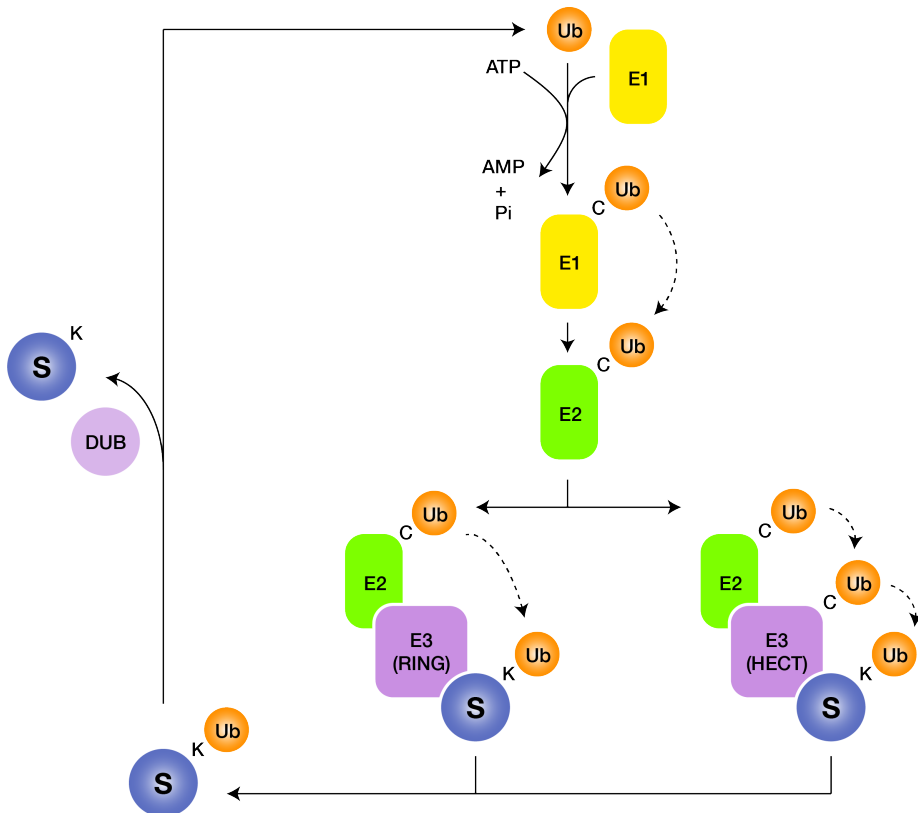
Figure 6 – **The ubiquitin cascade reaction.** Ubiquitin (Ub) is activated for transfer by E1 (ubiquitin-activating enzyme). Activated ubiquitin is transferred in thioester linkage from the active-site cysteine of E1 to the active-site cysteine of an E2 ubiquitin-conjugating enzyme. The E2-Ub thioester next interacts with an E3 ubiquitin ligase, which effects transfer of Ub from E2-Ub to a lysine residue of a substrate. E3 ligases are traditionally categorized into two main families: HECT E3s which accept Ub from E2s and then ligate the moiety onto the substrate, and RING ligases that facilitate Ub transfer from E2 enzymes to substrate lysine. Eventually, the substrate-Ub bond can be released *via* the action of a deubiquitinase (DUB).

Ub is particularly well described for its role as signal for the degradation of soluble cytosolic and nuclear proteins by the 26S proteasome (Weissman, 2001; Vierstra, 2009). This quality control system of proteins is also called ubiquitin-proteasome system (UPS) and involves K48 polyUb chains as signal (Smalle et al., 2004). Ub plays also a major role along the endomembrane system, controlling the fate of proteins and organelles. Ub has notably been described as crucial for quality control processes during membrane protein or secreted protein maturation in the ER (Meusser et al., 2005), and for the endocytosis of membrane proteins (Hicke, 2001; Hicke and Dunn, 2003). Finally, Ub has been demonstrated to act during autophagy, a process during which cytosolic compounds are degraded to the lysosome/vacuole *via* the formation of a double membrane compartment called autophagosome (Mizushima et al., 2011).

4.2   The ERAD pathway

The protein maturation process in the ER is an imperfect process that can produce defective proteins, which must be degraded. The first indication that certain ER proteins are eliminated came from studies in mammalian cells. Some subunits of the T-cell receptor, such as TCR-α, were described as retained in the ER and subsequently degraded (Bonifacino et al., 1989). A punctate mutant for the Cystic Fibrosis Transmembrane Conductance Regulator (CFTR) shares a similar fate. The mutation of the F508 residue in CFTR is the main cause for cystic fibrosis. This mutant is prematurely degraded and is therefore absent from the surface of epithelial cells (Cheng et al., 1990). The recognition of misfolded or mutated proteins depends on the detection of several factors such as exposed hydrophobic regions, unpaired cysteine residues and immature N-glycans. To be correctly targeted to the cytosol where degradation *via* the Ub-proteasome system occurs, defective proteins need to be released through the ER membrane and this step is called retro-translocation (Vembar and Brodsky, 2008). However, the molecular nature of the retro-translocon remains controversial (Hampton and Sommer, 2012). It was previously thought that SEC61 was responsible for retro-translocation of ERAD substrates through the ER membrane (Pilon et al., 1997). The yeast protein DER1 and its mammalian orthologs Derlins were also suspected to be the retro-translocon (Lilley and Ploegh, 2004; Ye et al., 2004). Eventually, because ERAD is an Ub-dependent process, the E3 ligase HRD1/DER3 implicated in the pathway was suggested to be also responsible for the retro-translocation step (Carvalho et al., 2010). It is possible that these three different factors could act as a retro-translocon for different misfolded substrate proteins thereby involving different adaptors for this retro-translocation.

As mentioned previously, the HRD1/DER3 was identified as the Ub ligase required for the ERAD pathway. This E3 ligase ubiquitinates denatured proteins *in vitro* suggesting that it functions as a quality control component (Bays et al., 2001). This ubiquitination of defective proteins led to their degradation *via* the proteasome 26S in the cytosol after the retro-translocation from the ER to the cytosol. Other key components of the ERAD pathway were identified so far such as the AAA-ATPase p97 (CDC48 in yeast) that is involved in the initiation of the substrate retro-translocation (Ye et al., 2001; Jentsch and Rumpf, 2007). HRD3 is another ER membrane protein and is a cofactor for HRD1/DER3 that may target substrates to the site of dislocation *via* its large lumenal domain (Gardner et al., 2000). Surprisingly, unconventional K11 linkages were also shown to be associated with ERAD pathway by quantitative proteomics analysis (Xu et al., 2009) (Fig. 4; Fig. 5). Thus, the UPS is not just associated with conventional K48 polyUb chains but also with unconventional linkages making ubiquitination a far more complex process than previously expected (Komander, 2009).

Homologs of yeast and mammalian ERAD components have been identified in the *Arabidopsis* genome and include E3 ubiquitin ligases that label substrate proteins for degradation, and accessory proteins such as the ATPase CDC48, the putative retro-translocon DER1 and the chaperone HRD3 (Su et al., 2011; Rancour et al., 2002; Kirst et al., 2005; Chen et al., 2016). However, recent genetic, biochemical and cell biological studies revealed unique aspects of the plant ERAD mechanisms and especially their connections with both stress tolerance and plant

defense (Liu and Li, 2014). For instance, the E2 enzyme UBC32 is an ERAD component implicated in brassinosteroid-mediated salt stress tolerance (Cui et al., 2012). Indeed, UBC32 is localized at the ER membrane and is involved in the degradation of *bri1-9*, a dwarf *Arabidopsis* mutant caused by retention of a defective brassinosteroid receptor in the ER (Cui et al., 2012). A suppressor screen of *bri1-9* made in the lab of Jianming Li lead to the discovery of either mammalian or yeast homologous proteins or plant specific factors implicated in the ERAD pathway (Jin et al., 2007b; Liu and Li, 2014). Among them, a plant specific calreticulin CRT3 was described as a key retention factor for a defective version of BRI1 in the ER (Jin et al., 2007b). Furthermore, a *crt3* null mutant does not accumulate the EFR innate immune receptor suggesting that EFR is also a substrate for CRT3 (Li et al., 2009).

4.3   Autophagy

Macroautophagy (or autophagy) is the process leading to the degradation of cytosolic compounds in the lysosome/vacuole during starvation. Indeed, upon starvation conditions, bulk cytosol is taken up by autophagosomes, transported to the lysosome/vacuole for degradation, and recycled into small biosynthetic precursors making a link between autophagy and a survival process. However, autophagy has broad roles in cellular housekeeping, including removal of damaged or unnecessary organelles and intracellular pathogens (Mizushima and Komatsu, 2011). Even the proteasome itself has been shown to be degraded by autophagy (Marshall et al., 2015). ATG8 is a well-described member of the autophagy-related (ATG) family and is required for the autophagosome formation. In plants, ATG5 has been shown to be in close contact with ATG8 in the growing phase of this autophagic compartment (Le Bars et al., 2014). In yeast, autophagosome biogenesis nucleates at the phagophore assembly site (PAS) (Stanley et al., 2014). The lipidation of yeast ATG8 or its mammalian counterpart LC3 begins at the PAS after the recruitment of all other ATG proteins and is required for phagophore expansion (Suzuki et al., 2007; Xie et al., 2008). The PAS is thought to be a dynamic structure that nucleates into a phagophore (Reggiori and Klionsky, 2013). It was suggested that various compartments including the ER, the Golgi apparatus and even the PM could contribute to the phagophore expansion (Reggiori and Klionsky, 2013). The cell indeed may mobilize membrane from multiple sources to respond to the demand from macroautophagy. As the phagophore grows, it can engulf the cytosol forming the autophagosome. The sequestration of a cytosolic compound requires a double membrane compartment to be thermodynamically favorable. When the external membrane of the autophagosome fuses to the vacuole/lysosome, the inner membrane, called the autophagic body, is released inside the lumen of the lytic compartment and further degraded. In plants, most of the genes coding for the ATG proteins have been identified (Michaeli et al., 2016).

This past decade, the implication of ubiquitination and particularly K63 polyUb chains in the autophagy process has been described. ATG8/LC3 can interact with adapter proteins through a LC3-interacting region (LIR) motif (Pankiv et al., 2007; Ichimura et al., 2008). These adapters have also the ability to bind ubiquitinated substrates (Kirkin et al., 2009). This co-interaction likely facilitates autophagic degradation. For instance, PARKIN is an E3 ligase that

can catalyze K63 polyUb chains leading to the recruitment of the Ub-binding adaptor p62 which is an autophagy receptor implicated in the clearance of protein inclusions (Tan et al., 2008; Kuang et al., 2013). PARKIN can also promote the degradation of misfolded proteins through K63-linked ubiquitylation, marking these proteins for clearance by autophagy *via* the adaptor protein HDAC6 (Olzmann and Chin, 2008). The implication of K63 polyubiquitination appears to be linked with selective autophagy in contrast with non-selective autophagy processes (Kraft et al., 2010).

In plants, FYVE1/FYVE domain protein for endosomal sorting 1 (FREE1) is a protein at the interplay between autophagy and sorting to the vacuole *via* the ESCRT complex (Gao et al., 2014; Gao et al., 2015). Depletion of FREE1/FYVE1 in an inducible *free1/fyve1* RNAi knock-down (KD) mutant leads to the accumulation of autophagosomes and an impaired autophagic degradation (Gao et al., 2014). FYVE1/FREE1 directly interacts with the autophagic regulator SH3 domain-containing protein 2 (SH3P2) which has been only described in plants (Zhuang et al., 2013). SH3P2 indeed binds to PI3P and ATG8 and regulates the formation of autophagosomes in plants (Zhuang et al., 2013). FYVE1/FREE1 also affects the association between autophagosomes and MVBs further suggesting the crucial role of this protein in the interplay between ESCRT-related endocytic and autophagic pathways (Gao et al., 2015). As mentioned later in this manuscript, FYVE1/FREE1 localizes to MVB/LE/PVC and interacts with IRT1 to control its trafficking. FYVE1/FREE1 overexpression therefore affects IRT1 localization between the plasma membrane and TGN/EE, and its polarity on the PM (Barberon et al., 2014). FYVE1/FREE1 likely acts on the recycling of IRT1 from endosomal compartments back to the plasma membrane.

Autophagy can also be implicated in the degradation of PM cargos in plants. The TRYPTO-PHAN-RICH SENSORY PROTEIN (TSPO) was initially described as a heme-binding protein whose interaction with ATG8 enables the degradation of porphyrins *via* autophagy (Vanhee et al., 2011). More recently, TSPO was shown to interact with the aquaporin PIP2;7 and to mediate its delivery from the plasma membrane to the vacuole in an autophagic-dependent pathway. This autophagic degradation of PIP2;7 seems to regulate water permeability, an important function under heat and drought stresses (Hachez et al., 2014).

Altogether, autophagy is a major process for recycling materials within cells and the implication of K63 polyubiquitination in selective autophagy is still poorly characterized particularly in the plant field. Despite its role in autophagy, K63 polyubiquitination has also been well-described for its role in the endocytosis of membrane proteins, especially in yeast and mammals, and will be discussed extensively in the next chapter.

Chapter 3

Ubiquitin-mediated endocytosis

The role of Ub as endocytosis signal has first been evidenced in yeast by Kolling and Hollenberg, who showed that mutants of S. cerevisiae deficient in the endocytic pathway accumulate ubiquitinated forms of the pheromone carrier STE6 at the PM (Kölling and Hollenberg, 1994). After that, the internalization of several membrane proteins has been correlated with their level of ubiquitination (Kölling and Hollenberg, 1994; Hicke and Riezman, 1996; Staub et al., 1997; Terrell et al., 1998). The following sections will review our current knowledge about Ub-mediated endocytosis in various model organisms.

1   Ubiquitination of PM proteins: internalization *versus* sorting

While only little is known on Ub-mediated endocytosis in plants, this process is well characterized in other model systems.

1.1   Yeast

The involvement of ubiquitination in the early steps of endocytosis, i.e. the internalization from the PM, came from the analysis of non-ubiquitinatable versions of cargos in yeast. GAP1 is highly active and stable at the plasma membrane in cells growing on poor nitrogen sources like proline (Springael and Andre, 1998). Upon addition of a favored nitrogen source like ammonium, GAP1 is ubiquitinated on its amino-terminal K9 and K16 thus causing its internalization (Springael and Andre, 1998; Soetens et al., 2001). K6R and K9R substitutions abolish its ubiquitination and provoke its accumulation at the PM (Soetens et al., 2001). GAP1 recycling requires the YPT6 GTPase involved in endosome to TGN transport (Nikko et al., 2003). After deletion of the YPT6 gene, GAP1 is internalized in these cells at a similar rate regardless of whether it is monoubiquitinated or polyubiquitinated and of whether one or two lysines are modified further indicating that monoubiquitination even on a single lysine residue is sufficient for GAP1

internalization from the PM (Lauwers et al., 2009). Zinc regulated transporter 1 (ZRT1) is another cargo that is endocytosed following its mono-, di- and/or multi-monoubiquitination (Gitan and Eide, 2000). Mutation on the K195 into arginine triggers a loss of both ubiquitination and internalization of ZRT1 (Gitan and Eide, 2000). Altogether, this suggests that mono- or multi-monoubiquitination of cargos is sufficient for the internalization step of endocytosis.

Other studies indicate that even if monoubiquitination constitutes a sufficient internalization signal for many membrane proteins, multi-monoubiquitination or a K63 polyUb chain can accelerate the process of internalization (Barriere et al., 2006; Hawryluk et al., 2006; Kim and Huibregtse, 2009; Lauwers et al., 2010). The internalization efficiency of the uracil permease FUR4 is proportional to the number of Ub monomers linked to this cargo (Blondel et al., 2004). Furthermore, when K63 polyubiquitination is impaired, the permease still undergoes endocytosis but at a reduced rate (Galan and Haguenauer-Tsapis, 1997). The SUB413 strain express no internal Ub pool which is counterbalanced by overproducing UbKR variant unable to form K63 polyUb chains (Spence et al., 1995). The JEN1 monocarboxylate transporter is stabilized at the PM in the strain producing the UbK63R variant (Paiva et al., 2009).

The RSP5 E3 ligase is the only member of the HECT family in yeast. First evidence supporting the role of RSP5 in endocytosis came from point mutations in some domains of the E3 ligase that impaired both STE2 ubiquitination and internalization (Dunn and Hicke, 2001). *END3* was the first gene shown to be necessary for the internalization step in yeast (Raths et al., 1993). JEN1 is not internalized in *end3* mutant cells and less ubiquitinated, as in the *rsp5* mutant strain (Paiva et al., 2009). Interestingly, overexpression of *RSP5* suppresses the growth defect of an *end3* mutant indicating the importance of this E3 ligase for the internalization step in yeast (Kaminska et al., 2002). As a result, RSP5 may function independently of END3 or downstream of it. RSP5 is now considered as responsible for the ubiquitination of most if not all internalized membrane proteins such as GAP1, JEN1, FUR4, ZRT1, or the siderophore iron transporter SIT1 (Hein et al., 1995; Galan et al., 1996; Gitan and Eide, 2000; Soetens et al., 2001; Erpapazoglou et al., 2008; Belgareh-Touzé et al., 2008). To recognize this myriad of substrates, RSP5 needs some adaptors to provide some specificity to the ubiquitination process. Emr and colleagues described in 2008 the arrestin-related trafficking adaptors (ART) family that have the ability to target specific PM proteins (Lin et al., 2008). ART1 is a protein with an arrestin motif that can interact with RSP5 (Lin et al., 2008). ART1 was initially identified from a genetic screen of 4652 knock-out yeast strains - each deleted for a nonessential gene - for increased sensitivity to canavanine, a toxic arginine analog that enters the cell *via* the arginine transporter CAN1 (Lin et al., 2008). A deletion of *ART1* gene led to a strong defect in CAN1 endocytosis and turnover (Lin et al., 2008). Furthermore, ART1 is recruited to the PM in response to high nutrient conditions suggesting its role in cargo downregulation (Lin et al., 2008). SMF1 is a metal transporter that is internalized in response to cadmium (Nikko et al., 2008). RSP5-mediated ubiquitination of K33 and K34 residues is implicated in the internalization of this transporter since a double mutant for these two lysines is slowly endocytosed from the PM (Nikko et al., 2008). Strikingly, ECM21 is an arrestin protein that can interact with both

RSP5 and SMF1 bridging the gap between the E3 ligase and the substrate (Peng et al., 2003; Nikko et al., 2008). Arrestins were also shown to regulate the final fate of the cargo, by acting on the balance between cargo recycling to the plasma membrane, or its vacuolar/lysosomal degradation. Indeed, arrestins have the ability to recruit E3 ligases and promote cargo ubiquitination, therefore acting as adaptor proteins (Shenoy et al., 2008). A phylogenetic study has revealed that proteins of the arrestin family are present in all eukaryotes except in plants (Alvarez, 2008; Aubry et al., 2009). Interestingly, arrestins are themselves targets of ubiquitination allowing further feedback (Shenoy et al., 2001; Lin et al., 2008). JEN1 undergoes Ub-mediated endocytosis and is degraded in response to glucose (Paiva et al., 2009). ROD1 is an adaptor of the arrestin family that is dynamically relocalized from cytosol to TGN compartment in response to glucose treatment. Furthermore, ROD1 is crucial for JEN1 sorting to the vacuole in response to glucose (Becuwe and Léon, 2014). Glucose removal promotes ROD1 relocalization to the cytosol and JEN1 deubiquitination, allowing transporter recycling when the signal is only transient (Becuwe and Léon, 2014). ROD1 indeed trigger ubiquitination or deubiquitination by interacting with JEN1 dynamically in response to glucose (Becuwe and Léon, 2014). Therefore, nutrient availability regulates the fate of this transporter through the localization of the ROD1/RSP5 ubiquitination complex at the TGN.? An ubiquitinated cargo protein can then be recognized by adaptors. The best characterized adaptors are Epsins (EPS15 interacting protein) (Traub, 2009). These adaptors are monomeric, contain a Ub-binding site (UIM) and are able to interact with clathrin, AP2 complex and PI(4,5)P$_2$ *via* their ENTH domain (Wendland, 2002; Traub, 2009). Arrestins can also interact with clathrin through a clathrin-binding motif (Goodman et al., 1996; Goodman et al., 1997; Krupnick et al., 1997). Altogether, arrestins may act at two different levels: first, for cargo ubiquitination, which could recruit Epsin endocytic adaptors, and, second, to assist the latter in the recruitment of a clathrin coat. Furthermore, Epsins are ideal candidates to coordinate ubiquitin recognition and cargo internalization. While such a function appears to be established in mammalian cells (Barriere et al., 2006; Kazazic et al., 2009; Sigismund et al., 2005), recent data in yeast favor a more complex model, where UIM domains would play a more general role in protein interactions and the assembly of the endocytic network (Dores et al., 2010). Ubiquitination is a reversible post-translational modification, counterbalanced by deubiquitination. Deubiquitination is involved in the regulation of CME, by acting directly on cargo ubiquitination status as well as on the endocytic machinery. EDE1 is ubiquitinated by RSP5 and allows the coat protein recruitment (Weinberg and Drubin, 2014). The deletion of UBP2 and UBP7 deubiquitinases (DUBs) implicated in EDE1 deubiquitination result in elongating the lifetime of cargos at the PM (Weinberg and Drubin, 2014). This mechanism emphasizes the existing balance to maintain protein level at the PM thereby controlling CME by dynamic ubiquitination and deubiquitination (Weinberg and Drubin, 2014).

In yeast, ubiquitination is also a signal driving to the lysosomal/vacuolar degradation of a cargo protein (Lauwers et al., 2010). The role of Ub in MVB sorting was difficult to establish given the crucial role of Ub in the early stages of endocytosis in yeast. This difficulty was bypassed in studies using cargo proteins which were directly addressed to the MVB. For instance,

the carboxypeptidase S 1 (CPS1) and the polyphosphatase PHM5 are directly sorted from the Golgi apparatus to the vacuole/lysosome through MVB/LE/PVC compartments (Odorizzi et al., 1998; Reggiori and Pelham, 2001). These two cargos are ubiquitinated, and non-ubiquitinatable variants of these proteins fail to reach the vacuolar lumen (Reggiori and Pelham, 2001; Katzmann et al., 2001). In addition, vacuolar delivery of PHM5 mutant cargos can be restored upon engineered fusion with Ub (Reggiori and Pelham, 2001). Whereas monoubiquitination of a protein may be sufficient for internalization, K63 polyubiquitination emerges as the signal required for lysosomal/vacuolar degradation (Erpapazoglou et al., 2008; Lauwers et al., 2009; Huang et al., 2013; Martins et al., 2015). The yeast GAP1 protein modified with a single diUb residue with K63 association is effectively directed to the vacuole whereas GAP1 modified with two monoubiquitins accumulates on the tonoplast following an internalization defect in ILVs of MVB/LE/PVC (Lauwers et al., 2009).

1.2 Mammals

In mammalian cell lines, the study of membrane protein ubiquitination is mainly focused on the EGF receptor (EGFR), the archetypal Receptor Tyrosine Kinase (RTK). EGFR was the first ubiquitinated cargo described in mammals (Galcheva-Gargova et al., 1995). Following EGF binding, EGFR is ubiquitinated by the RING E3 ligase CBL (Levkowitz et al., 1998). EGFR is ubiquitinated by the co-action of CBL, CIN85 and Endophilins that are bound constitutively with CIN85 and mediate CME (Soubeyran et al., 2002; Verstreken et al., 2002). EGFR is not properly internalized in CIN85-defective mutants (Soubeyran et al., 2002). The interaction between EGFR and CBL is mediated by the adaptor GRB2 (Waterman et al., 2002; Sorkin and Goh, 2009; Madshus and Stang, 2009). EGFR was first described as multi-monoubiquitinated (Haglund et al., 2003). The use of the FK1 and FK2 antibodies, specifically recognizing polyUb chains, failed to detect ubiquitination signals on EGFR immunoprecipitates, while the generic P4D1 antibody recognizing both mono- and polyubiquitin chains did. This observation suggested that multiple monoubiquitination were decorating EGFR in mammalian cells (Haglund et al., 2003). An EGFR-Ub$_{\Delta GG}$ chimera, depleted from the tyrosine kinase domain and translationally fused to an Ub moiety unable to be conjugated to additional Ub moieties, was used to evaluate the role of EGFR monoubiquitination. This monoUb-mimic version of EGFR is constitutively internalized and degraded in NR6 cells, indicating that monoubiquitination is sufficient for the endocytosis of the receptor (Haglund et al., 2003). Mass spectrometry analyses of EGFR revealed that it does not only carry multiple monoUb but can also be polyubiquitinated mostly with K63 polyubiquitin chains (Huang et al., 2006). Mutation of nine ubiquitination target lysines into arginines has however no effect the internalization of the receptor, whereas the loss of both GRB2 and CBL were crucial for this first step of endocytosis (Huang et al., 2006), suggesting that either ubiquitination of EGFR do not play a role in internalization or that additional ubiquitination sites exist. Ubiquitination of EGFR however appeared essential for its lysosomal targeting and degradation (Huang et al., 2006). In addition to the nine lysine residues mentioned above, six additional KR mutations in the kinase domain of EGFR were investigated to test whether resid-

ual ubiquitination of the 9KR mutant was responsible for its rapid internalization (Huang et al., 2007). A 15KR mutant version of EGFR revealed a partial internalization defect, with only low rates of endocytosis while its kinase activity is unchanged (Huang et al., 2007). Taken together, these results suggest that ubiquitination is not sufficient for internalization *per se*. However, siRNA used to knock-down the clathrin heavy chain (CHC), GRB2 and CBL strongly inhibited the internalization of EGFR (Huang et al., 2007). A more recent study shed light on the involvement of the AP2 adaptor complex and another post-translational modification, acetylation of lysine residues in the regulation of the CME of the receptor (Goh et al., 2010). The EGFR$_{15KR}$ mutant was mutated for its AP2 binding domain together with the mutation of five other lysines residues mutated into arginines implicated in both acetylation or ubiquination at the C terminal part of the protein (Goh et al., 2010). EGFR$_{21KR\Delta AP2}$ has a normal kinase activity but is impaired for internalization from the PM further suggesting that CME of EGFR involves at least four redundant mechanisms (Goh et al., 2010). However, the residual CME of this mutant version of EGFR was investigated in carcinoma cells more recently to further understand the mechanisms driving the EGFR internalization step (Fortian et al., 2015). The strong inhibition of the 21KRΔAP2 mutant endocytosis by siRNA knock-down of the UBCH5 E2 enzyme directly demonstrates the involvement of an ubiquitination event in this endocytosis process (Fortian et al., 2015). GRB2 has an essential function in the internalization of EGFR$_{21KR\Delta AP2}$ further supporting the role of ubiquitination in this process (Fortian et al., 2015). The authors finally uncovered the role of new Ub conjugation sites that may mediate the internalization of EGFR$_{21KR\Delta AP2}$ in carcinoma cells (Fortian et al., 2015). Analysis of the CCP dynamics using VA-TIRF microscopy in those cells indicated that the primary defect responsible for reduced internalization rates of EGFR$_{21KR\Delta AP2}$ is at the CCP recruitment step and an additional defect is the delayed completion of the CCP life cycle (Fortian et al., 2015). Altogether, these results led the authors to revise their previous model of the CME of EGFR that assumed at least four redundant mechanisms to be involved (Goh et al., 2010) and led to a new model whereby both receptor ubiquitination and interactions with AP2 mediate EGFR recruitment into CCP and endocytosis (Fortian et al., 2015). The internalization step of EGFR is controlled by at least two mechanisms but does not rely only on ubiquitination. This is a different situation compared with yeast where RSP5-mediated ubiquitination is absolutely necessary for the internalization of many cargos. The mammalian EGFR is also K63 polyubiquitinated and this modification triggers its degradation in lysosomal compartments (Huang et al., 2013). When EGFR is fused to the AMSH DUB, K63 polyubiquitination of the receptor is impaired and, as such, EGFR is slowly degraded in lysosomes (Huang et al., 2013).

1.3 Plants

In plants, the role of ubiquitination as endocytic signal was first suggested by the study of FLS2 (Robatzek et al., 2006; Göhre et al., 2008). The proteasome inhibitor MG132 was shown to prevent the internalization of the FLS2 flagellin receptor upon ligand binding. This observation led the authors to conclude that FLS2 degradation involves the UPS (Robatzek et al., 2006).

Considering the extensive knowledge accumulated in yeast and mammals on the degradation of PM proteins by endocytosis, this conclusion appeared rather inappropriate. FLS2 ubiquitination has later been demonstrated *in vitro* and *in vivo* in the context of a pathogen infection (Göhre et al., 2008). Ubiquitination of FLS2 is dependent on the AvrPtoB bacterial effector which acts as E3 ligase exploiting cellular machinery to ubiquitinate and accelerate the degradation of FLS2 and thus suppress the immune defense reaction (Göhre et al., 2008). More recently, a 22-amino-acid peptide containing a conserved epitope from bacterial flagellin, flg22 binding to FLS2 was shown to allow the recruitment of the U-box E3 ligases PUB12 and PUB13 and to promote their phosphorylation by the FLS2 co-receptor BAK1 (Lu et al., 2011). Once phosphorylated, PUB12 and PUB13 mediate the ubiquitination and degradation of FLS2 (Lu et al., 2011). Treatment with MG132 abolished the flg22-induced degradation of FLS2, leading the authors to conclude on the involvement of proteasome for the ubiquitin-mediated degradation of FLS2, although flg22-mediated endocytosis has been known for many years (Robatzek et al., 2006). A role of ubiquitination in endocytosis and degradation of PIN2 has also been suggested (Abas et al., 2006; Laxmi et al., 2008). PIN2 ubiquitination was shown *in vivo* and MG132 treatment is associated with an increased level of PIN2 ubiquitination and slower degradation in the vacuole, which highlights the indirect role of proteasome in the control of PIN2 turnover (Abas et al., 2006; Laxmi et al., 2008). For both PIN2 and FLS2, MG132 effect on the ubiquitination and degradation of membrane proteins is likely mediated *via* a depletion of free Ub pool for the ubiquitination of cargo proteins (Melikova et al., 2006), or *via* the stabilization of a protein that must be turned over to proceed with endocytosis. More recently, PIN2 was described as modified by K63 polyUb chains (Leitner et al., 2012). K63 polyubiquitination of the auxin efflux transporter is required for its vacuolar sorting *in planta* (Leitner et al., 2012). Consistently, mutation of 12K residues into arginines stabilized PIN2 protein levels together with a loss of ubiquitination for the cargo (Leitner et al., 2012). Altogether, PIN2 ubiquitination triggers its vacuolar targeting thereby affecting auxin distribution in root meristems and demonstrating a function in the control of gravitropic root growth (Leitner et al., 2012). The borate transporter BOR1 is another plant cargo that undergo ubiquitination (Kasai et al., 2011). Interestingly, BOR1 ubiquitination did not control its internalization but rather its vacuolar targeting (Kasai et al., 2011). Mutation of the K590 residue into alanine impaired the vacuolar sorting of BOR1-GFP (Kasai et al., 2011). In addition, BOR1 likely carries mono- or diUb residues at its K590 amino acid but this does not rule out the implication of K63 linkages between the two moieties (Kasai et al., 2011). The root iron transporter IRT1 is endocytosed following the monoubiquitination of its two K154 and K179 residues located in the large cytosolic loop of the protein (Barberon et al., 2011). However, there are no evidences for a role of ubiquitination in the vacuolar targeting of the transporter for now. The other plant cargo BRI1 fused to mCitrine fluorescent tag and attached with a single Ub moiety in its kinase domain is targeted to the vacuole and efficiently degraded (Martins et al., 2015). Mutations of 25K into arginines within the kinase domain of BRI1-mCitrine led to both ubiquitination defect and lower internalization rate compared with WT BRI-mCit (Martins et al., 2015). As such, BRI1$_{25KR}$-mCit is found at the PM compared

with non-mutated BRI1-mCit which is found at the PM and in endosomes (Martins et al., 2015). Indeed, using VA-TIRF microscopy in the hypocotyl, BRI125KR-mCit was found to be more stable at the PM but was still internalized (Martins et al., 2015). Pharmacological approaches indeed showed that $BRI1_{25KR}$-mCit accumulate in BFA bodies in presence of CHX suggesting an internalization of this mutated version of the cargo (Martins et al., 2015). However, loss of BRI1 ubiquitination impaired its vacuolar degradation indicating that this modification is at least essential for late events of endocytosis (Martins et al., 2015).

The implication of Ub along the endocytic pathway is undoubtedly established by now in several model organisms. However, while Ub-triggered internalization is well established in yeast, Ub functions has been more described to date in late events of endocytosis in animals and plants.

2 The endosomal sorting complex required for transport (ESCRT)

The ESCRT system is responsible for the recognition of ubiquitinated proteins at the MVB/LE/-PVC and their subsequent internalization on ILVs of this compartment (Spitzer et al., 2006; Haas et al., 2007; Spitzer et al., 2009; Schellmann and Pimpl, 2009; Raiborg and Stenmark, 2009) (Fig. 7). The ESCRT system is particularly well described in yeast. It is subdivided into 4 complexes of cytosolic proteins (ESCRT0, I, II and III) which are transiently recruited to endosomes and act sequentially by transmitting to each other the ubiquitinated cargo protein (Williams and Urbé, 2007; Schellmann and Pimpl, 2009; Raiborg and Stenmark, 2009). The cargo protein is then deubiquitinated by DOA4 DUB that interacts with the ESCRTIII complex (Amerik et al., 2000; Luhtala and Odorizzi, 2004). This complex then recruits the proteins that are necessary for the invagination step giving an internal vesicle of MVB/LE/PVC (Williams and Urbé, 2007; Schellmann and Pimpl, 2009; Raiborg and Stenmark, 2009). Disassembly and recycling of ESCRT subunits is performed *via* the AAA ATPase VPS4 that is associated with the ESCRTIII complex (Obita et al., 2007; Williams and Urbé, 2007; Schellmann and Pimpl, 2009). The invagination of the membrane in an ILV also depends on PI3P and $PI(3,5)P_2$ phosphoinositides recognized by the ESCRT system (Williams and Urbé, 2007).

The *A. thaliana* genome includes most of the genes encoding proteins of the ESCRT system (Winter and Hauser, 2006; Spitzer et al., 2006; Schellmann and Pimpl, 2009). ELC is a VPS23 homologous protein of the ESCRTI complex and was the first ESCRT component characterized in plants (Spitzer et al., 2006). ELC is able to bind directly to the Ub residue and is located at MVB/LE/PVC where it interacts with homologs of ESCRTI in *Arabidopsis* (Spitzer et al., 2006). The best characterized ESCRT component in plants is SKD1. SKD1 is a homolog of VPS4 which has ATPase activity and is recruited to the MVB/LE/PVC compartment (Haas et al., 2007). The expression of a dominant-negative form of SKD1 leads to the formation of an expanded MVB/LE/PVC compartment containing a reduced number of ILVs (Haas et al., 2007). In plants, CHMP1-A and CHMP1-B proteins are homologs of VPS46, a component of the ESCRTIII complex. They have also been characterized and are involved in the vacuolar
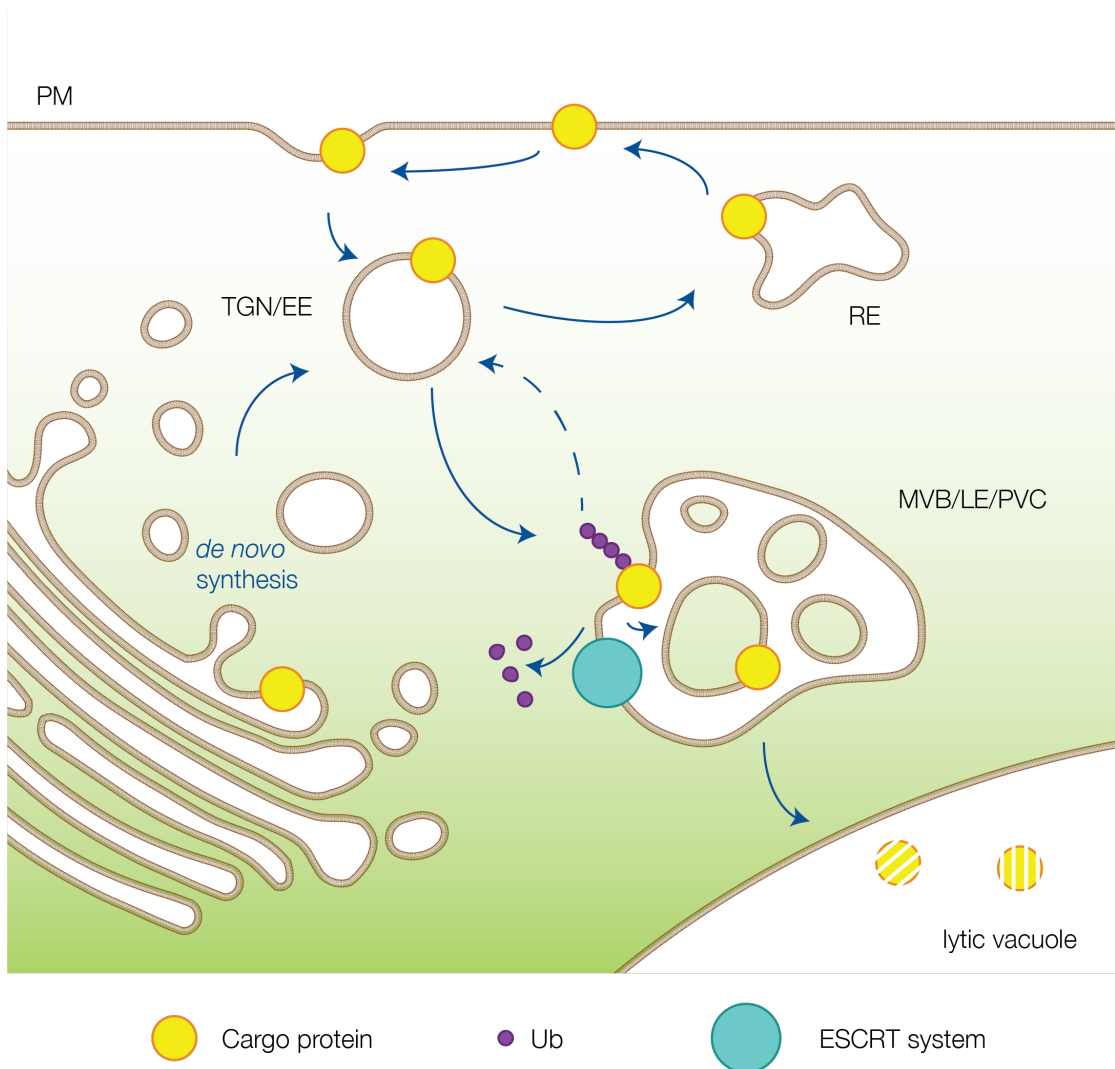
Figure 7 – **Model of action of the ESCRT complex in plants.** The ESCRT system is responsible for the recognition of ubiquitinated proteins (here the cargo carries a K63 polyUb chain) at the MVB/LE/PVC and their subsequent internalization on ILVs of this compartment and further degradation onto the vacuole.

targeting (Spitzer et al., 2009). In a double mutant *chmp1-a/chmp1-b*, PIN1, PIN2 and AUX1 are not internalized in ILVs of MVB/LE/PVC which results in an accumulation of these cargos on the tonoplast thus disrupting the degradation of these proteins in the vacuolar lumen (Spitzer et al., 2009). Recently, the AMSH3 DUB was described as involved in the vacuolar transport of cargo proteins and in the vacuolar biogenesis (Isono et al., 2010). AMSH3 hydrolyses K48 and K63 polyUb chains *in vitro* and is probably the main DUB enzyme in *A. thaliana* (Isono et al., 2010). In addition, an *amsh3* mutant has severe defect to target FM4-64 and PIN2 cargo protein to the vacuole (Isono et al., 2010). AMSH3 could therefore participate in the ESCRT system

by deubiquitinating cargo proteins recognized by the complex. However, no interaction between AMSH3 and the ESCRTIII complex proteins has been demonstrated to date (Isono et al., 2010). While most of the genes encoding components of the ESCRT complex exist in plants, ESCRT0 subunit is absent of the *Arabidopsis* genome and appears to be opisthokont-specific (Herman et al., 2011). However, in plants, the TOM1-LIKE (TOL) family was described to play the role of the ESCRT0 component in the degradative sorting of plant cargos (Korbei et al., 2013).

As mentioned in section II.d.iii, FYVE1/FREE1 localizes to MVB/LE/PVC and is essential for the formation of ILVs at such compartments (Gao et al., 2014). FYVE1/FREE1 is part of the ESCRTI complex as it is able to interact with VPS23 (Gao et al., 2014). Interestingly, as TOL proteins, FYVE1/FREE1 regulates the vacuolar sorting of cargos (Gao et al., 2014). However, this topic will be further discussed on the Discussion and perspectives part.

3 Crosstalk between phosphorylation and ubiquitination in endocytic pathways

Over the past twenty years, several studies suggested an interplay between the two major post-translational modifications phosphorylation and ubiquitination along the endocytic pathways. In yeast, STE2 ubiquitination at K337 by RSP5 requires hyperphosphorylation of the cargo (Terrell et al., 1998). The FUR4 yeast permease needs to be phosphorylated on its PEST-like sequence to be efficiently ubiquitinated and further degraded (Marchal et al., 1998; Marchal et al., 2000). In 2004, Kelm and colleagues suggested the existence of the PURE pathway as a multistep process of internalization involving Phosphorylation, Ubiquitination, Recognition of the substrate by the endocytic machinery and further Endocytosis of the cargo (Kelm et al., 2004). In their study, the authors showed the interplay of all these processes for the STE6 yeast α-factor transporter (Kelm et al., 2004). The monocarboxylate transporter JEN1 also necessitate YCK1/2 kinase activity to be properly degraded further suggesting the need of phosphorylation before JEN1 ubiquitination and endocytosis (Crapeau et al., 2014). In mammals, autophosphorylation at tyrosines 1045, 1068 and 1086 of the EGF receptor creates a major docking site for the E3 ligase CBL and its adaptor GRB2 (Levkowitz et al., 1999; Waterman et al., 2002; Jiang and Sorkin, 2003; Huang and Sorkin, 2005; Huang et al., 2006). Furthermore, the interferon α-receptor 1 (IFNAR1) necessitate phosphorylation at serine 535 and 539 to be efficiently ubiquitinated and degraded (Kumar et al., 2004). It was suggested ten years ago that a change of conformation and/or phosphorylation status of mammalian G protein-coupled receptors (GPCRs) might lead to recruitment of adaptors and subsequent ubiquitination (Reiter and Lefkowitz, 2006). The examples of phosphorylation-coupled ubiquitination of substrate proteins are numerous, although ubiquitination may also occur in the absence of prior phosphorylation.

The interplay between phosphorylation and ubiquitination of cargos can be at the effector level and not directly on the substrate. While auto-phosphorylation of EGFR is needed for further interaction with the E3 ligase CBL, phosphorylation of CBL itself by EGFR induces the interaction CIN85 that also necessitate to be phosphorylated for an effective EGFR ubiquitination

and sorting into MVBs (Levkowitz et al., 1999; Soubeyran et al., 2002; Schroeder et al., 2012). In plants, the PUB12 and PUB13 E3 ligases need a prior phosphorylation by BAK1 to efficiently ubiquitinate FLS2 (Lu et al., 2011).

Taken together, phosphorylation appears to be a major molecular switch to trigger ubiquitination of plasma membrane proteins.

4 Regulations of endocytosis by ligands and substrates

Controlling the level of proteins at the PM is crucial to respond to both endogenous and environmental cues. The turnover of proteins is essential for the quality control process, regulating the amount of proteins at the PM in response to a stimulus is a well described process in yeast and mammals. In plants however, only few plasma membrane proteins were described as regulated in response to their substrates, to biotic or abiotic stresses or even in response to their ligand in the case of receptors.

4.1 Ligand-mediated regulation

Many receptors in eukaryotes are internalized by endocytosis following the binding of their ligands. Ligand binding can trigger conformational changes and post-translational modifications such as phosphorylation and ubiquitination that lead to receptor-ligand endocytosis. In mammals, following the binding of EGF on its receptor, EGFR autophosphorylates on tyrosines 1045, 1068 and 1086 *via* its kinase domain (Levkowitz et al., 1999; Huang and Sorkin, 2005; Huang et al., 2006). This autophosphorylation allows the recruitment of the CBL-GRB2 complex, triggering ubiquitination of EGFR (Waterman et al., 2002; Jiang and Sorkin, 2003).

In plants, the receptor-like kinase FLS2 receptor is ubiquitinated, internalized, and degraded upon binding of flg22. Flg22 binding induces the interaction of FLS2 with another plasma membrane kinase called BAK1 (Chinchilla et al., 2007). This interaction promotes the activation of the whole complex and ultimately the internalization and degradation of FLS2 (Chinchilla et al., 2007). FLS2 binding to flg22 recruits the E3 ubiquitin ligases PUB12 and PUB13 and promotes their phosphorylation by BAK1 and the ubiquitination of FLS2 (Lu et al., 2011). The brassinosteroid receptor BRI1 is structurally related to FLS2 and also associates with BAK1 upon activation (Li et al., 2002; Nam and Li, 2002). However, in contrast to FLS2, the BRI1 endocytosis rate is not changed in the presence of its ligand (Geldner et al., 2007).

4.2 Substrate-mediated regulation

? The endocytic internalization and degradation of transporters in response to their substrates has been at the edge of recent publications in the literature. This substrate-induced ubiquitin-mediated endocytosis of transporters has mainly been explored in yeast and only a few evidence were published in plants (Dupre et al., 2004).

This downregulation mechanism was originally described for the inositol permease ITR1 (Lai et al., 1995). Since then, a lot of transporters in yeast were described as endocytosed in response to their substrate(s). For instance, K63 polyubiquitin-dependent degradation of SIT1 is mediated by iron, substrate of the transporter (Erpapazoglou et al., 2008). On the other hand, JEN1, a monocarboxylate transporter, is tightly controlled by glucose while it is not its direct substrate (Paiva et al., 2009; Becuwe and Léon, 2014). JEN1 is indeed ubiquitinated and degraded in response to glucose (Paiva et al., 2009; Becuwe and Léon, 2014). To further demonstrate the implication of K63 polyubiquitination in the glucose-induced degradation of the transporter, the authors expressed *JEN1* in a yeast strain defective for making K63 polyUb chains by mutating lysine 63 of ubiquitin into arginine (Paiva et al., 2009). JEN1 is stabilized at the PM and does not respond to glucose upon defective K63 polyubiquitin chain formation, further highlighting the glucose-induced K63 polyUb-mediated degradation of the transporter (Paiva et al., 2009). The glucose-induced internalization of JEN1 relies on ubiquitination of the transporter by RSP5 E3 ligase but also on another factor called ROD1 (Becuwe and Léon, 2014). As already mentioned, ROD1 is a protein of the arrestin family that is dynamically relocated from cytosol to TGN compartment in response to glucose treatment. Furthermore, ROD1 is crucial for JEN1 sorting to the vacuole in response to glucose (Becuwe and Léon, 2014). The well-described yeast permease GAP1 is ubiquitinated and internalized in response to ammonium (Crapeau et al., 2014). In cells growing on a poor nitrogen source, both BUL1 and BUL2 adaptors are phosphorylated by the NPR1 kinase and the phosphorylation state of BUL1/2 is stabilized by 14-3-3 proteins thereby inactivating BUL1/2 (Crapeau et al., 2014). In those conditions, GAP1 is not ubiquitinated by RSP5 and is found at the PM (Springael and Andre, 1998; Merhi and André, 2012; Crapeau et al., 2014). This inhibition of ubiquitination is relieved when NPR1 is itself phosphoinhibited by the TORC1 kinase complex when there is an increase of the internal amino acid pool (Merhi and André, 2012). As such, BUL1/2 are dephosphorylated thereby inducing RSP5-mediated ubiquitination on the N-terminal part of GAP1 and further degradation of the permease (Springael and Andre, 1998; Soetens et al., 2001; Merhi and André, 2012). Interestingly, another way of degradation exists through the inhibition of the TORC1 kinase complex by rapamycin (Crapeau et al., 2014). The arrestin-like ALY1 and ALY2 proteins together with BUL1/2 remain phosphorylated but still play a role in GAP1 ubiquitination and degradation (Crapeau et al., 2014). In a recent article, Ghaddar and colleagues showed that GAP1 and the arginine-specific permease CAN1 were ubiquitinated and endocytosed in response to their substrates (Ghaddar et al., 2014). This ubiquitin-dependent endocytosis is due to transport catalysis rather than intracellular substrate accumulation (Ghaddar et al., 2014).

A remaining question concerns the degradation of proteins found at the vacuolar/lysosomal membrane. Interestingly, recent publications by the Emr lab described a novel vacuole membrane recycling and degradation (vReD) pathway to downregulate vacuolar membrane transporters (Li et al., 2015b; Li et al., 2015a). The amino acid transporter YPQ1 is localized at the tonoplast and is selectively sorted and degraded in the vacuolar lumen following lysine withdrawal (Li et al., 2015b). This process requires a vacuole anchored ubiquitin ligase complex (VAcUL-1) that is

composed of RSP5 and one of its adaptor SSH4 (Li et al., 2015b). Eventually, the ESCRT complex allows the internalization of YPQ1 in ILVs and further degradation into the vacuolar lumen (Li et al., 2015b). The vReD pathway is conserved as zinc efflux ZRT3 and influx COT1 transporters are ubiquitinated and degraded in the vacuole following the application of zinc excess (Li et al., 2015a). However, COT1 is not ubiquitinated by RSP5 but by another RING E3 ligase TUL1 and more generally by the DSC complex (Li et al., 2015a). In the contrary, ZRT3 is ubiquitinated in response to its substrate by the co-action of both RSP5 and TUL1 E3 ligases and the DSC complex (Li et al., 2015a).

In plants, some metal transporters are internalized and degraded by high concentrations of their substrates, representing an important mechanism to regulate ion homeostasis. The boric acid exporter BOR1 is localized in the inner polar domain of root cells where it mediates boron loading into the root xylem (Takano et al., 2002; Takano et al., 2005). BOR1 is internalized and degraded in the presence of boron excess (Takano et al., 2005; Takano et al., 2010). Under low-boron conditions, BOR1 undergoes constitutive internalization and recycling from the TGN in a process dependent on a Tyr-based sorting signal in the large cytosolic loop of the transporter (Takano et al., 2010). When roots are exposed to high boron, BOR1 is ubiquitinated and the flux of BOR1 to the vacuole increases, although ubiquitination itself is not needed for internalization (Takano et al., 2005; Takano et al., 2010; Kasai et al., 2011). However, no phenotypes were associated with this high boron response decoupling cellular response and plant physiology.

IRT1 is a root transporter which mediates the uptake of iron in epidermal cells from the soil under iron-deficient conditions (Vert et al., 2002; Barberon et al., 2011). IRT1 is finely regulated at the transcriptional level by low iron notably through the action of FIT and other bHLH transcription factors (Vert et al., 2002; Vert et al., 2003; Séguéla et al., 2008; Sivitz et al., 2011). IRT1 is also able to transport other metals, such as zinc, manganese, cobalt and cadmium (Eide et al., 1996; Korshunova et al., 1999; Rogers et al., 2000; Vert et al., 2001; Vert et al., 2002). However, iron is the primary substrate of the transporter as it is able to complement an *irt1-1* knock-out mutant while the metals mentioned above failed to restore a normal phenotype and are then considered as secondary substrates (Vert et al., 2002). IRT1 protein levels are tightly regulated through both transcription and post-translational modification. Indeed, the multi-monoubiquitination of IRT1 at lysine residues 154 and 179 in the large cytosolic loop of the transporter is required for its constitutive internalization and recycling (Barberon et al., 2011). Although IRT1 abundance at the plasma membrane is not affected by iron concentration, it was subjected that the availability of non-iron substrates could affect the trafficking of IRT1 (Barberon et al., 2011; Zelazny et al., 2011). This hypothesis was at the basis of my thesis project and will be further discussed in the next part.

Part II

Context and objectives

The major objective of Grégory Vert's lab is to better understand the role(s) of K63 polyubiquitination in plant endocytosis and to unravel new roles associated with this poorly-characterized post-translational modification. Previous work from the group demonstrated for the first time the existence of Ub-mediated endocytosis in plants, taking advantage of the root iron transporter IRT1 as a model (Barberon et al., 2011). Following this pioneering work, two model PM proteins were implemented in the lab to grasp further how Ub, and more specifically K63 polyUb, is used to control the dynamics of these two PM proteins in the cell and its biological relevance. These models are IRT1 and the plant steroid hormone receptor BRI1.

I joined the group to follow up on the Ub-mediated endocytosis of IRT1. IRT1 was previously demonstrated by former lab members (Marie Barberon and Enric Zelazny) to be multi-monoubiquitinated on two lysine residues located in the large cytosolic loop of IRT1. At steady state, this transporter is localized to TGN/EE compartments. However, work from previous lab members unraveled the dynamic behavior of IRT1 between the cell surface and TGN/EE as a consequence of the constant and rapid endocytosis and recycling of IRT1. Mutation of the residues K154 and K179 into the non-ubiquitinatable arginine residues triggers accumulation of IRT1 at the PM. Furthermore, transgenic plants expressing $IRT1_{K154,179R}$ displayed a dramatic phenotype due to uncontrolled metal uptake, further indicating that the control of IRT1 protein levels and localization by ubiquitination is critical for proper iron homeostasis of plant root cells and the whole organism (Barberon et al., 2011). The availability of iron, which is the primary substrate of IRT1, has no apparent impact on the localization or the levels of IRT1, questioning the biological relevance of such a control by Ub-mediated endocytosis. IRT1 is a broad range metal transporter able to uptake other highly reactive divalent metals such as zinc, manganese, cobalt and cadmium (Eide et al., 1996; Korshunova et al., 1999; Rogers et al., 2000; Vert et al., 2001; Vert et al., 2002), raising the possibility that these non-iron metals may control IRT1 post-translationally by ubiquitin-mediated endocytosis. A first evidence for the involvement of non-iron metals in IRT1 dynamics came from observations made by Marie Barberon where IRT1 was shown to relocalize from early endosomal compartments to the outer polar PM domain facing the soil when secondary metal substrates of IRT1 are absent from the medium (Barberon et al., 2014).

The first objective of my PhD was to precisely dissect the impact of Zn, Mn and Co in the trafficking of IRT1 and to investigate deeper the relationship between non-iron metal nutrition, IRT1 localization and its ubiquitination profile. I also focused on the identification of the molecular mechanisms and actors involved in the metal-dependent Ub-mediated endocytosis of IRT1. Although one of the goal was to identify E3 ligases interacting with IRT1 and driving its response to non-iron metals, a paper reporting the characterization of the RING E3 ligase IRON-DEGRADATION FACTOR 1 (IDF1) came out at the beginning of my PhD. I therefore focused my attention on the potential role of IDF1 in the metal-triggered endocytosis of IRT1. I also shed light on the role of a histidine-rich stretch in the large cytosolic loop of IRT1 as potential direct metal-binding site, and the phosphorylation of IRT1.

The vast majority of the results accumulated during my PhD have been combined in a manuscript on which I am first author and that will serve as a basis for a submission within the next few weeks/months depending on the results from final ongoing experiments, notably on phosphorylation. This manuscript is presented in the fourth part of this thesis.

Marie Barberon also identified the FYVE domain-containing FYVE1 protein as interacting with IRT1 in a yeast two-hybrid (Y2H) assay. Interestingly, the overexpression of *FYVE1* led to the loss of polarity of IRT1 in root epidermal cells, allowing to tackle for the first time the functional relevance of outer polarity of transporters in the root epidermis for plant nutrition. This work was published in Proceedings of the National Academy of Sciences of the United States of America (PNAS) in 2014 in which I am the second author. Marie Barberon did most of the experiments illustrated in the paper but I contributed to several experiments, as described hereafter: I confirmed the localization of IRT1 at the outer polar domain at the PM in non-iron metals depleted conditions (Fig. 8A and C), I also performed imaging of FYVE1-mCit in response to Wm treatment (Fig. 10D and E), and I eventually imaged and quantified the FM4-64 uptake for wild-type and 35S::FYVE1 plants (Fig. 13D and E) to evaluate the possible impact of FYVE1 on general endocytosis. Furthermore, I wrote an addendum to this paper published in the journal Communicative and Integrative Biology (CIB) in 2015 to further discuss about the close parallel between mammals and plants in polarity of transporters to ensure proper uptake of nutrients. The PNAS and CIB articles are presented in two chapters of the third part of this thesis.

Part III

Polarity and dynamics of IRT1 mediate plant metal homeostasis

Chapter 1

Polarization of IRON-REGULATED TRANSPORTER 1 (IRT1) to the plant-soil interface plays crucial role in metal homeostasis

Marie Barberon[1], Guillaume Dubeaux[2], Cornelia Kolb[3], Erika Isono[3], Enric Zelazny[2], and Grégory Vert[2][4]

Keywords: *Arabidopsis*, Transport, Iron, Metals, Endocytosis, Polarity

[1]Department of Plant Molecular Biology, Biophore Building, UNIL-Sorge, Université de Lausanne, 1015-Lausanne, Switzerland

[2]Institut des Sciences du Végétal, Centre National de la Recherche Scientifique - Unité Propre de Recherche 2355, Avenue de la Terrasse Bâtiment 23A, 91190 Gif-sur-Yvette, France

[3]Department of Plant Systems Biology, Technische Universität München, 85354 Freising, Germany

[4]Correspondence should be addressed to G.V: Grégory.Vert@isv.cnrs-gif.fr

1   Abstract

In plants, the controlled absorption of soil nutrients by root epidermal cells is critical for growth and development. IRT1 is the main root transporter taking up iron from the soil, and is also the main entry route in plants for potentially toxic metals such as manganese, zinc, cobalt, and cadmium. Previous work demonstrated that the IRT1 protein localizes to early endosomes/*trans*-Golgi network (EE/TGN) and is constitutively endocytosed through a monoubiquitin- and clathrin-dependent mechanism. Here we show that the availability of secondary non-iron metal substrates of IRT1 (Zn, Mn and Co) controls the localization of IRT1 between the outer polar domain of the plasma membrane and EE/TGN in root epidermal cells. We also identify FYVE1, a phosphatidylinositol-3-phosphate (PI3P)-binding protein recruited to late endosomes (LE), as an important regulator of IRT1-dependent metal transport and metal homeostasis in plants. FYVE1 controls IRT1 recycling to the plasma membrane and impacts the polar delivery of this transporter to the outer plasma membrane domain. This work establishes a functional link between the dynamics and the lateral polarity of IRT1 and the transport of its substrates, and identifies a molecular mechanism driving polar localization of a cell surface protein in plants.

Significance Statement Plants take up iron from the soil using a broad spectrum transporter named IRT1. IRT1 mediates influx of potentially toxic elements such as manganese, zinc, cobalt and cadmium. We uncovered that the localization at the cell surface of IRT1 is directly controlled by its secondary toxic substrates. When these metals are found at low levels in soils, IRT1 is located at the plasma membrane in a polar fashion to face the soil. We identified a lipid-binding protein recruited to endosomes that controls the dynamics and the polarity of IRT1, and that plays an important role in the radial transport of metals. Altogether, our work points to an unexpected mode of radial transport of iron towards vascular tissues involving efflux transporters.

2 Introduction

Iron is an essential element for virtually all organisms because it plays critical roles in life-sustaining processes (Kobayashi and Nishizawa, 2012). Iron's ability to gain and lose electrons makes iron a cofactor of choice for enzymes involved in a wide variety of oxidation-reduction reactions, such as photosynthesis, respiration, hormone synthesis, and DNA synthesis. This essential role of iron is highlighted by the severe disorders triggered by iron deficiency, including anemia in mammals or chlorosis in plants (Kobayashi and Nishizawa, 2012). Although abundant in nature, iron is often available in limited amounts to plants because it is mostly found in rather insoluble Fe(III) complexes in soils (Kobayashi and Nishizawa, 2012). The IRON-REGULATED TRANSPORTER 1 (IRT1) root iron transporter from the model plant *Arabidopsis thaliana* takes up iron from the soil upon iron deficiency (Vert et al., 2002). IRT1 is a major player in the regulation of plant iron homeostasis, as attested by the severe chlorosis and lethality of an *irt1-1* knockout mutant (Vert et al., 2002). Consistently, *IRT1* gene is highly expressed in iron-starved root epidermal cells which face the rhizosphere (Vert et al., 2002). The resultant IRT1-dependent iron absorption allows proper growth and development under iron-limited conditions. Despite its absolute requirement, iron reacts in cells with oxygen and generates noxious reactive oxygen species that are deleterious for plant growth and development (Thomine and Vert, 2013). Cellular and whole-organism iron homeostasis must therefore be strictly balanced. Moreover IRT1 also participates in the absorption of manganese, zinc, cobalt and industrial pollutants such as cadmium and nickel (Eide et al., 1996; Korshunova et al., 1999; Nishida et al., 2011; Rogers et al., 2000; Vert et al., 2001). As such, IRT1 is the main entry route for such potentially toxic metals in iron-starved plants and in the food chain. Intricate regulatory networks control plant responses to low iron conditions, and more specifically *IRT1* gene expression. Several transcription factors directly binding to the *IRT1* promoter in root epidermal cells have been identified and control its inducibility by low iron conditions (Colangelo and Guerinot, 2004; Jakoby et al., 2004; Yuan et al., 2005; Wang et al., 2013). Other pathways including the cytokinin-mediated root growth control and the stress hormone ethylene impinge on iron uptake by converging at the level of the IRT1 promoter (Séguéla et al., 2008; Lingam et al., 2011). The integration of these regulatory networks aims at providing enough iron to sustain growth and avoid detrimental effects of iron overload. Recently, a post-translational control of IRT1 protein by ubiquitination was identified (Kerkeb et al., 2008; Barberon et al., 2011). IRT1 protein was shown to localize to Early Endosomes/trans-Golgi Network compartments (EE/TGN) as a result of monoubiquitin- and clathrin-dependent endocytosis, and is targeted to the vacuole for degradation via late endosomes (LE) (Barberon et al., 2011). The ubiquitin-mediated endocytosis of IRT1 is mediated by the IDF1 RING E3 ligase (Shin et al., 2013). IRT1 localization and ubiquitination however appeared to be unaffected by the availability of its primary substrate iron (Barberon et al., 2011), raising the question of the biological relevance of such post-translational control of IRT1. In the present study we show that the availability in secondary non-iron metal substrates of IRT1 (i.e. Zn, Mn and Co) controls its localization between the outer polar domain of the plasma membrane and EE/TGN in root epidermal cells. We identified a previously uncharacterized

phosphatidylinositol-3-phosphate (PI3P)-binding protein recruited to LE, FYVE1, as an important regulator of IRT1-dependent metal transport and metal homeostasis. FYVE1 controls IRT1 recycling to the plasma membrane and impacts the polar delivery of this transporter to the outer plasma membrane domain. This work establishes a functional link between the dynamics and the lateral polarity of IRT1 and the transport of its substrates, and identifies a molecular mechanism driving outer polar localization of a cell surface protein in plants.

3   Results and discussion

The root iron transporter IRT1 undergoes Ub-dependent endocytosis, although this process is not regulated by the availability in iron, its primary substrate (Barberon et al., 2011). To get further insight into the mechanisms driving IRT1 localization in EE/TGN, we tested the influence of the secondary metal substrates of IRT1 by immunolocalization using anti-IRT1 specific antibodies on plants constitutively expressing *IRT1*. Although IRT1 localized under standard conditions to intracellular vesicles that we previously characterized as EE/TGN (Barberon et al., 2011), depletion of non-iron metal substrates of IRT1 led to its accumulation at the cell surface of root hairs (Fig. 8A). The EE/TGN identity was not altered by non-iron metal deficiency since known EE/TGN markers failed to relocalize to the cell-surface under such growth conditions in differentiated root cells where *IRT1* is expressed (Fig. 9A) (Dettmer et al., 2006; Geldner et al., 2009). These observations highlight the ability of potentially toxic non-iron metals transported by IRT1 to specifically trigger its intracellular dynamics between the cell surface and EE/TGN. The non-ubiquitinatable $IRT1_{K154RK179R}$ was found at the cell surface in the presence of metals, as previously reported (Barberon et al., 2011), providing genetic evidence that the response to the secondary substrates of IRT1 is likely mediated by Ub-mediated endocytosis (Fig. 8A). Metal-dependent endocytosis appears as a protective mechanism to limit the absorption of the secondary substrates of IRT1. Indeed, depletion of Mn for example from the medium alleviates the deleterious consequences of $IRT1_{K154RK179R}$ expression (Fig. 8B). Under iron limitation where *IRT1* is strongly expressed, non-iron metals are readily available for transport by IRT1 and are heavily accumulated (Vert et al., 2002). In contrast, iron is not efficiently taken up due to its low level and the necessity of reduction by the FRO2 reductase whose activity is limiting for iron transport (Connolly et al., 2003). Taken together, these observations point to the existence of multiple layers of regulation for *IRT1* gene expression by metals. Iron indeed controls *IRT1* transcription while its secondary non-iron metal substrates act at the post-transcriptional level, as observed for Zn (Connolly et al., 2002), and at the post-translational level on the dynamics of IRT1 protein.

We also monitored IRT1 localization in response to metals in root epidermal cells. Interestingly, IRT1 accumulated under metal-depleted conditions at the outer polar domain of the plasma membrane facing the rhizosphere (Fig. 8C). Quantification of IRT1 fluorescence, represented as the fluorescence profile across root epidermal cells (Fig. 9B) or as the ratio between outer and inner plasma membrane fluorescence intensities (Fig. 8D), show a clear enrichment of IRT1 in the outer plasma membrane domain. Lateral polarity in plant roots was described first in rice for the As/Si transporters Lsi1, Lsi2 (Ma et al., 2007) and in *Arabidopsis* for the boron transporter BOR4 (Miwa et al., 2007). Then an increasing number of transporters were demonstrated to be laterally polarized in *Arabidopsis* roots such PDR8/PEN3, BOR1, NIP5;1, PIS1/PDR9/ABCG37, and NRT2.4 (Strader and Bartel, 2009; Langowski et al., 2010; Alassimone et al., 2010; Takano et al., 2010; Kiba et al., 2012). However, the molecular mechanisms controlling lateral polarity are still unclear. To shed light on the mechanisms controlling IRT1 metal-dependent dynamics and its localization at the outer plasma membrane domain of root epi-
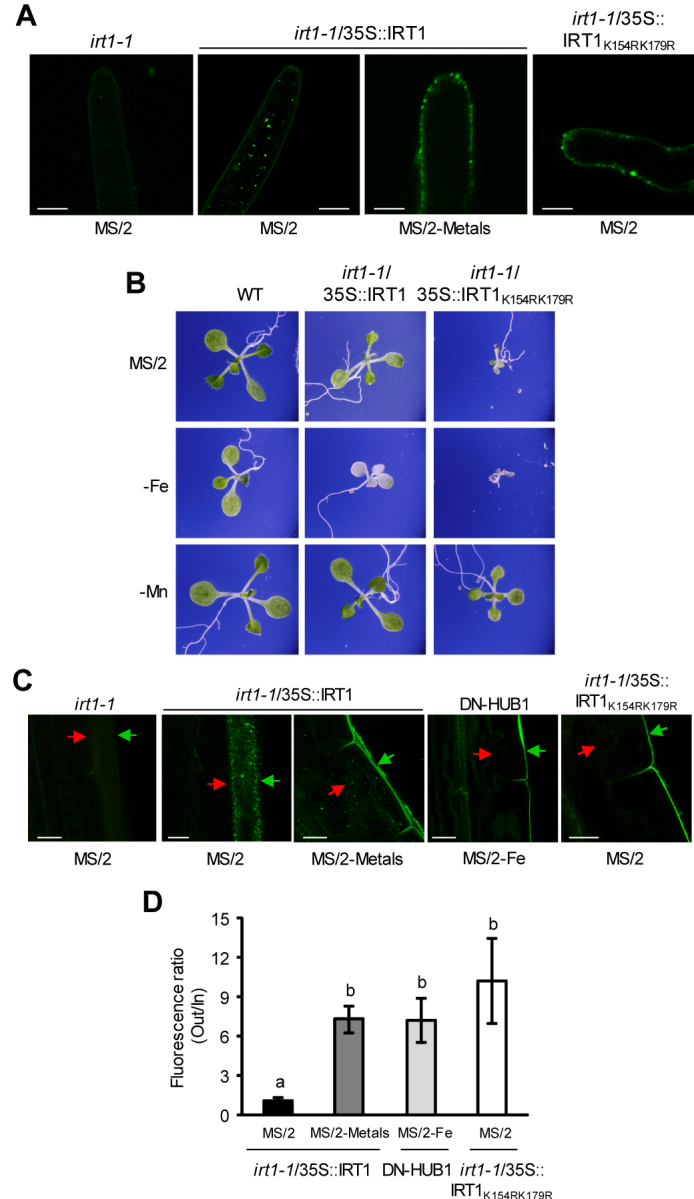
Figure 8 – **IRT1 localization to the outer polar domain in low metal conditions.** (A) IRT1 immunolocalization with anti-IRT1 antibodies on root hair cells of *irt1-1*, *irt1-1*/35S::IRT1, and *irt1-1*/35S::IRT1$_{K154RK179R}$ plants grown 7 days in different metal conditions. MS/2 refers to standard plant growth medium containing metals. Metal depleted conditions correspond to combined absence of Zn, Mn, and Co. Scale bar, 10μm. (B) Phenotype of wild-type, *irt1-1*/35S::IRT1 and *irt1-1*/35S::IRT1$_{K154RK179R}$ plants grown on standard medium (MS/2), iron-(-Fe) and manganese-depleted media (-Mn). (C) IRT1 immunolocalization with anti-IRT1 antibodies on root epidermal cells of *irt1-1*, *irt1-1*/35S::IRT1, tamoxifen-induced DN-HUB1, and *irt1-1*/35S::IRT1$_{K154RK179R}$ plants grown 7 days in different metal conditions. DN-HUB1 plants express an inducible dominant-negative clathrin HUB and are defective in CME. Scale bar, 10μm. Red and green arrows mark the inner and outer plasma membrane domains of root epidermal cells (PM$_{in}$ and PM$_{out}$) used for quantification of polarity profiles (Fig. 9B). (D) Quantification of the outer/inner polarity ratios in root epidermal cells. Data represents the mean ±SE (n=10). Different letters indicate means that were statistically different by one-way ANOVA and Tukey's multiple testing method (P < 0.05). Ratio = 1 indicates apolar plasma membrane localization, or non-plasma membrane localization in the case of wild-type plants, ratio < 1 indicates inner localization and ratio >1 indicates outer localization.

61
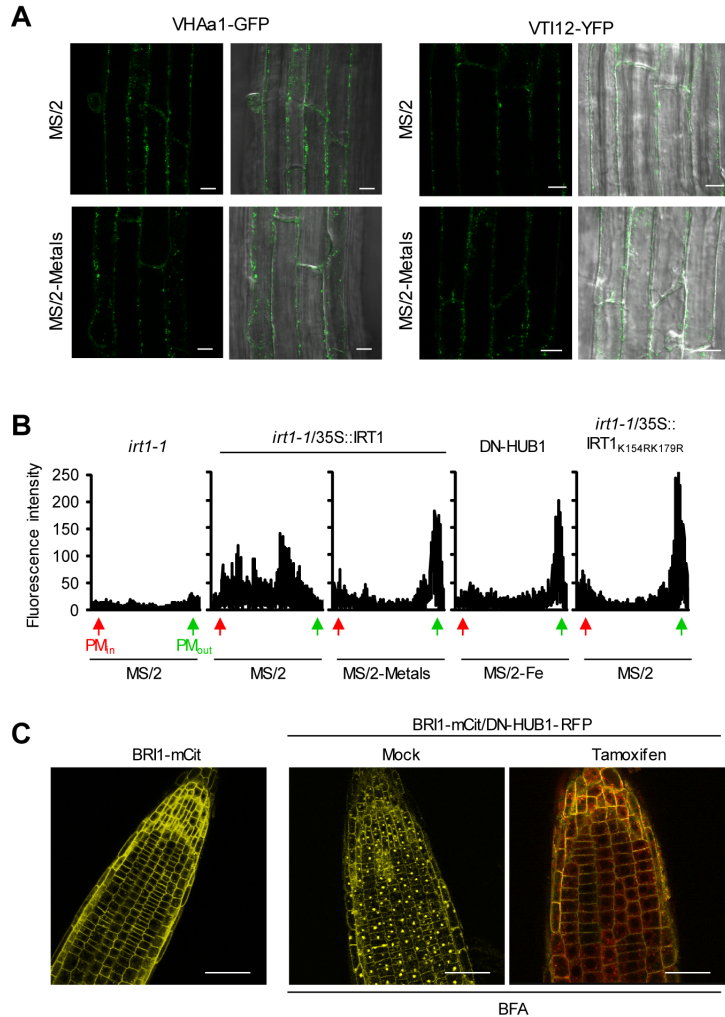
Figure 9 – **Metal-dependent dynamics and polar localization of IRT1.** (A) Confocal microscopy imaging of the EE/TGN markers VTI12-YFP and VHAa1-GFP in differentiated root cells of plants grown in control or metal-depleted conditions. Scale bar, 10μm. (B) Quantification of polarity profiles across epidermal cells (Fig. 8C). Data represent the best fitted curve corresponding to independent immunofluorescence experiments (n=10). (C) Confocal imaging of BRI1-mCitrine and BRI1-mCitrine/DN-HUB1-RFP. DN-HUB1 is induced by tamoxifen treatment prior to BFA application. The overlay between the yellow (BRI1-mCitrine) and red (DN-HUB1-RFP) channels is shown. Scale bar, 30μm.

dermal cells, we investigated the localization of the non-ubiquitinatable $IRT1_{K154RK179R}$ mutant version. $IRT1_{K154RK179R}$ localized to the outer polar domain in the presence of metals, similar to what is observed with wild-type IRT1 under non-iron metal depleted conditions (Fig. 8C and D; Fig. 9B). We previously demonstrated that IRT1 accumulates at the cell-surface in root hair cells when clathrin-mediated endocytosis (CME) is impaired (Barberon et al., 2011). Inhibition of CME in root epidermal cells, due to tamoxifen-inducible expression of a dominant-negative clathrin form, led to the redistribution of IRT1 at the outer plasma membrane domain (Fig.

8C and D; Fig. 9B). The same DN-HUB1 line prevented the accumulation of the BRI1 steroid hormone receptor in endosomal aggregates triggered by the fungal toxin brefeldin A (BFA) upon induction, ensuring that DN-HUB1 effectively inhibited CME (Fig. 9C). These results indicate that the presence of IRT1 in the outer plasma membrane polar domain is established independently of IRT1 ubiquitination and CME.

To identify factors involved in the control of IRT1 localization, we performed a yeast-two-hybrid screen using the hydrophilic cytosolic loop of IRT1 as bait. This screen identified several clones of an uncharacterized FYVE domain-containing protein named FYVE1 (Fig. 10A) (van Leeuwen et al., 2004). Expression analyses confirmed that *FYVE1* transcripts are found in roots, similar to *IRT1*, although not regulated by iron starvation (Fig. 11A). To further confirm the protein-protein interaction between FYVE1 and IRT1, we first generated transgenic plants expressing *FYVE1-mCitrine* in the wild-type background. Using anti-GFP antibodies, FYVE1-mCitrine was immunoprecipitated from wild-type or FYVE1-mCitrine iron-deficient plants where IRT1 is expressed. The presence of IRT1 was only observed in immunoprecipitates from FYVE1-mCitrine (Fig. 10B), attesting that both proteins are able to interact *in vivo*.

FYVE domains have been reported to recognize PI3P, leading to recruitment of FYVE domain-containing proteins to EE and LE (Burd and Emr, 1998; Gaullier et al., 1998; Gaullier et al., 2000; Vermeer et al., 2006). To assess whether FYVE1 binds to PI3P, we performed lipid overlay analyses using in vitro-transcribed/translated FYVE1-FLAG. FYVE1 interacted with PI3P, in agreement with previous reports on FYVE domain-containing proteins, as well as other acidic phospholipids although to a lesser extent (Fig. 10C). Confocal microscopy imaging of FYVE1-mCitrine showed that FYVE1 protein is found in the nucleus, the cytosol and in intracellular vesicles that may correspond to LE in root tip cells (Fig. 11B) as well as in differentiated root cells (Fig. 10D), although more difficult to visualize due to the large central vacuole. We further investigated FYVE1 localization in differentiated epidermal cells where IRT1 is expressed, as well as in root tip cells since they allow easy visualization of intracellular compartments, are readily accessible to drug and dye treatments and have been extensively characterized (Jaillais and Gaude, 2007). The recruitment of FYVE1 to LE was confirmed by its sensitivity to the inhibitor of PI3-kinase Wortmannin, which creates homotypic fusion and swelling of LE (Fig. 10E; Fig. 11C) (Jaillais et al., 2006). Consistently, FYVE1-mCitrine showed colocalization with the LE marker RabF2a (Fig. 10F and H; Fig. 11D and F) and the PI3P-recruited and LE-localized 2xFYVE$_{HRS}$ (Fig. 10G and H; Fig. 11E and F). Altogether those results demonstrate that IRT1 interacts with the LE-recruited and PI3P-binding protein FYVE1.

To functionally characterize FYVE1, we isolated the publicly available pst18264 RIKEN insertion line hereafter named *fyve1-1*. This line carries the DS transposon in the first exon of the *FYVE1* gene. We repeatedly failed to identify homozygous *fyve1-1* knock-out mutants in the progeny of *fyve1-1* heterozygous plants, suggesting that the corresponding mutation is likely lethal at the homozygous state. Consistently, *fyve1-1* segregating mutants produced about 26% of seeds that failed to germinate, corresponding to the ratio expected for plants segregating a recessive mutation impairing germination (Tab. 1). Genetic complementation of *fyve1-1*
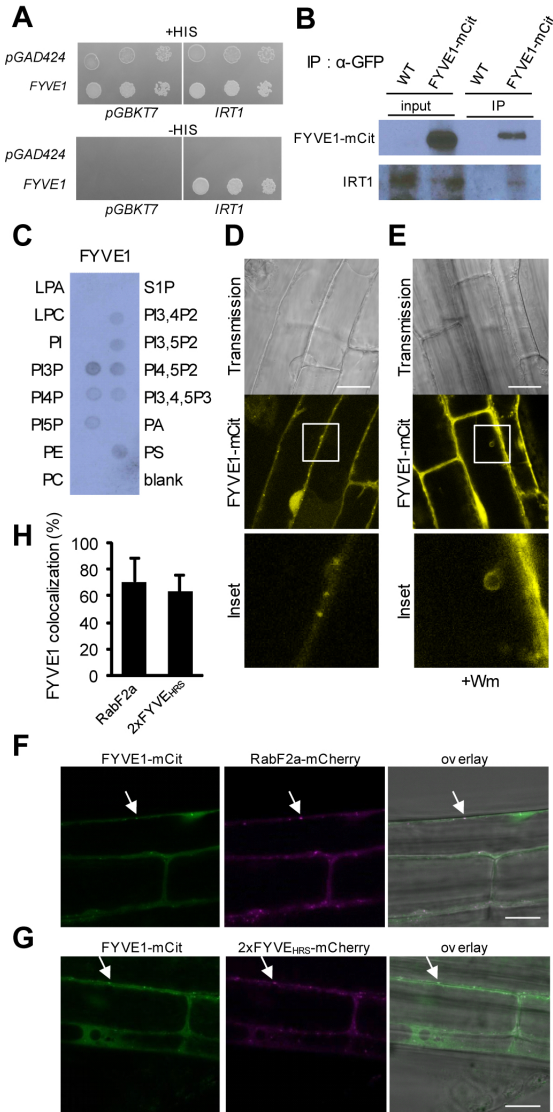
Figure 10 – FYVE1 interacts with IRT1 and PI3P and is recruited to late endosomes. (A) Yeast two hybrid screening using IRT1 as bait identified FYVE1. The interaction is revealed by the activation of *HIS3* transcription and growth on -HIS medium. (B) Co-immunoprecipitation analyses between FYVE1-mCitrine and IRT1 in iron-deficient roots. (C) Lipid binding assays of in vitro transcribed/translated FYVE1 protein. LPA, lysophosphatidic acic; LPC, lysophosphatidylcholine; PI, phosphatidylinositol; PI3P, PI-3-phosphate; PI4P, PI-4-phosphate; PI5P, PI-5-phosphate; PE, phosphatidylethanolamine; PC, phosphatidylcholine; S1P, sphingosine-1-phosphate; PI3,4P2, PI-3,4-bisphosphate; PI3,5P2, PI-3,5-bisphosphate; PI4,5P2, PI-4,5-bisphosphate; PI3,4,5P3, PI-3,4,5-triphosphate; PA, phosphatidic acid; PS, phosphatidylserine. (D) Localization of FYVE1-mCitrine fusion protein in differentiated root cells. Scale bar, 10μm. (E) Sensitivity of FYVE1-mCitrine trafficking to Wortmannin (Wm) in differentiated root cells. Scale bar, 10μm. (F-G) Colocalization of FYVE-mCitrine with the late endosomal marker RabF2a-mCherry (F) and 2xFYVE$_{HRS}$-mCherry (G) in differentiated root cells. Arrows show an example of colocalization. Scale bar, 10μm. (H) Quantification of FYVE1 colocalization with the late endosomal markers RabF2a and 2xFYVE$_{HRS}$. Colocalization of punctate structures was quantified in 10 cells from the F1 progeny from crosses between parental lines FYVE1-mCitrine and marker lines RabF2a and 2xFYVE$_{HRS}$. Data represents the mean $\pm$SE.
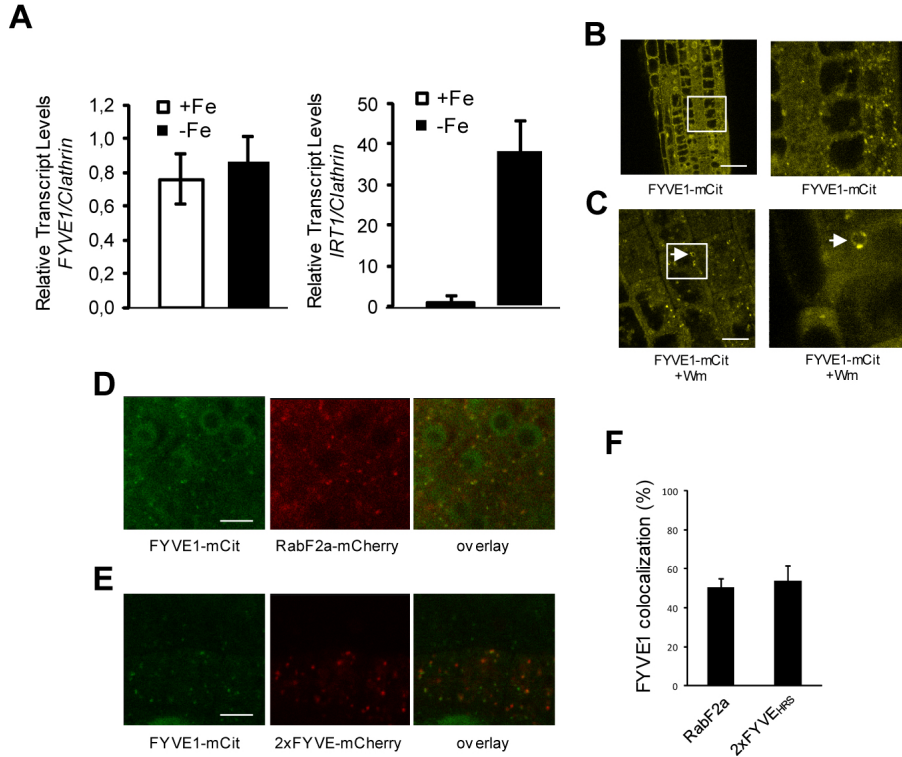
Figure 11 – Characterization of FYVE1 localization. (A) Quantitative RT-PCR analyses monitoring *FYVE1* (left panel) and *IRT1* (right panel) expression in roots of wild-type plants. Experiments were performed using 10-d-old plants transferred for 3 d in iron-sufficient (+Fe) or iron-deficient (-Fe) conditions. Results are presented as mean ±SD from 3 to 4 batches of 30 seedlings. (B) Confocal microscopy imaging of FYVE1-mCitrine plants in root tip cells. Scale bar, 25μm. The inset is shown on the right panel. (C) Sensitivity of FYVE1-mCitrine trafficking to Wortmannin (Wm) in root tip cells. Arrows show an example of a wortmannin compartment. Scale bar, 10μm. The inset is shown on the right panel. (D-E) Colocalization of FYVE-mCitrine with the late endosomal marker RabF2a-mCherry (D) and 2xFYVE$_{HRS}$-mCherry (E) in root tip cells. Scale bar, 5μm. (F) Quantification of FYVE1 colocalization with the late endosomal markers RabF2a and 2xFYVE$_{HRS}$. Colocalization of punctate structures was quantified in 10 cells from the F1 progeny from crosses between parental lines FYVE1-mCitrine and marker lines RabF2a and 2xFYVE$_{HRS}$. Results are presented as mean ±SE.

was carried out by crossing heterozygous *fyve1-1* mutant with a monoinsertional segregating line constitutively expressing Ubi10::FYVE1. The progeny now only showed 6.9% of seeds that failed to germinate, matching the expected segregation of 6.25% for plants carrying the homozygous *fyve1-1* mutation and that do not possess transgenic *FYVE1* (Tab. 1). Homozygous *fyve1-1* mutants carrying Ubi10::FYVE1 were also recovered in the progeny (Fig. 13A), further highlighting the genetic complementation of *fyve1-1* by *FYVE1*. Overall, this clearly demonstrates that the loss-of-function mutation in the *FYVE1* gene is the direct cause of *fyve1-1* lethality. Since the onset of IRT1 expression is at 3 days after germination, we cannot use *fyve1-1* to address the biological role of FYVE1 in iron homeostasis. We therefore generated transgenic plants constitutively expressing *FYVE1* under the control of the strong 35S promoter, leading to overaccumulation of *FYVE1* transcripts in transgenic plants (Fig. 13B). Such plants showed no phenotype when grown in the presence of iron in the medium (Fig. 12A and B). When
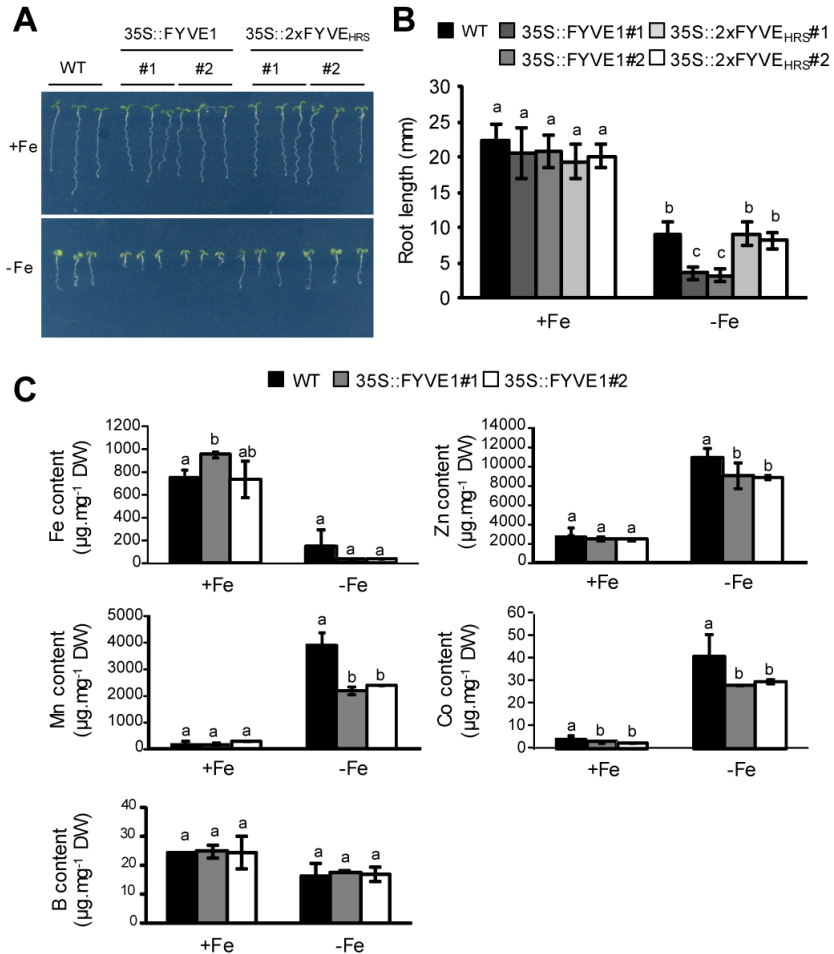
Figure 12 – *FYVE1* overexpression leads to iron deficiency and impaired transport of IRT1 substrates. (A) Phenotype of wild-type (WT), two independent 35S:FYVE1 and two independent 35S::2xFYVE$_{HRS}$ transgenic lines grown 5 days in +Fe (upper panel) or in -Fe (bottom panel). (B) Root length of 5-old-day wild-type (WT), 35S::FYVE1 and 35S::2xFYVE$_{HRS}$ grown in + or -Fe. Results are presented as mean ±SD (n=20). Statistical differences were calculated by one-way ANOVA. Different letters indicate means that were statistically different by Tukey?s multiple testing method (P < 0.05). (C) Metal content determined by ICP-MS on roots of 7-day old plants grown in + or -Fe. Results are presented as mean ±SD from 3 to 4 batches of 30 seedlings. Statistical differences were calculated by one-way ANOVA. Different letters indicate means that were statistically different by Tukey's multiple testing method (P < 0.05) for genotypes within a given growth condition (+Fe or -Fe).

grown on iron-depleted media, 35S::FYVE1 plants displayed shorter roots than wild-type (Fig. 12A and B), a hallmark of iron-deficient plants. The hypersensitivity of 35S::FYVE1 plants to low iron conditions is abolished when plants are grown on medium containing Wortmannin (Fig. 13C), indicating that PI3P is necessary for the role of FYVE1 in iron homeostasis. Plants overexpressing the well-established PI3P-binding 2xFYVE$_{HRS}$ reporter showed wild-type sensitivity to low iron, attesting the specific involvement of FYVE1 in plant responses to low iron (Fig. 12A and B) (Vermeer et al., 2006). To further evaluate the biological role of FYVE1 in
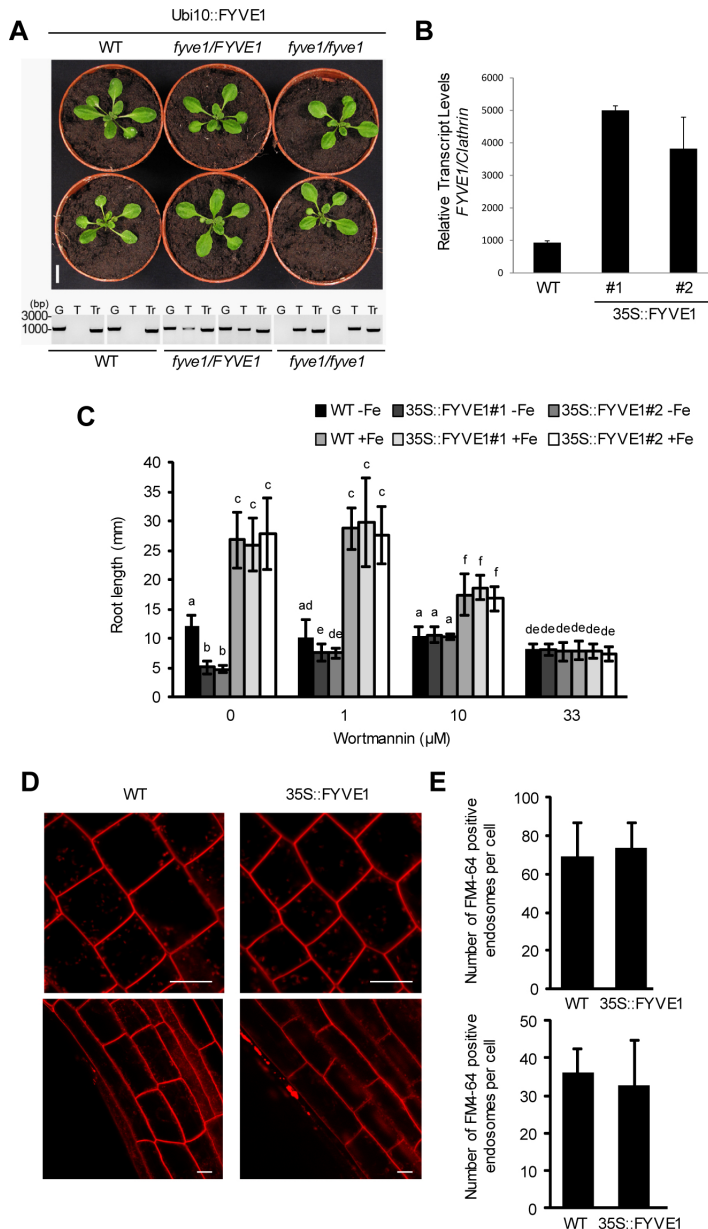
Figure 13 – Genetic characterization of $FYVE1$. (A) Phenotype of 3-week-old wild type (WT), heterozygous *fyve1/FYVE1* and homozygous *fyve1/fyve1* carrying Ubi10::FYVE1 transgene (upper panel). The genotypes of the photographed plants were verified by PCR-based genotyping (lower panel). Genotyping was performed for the endogenous gene (G), for the T-DNA (T) and for the transgene (Tr). (B) Quantitative RT-PCR analyses monitoring *FYVE1* (left) and *IRT1* (right) expression in roots of wild-type and two 35S::FYVE1 independent transgenic lines. Experiments were performed using 10-d-old plants grown in MS/2. Results are presented as mean ±SD from 3 to 4 batches of 30 seedlings. (C) Root length of 7-old-day wild-type (WT) and two independent transgenic lines of 35S:FYVE1 grown in +Fe or ?Fe conditions with various concentrations of Wortmannin. Results are presented as mean ±SD (n?8). Different letters indicate means that were statistically different by one-way ANOVA and Tukey's multiple testing method (P < 0.05). (D) FM4-64 internalization assays. 7-day-old wild-type and 35S::FYVE1 plants were treated with FM4-64, rinsed and imaged every 5 minutes after treatment. Representative images of FM4-64 signals obtained in root tip cells (upper panel) and differentiated root cells (bottom panel) after twenty five minutes are shown. Scale bar, 10μm. (E) Quantification of FM4-64 internalization on root tip cells (top) and differentiated root cells (bottom). Results are represented as mean ±SE (n=10).

67

Parental genotype	Germinated(%)	Ungerminated(%)	n	χ^2	p-value
WT	97.7	2.3	176		
fyve1/FYVE1	70.9	29.1	617	2.628	0.019*
fyve1/FYVE1 Ubi10::FYVE1 +/-	91.8	9.2	455	2.634	0.011*
fyve1/FYVE1 (corrected)	73.2	26.8	617	0.390	0.373
fyve1/FYVE1 Ubi10::FYVE1 +/- (corrected)	93.1	6.9	455	0.037	0.729

Table 1 – *fyve1-1* germination phenotype and genetic complementation. Segregation of the progeny phenotypes (germinated:ungerminated) were corrected for the germination defect of wild-type (WT) Nossen ecotype and evaluated with the chi-square goodness-of-fit test by using 3:1 segregation as a null hypothesis for *fyve1* and 15:1 segregation as a null hypothesis for *fyve1* Ubi10::FYVE1. Chi-square values (χ^2) and corresponding p-value are indicated. * indicates significant difference (P < 0.05).

metal homeostasis, we determined the metal content of both wild-type and 35S::FYVE1 plants by Inductively-Coupled Plasma Mass Spectrometry (ICP-MS). Under metal replete conditions, both wild-type and 35S::FYVE1 plants showed comparable metal accumulation profile (Fig. 12C). When grown in the absence of iron, however, 35S::FYVE1 roots accumulated slightly less Fe and showed significantly reduced levels of non-iron IRT1 substrates. As a control, we monitored accumulation of boron that is not transported by IRT1 and observed no difference between the two genotypes (Fig. 12C).

The fact that 35S::FYVE1 showed hypersensitivity to low iron growth conditions and reduced accumulation of metals transported by IRT1 prompted us to investigate *IRT1* expression in both wild-type and 35S::FYVE1 plants. *FYVE1*-overexpressing plants accumulated wild-type levels of IRT1 protein (Fig. 14A), indicating that the phenotypes displayed by 35S::FYVE1 plants are not explained by lower accumulation of IRT1 transporter. We then analyzed IRT1 protein localization by immunolocalization to highlight possible defects in IRT1 localization. Wild-type plants grown in the absence of iron showed strong accumulation of IRT1 in EE/TGN, as previously reported (Barberon et al., 2011), while FYVE1-overexpressors readily accumulated IRT1 at the plasma membrane in a non-polar fashion (Fig. 14B). The ratio of plasma membrane fluorescence intensity out/in is 1 for both genotypes (Fig. 14C), although corresponding to intracellular EE/TGN and apolar plasma membrane localization respectively. However, quantification of fluorescence profiles across root epidermal cells clearly argues for IRT1 accumulating at the plasma membrane in a non-polar fashion in 35S::FYVE1 plants (Fig. 14B). *FYVE1* overexpression therefore affects IRT1 localization between the plasma membrane and EE/TGN as well as its polarity on the plasma membrane. The presence of IRT1 at the cell-surface in 35S::FYVE1 transgenic plants is not explained by a defect in general endocytosis since both wild-type and 35S::FYVE1 show comparable internalization of the endocytic tracer FM4-64 in both root tip and differentiated cells (Fig. 13D and E). Taken together, these observations suggest that FYVE1 acts more on the recycling of IRT1 from endosomal compartments back to the plasma membrane.

The polar localization of PIN proteins at the apico-basal domain of root cells requires clearance from the PM by endocytosis involving clathrin (Dhonukshe et al., 2007; Kitakura et al., 2011), retargeting to and retention at the polar domain (Kleine-Vehn and Friml, 2008; Kleine-Vehn et al., 2011). Similarly, possible tyrosine-based motives have been involved in the lateral
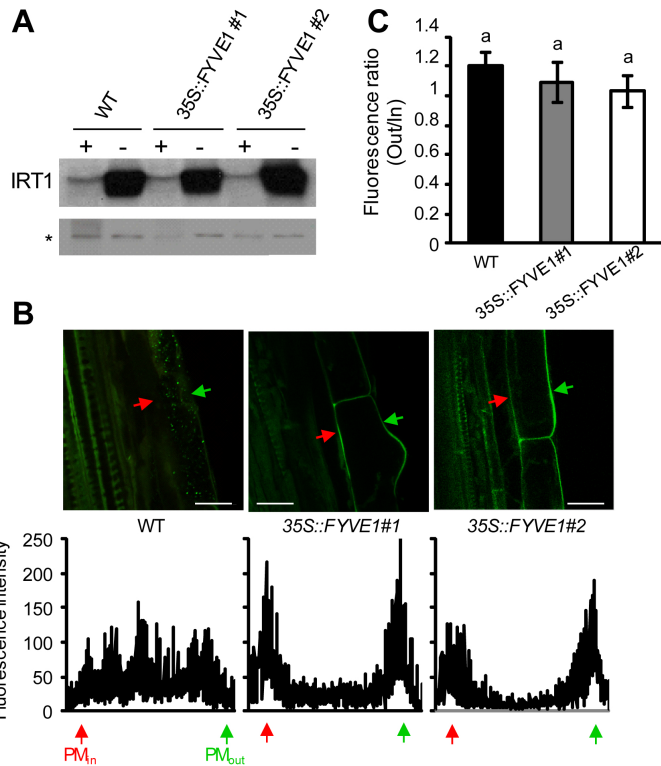
Figure 14 – *FYVE1* overexpression leads to apolar IRT1 accumulation at the cell surface. (A) IRT1 protein accumulation in roots of 7-day-old wild-type (WT) and 35S::FYVE1 independent transgenic lines grown in presence (+) or in absence (-) of Fe. Total protein were extracted and analyzed by western bolt with anti-IRT1 antibodies. (B) IRT1 immunolocalization with anti-IRT1 antibodies, in differentiated roots of wild-type (WT) and 35S::FYVE1 plants grown in Fe deficient conditions. Scale bar, 10μm. Red and green arrows mark the inner and outer plasma membrane domains of root epidermal cells (PM_{in} and PM_{out}), respectively. Quantification of polarity profiles across corresponding epidermal cells is shown below each panel and represents the best fitted curve from independent immunofluorescence experiments (n=10). (C) Quantification of the outer/inner polarity ratios in differentiated root epidermal cells. Data represents the mean $\pm$SE (n=10). Statistical differences were calculated by one-way ANOVA. Different letters indicate means that were statistically different by Tukey's multiple testing method (P < 0.05). Ratio = 1 indicates apolar localization or non-plasma membrane localization in the case of wild-type plants, ratio < 1 indicates inner localization and ratio >1 indicates outer localization.

polarity of BOR1, suggesting a role for endocytosis dependent on clathrin in this process (Takano et al., 2010). CME appears not to be required for IRT1 polarization, as evidence by the lateral polarity of IRT1 in DN-HUB1 transgenic plants (Fig. 8C and D; Fig. 9B). Our work rather points to role for the LE-recruited PI3P-binding FYVE1 protein in the recycling of IRT1 from endosomal compartments. Although the ability of LE to function in recycling have been debated in the recent years (Niemes et al., 2010; Viotti et al., 2010), the presence of vacuolar sorting receptors (Tse et al., 2004) and retromer subunits (Oliviusson et al., 2006) in LE suggest a function as a recycling compartment (Foresti and Denecke, 2008; Jaillais et al., 2008; Otegui and Spitzer, 2008). Overexpression of *FYVE1* may therefore misroute IRT1 beyond the outer polar plasma membrane domain on its way back to the cell surface.

We previously reported that IRT1 mis-localization at the plasma membrane, resulting from

impaired ubiquitination of IRT1, leads to severe growth defects and oxidative stress due to metal toxicity (Barberon et al., 2011). In this particular case, IRT1$_{K154RK179R}$ showed lateral polarity, as observed for endogenous IRT1 protein (Fig. 8C and D; Fig. 9B). We now observe that the apolar presence of IRT1 at the cell surface leads to metal deficiency (Fig. 12, Fig. 14B and C). A possible explanation is that, although accumulating at the plasma membrane in 35S::FYVE1, IRT1 has decreased transport activity. Impaired metal transport may for example result from IRT1 being localized to different membrane subdomains in 35S::FYVE1, or lacking a partner or post-translational modification required for full transport activity. Alternatively, a tantalizing hypothesis is that the polarity of IRT1 is critical for proper radial transport of metal in the root. We demonstrated that the vast majority of iron is taken up by root epidermal cells (Vert et al., 2002). Whether iron is transported from epidermal cells to underlying cortical cells symplasmically using cell-cell connections called plasmodesmata or via efflux transporters remains elusive. Our observations showing that IRT1 polarity is critical for iron and metal homeostasis suggest that these metals exit root epidermal cells using efflux transporters rather than the symplasmic route. The loss of polarity would result in IRT1 working against such efflux transporter, leading to radial transport defects within the root and thus impaired metal accumulation. This is supported by several studies based on dye-coupling approaches showing that differentiated root epidermal and root hair cells of several plant species including *Arabidopsis thaliana* are symplasmically isolated from neighboring cells (Erwee and Goodwin, 1985; Duckett et al., 1994). Although one can argue that dyes used in these studies may have a larger radius than many hydrated ions, most highly-reactive metals appear to be chelated to various organic molecules (i.e. nicotianamine, citrate) and metallochaperones in the cell (Puig and Peñarrubia, 2009; Kobayashi and Nishizawa, 2012). Altogether, the lack of symplasmic transport between epidermal and underlying cortical cells, associated to the specific requirement for a polar localization of IRT1 strongly suggest that iron and metals transported by IRT1 exits epidermal cells using efflux transporters. Homologs of mammalian metal efflux transporters from the IREG/ferroportin family have already been described in *Arabidopsis* and play a role in metal homeostasis (Schaaf et al., 2006; Morrissey et al., 2009). Whether such proteins play a role in iron and metal exit from epidermal cells will have to be addressed in the future.

In plants, the necessity of a functional interface between the root and the soil is obvious, but virtually nothing is defined. Here, we demonstrated that the localization of the IRT1 root iron transporter is dynamically controlled between the EE/TGN and the cell surface by its potentially toxic secondary substrates to avoid non-iron metal toxicity. In addition, we identified a novel endosomal-recruited protein controlling not only the localization but also the polarity of IRT1, and thus establishing the functional link between lateral polarity of a transporter and transport of its substrate. Finally, our work also opens the door to a better understanding on the establishment of polarity for other proteins targeted to the outer plasma membrane domain and acting as nutrient and hormone transporters or mediators of pathogen defense (Ma et al., 2007; Miwa et al., 2007; Strader and Bartel, 2009; Langowski et al., 2010; Takano et al., 2010; Kiba et al., 2012).

Name	Use	Sequence (5' to 3')
FYVE1 F	Construct	GGGAGCTCATGCAACAGGGAGATTACAATTCG
FYVE1 R	Construct	GCGGATCCTCAATGTGCGCTAACGAGGAAAGG
FYVE1attB1	Construct	GGGGACAAGTTTGTACAAAAAAGCAGGCTGGGCCATGCA
FYVE1attB2	Construct	GGGGACCACTTTGTACAAGAAAGCTGGGTCATGTGCGCTA
qFYVE1 F	qRT-PCR	CGTCTGGTTTGAGGGAAGGAT
qFYVE1 R	qRT-PCR	CGGGTAGGAAGATCAATGTGC
IRT1 F	qRT-PCR	CGGTTGGACTTCTAAATGC
IRT1 R	qRT-PCR	CGATAATCGACATTCCACCG
Clathrin F	qRT-PCR	AGCATACACTGCGTGCAAAG
Clathrin R	qRT-PCR	TCGCCTGTGTCACATATCTC
EI511	Genotyping	GCGACATCACTAAACCC
EI512	Genotyping	AACCCAC CAACATAAGAAC
Ds5-2a	Genotyping	TCCGTTCCGTTTTCGTTTTTTAC
CK150	Genotyping	GGACGATCCATTAGCTTTT
EI2	Genotyping	GGGGACCACTTTGTACAAGAAAGCTGGGT

Table 2 – List of primers used in this article.

4 Methods

4.1 Materials and growth conditions

Wild-type and the various transgenic lines used in this study were grown in sterile conditions on vertical plates at 21°C with 16-h light/8-h dark cycles, as previously described (Séguéla et al., 2008). For expression analyses, plants were cultivated in the conditions described above for 7 d and then transferred on iron-sufficient (50 μM Fe-EDTA) or iron-deficient (300 μM Ferrozine [3-(2-pyridyl)-5,6-diphenyl-1,2,4-triazine sulfonate], a strong iron chelator) medium for an additional 3 d. For immunolocalization studies, iron starvation was applied by directly germinating seeds on half-strength Murashige and Skoog (MS) medium lacking exogenous iron to preserve root integrity. All reagents were purchased from Sigma-Aldrich. The *irt1-1*, *irt1-1*/35S::IRT1, *irt1-1*/35S::IRT1$_{K154RK179R}$, dominant negative clathrin hub DN-HUB1, RabF2a-mCherry, 2xFYVE$_{HRS}$-mCherry, 2xFYVE$_{HRS}$, BRI1-mCitrine, VHAa1-GFP and VTI112-YFP lines were described in previous studies (Vert et al., 2002; Barberon et al., 2011; Dettmer et al., 2006; Geldner et al., 2009; Vermeer et al., 2006; Dhonukshe et al., 2007; Jaillais et al., 2011; Simon et al., 2014). The *fyve1-1* insertion mutant (pst18264, Nossen ecotype) was isolated from the RIKEN collection. Genotyping of *fyve1-1* was carried out with the primers listed in the Table 2. The *FYVE1* open reading frame was cloned into pCHF3 binary vector under the control of 35S promoter, or recombined by multisite Gateway technology to generate Ubi10::FYVE1-mCitrine in the pB7m34GW binary vector. For lipid binding assays, FYVE1 was recombined in pTnT GW-HF, a gateway compatible in vitro transcription/translation vector carrying a FLAG tag (Nito et al., 2013).

4.2   Yeast Two-Hybrid Screen

A fragment of the *IRT1* cDNA, encoding the cytosolic loop of IRT1 (amino acids 146-194), was cloned into the pGBKT7 vector (Clontech) and transformed in the AH109 yeast strain, as described previously (Barberon et al., 2011). The resulting yeast cells were then transformed with plasmid DNAs derived from the CD4-10 *Arabidopsis* cDNA library prepared with roots and shoots of 4-week-old plants. Approximately 106 transformants were screened for activation of the HIS3 and LacZ reporters. Positive clones were sequenced, and interesting candidates in which GAL4AD was in frame with the corresponding cDNA were rescued. Candidate clones isolated from the screen were then individually retransformed in yeast cells expressing GALDB alone or the GAL4DB-IRT1 prey fusion for confirmation.

4.3   Lipid overlay assays

Lipid binding assays were performed using PIP Strips (Echelon). PIP strips were blocked in 1x TBS, 0.1% Tween 20, and 5% fatty acid free BSA and then incubated overnight at 4°C in vitro transcribed/translated FYVE1-FLAG using reticulocytes (Promega). Next, the PIP strips were washed with 1x TBS, 0.1% Tween 20, incubated with anti-FLAG antibodies (1:2000 in blocking solution) for 1 h at room temperature, washed with 1xTBS, 0.1% Tween 20, and then incubated with anti-rabbit HRP secondary antibodies (1:1000) for 1 h at room temperature. Finally, the PIP strips were washed with 1x TBS, 0.1% Tween 20 before developing with enhanced chemiluminescent reagent.

4.4   Immunolocalization

Whole-mount Immunolocalization experiments were performed as described (Barberon et al., 2011).

4.5   Imaging

FM4-64 (Invitrogen) was applied at a concentration of 5 μM; Cycloheximide (Sigma-Aldrich) was applied at a concentration of 100 μM for 1 hour prior to treatment with BFA; BFA and Wortmannin (Sigma-Aldrich) were applied at a concentration of 50 μM and 33 μM for 1 hour in liquid medium, respectively. Imaging was performed on an inverted Leica SP2 and Zeiss 700 confocal microscopes. The percentage of FYVE1-mCitrine dotted structures showing overlap with RabF2a-mCherry or 2xFYVE$_{HRS}$-mCherry was manually determined. Induction of DN-HUB1 was performed with 2μM 2-hydroxytamoxifen for 24 hours. For polarity profiles epidermal cell width was normalized and fluorescence intensity determined across cells with ImageJ. Intensity values as a function of distance were plotted for each experiment, and the moving average applied to the scatterplot. The ratios between outer (PM$_{out}$) and inner (PM$_{in}$) plasma membrane domains were determined with ImageJ. For FM4-64 internalization assays, z-stacks encompassing

the whole cell volume were acquired every 5 minutes until internalization is observed. Three independent experiments obtained 25 minutes after FM4-64 addition were analyzed using ImageJ. To better visualize the endosomes, images were treated with the Difference of Gaussian filter and the number of FM4-64-positive endosomes in a cell was quantified on the treated images using the 3D Object Counter plugin of ImageJ.

4.6 Elemental analyses

Tissues were desorbed by washing for 10 min with 2 mM CaSO4 and 10 mM EDTA and then rinsed for 5 min with deionized water. Samples were dried at 80°C for 2 d. For mineralization, tissues were digested completely (1?3 h) in 70% (vol/vol) HNO3 at 120°C. Elemental analyses were performed by ICP-MS.

4.7 RNA Extraction and Real-Time Quantitative PCR

Total RNA was extracted using TRIzol reagent (Invitrogen) and purified using the RNeasy MinElute Cleanup Kit (Qiagen) after DNase treatment (Qiagen). The integrity of DNA-free RNA was verified by agarose gel electrophoresis, and an equal amount of total RNA (2 μg) was used for RT with anchored oligo(dT23). Real-time PCR was performed exactly as previously described (Séguéla et al., 2008), using gene-specific and control primers. The experiments were done in three biological replicates, with each containing two technical replicates.

4.8 Protein Extraction and Western Blot Analysis

Western blot analyses of IRT1 were performed on total proteins exactly as previously described (Séguéla et al., 2008; Barberon et al., 2011). Immunodetection of mCitrine was performed using the same protocol, but using the HRP-coupled GFP antibodies (Miltenyi Biotech).

4.9 Immunoprecipitation

Roots of plants cultivated in the conditions described above were subjected to immunoprecipitation as previously described (Jaillais et al., 2011), and following manufacturer's instruction (Miltenyi Biotech).

5 Acknowledgements

Chapter 2

Addendum: Getting to the root of plant iron uptake and cell-cell transport - polarity matters!

Guillaume Dubeaux[1], Enric Zelazny[12] and Grégory Vert[12]

---

[1]Institut des Sciences du Végétal, Unité Propre de Recherche 2355, Centre National de la Recherche Scientifique, Saclay Plant Sciences, Avenue de la Terrasse, 91190 Gif-sur-Yvette, France

[2]Correspondence to: Enric.Zelazny@isv.cnrs-gif.fr, Gregory.Vert@isv.cnrs-gif.fr

1   Abstract

Plasma membrane proteins play pivotal roles in mediating responses to endogenous and environmental cues. Regulation of membrane protein levels and establishment of polarity are fundamental for many cellular processes. In plants, IRON-REGULATED TRANSPORTER 1 (IRT1) is the major root iron transporter but is also responsible for the absorption of other divalent metals such as manganese, zinc and cobalt. We recently uncovered that IRT1 is polarly localized to the outer plasma membrane domain of plant root epidermal cells upon depletion of its secondary metal substrates. The endosome-recruited FYVE1 protein interacts with IRT1 in the endocytic pathway and plays a crucial role in the establishment of IRT1 polarity, likely through its recycling to the cell surface. Our work sheds light on the mechanisms of radial transport of nutrients across the different cell types of plant roots towards the vascular tissues and raises interesting parallel with iron transport in mammals.

2   Discussion

Because plants are fixed to a specific location, they have to constantly monitor and quickly respond to environmental changes. In particular, nutrient uptake must be tightly controlled to optimize plant growth and development to nutrient availability in soils. This is achieved in part by a tight regulation of transporter levels at the cell surface. In addition, many nutrient transporters driving the uptake of nutrient from the soil are polarly localized in root epidermal cells and enriched in the outer plasma membrane domain facing the soil. Lateral polarity of plasma membrane transporters has been previously demonstrated in rice for the Low silicon rice 1 (Lsi1) silicon influx channel and the Low silicon rice 2 (Lsi2) silicon exporter localized at the outer and the inner polar domain of the plasma membrane, respectively (Ma et al., 2006; Ma et al., 2007). The radial transport of boron across the root of the model plant *Arabidopsis thaliana* involves the boric acid channel NIP5;1, which is laterally polarized at the outer domain of the plasma membrane of root epidermal cells, and the borate efflux transporter BOR1 localized at the inner polar domain of root cells (Takano et al., 2010). Such lateral polarity is believed to be important for the radial transport of nutrients across cells found between the root epidermis and the vascular tissues, although no clear demonstration currently exists in the literature. Recently, we identified the mechanisms driving the dynamics and the polarity of IRON-REGULATED TRANSPORTER 1 (IRT1), a metal iron transporter involved in iron acquisition from the soil and that also transports highly reactive metal substrates such as Zinc (Zn), Manganese (Mn), Cobalt (Co) and Cadmium (Cd) (Rogers et al., 2000; Vert et al., 2001; Vert et al., 2002). IRT1 is found at the outer polar plasma membrane domain of root epidermal cells, but exclusively when plants are grown in the absence of its secondary metal substrates (Fig. 15A) (Barberon et al., 2014).

In the presence of such metals, IRT1 undergoes internalization from the plasma membrane into early endosomes/*trans*-Golgi network (EE/TGN) (Fig. 15B) (Barberon et al., 2011; Barberon et al., 2014). IRT1 ubiquitin-mediated endocytosis requires monoubiquitination of two

cytosolic lysine residues and the IRT1 DEGRADATION FACTOR 1 (IDF1) RING-type E3 ubiquitin ligase (Barberon et al., 2011; Shin et al., 2013). This mechanism is crucial to limit the overaccumulation of noxious heavy metals through IRT1 and for the control of metal homeostasis (Barberon et al., 2011; Zelazny et al., 2011; Barberon et al., 2014), as plants expressing the non-ubiquitinatable $IRT1_{K154RK179R}$ form rapidly die of metal overload. In parallel, we identified the endosomal FYVE1 protein as an IRT1 partner *in vivo*. Interestingly, *Arabidopsis* plants overexpressing *FYVE1* accumulate IRT1 at the cell surface in an apolar fashion, making of FYVE1 an important regulator of IRT1 polarity and a great tool to investigate the role of transporter polarity in nutrient distribution (Fig. 15C) (Barberon et al., 2014). *FYVE1*-overexpressing plants show hypersensitivity to low iron content and decreased metal content, although harboring wild-type levels of IRT1 protein. Altogether, these observations point to a defect in the radial transport of metals associated with the loss of IRT1 polarity.

Once taken up by root epidermal cells through IRT1, iron has to travel through the root
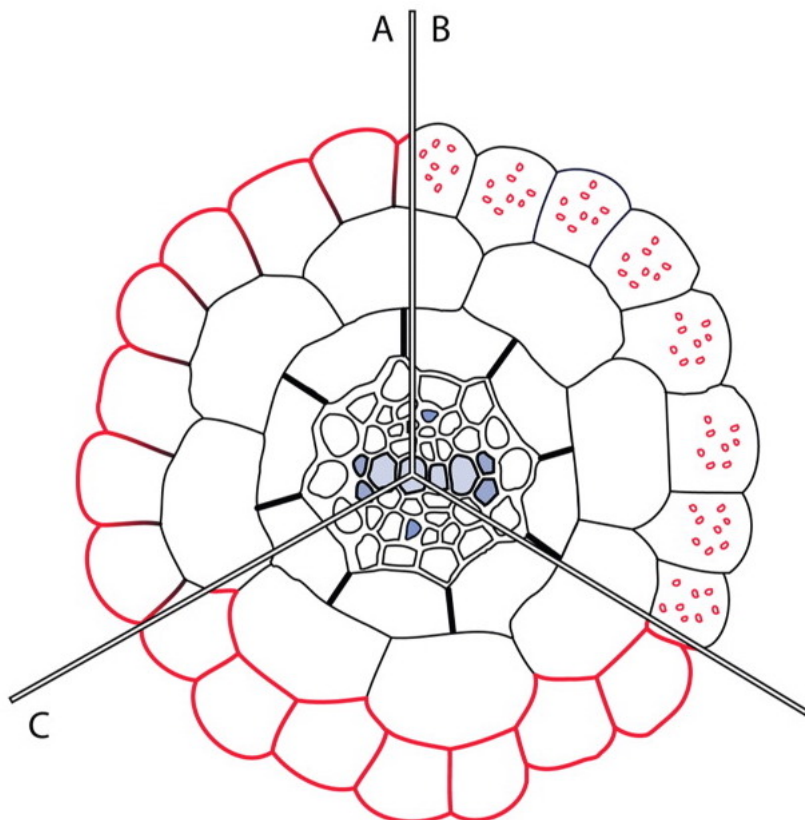
Figure 15 – **Trafficking and lateral polarity of IRT1 in plant root epidermal cells.** (A) *IRT1* (red) is expressed in root epidermal cells and localized at the outer polar domain of the plasma membrane when grown in the absence of its non-iron metal substrates, i.e. zinc, manganese and colbalt, or in standard conditions for the non-ubiquitinatable $IRT1_{K154K179R}$ mutant form. (B) IRT1 localizes to the early endosome/*trans*-Golgi network in standard growth conditions, i.e. in the presence of its secondary metal substrates Zn, Mn and Co. (C) IRT1 accumulates at the cell surface in an apolar fashion upon overexpression of endosomal FYVE1 protein.
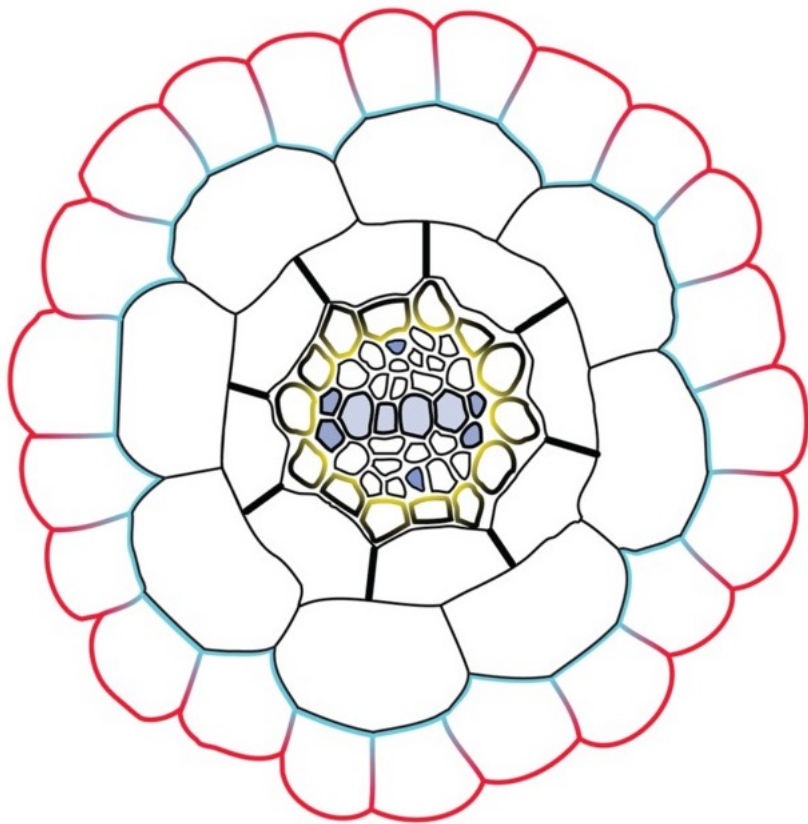
Figure 16 – Model of radial transport of iron in plant roots. In plants, iron absorption from the rhizosphere is mediated by IRT1 (red). A putative efflux transporter (blue) is likely located at the inner polar domain of the plasma membrane to allow iron exit from root epidermal cells.

cortex, the endodermis - including the Casparian strip, a physical barrier blocking the apoplastic flow - and the pericycle where it is released in the vasculature through the FERROPORTIN 1 (FPN1) (Morrissey et al., 2009). The fact that the loss of IRT1 polarity impairs the radial transport of iron and metals suggests that metals don't travel through the plant cell-cell communications called plasmodesmata. This idea is further supported by the loss of symplasmic connection between differentiated root epidermal cells, where IRT1 is expressed, and underlying cortical cells (Duckett et al., 1994). We can therefore hypothesize that efflux transporters polarized to the inner plasma membrane domain of root epidermal cells are required for the exit of iron from epidermal cells (Fig. 16). How iron and metals are then transported into underlying cortical cells remains an open question. Several multigenic families of metal transporters able to transport metal ions or metal-chelates are found in the *Arabidopsis* genome (Kobayashi and Nishizawa, 2012). Deciphering the identity of the metal transporters driving the radial movement of metals between the different root cell types represents a major challenge in our understanding of the physiology of plant nutrition. This will notably require a careful investigation of the expression territories and subcellular localization of these different metal transporters.

The mechanisms of iron nutrition in plants share similarities with the well-known absorption and transport of iron in mammals. In enterocytes, DIVALENT METAL TRANSPORTER 1 (DMT1) is the major iron influx transporter driving dietary iron absorption from the lumen of the duodenum (Anderson and Vulpe, 2009). DMT1 is polarized at the apical domain of the enterocyte (Anderson and Vulpe, 2009). Working in concert with DMT1, the efflux transporter FPN1 is localized to the basal plasma membrane domain of enterocytes and is responsible for iron secretion in the bloodstream (Donovan et al., 2000). Interestingly, DMT1 is also regulated by an ubiquitin-dependent mechanism. DMT1 ubiquitination involves WWP2, a HECT-type ubiquitin ligase of the Nedd4 family and Ndfip1/2, that constitute adaptors of this E3 ligase (Foot et al., 2008; Howitt et al., 2009). In contrast to animals that possess a single cell type to perform the influx of iron from the duodenum and efflux into the bloodstream, plants have several cell layers and probably many transporters at stake between the root epidermis and the vascular tissues. This greatly increases the complexity of iron transport and has greatly hampered our ability to decipher the precise molecular and physiological mechanisms of plant iron nutrition.

Our work opens new field of investigation on the establishment of lateral polarity of plasma membrane proteins and on the physiology of radial transport of nutrients in plant roots. Taking animals as a source of inspiration may be motivating but plant specificities, including numerous cell types to cross before reaching the vasculature and a polarized epithelia located deeper inside the root, must be obviously considered to fully grasp the mechanisms involved in plant nutrition.

3 Acknowledgements

Part IV

Integrated control of plant metal uptake

Substrate-dependent phosphorylation and K63 polyubiquitin-mediated endocytosis of IRON-REGULATED TRANSPORTER1 integrates plant metal nutrition.

Guillaume Dubeaux[1], Julie Neveu[1], Enric Zelazny[1] and Grégory Vert[1][2]

Keywords: ubiquitin, endocytosis, plant cell biology, metal nutrition, phosphorylation

[1]Institute for Integrative Biology of the Cell (I2BC), CNRS/CEA/Univ. Paris Sud, Université Paris-Saclay, 91198 Gif-sur-Yvette, France

[2]Correspondence should be addressed to G.V: Gregory.Vert@i2bc.paris-saclay.fr

1 Abstract

Plants take up iron from the soil using the IRON-REGULATED TRANSPORTER 1 (IRT1) iron transporter expressed in root epidermis, at the interface with the rhizosphere. Sophisticated transcriptional networks regulate the levels of the root iron uptake machinery, ensuring optimal absorption of iron which is essential for plant growth. Additional post-translational mechanisms controlling the levels of IRT1 in root epidermal cells and critical for proper metal homeostasis recently emerged. In *Arabidopsis thaliana*, IRT1 is indeed internalized from the cell surface to *trans*-Golgi Network/early endosomes (TGN/EE) following the multi-monoubiquitination of two lysine residues located in its large cytosolic loop. However, the molecular mechanisms driving the ubiquitin-mediated endocytosis of IRT1 and its biological relevance remains unclear. Here, we uncovered that IRT1 dynamics is controlled by the highly reactive secondary metal substrates aspecifically transported by IRT1 (zinc, manganese and cobalt). Increasing non-iron metal substrate availability triggers both an increase in the pool of ubiquitinated IRT1 and an extension of multi-monoubiquitination into lysine 63-linked polyubiquitin chains, leading to IRT1 degradation in the vacuole. This process is dependent on the IRT1-interacting E3 ubiquitin ligase IDF1. We also demonstrate that direct metal binding to a histidine-rich stretch and phosphorylation of IRT1 are required for the metal-dependent and K63 polyubiquitin-mediated degradation of IRT1 and proper plant responses to metal excess. Altogether, the transcriptional and post-translational regulations of *IRT1* by its different metal substrates are integrated to optimize iron uptake while limiting the transport of highly reactive and potentially harmful metals.

2 Introduction

Plants are fixed organisms that have to constantly monitor their outside environment and adjust their growth and development for survival (Vert and Chory, 2011). The acquisition of nutrients from the soil is absolutely essential for plant development. Among them, iron is of the utmost importance because of its ability to change redox states, making it an indispensable co-factor in electron transport chains and catalytic processes (Balk and Schaedler, 2014). This essential role of iron is highlighted by the severe disorders promoted by its deficiency such as anemia in mammals and chlorosis in plants (Briat et al., 2015). Despite its absolute necessity, iron is also noxious when present in excess since it reacts with oxygen further generating toxic reactive oxygen species (ROS) that interfere with proper plant development (Thomine and Vert, 2013). As such, iron homeostasis has to be tightly regulated within cells. Although abundant in nature, iron is often poorly available in soils because it is found in rather insoluble ferric complexes in soils (Brumbarova et al., 2014). Dicotyledonous plants, such as the model plant *Arabidopsis thaliana*, rely on a multistep iron uptake strategy involving rhizosphere acidification, reduction of iron and transport (Curie and Briat, 2003). Soil acidification results from the combined action of the AHA2 H^+-ATPase and secreted organic acids, and increases the solubility of ferric iron (Jin et al., 2007a; Santi and Schmidt, 2009; Schmid et al., 2014). Ferric iron is then reduced into ferrous iron by the root epidermis-expressed ferric chelate reductase FRO2 before uptake by the ferrous iron transporter IRT1 (Eide et al., 1996; Robinson et al., 1999; Vert et al., 2002). Iron is then radially distributed in the root using a coupled-transcellular pathway, at least between the epidermis and the cortex (Barberon et al., 2014), before reaching the vasculature. Loading of iron into the xylem sap and distribution to shoots requires the pericycle- and xylem parenchyma-localized FRD3 citrate effluxer (Green and Rogers, 2004).

Iron transport into root peripheral cells by IRT1 is critical for proper plant nutrition and establishment of iron homeostasis. An *irt1* loss-of-function mutant is severely chlorotic and dies early in development, unless fertilized with massive amounts of iron (Vert et al., 2002). To meet the plant demand in iron, the root iron uptake machinery is regulated at the transcriptional level by iron starvation. The activity of both *FRO2* and *IRT1* promoters is strongly and rapidly induced upon iron limitation by direct binding of the heterodimer between FIT and two subgroup Ib bHLH transcription factors (Colangelo and Guerinot, 2006; Yuan et al., 2008; Sivitz et al., 2012). The acquisition of iron from the soil is highly integrated at the level of *IRT1* transcription. *IRT1* expression is controlled diurnally (Vert et al., 2003). In addition, the circadian clock regulates the transcription and mRNA accumulation of each of these *IRT1*, *FER1* - which encodes a plant iron storage protein named ferritin - and *bHLH39* iron homeostasis genes (Hong et al., 2013). Iron status also affects the circadian period length, indicating that the iron homeostasis network is not only an output of the circadian clock but that iron status is a nutritional input that modulates the pace of the clock (Hong et al., 2013). A linear relationship between increased iron deficiency and period lengthening further suggests a finely tuned response mechanism (Salomé et al., 2013). This mechanism was not observed for copper, zinc or manganese implying that not all nutrients act as clock inputs (Chen et al., 2013; Salomé et al., 2013).

IRT1 is repressed at the transcriptional level by exogenous addition of cytokinins (CKs) or abscissic acid (ABA) (Séguéla et al., 2008). In contrast, upon ethylene signaling, direct interaction between EIN3/EIL1 and FIT led to an accumulation of the latter thereby increasing the expression level of *IRT1 in planta* (Lingam et al., 2011).

IRT1 served for many years as model to deconstruct the mechanisms driving iron deficiency responses in plants. More recently, IRT1 became one of the reference plant plasma membrane protein to study the intricate mechanisms of endocytosis and endosomal trafficking in plants and its interplay with plant nutrition (Barberon et al., 2011; Shin et al., 2013; Barberon et al., 2014; Ivanov et al., 2014). Multi-monoubiquitination was shown to control the internalization of IRT1 from the cell surface to the *trans*-Golgi network/early endosomes (TGN/EE) (Barberon et al., 2011). A non-ubiquitinatable IRT1 variant, in which two lysine residues (K159 and K174) are mutated in arginines, accumulates to the outer plasma membrane domain facing the soil, and yields uncontrolled metal uptake leading to plant death (Barberon et al., 2011). The IDF1 RING E3 ligase interacts with IRT1 and proposed to destabilize IRT1 protein in the cell (Shin et al., 2013). The ubiquitin-mediated endocytosis of IRT1 therefore appears as a crucial mechanism controlling the distribution of IRT1 in the cell by endocytosis and iron uptake. The FYVE1/FREE1 protein is recruited to late endosomes (LE) via phosphatidylinositol-3-phosphate binding, and was shown to directly interact with IRT1 and ubiquitin (Barberon et al., 2014; Gao et al., 2014). FYVE1/FREE1 is incorporated in the Endosomal Sorting Complex Required for Transport (ESCRT) complex (Gao et al., 2014), required for the sorting and the vacuolar targeting of endocytosed proteins (Hurley, 2008). Surprisingly, interference with *FYVE1/FREE1* expression leads to apolar localization of IRT1 at the plasma membrane and is associated with impaired radial transport of metals in the root. This greatly contrasts with the outer lateral polarity observed when ubiquitination or clathrin-mediated endocytosis are impaired (Barberon et al., 2014), and indicates that endosomal sorting of IRT1 is essential for its proper partitioning in the cell. Retrieval of IRT1 from endosomes and recycling to the cell surface also requires the SNX1 protein (Ivanov et al., 2014).

Neither the levels, nor the endocytosis of IRT1 are regulated by iron availability (Barberon et al., 2011), raising the question about the biological relevance of IRT1 ubiquitination. Although ubiquitin-mediated endocytosis of IRT1 may control constitutive turnover of the protein, it is very likely that this is regulated by a signal/stimulus to fine tune plant nutrition. IRT1 is a broad-spectrum divalent metal transporter, involved in the uptake of iron but also zinc, manganese, cobalt and cadmium (Eide et al., 1996; Korshunova et al., 1999; Rogers et al., 2000; Vert et al., 2001; Vert et al., 2002). As such, IRT1 is the main entry route for these highly reactive and potentially toxic metals in plants and in the food chain. The deficiencies in Zn, Mn and Co observed in *irt1* however do not contribute to its chlorosis and growth defects (Vert et al., 2002). This indicates that iron is the primary substrate of this transporter, and non-iron metals only secondary substrates resulting from its lack of selectivity. In the present study, we demonstrate that IRT1 undergoes ubiquitin-mediated endocytosis in response to excess of its non-iron metal substrates (i.e., Zn, Mn and Co). Whereas multi-monoubiquitination drives

IRT1 internalization from the cell surface to TGN/EE in a constitutive manner, non-iron metal excess triggers extension of these single ubiquitin moieties into K63 polyubiquitin chains in endosomes and vacuolar targeting of IRT1. This metal-dependent destabilization of IRT1 is mediated by the E3 ubiquitin ligase IDF1. We also provide biochemical and genetic evidence that non-iron metals are directly sensed by a histidine-rich stretch in IRT1 protein, triggering the phosphorylation and IDF1-mediated K63 polyubiquitination of IRT1 upon metal stress. Altogether the dual regulation of IRT1 at the transcriptional and post-translational levels by its different metal substrates are integrated to maximize iron uptake while limiting the absorption of highly reactive and potentially toxic non-iron metals.

3   Results

3.1   Generation of a functional fusion of IRT1 with a fluorescent protein

The subcellular localization of IRT1 protein in plant cells was previously investigated by immunofluorescence analyses in *Arabidopsis* roots using anti-IRT1 antibodies (Barberon et al., 2011; Barberon et al., 2014) or using transient expression of a translational IRT1 fusion with Green Fluorescent Protein (GFP) in tobacco (Vert et al., 2002; Ivanov et al., 2014). To obtain a better spatial and temporal resolution on IRT1 localization and dynamics in plant root cells, we generated a stable transgenic *Arabidopsis* line expressing IRT1 protein fused to the Yellow Fluorescent Protein variant mCitrine. The mCitrine (mCit) fluorescent tag was inserted at the N- or C-terminus of IRT1, and the corresponding IRT1-mCit fusion proteins were expressed under the control of *IRT1* promoter in the *irt1-1* loss-of-function mutant. *irt1-1* shows severe chlorosis due to impaired iron uptake from the soil unless watered with massive amount of iron (Vert et al., 2002). Neither N- nor C-terminal fusions of IRT1 to mCitrine appeared to be functional, as attested by the lack of complementation of *irt1-1* (data not shown). Insertion of the mCitrine in cytosolic and extracellular loops of IRT1 also yielded non-functional fusions, except when mCitrine was inserted between the predicted signal peptide and the first transmembrane domain of IRT1 protein (hereafter called IRT1-mCit) (Fig. 18A). The *IRT1* promoter drove *IRT1-mCit* expression in the root epidermis in response to iron deficiency, consistent with previous reports (Vert et al., 2002), including in peripheral cells from the meristem and in the lateral root cap (Fig. 18B).

3.2   Local metal availability regulates IRT1 subcellular localization

The metal transport spectrum of IRT1 is broad, and includes iron, manganese, zinc, cobalt and cadmium (Eide et al., 1996; Korshunova et al., 1999; Rogers et al., 2000; Vert et al., 2001; Vert et al., 2002). Among these metals, the primary substrate of IRT1 is iron, as attested by the sole complementation of *irt1-1* lethal phenotype by iron fertilization (Vert et al., 2002). Previous work suggested the existence of a post-translational regulation of IRT1 by non-iron metals such as Zn, Mn and Co that are secondary substrates of the transporter (Zelazny et al., 2011; Barberon et al., 2014). To get further insight into the regulation of IRT1 by its non-iron metal substrates, we grew *IRT1-mCit*-expressing plants on media lacking iron to activate the *IRT1* promoter, and containing different concentrations of all three metals combined. Under physiological non-iron metal provision found in half-strength Murashige and Skoog medium (Murashige and Skoog, 1962), IRT1-mCit protein is found at the plasma membrane in a polar manner and in intracellular vesicles (Fig. 17A), which likely correspond to TGN/EE where IRT1 was previously found by immunofluorescence (Barberon et al., 2011). When *IRT1-mCit*-expressing plants were grown in the combined absence of Zn, Mn and Co, IRT1-mCit mostly accumulated at the cell surface
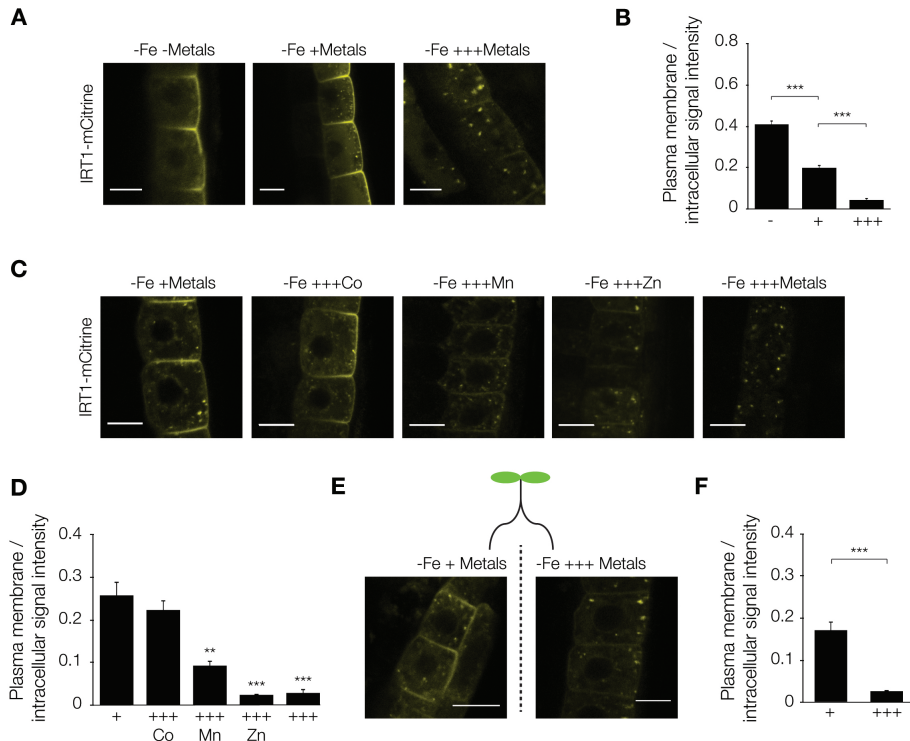
Figure 17 – **IRT1 trafficking is regulated by its non-iron substrates in a local environment**
(A) Confocal microscopy analyses of *irt1-1*/IRT1::IRT1-mCit plants grown in iron-deficient conditions with low levels of non-iron metal substrates of IRT1 (Zn, Mn, Co ; -Fe -Metals), physiological concentrations of non-iron metals (Zn, Mn, Co ; -Fe +Metals), or subjected to a 2d non-iron metal excess (Zn, Mn, Co ; -Fe +++Metals). Representative images are shown. Scale bars = 10 μm. (B) Quantification of plasma membrane and intracellular signal intensities of IRT1-mCit from experiments performed as in (A). Experiments were carried out in triplicates on stacks encompassing epidermal cells at the root tip. Error bars represent s.d. (n=18). The asterisks indicate significant differences (Mann-Whitney, P<0.0001). (C) Subcellular localization of *irt1-1*/IRT1::IRT1-mCit in response to 2d treatment with physiological concentrations of non-iron metals (-Fe +Metals), combined non-iron metal excess (-Fe +++Metals), or separate non-iron metal oversupply (-Fe +++Zn, Mn, or Co). Representative images are shown. Scale bars = 10 μm. (D) Ratio between plasma membrane and intracellular fluorescence signal intensities of *irt1-1*/IRT1::IRT1-mCit from experiments performed as in (C). Experiments were carried out in triplicates on stacks encompassing epidermal cells at the root tip. Error bars represent s.d. (n=18). The asterisks indicate significant differences (Mann-Whitney, P<0.0001) (E) Split-root experiments of *irt1-1*/IRT1::IRT1-mCit plants transferred for 2d to a plate with one half containing physiological concentrations of non-iron metals (-Fe +Metals) and one half containing non-iron metal excess (-Fe +++Metals). Representative images are shown. Scale bars = 10 μm. (F) Ratio between plasma membrane and intracellular fluorescence signal intensities of split-root-grown *irt1-1*/IRT1::IRT1-mCit plants as in (E). Experiments were carried out in triplicates on stacks encompassing epidermal cells at the root tip. Error bars represent s.d. (n=18). The asterisks indicate significant differences (Mann-Whitney, P<0.0001).

(Fig. 17A and B). To evaluate the influence of non-iron metal excess on IRT1-mCit localization, we transferred 10-day-old plants grown under standard metal conditions for 2 days in a medium containing a 10-fold excess of Zn, Mn and Co. These conditions triggered depletion of IRT1-mCit from the plasma membrane and accumulation in large intracellular vesicles (Fig. 17A and B). This metal-dependent change in localization is specific of IRT1-mCit since other root cell surface proteins, such as the boron transporter BOR4, failed to respond (Fig. 18C). To decipher the
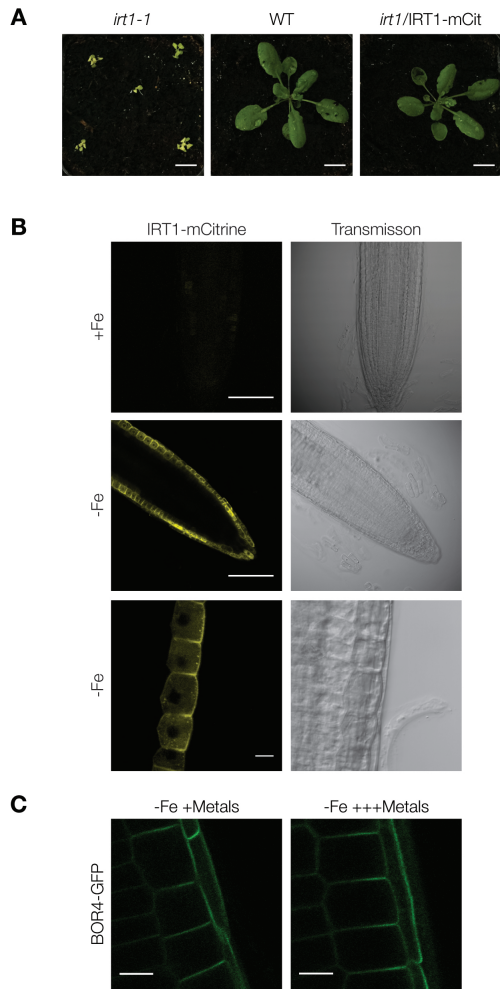
Figure 18 – Functional fusion of IRT1 with a fluorescent mCit tag. (A) Phenotypic analyses of *irt1-1* KO mutant, WS accession (WT) and *irt1-1*/IRT1::IRT1-mCit (*irt1-1*/IRT1-mCit). Scale bars = 1cm. (B) Confocal microscopy analyses of *irt1-1*/IRT1::IRT1-mCit (IRT1-mCit) grown for 12d in iron-sufficient or iron-deficient media. Scale bars (top and center) = 100 μm and scale bar (bottom) = 10 μm. (C) Confocal microscopy analyses of 35S::BOR4-GFP (Kasai et al., 2011) grown for 12d in iron-deficient media and transferred on iron-deficient with physiological (-Fe +Metals) or an excess of secondary substrates of IRT1 (-Fe +++Metals). Scale bars = 10 μm.

nature of the non-iron metal driving the change in IRT1-mCit localization, we added a ten-fold excess of Zn, Mn and Co separately. Both Zn and Mn excess triggered the depletion of IRT1-mCit from the cell surface and an accumulation in intracellular vesicles, whereas Co had very little effect at the concentrations used (Fig. 17C and D).

The transcriptional activation of *IRT1* gene expression by iron starvation responds to shoot-borne systemic starvation signals. Split-root experiments, where only half of the root system is subjected to iron deficiency, indeed revealed the ability of plants to express IRT1 in the iron-replete half of the root system (Vert et al., 2003). To investigate whether the signals triggering

the retrieval of IRT1 from the cell surface are of local or systemic nature, we carried out split-root approaches in which half of the root system was challenged with a combined excess of non-iron metal excess. Interestingly, IRT1 was depleted from the plasma membrane and accumulated in intracellular vesicles only in the half subjected to metal excess (Fig. 17E and F), indicating that IRT1 is locally regulated at the post-translational level by metals.

3.3   Non-iron metals change the fate of IRT1 protein

To evaluate the nature of the subcellular compartments associated with IRT1, we co-localized IRT1-mCit with several endocytic marker proteins upon various metal regimes. When plants were grown in the presence of physiological concentrations of non-iron metals, the intracellular pool of IRT1-mCit protein strongly co-localized with Vha-a1, a TGN/EE marker (Dettmer et al., 2006). Consistently, very little overlap was observed between IRT1-mCit and the RabF2a late endosomal marker (Fig. 19A and B) (Geldner et al., 2009). Two days of metal excess redistributed IRT1-mCit in the cell, with a decrease of the cell-surface and early endosomal pools of IRT1. Rather IRT1-mCit was mostly found associated with late endosomal compartments, as visualized by the strong overlap with RabF2a (Fig. 19A and B). The removal of IRT1 from the cell surface and the shift in IRT1 localization to the late endosomal compartments likely reflects a change into IRT1 degradative fate.

The metal-dependent change in IRT1 localization observed after 2 days of metal excess actually occurred within hours of high metal level exposure. A metal excess of a few hours was indeed sufficient to deplete IRT1 from the cell surface (Fig. 19C and D). To confirm that IRT1 is targeted to the vacuole upon metal excess, we took advantage of dark growth conditions that impair the lytic activity of the vacuole and allow visualization of vacuolar targeted fluorescent proteins (Tamura et al., 2003). Plants expressing IRT1-mCit grown under standard conditions showed weak vacuolar fluorescence after 4h of darkness, whereas plants subjected to non-iron metal excess displayed dramatically enhanced fluorescence in the vacuole traducing an increased degradation of the protein (Fig. 19C and D).

To better visualize the degradation of IRT1 upon metal stress, we sought to follow the accumulation of IRT1-mCit protein over time after transfer to metal excess by western blot. Since non-iron metals compete with iron for uptake by IRT1, they interfere with *IRT1* promoter activity (Fig. 20A). To avoid interference of non-iron metals with IRT1 levels, we generated transgenic plants expressing the functional IRT1-mCit fusion under the control of the strong and constitutive CaMV35S promoter in wild-type plants (Fig. 20B). Metal excess led to a rapid internalization and degradation of constitutively-expressed IRT1-mCit protein and degradation, as visualized by the drop in IRT1-mCit levels (Fig. 19E and G) with no change in *IRT1-mCit* mRNA (Fig. 20C).

A

B

C

D

E

F
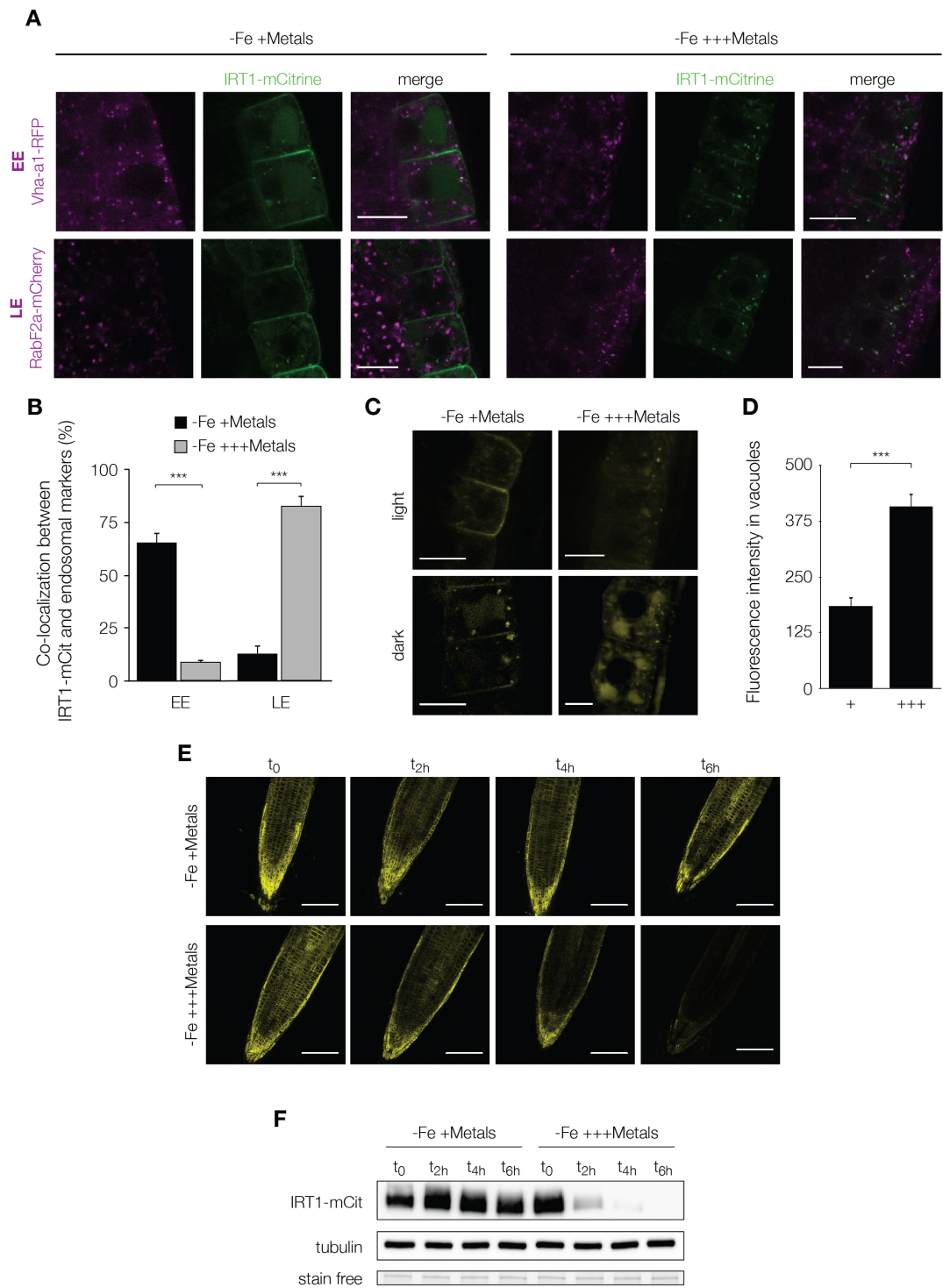
Figure 19 – IRT1 is degraded in response to its non-iron substrates. (Legend continued on next page.)

Figure 19 – IRT1 is degraded in response to its non-iron substrates (continued). (A) Co-localization between *irt1-1*/IRT1::IRT1-mCit and markers from the TGN/EE (Vha-a1-RFP) and LE (RabF2a-mCherry) after a transfer for 2d in physiological (-Fe + Metals) or non-iron metal excess conditions (-Fe +++Metals). Representative images are shown. Scale bars = 10μm. (B) Quantification of the co-localization between IRT1-mCit and endosomal markers from the same experiments as (A). The center of mass of each particle was used to determinate the percentage of coincidence. Experiments were carried out in triplicates on stacks encompassing epidermal cells at the root tip. Error bars represent s.d. (n=18). The asterisks indicate significant differences (Mann-Whitney, P<0.0001). (C) Sensitivity of *irt1-1*/IRT1::IRT1-mCit to dark growth conditions. Light grown seedlings were incubated in the dark for 4h in physiological (-Fe + Metals) or non-iron metal excess conditions (-Fe +++Metals) conditions. Representative images are shown. Scale bars = 10μm. (D) Vacuolar fluorescence intensity upon darkness treatment performed as in (C). Experiments were carried out in triplicates. Error bars represent s.d. (n=18). The asterisks indicate significant differences (Mann-Whitney, P<0.0001). (E) Confocal microscopy analyses of 35S::IRT1-mCit in response to physiological (-Fe +Metals) or to metal excess conditions (-Fe +++ Metals). Representative images are shown. Scale bars = 10μm. (F) Western-blot analyses on 35S::IRT1-Cit-expressing plants in response to (-Fe +Metals) or to non-iron metal excess conditions (-Fe +++ Metals) using anti-GFP and anti-tubulin antibodies.. Stain free staining was used as a supplemental control of charge. A representative blot is shown.

3.4 Metal-dependent ubiquitin-mediated endocytosis of IRT1 in response to metal excess

The ubiquitination of plant plasma membrane proteins has recently been shown to drive their endocytosis (Kasai et al., 2011; Barberon et al., 2011; Leitner et al., 2012; Barberon et al., 2014; Martins et al., 2015). More specifically, we previously demonstrated that IRT1 is ubiquitinated *in vivo* on two lysine residues (K154 and K179) and that IRT1 ubiquitination is not regulated by iron nutrition (Barberon et al., 2011). The metal-dependent endocytosis of IRT1 led us to investigate the influence of non-iron metal nutrition on IRT1 ubiquitination. To avoid interference of non-iron metal substrates on IRT1-mCit levels, we first used plants constitutively-expressing IRT1-mCit as described above. Immunoprecipitation of IRT1-mCit from plants grown in standard conditions or subjected to a 2-hour-metal excess were enriched for IRT1-mCit (Fig. 21A). When probed with the P4D1 general anti-ubiquitin antibodies, IRT1-mCit immunoprecipitates showed a high molecular weight smear that is typical of ubiquitinated proteins. However, the pool of ubiquitinated IRT1-mCit protein appeared more intense and larger after non-iron metal excess, indicating that metal stress triggers IRT1 ubiquitination (Fig. 21A). The same pattern was also observed using plants expressing *IRT1-mCit* driven by the *IRT1* promoter (Fig. 22B).

To investigate deeper the role of ubiquitination in IRT1 endocytosis, we generated transgenic lines expressing the non-ubiquitinatable IRT1$_{2KR}$ mutant version, carrying the K154R and K179R substitutions (previously called IRT1$_{K154RK179R}$; Barberon et al., 2011), fused to mCit in the *irt1-1* mutant background. Expression of IRT1$_{2KR}$-mCit complemented the chlorosis and growth defects of *irt1-1*, indicating that it is fully functional (Fig. 22A). IRT1$_{2KR}$-mCit protein was found at the plasma membrane upon standard conditions, consistent with previous results (Fig. 21B) (Barberon et al., 2011; Barberon et al., 2014). Interestingly, IRT1$_{2KR}$-mCit failed to be endocytosed upon metal excess (Fig. 21B and C), indicating that responses to non-iron metals requires ubiquitination of lysine residues K154 and K179. The loss of ubiquitination for several plant cargos has been associated with vacuolar targeting defects and forced recycling rather than impaired internalization from the cell surface (Kasai et al., 2011; Leitner et al., 2012; Martins
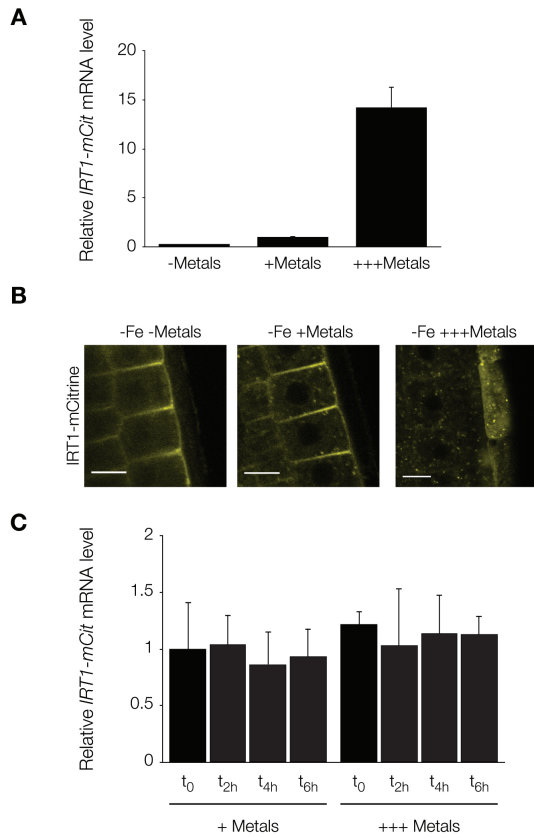
Figure 20 – **Generation of a constitutive Col0/35S::IRT1-mCit line.** (A) *IRT1-mCit* mRNA accumulation of *irt1-1*/IRT1::IRT1-mCitrine plants grown for 12d in iron-deficient conditions with ten-fold less non-iron substrates of the transporter (-Fe -Metals) or 10d in iron-deficient conditions (-Fe +Metals) subjected or not to a transfer in a medium containing a ten-fold increase of Zn, Mn and Co (-Fe +++Metals) for 2d. (B) Confocal microscopy analyses of Col0/35S::IRT1-mCit (IRT1-mCit) plants grown for 7d in iron-deficient conditions with ten-fold less non-iron substrates of the transporter (-Fe -Metals) or in iron-deficient conditions (-Fe +Metals) subjected or not to a transfer in a medium containing a ten-fold increase of Zn, Mn and Co (-Fe +++Metals) for 2h. Scale bars = $10\mu m$. (C) *IRT1-mCit* mRNA accumulation of Col0/35S::IRT1-mCit plants grown for 7d in iron-deficient conditions with ten-fold less non-iron substrates of the transporter (-Fe -Metals) or in iron-deficient conditions (-Fe +Metals) subjected or not to a transfer in a medium containing a ten-fold increase of Zn, Mn and Co (-Fe +++Metals) for 2h, 4h or 6h as described in Figures 2E and 2G. (D) Quantification of the signal intensity of images taken in Figure 2E.

et al., 2015). To decipher where ubiquitination and metals act on the endocytic trafficking of IRT1, plants expressing IRT1- or IRT1$_{2KR}$-mCit were treated with the fungal drug Brefeldin A (BFA), which creates an aggregation of endocytosed proteins in so-called BFA bodies, in the absence of *de novo* protein synthesis. While wild-type IRT1-mCit largely accumulated in BFA bodies, IRT1$_{2KR}$-mCit appeared completely insensitive to BFA indicating that ubiquitination of residues K154 and K179 is essential for retrieving IRT1 from the cell surface (Fig. 21D).
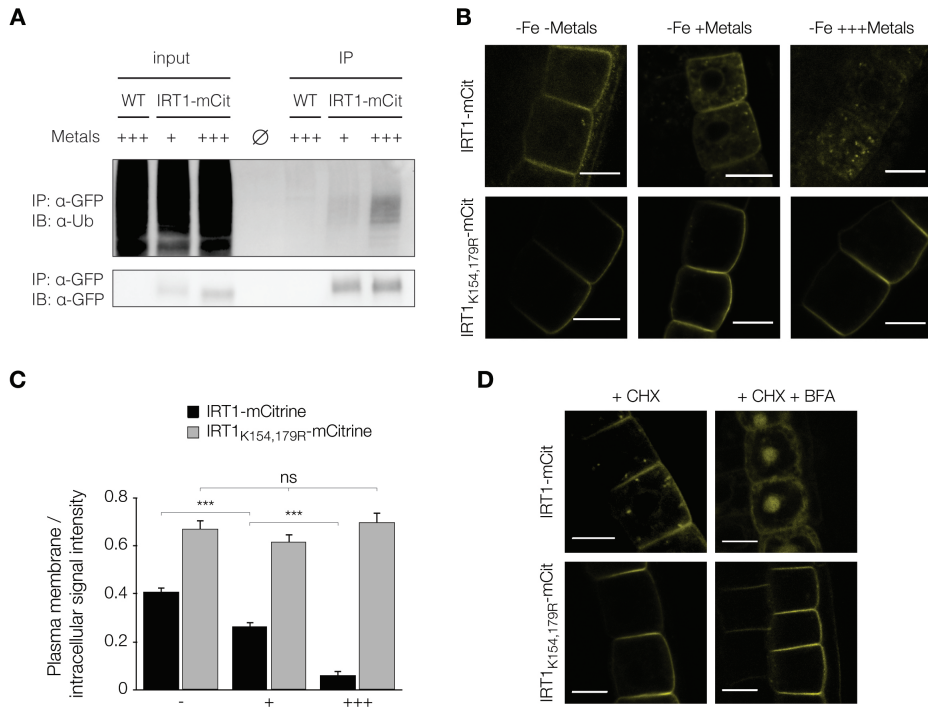
Figure 21 – IRT1 is ubiquitinated in response to metal excess and this regulation drives its endocytosis. (A) *In vivo* ubiquitination analyses of IRT1 in response to non-iron metals. Immunoprecipitation was performed using anti-GFP antibodies on solubilized protein extracts from wild-type and mono-insertional homozygous 35S::IRT1-mCit plants and subjected to immunoblotting with anti-Ub P4D1 (top) and anti-GFP (bottom). A representative blot is shown. IB, immunoblotting; IP, immunoprecipitation; +, -Fe +Metals; +++, -Fe +++Metals. (B) Confocal microscopy analyses of *irt1-1*/IRT1::IRT1-mCit and *irt1-1*/IRT1::IRT1$_{2KR}$-mCit grown in iron-deficient conditions with low non-iron metals (-Fe -Metals), physiological non-iron metals (-Fe +Metals), or transferred for 2h to a ten-fold increase of non-iron metals (-Fe +++Metals). Representative images are shown. Scale bars = 10μm. (C) Ratio between plasma membrane and intracellular fluorescence signal intensities of IRT1-mCit from experiments performed as in (B). Experiments were carried out in triplicates on stacks encompassing epidermal cells at the root tip. Error bars represent s.d. (n=18). The asterisks indicate significant differences (Mann-Whitney, P<0.0001). No significant difference was observed for *irt1-1*/IRT1::IRT1$_{2KR}$-mCit in the three different metal conditions. (D) Sensitivity of *irt1-1*/IRT1::IRT1-mCit and *irt1-1*/IRT1::IRT1$_{2KR}$-mCit plants to BrefelfinA (BFA). Plants were pretreated with 100 μM cycloheximide (CHX) for 1h and exposed to 100 μM CHX and 50 μM BFA for 4h. Representative images are shown. Scale bars = 10 μm.

3.5 The IDF1 RING E3 ligase drives the metal dependent K63 polyUb-mediated endocytosis of IRT1

The ubiquitination of IRT1 requires the IDF1 RING E3 ligase (Shin et al., 2013). Notably, the *idf1-1* loss-of-function mutant appeared to be defective in IRT1 ubiquitination and accumulated more IRT1 protein. However, the biological role of IDF1 remains unclear since the ubiquitination of IRT1 was thought to be constitutive (Barberon et al., 2011). The metal-dependent ubiquitination of IRT1 uncovered in the present study now provides a possible role for IDF1 in mediating plant responses to non-iron metal stress. We therefore scored the root length of wild-type and *idf1-1* loss-of-function mutant plants on media containing standard or metal excess conditions. Wild-type plants showed slightly decreased root length when grown in the presence of non-iron
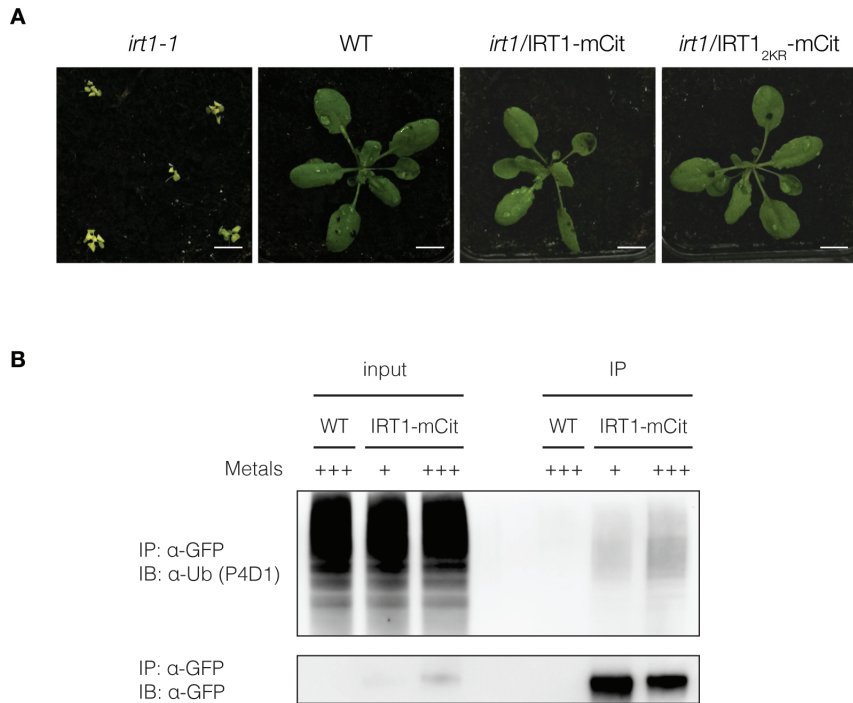
Figure 22 – Functional fusion of IRT1$_{2KR}$-mCit and ubiquitination status of *irt1-1*/pIRT1::IRT1-mCit in response to metals. (A) Phenotypic analyses of *irt1-1* KO mutant, WS accession (WT), *irt1-1*/IRT1::IRT1-mCit (*irt1*/IRT1-mCit) and *irt1-1*/IRT1::IRT1$_{K154,179R}$-mCit (*irt1*/IRT1$_{2KR}$-mCit).. Scale bars = 1cm. (B) In vivo ubiquitination analyses of IRT1 in response to different 2h-non-iron-metals treatments. Immunoprecipitation was performed using anti-GFP antibodies on solubilized protein extracts from wild-type and mono-insertional homozygous *irt1-1*/IRT1::IRT1?mCit plants and subjected to immunoblotting with anti-Ub P4D1 (top) and anti-GFP (bottom). IB, immunoblotting; IP, immunoprecipitation; +, -Fe +Metals; +++, -Fe +++Metals.

metal excess compared to standard conditions. In contrast, *idf1-1* showed increased sensitivity to metal stress, as attested by the strong reduction in root length observed in the presence of metal excess (Fig. 23A and B). Although clearly hypersensitive to the oversupply of IRT1 secondary metal substrates, *idf1-1* displayed longer roots than wild-type plants likely resulting from other roles of IDF1. The hypersensitivity of *idf1-1* to metal excess was accompanied with greater leaf content in Zn, Mn and Co compared to wild-type plants (Fig. 24A). Consistently, IRT1 protein accumulated at higher levels in *idf1-1* than in wild-type plants in response to non-iron metal excess, with no change in mRNA accumulation (Fig. 23C; Fig. 24B). When expressed in the *idf1* mutant background, IRT1-mCit was unable to relocate to endosomal compartments in response to non-iron metals and was still found at the cell surface (Fig. 23E and F). This was associated with a strong reduction of IRT1-mCit ubiquitination in *idf1* upon metal stress (Fig. 23G).

To further examine how IDF1 and non-iron metal excess regulate IRT1 ubiquitination, we took advantage of the Apu3 anti-ubiquitin antibodies, which show specificity towards K63 polyubiquitin chains. K63 polyubiquitination indeed controls the endocytosis of plant plasma membrane proteins (Kasai et al., 2011; Leitner et al., 2012; Martins et al., 2015; Johnson and Vert,
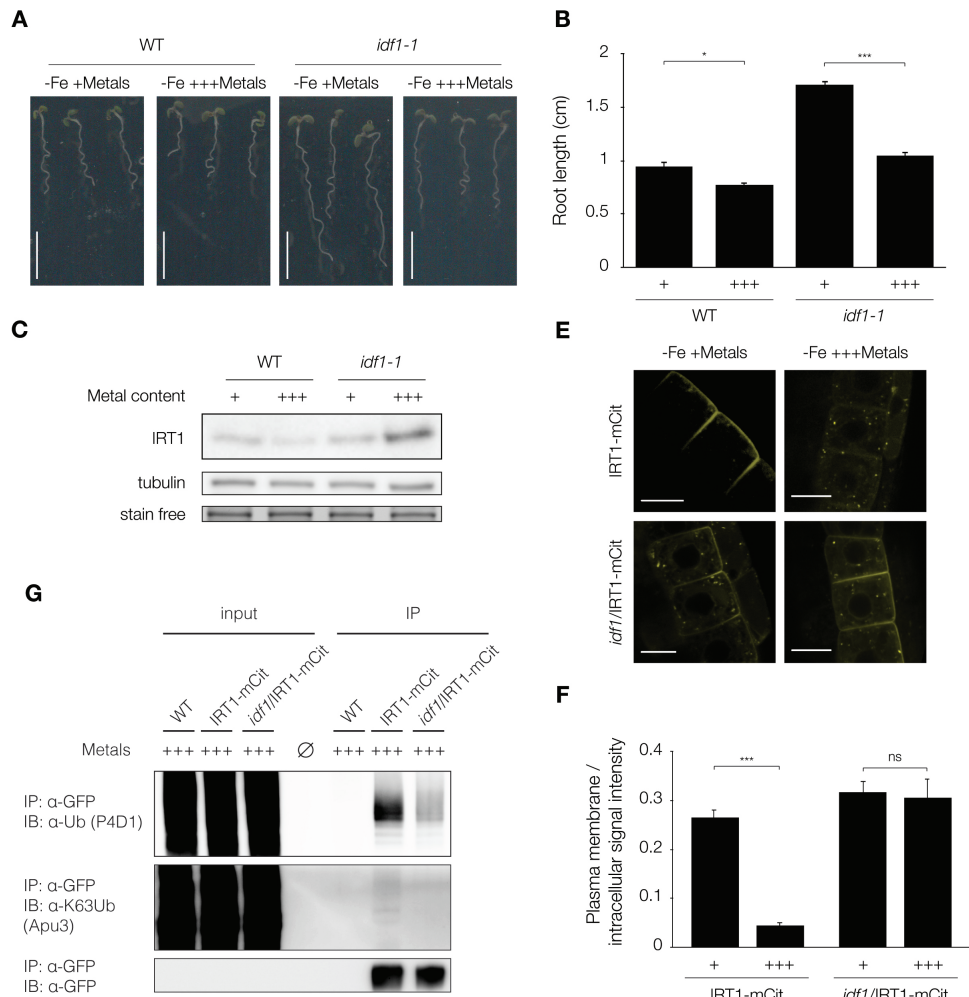
Figure 23 – **IDF1 mediates the K63 polyUb-mediated endocytosis of IRT1 in response to metal excess.** (A) Phenotypic analyses of 7d-old wild-type (WT) and *idf1-1* seedlings grown in ?Fe +Metals (+) or ?Fe +++Metals (+++) conditions. Representative images are shown. Scale bars = 5mm. (B) Root length quantification of plants grown as in (A). Experiments were carried out in triplicates. Error bars represent s.d. (n=40). The asterisks indicate significant differences (Mann-Whitney, P<0.0001). (C) Western-blot analyses of plants cultivated as described in (A), using anti-IRT1 antibodies. Stain free staining was used as a loading control. (D) Confocal microscopy analyses of *irt1-1* /IRT1::IRT1-mCit and *idf1-1* /IRT1::IRT1-mCit grown in ?Fe +Metals (+) for 12d and subjected or not to a 2h-short-term-metal-treatment (-Fe +++Metals, +++). Representative images are shown. Scale bars = 10μm. (E) Quantification of IRT1-mCit plasma membrane and intracellular fluorescence signal intensities in experiments performed as in (D). Experiments were carried out in triplicates on stacks encompassing epidermal cells at the root tip. Error bars represent s.d. (n=15). The asterisks indicate significant differences (Mann-Whitney, P<0.0001). No significant difference was observed for *idf1-1* /IRT1::IRT1-mCit in the different metal conditions (F) *In vivo* ubiquitination analyses of IRT1. Immunoprecipitation was performed using anti-GFP antibodies on solubilized protein extracts from wild-type (WT) and mono-insertional homozygous *irt1-1* /IRT1::IRT1-mCit and *idf1-1* /IRT1::IRT1-mCit plants and subjected to immunoblotting with anti-Ub P4D1 (top), anti-K63-polyUb Apu3 (center) and anti-GFP (bottom) antibodies. IB, immunoblotting; IP, immunoprecipitation; +, -Fe +Metals; +++, -Fe +++Metals.

95

A

B
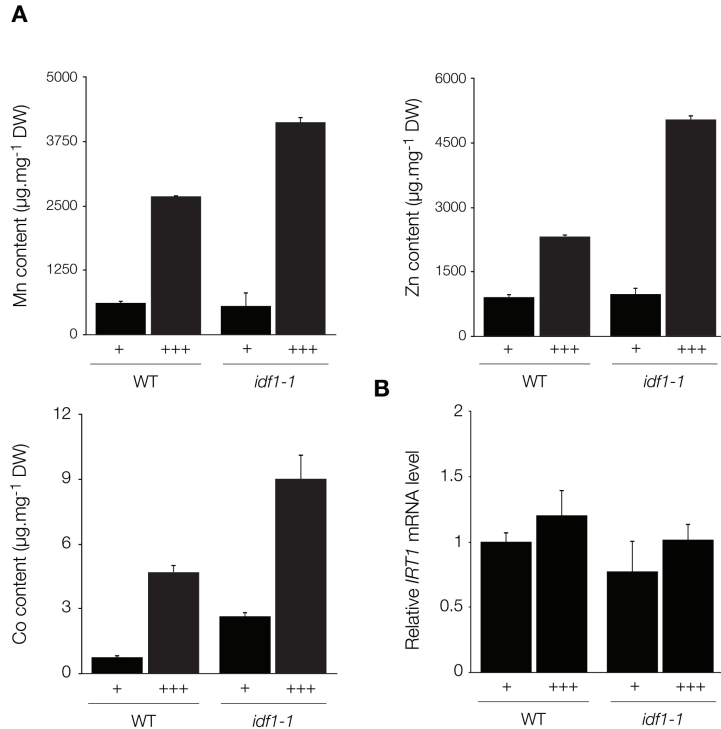
Figure 24 – **Non-iron metals overaccumulation in the *idf1-1* mutant background.** (A) Zn, Mn and Co content analyses by atomic absorption spectrometry of 7d old seedlings described in Fig. 4A. Experiments were carried out in triplicates. Error bars represent s.d. (n=3). The asterisks indicate significant differences between ?Fe +Metals (+) and ?Fe +++Metals (+++) (Mann-Whitney, P<0.0001). (B) *IRT1* mRNA accumulation from plants described in Figure 4A.

2016), and is known in yeast and mammals to be critical for intracellular sorting and lysosomal/vacuolar targeting (Lauwers et al., 2009; Lauwers et al., 2010; Huang et al., 2013). A high molecular weight smear was observed for IRT1-mCit upon metal oversupply, suggesting that IRT1 is K63 polyubiquitinated *in vivo*. Strikingly, no smear was detected for IRT1-mCit when expressed in *idf1* background, indicating that IDF1 is the E3 ligase responsible for the K63 polyubiquitination of IRT1 *in planta* (Fig. 23G). Taken together, these results indicate that IDF1 mediates IRT1 endocytosis and vacuolar sorting through K63 polyubiquitin-chains in response to metal excess.

3.6   IRT1 phosphorylation mediates its IDF1 dependent K63 polyubiquitination in response to metals

To better understand the mechanism by which non-iron metals trigger the recruitment of IDF1 and the K63 polyubiquitination-dependent vacuolar targeting of IRT1, we assessed whether IRT1 was phosphorylated in response to metals. Phosphorylation of the substrate or the E3 ligase itself is often a prerequisite to mediate their interaction (Huang et al., 2006; Lu et al., 2011). We
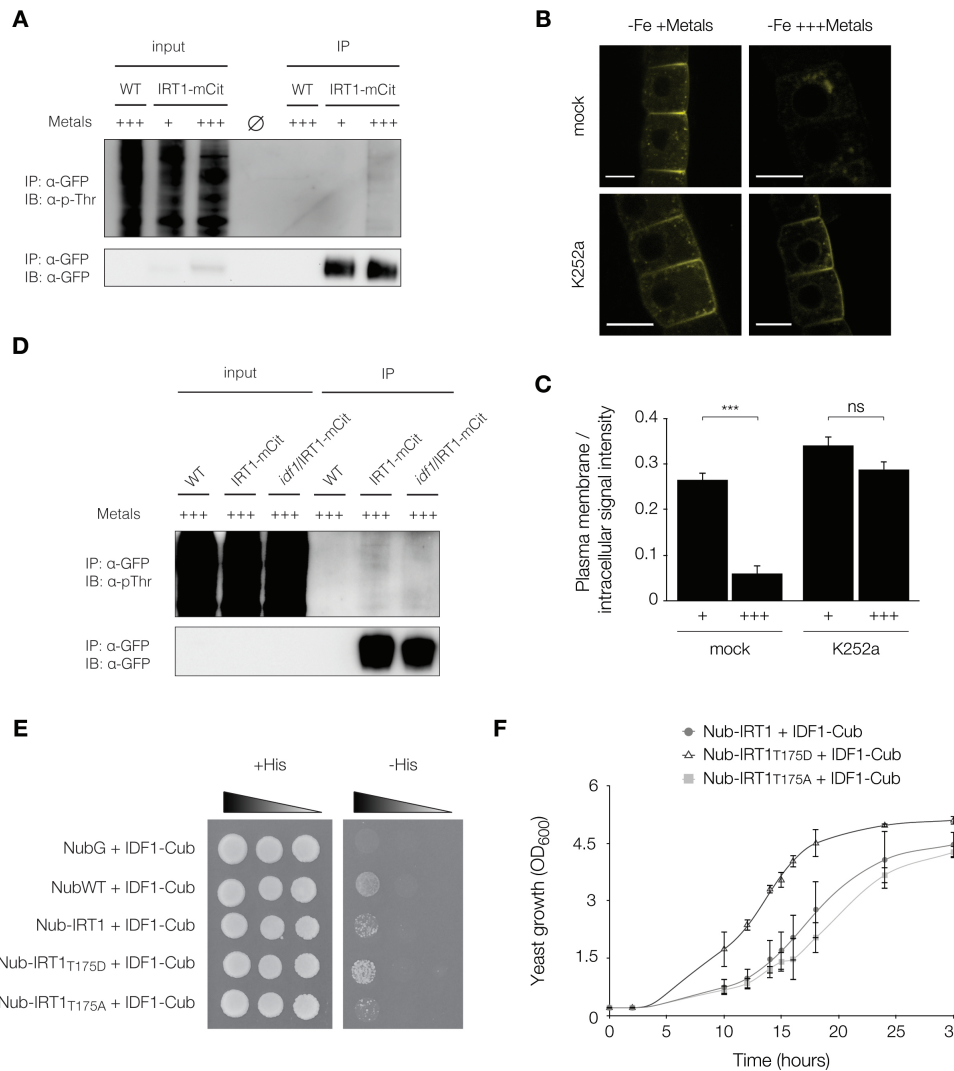
Figure 25 – IRT1 is phosphorylated in response to metals mediating its IDF1-dependent K63 polyubiquitination. (Legend continued on next page.)

therefore probed IRT1-mCit immunoprecipitates from plants grown under standard conditions, or subjected to a short term metal excess, with anti-phosphothreonine antibodies. No signal could be detected for wild-type and IRT1-mCit-expressing plants grown under standard grown conditions (Fig. 25A). However, a smear was specifically observed for IRT1-mCit challenged with metals. This smear is reminiscent of what we observed for ubiquitinated forms of IRT1 and suggests that IRT1 is both K63 polyubiquitinated and phosphorylated.

To grasp the role of phosphorylation in plant metal responses, we first took a pharmacological approach using the K252a general kinase inhibitor. No removal of IRT1 from the cell surface was observed upon metal excess when plants were treated with K252a treatment (Fig. 25B;

Figure 25 – **IRT1 is phosphorylated in response to metals mediating its IDF1-dependent K63 polyubiquitination (continued).** (A) *In vivo* phosphorylation analyses of IRT1 in response to non-iron-metals. Immunoprecipitation was performed using anti-GFP antibodies on solubilized protein extracts from wild-type (WT) and mono-insertional homozygous 35S::IRT1?mCit plants and subjected to immunoblotting with anti-P-Thr (top) and anti-GFP (bottom) antibodies. A representative blot is shown. IB, immunoblotting; IP, immunoprecipitation; +, -Fe +Metals; +++, -Fe +++Metals. (B) Sensitivity of irt1-1/IRT1::IRT1-mCit plants to kinase inhibition. Plants were grown for 12d in physiological non-iron metals conditions and treated for 2h with the same medium (-Fe +Metals) or with non-iron metal excess (-Fe +++Metals) in the presence of 1 μM K252a. Representative images are shown. Scale bars = 10 μm. (C) Quantification of the ratio between plasma membrane and intracellular fluorescence signal intensities of IRT1-mCit from plants grown as in (B). Experiments were carried out in triplicates on stacks encompassing epidermal cells at the root tip. Error bars represent s.d. (n=15). The asterisks indicate significant differences (Mann-Whitney, P<0.0001). No significant difference was observed of K252a-treated *irt1-1*/IRT1::IRT1-mCit plants in response to non-iron metals. (D) In vivo phosphorylation analyses of IRT1 in ubiquitination-defective backgrounds, in response to non-iron-metals. Immunoprecipitation was performed using anti-GFP antibodies on solubilized protein extracts from wild-type (WT), mono-insertional homozygous *irt1-1*/IRT1::IRT1-mCit, *irt1-1*/IRT1::IRT1$_{2KR}$-mCit and *idf1-1*/IRT1::IRT1-mCit plants and subjected to immunoblotting with anti-P-Thr (top) and anti-GFP (bottom) antibodies. A representative blot is shown. IB, immunoblotting; IP, immunoprecipitation; +++, -Fe +++Metals. (E) Split-ubiquitin interaction between IDF1 and IRT1 variants for threonine residue T175. NubG and NubWT were used as negative and positive controls, respectively. Controls, and yeast expressing IDF1-Cub together with NubG-IRT1 (plain circle), NubG-IRT1$_{T175D}$ (open triangle) and NubG-IRT1$_{T175A}$ (square) were spotted in serial dilutions on selective (SD-Leu-Trp-Ade-His) or non-selective (SD-Leu-Trp) media. Experiments were done in triplicates. (F) Growth rate analysis of split ubiquitin interactions shown in (E). Yeast were inoculated at OD = 0.2 in selective medium (SD-Leu-Trp-Ade-His) and growth recorded over 30h. Experiments were done in triplicates.

23C), suggesting that phosphorylation events are directly or indirectly required for the K63 polyubiquitin-dependent vacuolar degradation of IRT1. Consistently, phosphorylation of IRT1-mCit was still observed in the *idf1* mutant background upon metal excess (Fig. 25D), arguing that metal-dependent phosphorylation is likely upstream of IRT1 K63 polyubiquitination.

To better evaluate the respective roles of phosphorylation and IDF1-mediated K63 polyubiquitination in IRT1 degradation, we used bioinformatics prediction tools to locate possible phosphorylation sites in IRT1. We filtered the data obtained keeping phosphorylation sites with the highest scores and targeting cytosolic loops. Using these criteria, we identified threonine residue T175 located in the large cytosolic loop and in close proximity with K154 and K179 as a good candidate. We monitored the influence of IRT1 phosphorylation on its ability to interact with IDF1 in split ubiquitin assays. IDF1 interacted with wild-type IRT1 in split ubiquitin assays, as previously shown (Shin et al., 2013). Interestingly, the IRT1 variant carrying the non-phosphorylatable T175A substitution grew slightly slower than wild-type IRT1, while the T175D phosphomimic substitution yielded better growth in selective conditions (Fig. 25E). No difference in growth rate was however observed in non-selective medium. To accurately monitor the split ubiquitin interactions, we monitored yeast growth in selective liquid cultures and observed a sharp difference between yeast expressing *IRT1*, *IRT1$_{T175D}$* and *IRT1$_{T175A}$* (Fig. 25F). Taken together, these observations strongly suggest that phosphorylation of residue T175 serves as a platform allowing the interaction with IDF1 and subsequent K63 polyubiquitination of IRT1.
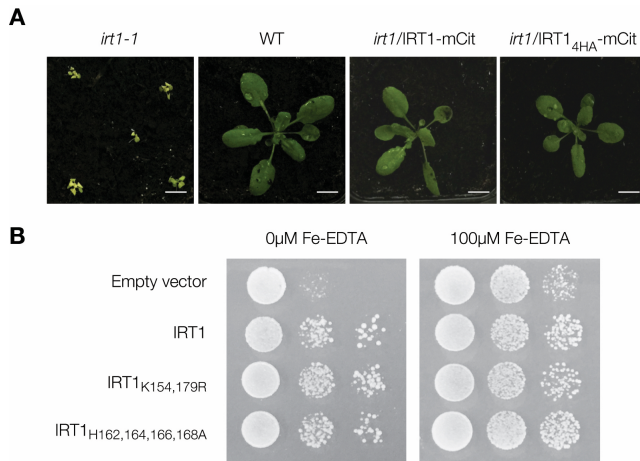
Figure 26 – **IRT1$_{4HA}$ is functional *in planta* and in yeast heterologous system.** (A) Phenotypic analyses of *irt1-1* KO mutant, WS accession (WT), *irt1-1*/IRT1::IRT1-mCit (*irt1*/IRT1-mCit) and *irt1-1*/IRT1::IRT1$_{H162,164,166,168A}$-mCit (*irt1*/IRT1$_{4HA}$-mCit).. Scale bars = 1cm. (B) Functional expression of IRT1, IRT1$_{2KR}$ and IRT1$_{4HA}$ in *fet3fet4* yeast strain. The different SD media were supplemented or not with 100 μM Fe-EDTA.

3.7 Histidine residues in IRT1 play a role in its metal-triggered ubiquitin-mediated endocytosis

A stretch of 4 histidine residues (HGHGHGHG) located in the large cytosolic loop of IRT1 between the two lysines K154 and K179 has been shown to directly bind metals by isothermal titration calorimetry (Grossoehme et al., 2006). We confirmed this observation using full length IRT1-mCit protein and the IRT1$_{4HA}$-mCit mutant variant, where histidines were mutated to alanines. The corresponding proteins were purified from plants and their ability to bind to a metal-NTA agarose resin measured. IRT1$_{4HA}$-mCit bound poorly to the metal resin compared to wild-type IRT1 (Fig. 27E), pointing to the crucial role of the His-rich motif for the direct interaction with divalent metals *in vitro*. To address whether such histidine stretch may play a role in the metal sensing and response leading to IRT1 metal-dependent degradation, we generated a transgenic line expressing *IRT1$_{4HA}$-mCit* in the *irt1-1* mutant background. Expression of *IRT1$_{4HA}$* restored the growth of the *irt1-1* loss-of-function mutant demonstrating that these four histidine residues are not required for metal transport *per se* (Fig. 26A). This is further confirmed by the ability of IRT1$_{4HA}$ to functionally complement the iron uptake-defective *fet3fet4* yeast mutant to the same extent than wild-type IRT1 (Fig. 26B). We then scored the root length of IRT1-mCit and IRT1$_{4HA}$-mCit lines on standard media or in metal excess conditions. IRT1$_{4HA}$-mCit-expressing plants grew similar to wild-type under standard conditions, they were clearly hypersensitive to metal excess (Fig. 27A and B) and accumulated massive amounts of non-iron metal substrates of IRT1 (Preliminary results). Interestingly, IRT1$_{4HA}$-mCit failed to relocalize to endosomes upon non-iron metal oversupply and remained mostly at the cell surface (Fig. 27C and D). This is further corroborated by the lack of phosphorylation, ubiquitination and more

specifically K63 polyubiquitination for IRT1$_{4HA}$-mCit upon metal (Fig. 27G). Split-ubiquitin assay further indicated that the mutation of the histidine stretch prevented the interaction between IRT1 and IDF1 (Fig. 27F), providing further insight into the molecular mechanism driving IRT1 response to its non-iron metal substrates. This histidine-rich stretch likely serves as a sensing area to coordinate non-iron metal excess degradation mediated by phosphorylation and K63 polyUb linkages.

4 Discussion

Despite its regulation at the transcriptional level by low iron (Vert et al., 2002), IRT1 is also controlled at the post-translational level by multi-monoubiquitination of two lysine residues in its large cytosolic loop triggering its internalization into early endosomes (Barberon et al., 2011). This mechanism, although not regulated by iron nutrition, is critical for the control of metal homeostasis since the expression of a non-ubiquitinatable version of IRT1 is detrimental to plant growth due to uncontrolled metal uptake. In the present study, we uncovered that IRT1 is differently ubiquitinated by the availability of its non-iron metal substrates. In response to metal excess, IRT1 is relocalized from PM and TGN/EE compartments to the vacuole via late endosomal compartments. This metal-dependent degradation appears to rely on K63 polyubiquitination of the transporter by the IDF1 E3 ligase. Since a non-ubiquitinatable mutant fails to relocalize upon metal excess, K63 polyubiquitin chains are likely extended on the monoubiquitinated K154 and K179 residues. Because K63 polyubiquitination seems to be implicated only in metal excess conditions, one of our hypothesis is the involvement of another E3 ligase in the early endocytosis events. In contrast with the IRT1$_{2KR}$ mutant that is stabilized at the PM, IRT1$_{4HA}$ or *idf1*/IRT1 proteins are still found in endosomal compartments indicating that IDF1 only acts in the sorting at the LE compartments and further degradation of the cargo. It would also be really interesting to discover new factors implicated in both ub- or deubiquitination of IRT1. In addition to ubiquitination, deubiquitination is the reverse process that release the Ub moiety from the linkage allowing to remobilize a free pool of Ub in the cytososol (Schmidt and Teis, 2012). While the DUB acting between TGN/EE and PM is likely specific of IRT1, the one acting in the sorting in LE through the ESCRT complex would rather be ubiquitous and could function for all ubiquitinated plant cargos. In mammals, the *AMSH* gene encodes a deubiquitinase (DUB) that is recruited by the ESCRTIII complex (Agromayor and Martin-Serrano, 2006). In plants, AMSH3 is a good candidate for deubiquitinating cargos that are sorted into intraluminal vesicles (ILVs) of LE by the ESCRT system. AMSH3 is a plant DUB that interacts with the ESCRTIII complex and catalyzes both K48 and K63 polyubiquitin chains (Isono et al., 2010; Katsiarimpa et al., 2011). AMSH3 is certainly playing the same role in plants as AMSH in mammals for cargo deubiquitination by the ESCRT system and its involvement in IRT1 sorting to ILVs by the ESCRT system should be investigated in the future.

We also show here that phosphorylation adds another layer of complexity on the regulation of IRT1 ubiquitin-mediated endocytosis in response to metal excess. The role of a single
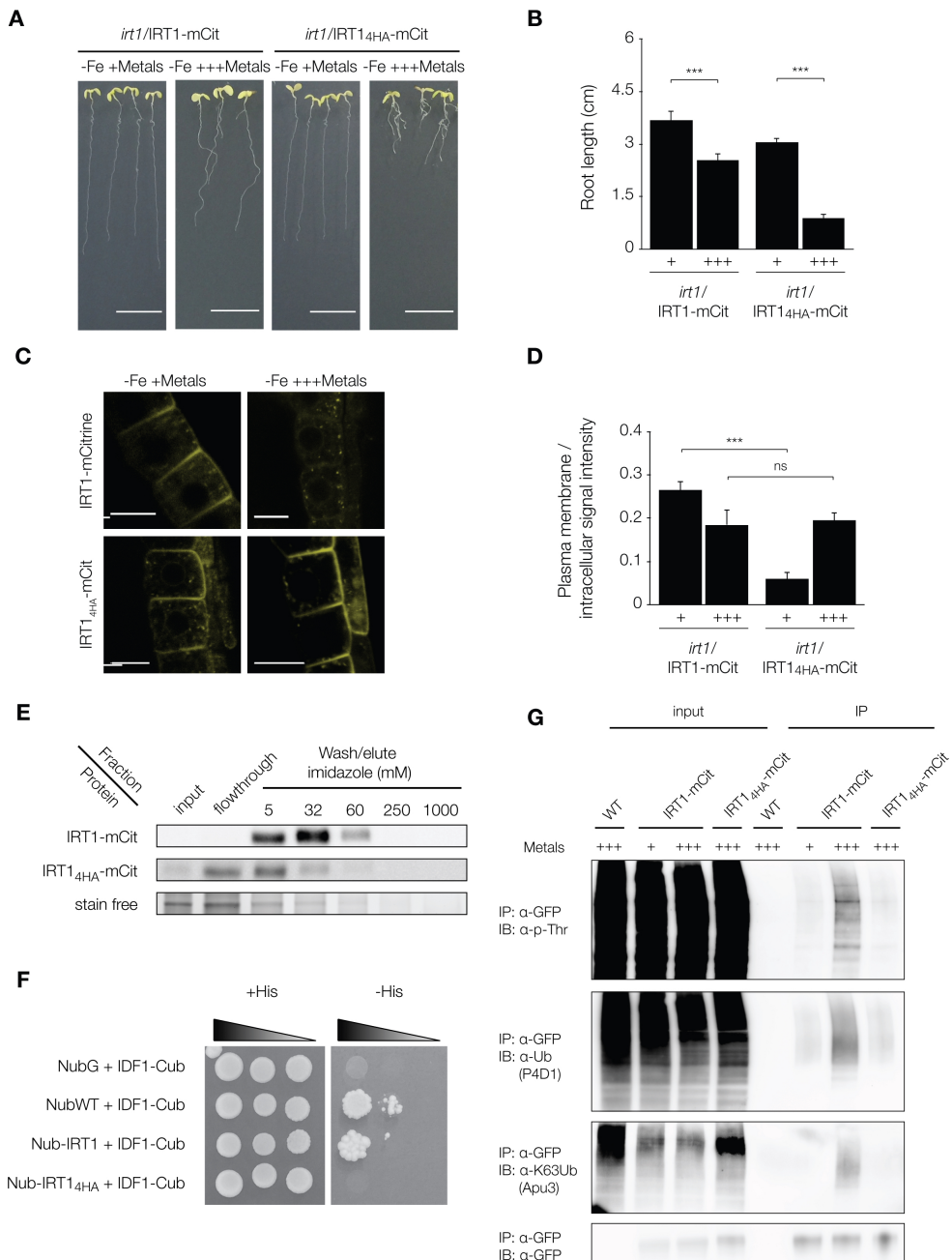
Figure 27 – **A histidine-rich stretch is implicated in metal binding and is necessary for metal-triggered ubiquitin-mediated endocytosis of IRT1.** (Legend continued on next page.)

phosphorylation site (T175), identified by in silico prediction, was investigated. The sole phosphorylation of IRT1 at this phosphosite appears to be sufficient to promote the interaction of IRT1 with IDF1. However, we cannot rule out the potential implication of other residues in this

Figure 27 – **A histidine-rich stretch is implicated in metal binding and is necessary for metal-triggered ubiquitin-mediated endocytosis of IRT1 (continued).** (A) Phenotypic analyses of 12-d-old *irt1-1*/IRT1::IRT1-mCit and *irt1-1*/IRT1::IRT1$_{4HA}$-mCit seedlings grown in physiological (-Fe +Metals) or non-iron metal excess (-Fe +++Metals) conditions. Scale bars = 1 cm. (B) Root length quantification of plants grown as in (A). Experiments were carried out in triplicates. Error bars represent s.d. (n=40). The asterisks indicate significant differences (Mann-Whitney, P<0.0001). (C) Confocal microscopy analyses of *irt1-1*/IRT1::IRT1-mCit and *irt1-1*/IRT1::IRT1$_{4HA}$-mCit plants grown in iron-deficient conditions with low non-iron metals (-Fe -Metals), physiological non-iron metal conditions (-Fe +Metals), or transferred for 2h to a ten-fold oversupply of non-iron metals (-Fe +++Metals). Representative images are shown. Scale bars = 10 μm. (D) Quantification of the ratio between plasma membrane and intracellular fluorescence signal intensities plants grown as in (C). Experiments were carried out in triplicates on stacks encompassing epidermal cells at the root tip. Error bars represent s.d. (n=18). The asterisks indicate significant differences (Mann-Whitney, P<0.0001). No significant difference was observed for *irt1-1*/IRT1::IRT1$_{4HA}$-mCit in the three different metal conditions. (E) Metal binding analyses of IRT1-mCit and IRT1$_{4HA}$-mCit. Proteins from 35S::IRT1-mCit and 35S::IRT14HA-mCit plants were solubilized and subjected to metal ion purification. Increasing imidazole concentrations were used to eluate proteins from the metal ion resin. Stain free staining was used to illustrate the serial elutions with imidazole. Experiments were done in triplicates. (F) Split-ubiquitin assay between IDF1 and IRT1 variants. NubG and NubWT were used as negative and positive controls, respectively. Serial dilutions were spotted in selective (SD-Leu-Trp-Ade-His) and non-selective (SD-Leu-Trp) media. Experiments were carried out in triplicates. (G) In vivo phosphorylation and ubiquitination analyses of IRT1 and its IRT1$_{4HA}$ in response to non-iron metals. Immunoprecipitation was performed using anti-GFP antibodies on solubilized protein extracts from wild-type (WT) and mono-insertional homozygous 35S::IRT1-mCit and 35S::IRT1$_{4HA}$-mCit plants and subjected to immunoblotting with from top to bottom : anti-P-Thr, anti-Ub P4D1, anti-K63-polyUb Apu3, and anti-GFP antibodies. A representative blot is shown. IB, immunoblotting; IP, immunoprecipitation; +, -Fe +Metals; +++, -Fe +++Metals

mechanism. It would also be really interesting to discover the kinase implicated in IRT1 phosphorylation triggering the K63 polyubiquitination of the transporter by IDF1. The imbrication of IDF1 together with the ESCRT system could also be investigated since some adaptor proteins were shown as implicated in the recruitment of E3 ligases in mammals directly by the ESCRT complex (Sette et al., 2010). Altogether, this complex mechanism unraveled here serves the plant to tightly adapt both IRT1 localization and protein levels within the epidermis in response to metal content.

As a crucial root iron transporter, IRT1 is needed for the uptake of this element from the soil (Vert et al., 2002). However, the cargo also pumps other divalent metals from the soil that can be toxic if present in excess. To protect the plant from metal overload, IRT1 is only expressed in iron starved conditions to only uptake iron when limiting in soils. At another level, when iron is lacking together with high concentrations of non-iron metals, IRT1 is internalized and degraded. Altogether, this dual regulation optimizes iron absorption and also limits the toxicity associated with uptake of other harmful elements of the soil.

5 Methods

5.1 Materials and constructs

The *irt1-1*, *idf1-1*, VHAa1-RFP, RabF2a-mCherry and BOR4-GFP *Arabidopsis* lines were described in previous studies (Vert et al., 2002; Shin et al., 2013; Dettmer et al., 2006; Geldner et al., 2009; Kasai et al., 2011). The *IRT1* ORF coding sequence was cloned into pDONR221 Gateway entry vector. mCitrine coding sequence was cloned in 5', 3' or in corresponding loops of IRT1 by inserting BamHI restriction sites, yielding pDONR221-IRT1-mCit. The mutated IRT1-mCit versions (IRT1$_{2KR}$-mCit and IRT1$_{4HA}$-mCit) were generated using the Single-Primer Reactions In Parallel method (Edelheit et al., 2009), with mutagenic primers described in Table 3. Entry vectors carrying the IRT1 and 35S promoters, and the mCitrine fluorescent protein were previously described (Marquès-Bueno et al., 2016; Jaillais et al., 2011). Final destination vectors were obtained by using three-fragment recombination system (Life Technologies), using the pG7m34GW destination vector and the various pDONR221-IRT1-mCit entry clones to generate the pIRT1::IRT1-mCit and p35S::IRT1-mCit constructs. All these constructs were inserted in *irt1-1*, *idf1-1* mutant backgrounds or wild-type *Arabidopsis thaliana* plants floral dipping technique using *Agrobacterium tumefaciens* (Clough and Bent, 1998). For all constructs, around 20 independent T1 lines were isolated and six representative mono-insertion lines were selected in T2. Independent lines homozygous for the transgene were selected in T3. For yeast growth assay, IRT1 cDNA was cloned into pDR195 by Gateway technology. For split-Ub assay, the same IRT1 cDNA was used and inserted into pNubG vector. IDF1 cDNA was inserted into pCub vector containing the PLV transcription factor. Sub-versions of IRT1 mutated for its histidine-rich stretch (IRT1$_{4HA}$) or for the threonine 175 residue (IRT1$_{T175D}$ and IRT1$_{T175A}$) were generated and inserted in the pNubG vector. The mutagenic primers are described in Table 3.

5.2 Growth Conditions

Wild-type and the various transgenic lines used in this study were grown in sterile conditions on vertical plates at 21°C with 16h light/8h dark cycles. For confocal microscopy analyses of transgenic plants using the IRT1 promoter, iron starvation was performed by directly germinating seeds on half-strength Murashige and Skoog (MS) (Murashige and Skoog, 1962) medium lacking exogenous iron for 10d. Plants were then then transferred for 2d in the same conditions (standard ; +) or in a medium containing ten times more Zn, Mn and Co (metal excess ; +++). Non-iron metal deficiency was carried out by germinating seeds on medium lacking Fe, Zn, Mn and Co (deficiency ; -). Short term metal excess used a 2h-transfer in physiological or metal excess liquid medium. 35S::IRT1-mCitrine and mutated versions were imaged 7d after germination, following a 2h-transfer in physiological or metal excess conditions. For biochemistry approaches, transgenic lines expressing *IRT1-mCit* under the control of its own promoter were cultivated in iron-deficient conditions for 12d before collecting samples. Constitutively-expressing *IRT1-mCit* lines were grown in iron-deficient conditions for 9d. Plants were then transferred for a 2h in liquid medium lacking iron but containing either physiological levels of Zn, Mn and Co (+) or a

Name	Use	Sequence (5' to 3')
EF1a qPCR F	qRT-PCR	GTCGATTCTGGAAAGTCGAC
EF1a qPCR R	qRT-PCR	AATGTCAATGGTGATACCACGC
mCit qPCR F	qRT-PCR	GACTTCTTCAAGTCCGCCATG
mCit qPCR R	qRT-PCR	GTCCTCCTTGAAGTCGATGC
IRT1 qPCR F	qRT-PCR	CGGTTGGACTTCTAAATGC
IRT1 qPCR R	qRT-PCR	CGATAATCGACATTCCACCG
IDF1 qPCR F	qRT-PCR	GGTTTCACCTTCTTCTTCGC
IDF1 qPCR R	qRT-PCR	ACGCATCTTGGAGATAACCC
IRT1 K154R F	SDM	GCCTATACACCAGCAGGAACGCAGTTGGTATC
IRT1 K154R R	SDM	GATACCAACTGCGTTCCTGCTGGTGTATAGGC
IRT1 K179R F	SDM	GTTACCTTACCAATAAGAGAAGATGATTCGTC
IRT1 K179R R	SDM	GACGAATCATCTTCTCTTATTGGTAAGGTAAC
IRT1 H162,164A F	SDM	GTTGGTATCATGCCCGCTGGTGCTGGTCATGGTCACGGC
IRT1 H162,164A R	SDM	GCCGTGACCATGACCAGCACCAGCGGGCATGATACCAAC
IRT1 H166,168A F	SDM	CCCGCTGGTGCTGGTGCTGGTGCCGGCCCCGCAAATGATG
IRT1 H166,168A R	SDM	CATCATTTGCGGGGCCGGCACCAGCACCAGCACCAGCGGG
IRT1 T175D F	SDM	CCCGCAAATGATGTTGACTTACCAATAAAAGAAG
IRT1 T175D R	SDM	CTTCTTTTATTGGTAAGTCAACATCATTTGCGGG
IRT1 T175A F	SDM	CCCGCAAATGATGTTGCCTTACCAATAAAAGAAG
IRT1 T175A R	SDM	CTTCTTTTATTGGTAAGGCAACATCATTTGCGGG

Table 3 – List of primers used in this article.

ten-fold increase of secondary substrates of IRT1 (+++). For split-root experiments, lateral root initiation was stimulated by cutting the primary root of 5d-old-seedlings grown in iron-deficient conditions at the root-shoot junction, and further grown for 12d. Plants were then transferred for 2 more days on a split plate containing one half with standard non-iron metal conditions, and one half subjected to a ten-fold metal excess. For root growth analyses, plants were grown for 7d in iron-deficient conditions and with either physiological level of non-iron metals (+) or with a ten-fold excess of these metals (+++). Aerial parts were then collected for elemental analyses. Roots were harvested for mRNA and protein extraction.

5.3 Imaging

Imaging was performed on inverted Leica SP2 and SP8X confocal microscopes. Within a given experiment, images were taken using similar laser and detection settings for direct comparison of signal intensities and patterns between conditions and genotypes. For quantifications, z-stacks encompassing the whole cell volume were imaged on at least three different cells of three different plants during three independent experiments. The stacks were then subjected to maximum projection. The ratios of PM over intracellular relative signal content were obtained by selecting whole cell and intracellular content mean fluorescence with ImageJ. The fluorescence intensity in vacuoles was determined using same ROI for two different cells of three different plants during three independent experiments. The percentage of IRT1-mCit-positive endosomal structures showing overlap with Vha-A1-RFP or RabF2a-mCherry was determined using the center of mass of every particle with ImageJ plugin JACoP (Bolte and Cordelières, 2006). Cycloheximide (Sigma-Aldrich) was applied at a concentration of 100 μM for 1 h before treatment with BFA;

BFA (Sigma-Aldrich) was applied at a concentration of 50 μM for 3 h in liquid medium. For dark treatment, plants were transferred in light or dark for 4 hours in liquid medium containing physiological level $(+)$ or excess of non-iron metals $(+++)$.

5.4 Elemental Analyses

Leaves were harvested and rinsed for 5 min with deionized water before being dried at 65°C for 7 days. Tissues were digested completely in 2 mL of 70% (v/v) nitric acid in a DigiBlock ED36 (LabTech) at 80°C for 1 h, 100°C for 1 h, and 120°C for 2 h. After dilution to 12 mL with ultrapure water, Mn, Zn and Co contents of the samples were determined by atomic absorption spectrometry using an AA240FS flame spectrometer (Agilent Technologies). Metal content analyses were performed in triplicates.

5.5 RNA Extraction and Real-Time Quantitative PCR

Total RNA was extracted using QIAzol reagent (Qiagen) and purified using the RNeasy MinElute Cleanup Kit (Qiagen) after DNase treatment (Qiagen). The integrity of DNA-free RNA was verified by agarose gel electrophoresis, and an equal amount of total RNA (2 μg) was used for reverse transcription with anchored oligo (dT18) and RevertAid enzyme (ThermoFischer Scientific). For real-time PCR analyses, IRT1-mCit, IRT1, IDF1 or EF1α were amplified with a Lightcycler 96 with SYBR Green I Master (Roche), using the primers described in Table 3. Experiments were done using three technical and three biological replicates. Relative expression of IRT1-mCit, IRT1 or IDF1 was quantified with the $2^{-\Delta\Delta Ct}$ method (Livak and Schmittgen, 2001) using EF1α as a reference gene.

5.6 Protein Extraction and Western Blot Analysis

Protein extraction and immunoprecipitation experiments were conducted using 12-day-old seedlings. For western blot analyses, total proteins were extracted from 100 mg of starting material. For protein detection, the following antibodies were used: Monoclonal anti-GFP horseradish peroxidase-coupled (Miltenyi Biotech 130-091-833, 1/5,000), anti-ubiquitin P4D1 (Millipore 05-944, 1/2,500), anti-K63 polyubiquitin Apu3 (Millipore 05-1,308, 1/2,000), anti-P-Thr (Cell Signaling 9381, 1/1,000) anti-IRT1 (Barberon et al., 2011). Quantification of western blot was performed using the stain free technology with the help of the ImageLab software (BioRad). Immunoprecipitation experiments were performed using approximately 2 g of roots. Tissues were ground in liquid nitrogen and resuspended in 3 volumes of RIPA buffer as previously described (Barberon et al., 2011). Samples were then centrifuged for 10 min at 5,000 g at 4°C. Total proteins contained in the supernatant were placed for 1h at 4°C on a rotating wheel to solubilize membrane proteins. Non-resuspended material was then pelleted for 45 min at 100,000 g. Immunoprecipitations were carried out using the μMACS GFP isolation kit (Miltenyi Biotec). For quantification of IRT1 ubiquitinated pools, the ratio of normalized immunoprecipitation

signal intensity obtained with anti-GFP and anti-Ub antibodies was determined using ImageJ. Immunoprecipitation and western blot analyses were performed in triplicates.

5.7   Immobilized metal ion affinity chromatography

The metal-binding capacity of IRT1-mCit and its IRT1$_{4HA}$-mCit was analyzed following the instruction of TALON Metal Affinity Resin Kit (Clontech) with modifications as follows. Samples were prepared as described above for immunoprecipitation experiments, but 100 μL of the TALON resin instead of μMACS GFP beads was added to the solubilized protein extract and incubated for 1h at 4°C on a rotating wheel. After a first centrifuge at 1000rpm, 100 μL of the supernatant was collected as the flow through fraction. Three washes were performed with 200 μL of RIPA buffer supplemented with 5 mM imidazole. Unbound and bound proteins were serially washed out and collected in each fraction by applying 200 μL each of RIPA buffer containing 5, 32, 60, 250, or 1000 mM imidazole. 20 μL of each fraction was subjected to SDS-PAGE. Detection of HRP chemiluminescence was done on a ChemiDoc Touch (BioRad) with the help of Super-Signal West Dura Extended Duration Substrate (ThermoScientific). Metal binding experiments were done in triplicates.

5.8   Functional Expression in Yeast

The *fet3fet4* mutant strain from Saccharomyces cerevisiae (MATa; leu2Δ0; ura3Δ0; lys2Δ0; YMR058w::kanMX4; YMR319c::kanMX4) was transformed with either the empty pDR195 vector as a negative control, or pDR195 plasmids containing IRT1 or mutant versions under the control by the lithium acetate method (Gietz et al., 1992). Transformed cells were selected on SD-Ura medium (Sigma). Complementation of *fet3fet4* was tested by spotting serial dilutions of three clone per construct on SD-Ura medium supplemented or not with 100 μM Fe-EDTA. Plates were placed at 30°C for 2d. Yeast complementation experiments were done in triplicates.

5.9   Split-ubiquitin assay

The C-terminus of ubiquitin (Cub) linked to the PLV transcription factor was fused to the C-terminal end of IDF1 (IDF1-Cub) and expressed in yeast together with the mutated N-terminal fragment of ubiquitin (NubG) fused to the N-terminal end of IRT1 (NubG-IRT1), IRT1 carrying a phosphomimic- or non-phosphorylatable residue at position 175 (NubG-IRT1$_{T175D}$ and NubG-IRT1$_{T175A}$, respectively). The wild- type ubiquitin N-terminal fragment (NubWT) was used as a positive control. THY.AP4 cells (MATa; ura3 leu2 lexA::lacZ::trp1 lexA::HIS3 lexA::ADE2) were transformed using the lithium acetate method (Gietz et al., 1992). Transformed THY.AP4 cells were selected on SD-Leu-Trp medium (Sigma). Protein-protein interaction was assessed by following the growth of transformed cells inoculated at OD 0.2 over time.

106

5.10   Bioinformatic and statistical analyses

Prediction of phosphorylation sites in IRT1 was achieved using the PhophAt 4.0 interface. Statistical analyses were performed using the software GraphPad Prism. Physiological plant parameter (root length), confocal microscopy analyses quantifications used the non-parametric Mann-Whitney test.

6   Acknowledgements

7   Author contribution

G.D., E.Z., and G.V. designed research; G.D. and J.N. performed experiments; G.D., E.Z. and G.V. analyzed data; and G.D. and G.V. wrote the paper. The authors declare no conflict of interest.

Part V

Discussion and perspectives

Chapter 1

Discussion and perspectives

Despite its regulation at the transcriptional level, IRT1 is also controlled at the post-translational level by multi-monoubiquitination of two lysine residues in its large cytosolic loop triggering its internalization into early endosomes (Barberon et al., 2011). This mechanism, although not regulated by iron nutrition, is absolutely critical for the control of metal homeostasis since the expression of a mutated and non-ubiquitinatable version of *IRT1* is detrimental to plant growth due to uncontrolled metal uptake. Despite the discovery of this control of IRT1 subcellular localization and its biological relevance, the intricate molecular mechanisms driving IRT1 ubiquitination and endocytosis were elusive when I began my PhD.

1   Differential ubiquitination of IRT1

IRT1 is differently ubiquitinated by the availability of its non-iron metal substrates. While K63 polyubiquitinated versions of IRT1 are observed only for metal excess conditions, the smeary pattern obtained on a blot (Fig. 21A) using the P4D1 generic anti-Ub antibody appears to be rather similar in size under both physiological and excess treatments although the smear intensity is clearly enhanced in the latter conditions. We would have expected different profiles that clearly distinguish multi-monoUb and K63 polyUb versions of IRT1, with a shift towards higher molecular weight under metal excess conditions as a result of conversion of multi-monoubiquitin moieties into K63 polyUb chains. However, signals derived from anti-ubiquitin antibodies are very intense for long Ub chains (i.e. K63 polyUb chains) while monoUb or short chains only yield very weak signals that may not be clearly observed on a western blot. This likely explains why no signal corresponding to multi-monoUb forms of IRT1 were observed in IRT1 Ub profiles, expecially in lower molecular weight. For now, no direct tools were developed to detect monoUb *per se*. Indirect investigations are the only way to decipher mono- from polyUb. In 2011, to investigate the monoubiquitinated versions of IRT1, immunoprecipitates were subjected to western-blot analysis with both the generic P4D1 anti-Ub and polyubiquitination-specific FK1 antibodies (Barberon et al., 2011). The absence of signal with the latter antibody further prompted the team to deduce the involvement of monoubiquitination rather than other forms of ubiquitination (Barberon

et al., 2011). To further study the possibility of IRT1 being K63 polyubiquitinated in response to metal excess, we could take advantage of AMSH3, a K48- and K63-specific deubiquitinase in plants (Isono et al., 2010). The *amsh3* loss-of-function mutant is lethal. However, it is possible to express a dominant-negative form of AMSH3, mutated for its active site AXA, under the control of an inducible promoter (Isono et al., 2010). As AMSH3-AXA plants accumulate ubiquitin conjugates, it would be interesting to cross *AMSH3-AXA*-expressing plants with IRT1-mCit to assess if impairing AMSH3 would impact IRT1 ubiquitination profile. If the profile remains the same with only an increase in the signal, it will further attest an enrichment with polyubiquitinated versions of the cargo in addition with the presence of monoubiquitinated forms of IRT1. In the contrary, a different pattern will attest that monoUb is the major form detected in our blots using the generic P4D1 antibody. However, it would be hard to understand why the profiles obtained with K63 polyUb Apu3 antibody look rather similar with the ones obtained with the P4D1 antibody without the lower bands. To further support the fact that IRT1 is K63 polyUb upon metal stress, we could take advantage of the recently-developed Vx3K0 K63 polyubiquitin-specific sensor that was developed in the lab (Johnson and Vert, 2016). One would predict that immunoprecipitating K63 polyUb proteins with Vx3K0 only recover IRT1 protein under metal excess conditions.

Recently, the Komander lab developed an Ub chain restriction protocol (UbiCRest) to decipher the Ub chain architecture (Mevissen et al., 2013; Hospenthal et al., 2015). This strategy uses several DUBs that can catalyze deubiquitination of specific chains or with less specificities. The use of K63 polyUb-specific DUB or a broad spectrum DUB that can catalyze all the linkages between Ub moieties would allow to characterize further the presence of K63 polyUb chains linked to IRT1 upon metal stress.

Because K63 polyubiquitination seems to be implicated only in metal excess conditions, to trigger IRT1 sorting to MVB/LE/PVC and further degradation to the vacuole, one of my hypothesis is the involvement of another E3 ligase in the early endocytosis events (Fig. 28; Fig. 29). Indeed, IRT1$_{2KR}$ is completely stabilized at the PM suggesting the role of ubiquitination for the internalization of the transporter (Fig. 21B, C and D). In the contrary, IRT1-mCit expressed in *idf1-1* knock-out mutant background is still found at the PM and in endosomes in response to metal excess but is not degraded (Fig. 23E and F) indicating that IDF1 only acts in the sorting at the MVB/LE/PVC compartments and further degradation of the cargo. Altogether, these results suggest the implication of another E3 ligase for the internalization of IRT1 from the PM (Fig. 28). The concerted action of this unidentified E3 ligase together with IDF1 would allow a tight control of IRT1 dynamics at the level of early endosomes by targeting to the vacuole. An imaging-based forward genetic screen has been initiated in the team to find new proteins involved in the trafficking of IRT1. A line expressing in a constitutive manner *IRT1-mCit* under the control of the *PIN2* promoter has been mutagenized using the ethyl methanesulfonate (EMS) agent. M1 seeds were planted in soils individually and ≈1600 M2 lines were collected. All these M2 lines will be screened at the confocal for a metal excess response. The M2 plants impaired for the non-iron metals response will be of great interest including either a PM-associated pattern
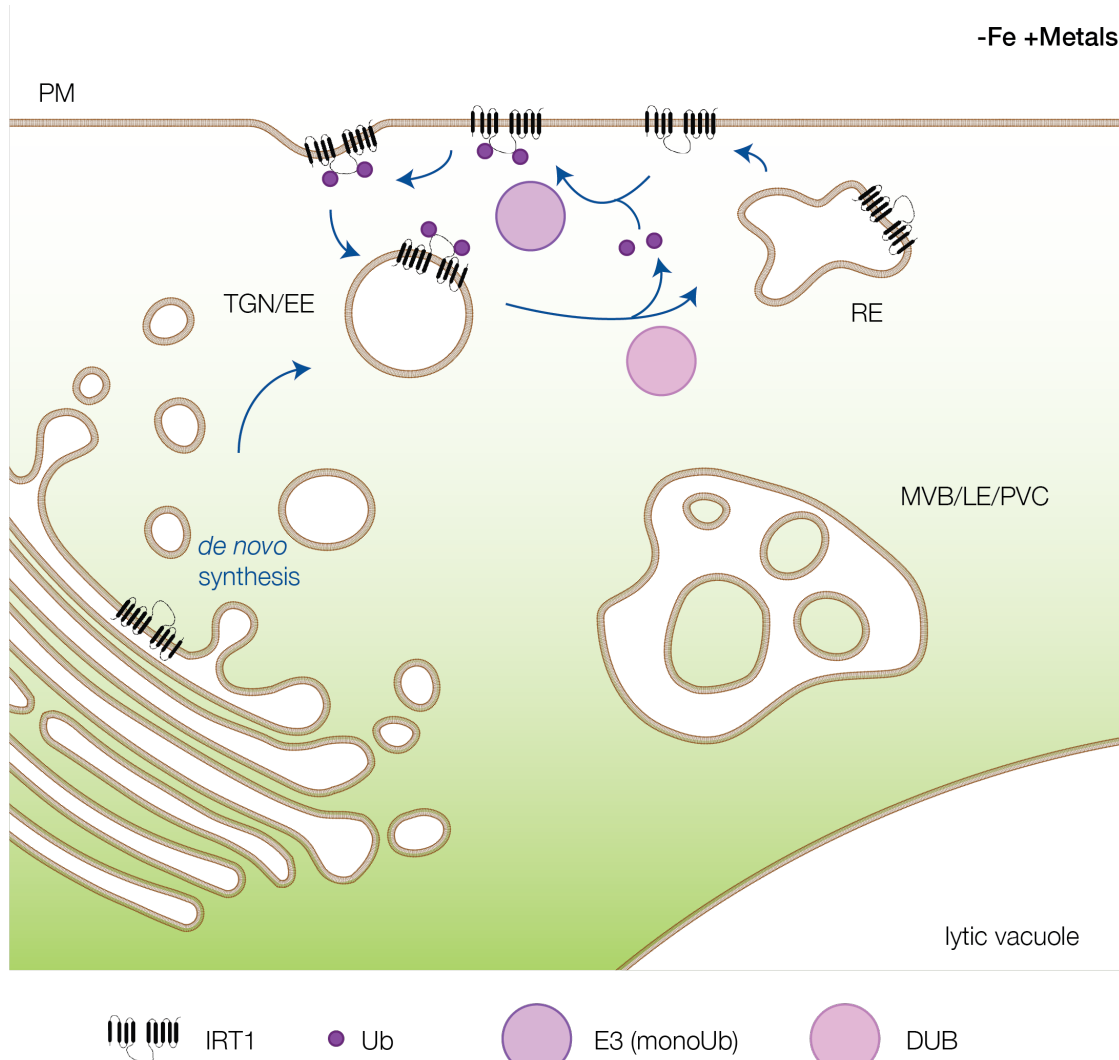
Figure 28 – **IRT1 cycles constitutively from PM to TGN/EE compartments through multi-monoubiquitination/deubiquitination in standard conditions.**

like IRT1$_{2KR}$-mCit or a PM together with endosomal localization like the *idf1-1* and IRT1$_{4HA}$-mCit. Such a screen may identify many factors involved in the endocytosis of IRT1 including the E3 ligase that can multi-monoubiquitinate IRT1 and that allows its internalization from the PM to TGN/EE compartments (Fig. 28).

Finally, it would be of importance to uncover the putative DUBs implicated in both the recycling from TGN/EE to the PM, as well as in the sorting in MVB/LE/PVC through the ESCRT complex function. Respectively, the first DUB is likely specific of IRT1 while the one acting together with the ESCRT system is rather ubiquitous and could function for all ubiquitinated cargos. In yeast and mammals, *DOA4* and *AMSH* genes encode deubiquitinases which are
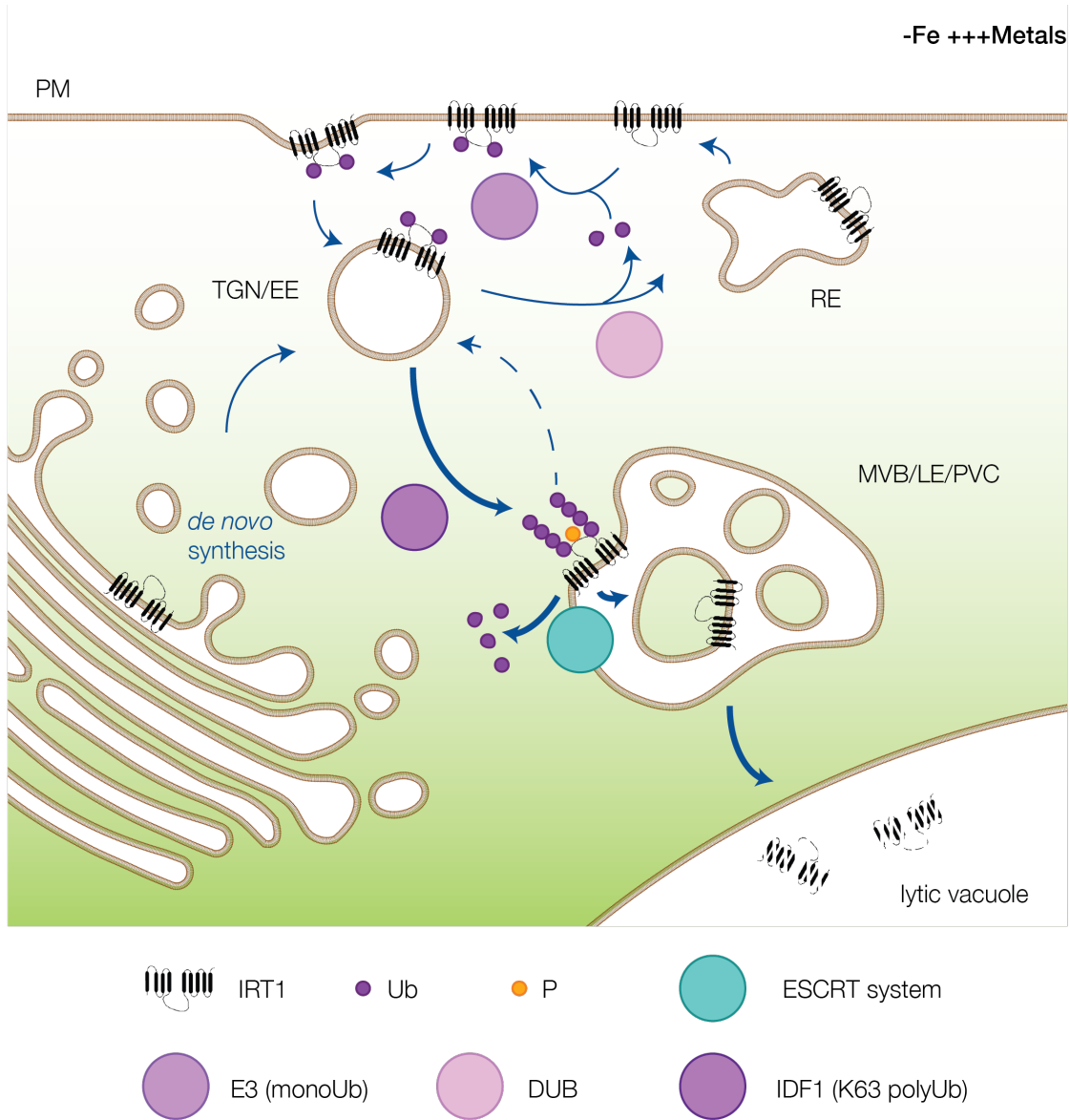
Figure 29 – **IDF1 mediates IRT1 K63 polyubiquitination triggering its degradation in response to metal excess.**

recruited by the ESCRTIII complex (Amerik et al., 2000; Agromayor and Martin-Serrano, 2006; Nikko and André, 2007; Richter et al., 2013). DOA4 was the first DUB identified as playing a role in the sorting of cargos in yeast (Amerik et al., 2000). Furthermore, deubiquitination by DOA4 is required for cargoes to be sorted into ILVs of MVB/LE/PVC (Nikko and André, 2007). In mammals, AMSH is a DUB required for cargo sorting into ILVs through the direct interaction with CHMPs subunits of the ESCRTIII complex (Agromayor and Martin-Serrano,

2006). In plants, AMSH3 is a good candidate for the deubiquitination step together with the ESCRTIII-mediated ILV formation. AMSH3 is a plant deubiquitinase that catalyze both K48- and K63 polyUb chains (Isono et al., 2010). AMSH3 also interacts with VPS2.1 and VPS24.1 subunits of the ESCRTIII complex (Katsiarimpa et al., 2013). In addition, the protein ALIX is required for the MVB/LE/PVC localization of AMSH3 (Kalinowska et al., 2015). AMSH3 is certainly playing the same role in plants as DOA4 in yeast or AMSH in mammals in cargo deubiquitination required for a proper internalization and recycling of Ub by the ESCRT system at the MVB/LE/PVC.

Altogether, all these results and hypotheses suggest that IRT1 is a great model to decipher the implication of both monoUb and K63 polyUb chains all along the endocytic pathway (Fig. 28; Fig. 29).

2   Going further on the phosphorylation mediating Ub-dependent degradation

Although phosphorylation seems to be acting before ubiquitination, as suggested in the second chapter of this thesis, some proofs are needed to strengthen this conclusion (Fig. 30). We initiated phosphoproteomics analysis but we fail to identify phosphosites within IRT1 sequence. The presence of Ub moieties likely prevents us from detecting phosphopeptides and new investigations will be initiated using IRT1$_{2KR}$-mCit to prevent the formation of ubiquitinated versions of the transporter in the fraction submitted to analysis. So far, the role of a single phosphorylation site (T175), identified by *in silico* predictions, has been initiated (Fig. 30). However, we cannot rule out the potential implication of other threonine, serine or even tyrosine residues in the ubiquitin-mediated degradation of IRT1. It would be of interest to mutate all the putative residues which can be phosphorylated into aspartic acid or alanine to have phospho- or non-phosphodead versions of IRT1 and test 1) their ability to interact with IDF1 in a split-ubiquitin assay 2) the localization of the corresponding proteins and their response to metals, and 3) the phenotype of the corresponding plants. The obvious missing link is the kinase mediating the phosphorylation of IRT1 in response to metals. Interestingly, many transporters were shown to be phosphorylated by the CBL-interacting protein kinase (CIPK) family *via* their co-action with calcineurin B-like (CBL) proteins (Xu et al., 2006; Ho et al., 2009; Maierhofer et al., 2014; Tang et al., 2015). The activity of the root epidermis-expressed potassium channel AKT1 is regulated under potassium starvation by the protein kinase CIPK23-CBL1/9 (Xu et al., 2006). Phosphorylation of AKT1 is counterbalanced by the AKT1-interacting PP2C 1 (AIP1) phosphatase (Lee et al., 2007). CHL1/NRT1.1 is a dual affinity nitrate transporter that mediates nitrate uptake in plants (Wang et al., 1998; Liu et al., 1999). When phosphorylated on residue T101, CHL1/NRT1.1 shows high affinity nitrate transport activity while dephosphorylation of T101 switches CHL1/NRT1.1 towards the low affinity mode (Liu and Tsay, 2003). CHL1/NRT1.1 also interacts with CIPK23 which mediates the phosphorylation of residue T101 (Ho et al., 2009). CIPK23 therefore appears to regulate several root-expressed nutrient transporters. Recently, the involvement of CIPK23

114
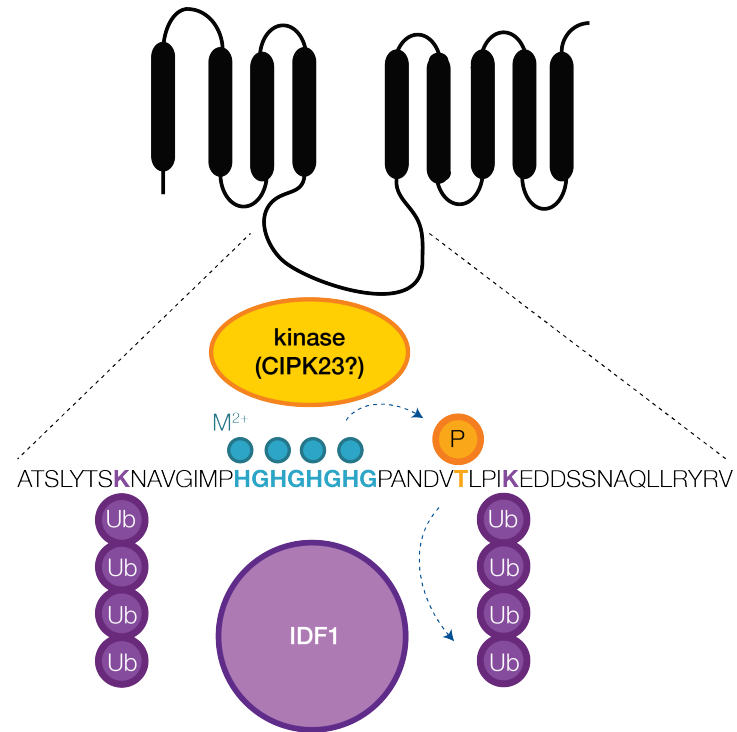
Figure 30 – Model of the substrate-dependent phosphorylation and K63 Ub-mediated endocytosis of IRT1.

in iron homeostasis was suggested (Tian et al., 2016). In iron starved conditions, ferric chelate reductase (FCR) activity was reduced in *cipk23-2* and *cipk23-3* mutants compared with WT plants consistently with the chlorotic phenotype of such mutants (Tian et al., 2016). The authors concluded on the role of this protein kinase on FCR that co-act with IRT1 to mediate the entry of iron from the rhizosphere (Brumbarova et al., 2014; Tian et al., 2016).

To evaluate the possible role of CIPK23 in the metal-dependent phosphorylation of IRT1, we characterized the corresponding *cipk23* loss-of-function mutant. Preliminary results indicate that the *cipk23-1* mutant is hypersensitive to metals, similar to what is observed for *idf1-1* and the histidine stretch mutant version of IRT1. To further strengthen these genetic evidence supporting a role of CIPK23 in the regulation of IRT1, the interaction between the two proteins has to be investigated. We initiated a collaboration with the Kudla lab to make a yeast two hybrid screen and further detect the putative interaction between the large cytosolic loop of IRT1 and all the CIPK family together with their co-actors CBLs. Furthermore, we will investigate the impact of the overexpression of *CIPK23* on the interaction between IRT1 and IDF1 in split-Ub assay in yeast. Finally, the impact of the *cipk23* mutation on the subcellular localization of IRT1 and its ability to be degraded in response to metal excess will have to be investigated.

As we proposed in the fourth part of the thesis, the histidine-rich stretch of IRT1 is binding metals and this would probably allow the direct or indirect recruitment of a kinase (Fig. 30).

If CIPK23 is confirmed as an interactor of IRT1 allowing the phosphorylation of the latter in response to metal excess, it would be really interesting to check if the kinase could still interact with a mutated version of the transporter for this histidine stretch (Fig. 30).

3   How IDF1 acts at the molecular level?

IDF1 is the RING E3 ligase implicated in the sorting and degradation of IRT1 in response to metal excess (Fig. 29; Fig. 30). To study deeper the role of IDF1 in the metal-dependent endocytosis of IRT1, we generated lines expressing *IDF1* with a fluorescent tag both in *idf1-1* mutant background, to check the functionality of the fusion, and in a line stably expressing IRT1-mCit. IDF1 was not detected using both microscopy or western-blot analysis in standard conditions indicating either a transient behavior of the protein or an absence of translation in those conditions. Preliminary results however indicate a co-localization of IDF1-mCherry with IRT1-mCit in response to metal excess. IDF1 therefore appears to be stabilized following metal excess. Considering that *IDF1* mRNA accumulate regardless of metal availability, IDF1 is likely regulated at the translational or post-translational levels by non-iron metals. IDF1 being an E3 ligase with a RING domain requiring zinc for proper function (Borden and Freemont, 1996), it is also tempting to speculate that incorporation of zinc upon metal excess into the RING domain may stabilize IDF1.

The accumulation of IDF1 protein specifically in response to metals represents a second regulatory level mediated by metals, in addition to IRT1 phosphorylation. The sole phosphorylation of IRT1 appears sufficient in theory to promote the interaction of IRT1 with IDF1 (Fig. 30). Why do plants also control the accumulation of IDF1 in parallel? It is conceivable that IDF1 targets other proteins than IRT1 in response to metal excess that do not undergo prior metal-dependent phosphorylation. In that case, the accumulation of IDF1 specifically in response to metals would represent the major regulatory mechanism to control the fate of such proteins.

As presented in the third part of this thesis, IRT1 also interacts with FYVE1/FREE1 that is a ESCRT-related protein directly implicated in the vacuolar sorting of PIN2 (Gao et al., 2014). The ability of FYVE1/FREE1 to interact with K63 polyUb chains could also be investigated as it was previously shown to interact with Ub (Gao et al., 2014). In a tempting model, we could speculate that IDF1-triggered K63 polyubiquitination of IRT1 in response to metal stress would be directly recognized by the FYVE1/FREE1 protein and the rest of the ESCRT system to allow the invagination of the transporter into MVB/LE/PVC and release of the Ub moieties into the cytosol (Fig. 29). This would ensure a proper degradation of IRT1 inside the vacuolar lumen to further protect the plant from the uptake of putative harmful elements from the soil. This however is not consistent with the *FYVE1*-overexpressing plants showing recycling of IRT1 protein back to the cell surface. This particular statement will be further debated in the next part of the discussion.

To further decipher the mechanism proposed in this thesis, it would be really interesting to find possible intermediate proteins acting between the IDF1-mediated K63 polyubiquitination of

IRT1 and the ESCRT complex. The ALIX protein has been demonstrated in plants to be required for the endosomal localization of AMSH3 and further interacts with the DUB (Kalinowska et al., 2015). ALIX is also implicated in the recruitment of the E3 ligase NEDD4 in mammals in order to facilitate the release of the HIV virus (Sette et al., 2010). Similarly, an ESCRT-associated protein could bridge the gap between IDF1 and the ESCRT system to elicit the sorting of IRT1 in favor of vacuolar degradation in response to metal excess.

4 FYVE1/FREE1: an important ESCRT-associated protein at the crossroads of endocytosis and autophagy

As mentioned above and in addition with the results we described in the third part of this thesis, FYVE1/FREE1 is crucial for the formation of ILVs in MVB/LE/PVC compartments in plants (Gao et al., 2014). Further, FYVE1/FREE1 is part of the ESCRTI complex as the protein is able to interact with VPS23 (Gao et al., 2014). FYVE1/FREE1 also binds to ubiquitin itself and is implicated in the vacuolar sorting of PIN2 (Gao et al., 2014). PIN2 undergo ubiquitin-mediated degradation and requires the ESCRT complex (Abas et al., 2006; Kleine-Vehn et al., 2008; Spitzer et al., 2009; Leitner et al., 2012; Korbei et al., 2013). PIN2-GFP is found at the tonoplast in a *fyve1/free1* mutant background explained by an absence of ILV formation (Gao et al., 2014). Strikingly, overexpression of *FYVE1/FREE1* disturbs the endosomal sorting of IRT1 and triggers recycling to the cell surface while one would have expected more degradation. This could be explained by the involvement of FYVE1/FREE1 in both recycling and sorting events, depending on the cargo. Alternatively, overexpression of a subunit of the ESCRTI complex may titrate ESCRTII and III away from endosomal membranes, preventing them to properly sort IRT1 in ILV and triggering its recycling. The influence of FYVE1 on IRT1 trafficking must therefore be tested in weak loss-of-function mutants, considering that *fyve1* null mutants are lethal. FYVE1/FREE1 directly interacts with the autophagic regulator SH3 domain-containing protein 2 (SH3P2) which has been only described in plants (Zhuang et al., 2013). SH3P2 indeed binds to PI3P and ATG8 and regulates the formation of autophagosomes in plants (Zhuang et al., 2013). FYVE1/FREE1 also affects the association between autophagosomes and MVBs, further suggesting a crucial role of this protein in the interplay between ESCRT-related endocytic and autophagic pathways (Gao et al., 2015). Being at the crossroads of such important pathways underlies the role of the ESCRT complex in the cell. It is tempting to suggest a direct role of the ESCRT complex on the autophagosome closure but no proof have been discovered so far. Ubiquitination processes appear to be much more important than expected in the trafficking of plasma membrane proteins and it opens a great new field of investigation of imbrication of both quality control process and response to nutrient availability.

5 Polarity and dynamics of IRT1 mediate plant metal homeostasis

We initially studied the localization of IRT1 by immunofluorescence (IF) analyses, using anti-IRT1 antibodies. To finely track the dynamics of the transporter within cells, we next generated a functional fusion of IRT1 with the fluorescent protein. Since IRT1 can only be tagged in an extracellular loop, we chose the pH-resistant mCitrine protein. Consistent with what we observed by IF, IRT1-mCit also showed metal-dependent trafficking. However, in contrast to endogenous IRT1 protein that we detected by IF in the early endosomes, IRT1-mCit is mostly found at the PM as well as in early endosomes under standard non-iron metal conditions. The different patterns between the two approaches may first reside in the techniques themselves. Indeed, IF need a prior fixation of tissues and uses the anti-IRT1 antibody that may only recognize a sub-pool of total IRT1 protein. The presence of the mCitrine tag may also influence the dynamics of IRT1 protein, although the protein appears functional on the basis of *irt1-1* complementation. Alternatively, the developmental stage of root cells may impact on IRT1 distribution in the cell. Although IRT1 is strongly expressed in differentiated root epidermal cells (Vert et al., 2002), we found that the endogenous promoter was also active at the root tip in young seedlings. Root tip cells are not differentiated and have a small vacuole facilitating the imaging of endosomal compartments. IF was performed on differentiated root hair cells, while more recent analyses using IRT1-mCit were carried out in root tip cells for more convenient imaging. The IRT1-mCit fusion protein is not suitable for imaging in older parts of the root because of cleavage of the mCit tag. To demonstrate that IRT1 is differentially distributed in differentiated *versus* non-differentiated cells or if the mCit tag interferes with IRT1 dynamics, it would be interesting to perform IF on root tip cells from wild-type and *IRT1-mCit*-expressing plants using anti-IRT1 and anti-GFP antibodies, respectively.

In metal excess conditions, IRT1 is relocalized from PM and TGN/EE compartments to MVB/LE/PVC and further degraded in the lytic vacuole. While a few hours are sufficient to trigger a metal-dependent degradation of IRT1-mCit (Fig. 19E and F), long-term treatment with metal excess leads to a strong accumulation of IRT1 in late endosomal compartments visualized by the colocalization with Rha1 (Fig. 19A and B). The biological relevance of the localization of the transporter in MVB/LE/PVC compartment after two days of transfer is not clear. Prolonged metal excess provokes the transcriptional activation of *IRT1*, due to the competition for uptake with iron (Fig. 20A). Under long-term non-iron metal excess, the plant is synthesizing loads of IRT1 protein but accumulates it in LE/MVB/PVC. This seems like a massive waste of energy, unless this pool of IRT1 can be remobilized when the availability in secondary metal substrates lowers. This would imply recycling from LE/MVB/PVC, a concept highly debated (Niemes et al., 2010; Scheuring et al., 2011; Robinson, 2015). IRT1-mCit overlaps with Rha1, a well-established marker of LE/MVB/PVC. The actual ultrastructure of Rha1-positive endosome is however unclear. Does Rha1 localizes only to mature MVB/LE/PVC where ILVs are already formed or does it also label earlier forms of MVB/LE/PVC or late forms of TGN/EE where ILVs

are not formed yet? While recycling appears impossible when proteins are already sorted into ILV, recycling from the limiting membrane of earlier LE is conceivable. To decipher if IRT1-mCit can recycle back to the cell surface after a long-term episode of metal excess, one could take advantage of plants expressing the photoconvertible mEos version of IRT1. Photoconversion of the LE/MVB/PVC pool of IRT1 observed after such plants are challenged with metal excess for 2 days, in the presence of CHX, should help visualize possible recycling to the cell surface. However, since part of IRT1 is found in TGN/EE even under long-term metal excess, the conclusions drawn from such an experiment may be limited.

To further characterize the nature of endosomal compartments where IRT1 is found after long-term metal excess, and more specifically if these structures already contain ILV, we performed correlative light/electron microscopy (CLEM). This technique uses the combination of both photonic and electronic miscrocopy and is particularly well described for mammalian tissues (Cortese et al., 2009). Among all the correlative microscopy sample preparation, Tokuyasu cryosections allow to keep an almost perfect ultrastructure and the integrity of epitopes while usual resin fixation alters protein structure thereby triggering a loss of fluorescence in the case of CLEM (Oorschot et al., 2014). It would be crucial in our case to have the nicest preparation in order to couple the characteristic structure of MVB/LE/PVC as it was observed in the plant literature (Scheuring et al., 2011) and the observation of IRT1-mCit in confocal microscopy in the same cryosections. From now, we were able to detect putative MVB/LE/PVC compartments by EM but no signal for IRT1-mCit was detected in confocal microscopy. Considering the thin cryosections, a very bright signal is needed to perform CLEM. New investigations will be initiated using a brighter *IRT1-mCit* expressing line.

Plants take up nutrient from the soil and transport them radially to the vasculature for distribution in the plant *via* the xylem sap. As proposed in the third part of this thesis, the outer lateral polarity displayed by IRT1 is required for proper radial transport of metals out of epidermal cells (Barberon et al., 2014). Once taken up, a nutrient like iron faces several routes to reach the vasculature. The symplastic route involves cell to cell transport *via* plasmodesmata, which are specific cell-cell communications found in plants (Fig. 31). In the symplastic pathway, the PM acts as a selective surface at the soil-plant interface controlling the uptake of nutrients (Barberon and Geldner, 2014). The existence of an apoplastic pathway adds more complexity to the process of radial transport of nutrients, providing a route for mass flow and the diffusion of water and nutrients towards the stele through free spaces and cell walls of the epidermis and cortex (Fig. 31). However, the Casparian strip (CS) in the endodermis constitute a physical barrier which blocks this apoplastic flow (Fig. 31) Because of the physical barrier, radial transport of nutrients from the rhizosphere to the stele need opposite polarization transporters in the endodermis. In this specific tissue, an influx transporter should be found at the outer polar domain of the PM and an efflux channel at the inner domain. This has been notably shown for the boric acid influx channel NIP5;1 and the boric acid/borate efflux transporter BOR1, localizing to the outer and inner PM domains of endodermal cells, respectively (Alassimone et al., 2010; Takano et al., 2010). The coupled trans-cellular pathway allows the radial transport
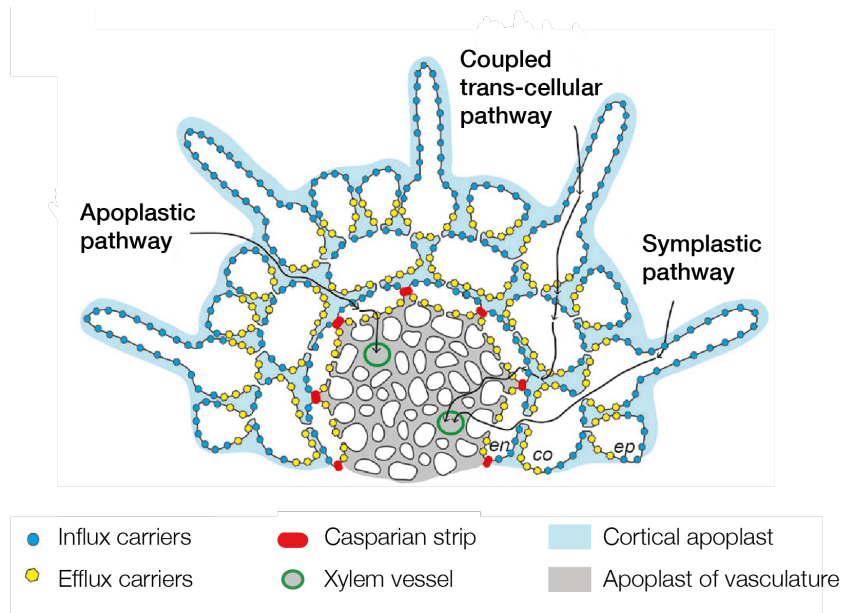
Figure 31 – Model of the radial transport of nutrients in differentiated roots (adapted from (Barberon et al., 2016)).

of nutrients from one cell to another *via* a succession of influx and efflux transporters showing outer and inner polarity, respectively (Barberon and Geldner, 2014). In *Oryza sativa*, the silicic acid importer Low-Silicon1 (LSI1) and the silicic acid exporter LSI2, are reciprocally localized at the outer and inner PM domains of both exodermis and endodermis in roots permitting an effective and directional trans-cellular transport of nutrient in plants (Ma et al., 2006; Ma et al., 2007).

In the case of iron, apoplastic transport plays a minor role since most of iron is taken up by IRT1 in root epidermal cells (Vert et al., 2002). In the epidermis of *Arabidopsis thaliana*, IRT1 is localized at the outer domain of the PM further ensuring a proper uptake of iron from the soil as we described in the first chapter of this thesis (Barberon et al., 2014). The contribution of the symplastic or trans-cellular pathway was however elusive. The loss of IRT1 polarity associated with interference with *FYVE1/FREE1* expression is associated with less accumulation of the secondary metal substrates of IRT1 in shoots (Barberon et al., 2014). We hypothesized that metals taken up by IRT1 fail to exit the epidermis when IRT1 is non polar, resulting in defective radial metal transport. This argues the existence of coupled trans-cellular pathway in the epidermis, consistent with the loss of cell-cell communications during the differentiation of root epidermal cells (Duckett et al., 1994). In this scenario, radial transport of metals needs the intervention of successive importers and exporters, at least in the epidermis, to reach the vasculature. A loss of IRT1 polarity would therefore counteract the action of an effluxer in the epidermis by re-uptaking metals in epidermal cells. Among possible metal effluxers are members of the ZRT/IRT-LIKE PROTEIN (ZIP) family that are well described transporters of

metals (Guerinot, 2000; Thomine and Vert, 2013; Socha and Guerinot, 2014). Another possibility comes with the proteins of the CDF or FERROPORTIN families that are well-established metal effluxers in bacterias and mammals (Nies, 2003; Ward and Kaplan, 2012).

Altogether, plants developed several strategies for the radial transport of nutrient with and their respective contribution may differ depending on the mobility of nutrients (Fig. 31).

Chapter 2

Conclusion

Altogether, the work done within the context of my PhD provides a detailed picture of the mechanism driving the degradation of IRT1 following a metal excess treatment. The cascade of events from the direct sensing of the non-iron substrates by a histidine-rich stretch, to the phosphorylation and, eventually the elongation of monoUb into K63 polyUb chains by the IDF1 E3 ligase allows the plant to degrade IRT1 in response to metal excess. The dual role of the different metal substrates in the regulation of IRT1 is quite unique. The transcriptional regulation by low iron allows the plant to uptake this element when it is limiting in soils. However, when the non-iron substrates are in high concentrations in the rhizosphere, the plant has elaborated an elegant mechanism to deplete IRT1 from the PM and to degrade it, avoiding the uptake of these potential harmful elements. This integrated control of IRT1 by its metal substrate is critical for proper plant responses to the availability of metals in soils. The post-translational control of IRT1 by non-iron metals highlights the danger associated with these highly reactive noxious heavy metals when present at high concentrations. Plants would rather starve for iron than risking the uptake of harmful elements. This phenomenon is certainly limiting the accumulation of zinc, manganese, cobalt or cadmium in the food chain but biotechnological perspectives would be necessary to further limit the accumulation of metals aspecifically transported by IRT1. Mutagenesis of certain residues in IRT1 do change its metal selectivity, notably mutation of the glutamic acid 111 mutated into alanine increases the specificity for iron (Rogers et al., 2000). Expressing such a mutant IRT1 version in plants may help lower the concentration of metal pollutants entering the food chain. In addition, phytoremediation strategies based on stabilized forms of IRT1 transporting Zn and Cd may also be implemented. However, these approaches have to be coupled to sequestration of metals to limit their toxicity and thereby maximize the biomass production and extraction capacities.

Bibliography

Abas, L., Benjamins, R., Malenica, N., Paciorek, T., Wiśniewska, J., Wirniewska, J., Moulinier-Anzola, J. C., Sieberer, T., Friml, J. and Luschnig, C. (2006). Intracellular trafficking and proteolysis of the Arabidopsis auxin-efflux facilitator PIN2 are involved in root gravitropism. Nat Cell Biol *8*, 249–256.

Agromayor, M. and Martin-Serrano, J. (2006). Interaction of AMSH with ESCRT-III and deubiquitination of endosomal cargo. J Biol Chem *281*, 23083–23091.

Alassimone, J., Fujita, S., Doblas, V. G., van Dop, M., Barberon, M., Kalmbach, L., Vermeer, J. E. M., Rojas-Murcia, N., Santuari, L., Hardtke, C. S. and Geldner, N. (2016). Polarly localized kinase SGN1 is required for Casparian strip integrity and positioning. Nature plants *2*, 16113.

Alassimone, J., Naseer, S. and Geldner, N. (2010). A developmental framework for endodermal differentiation and polarity. Proc Natl Acad Sci U S A *107*, 5214–5219.

Alvarez, C. E. (2008). On the origins of arrestin and rhodopsin. BMC evolutionary biology *8*, 222.

Amerik, A. Y., Nowak, J., Swaminathan, S. and Hochstrasser, M. (2000). The Doa4 deubiquitinating enzyme is functionally linked to the vacuolar protein-sorting and endocytic pathways. Mol Biol Cell *11*, 3365–3380.

Anderson, G. J. and Vulpe, C. D. (2009). Mammalian iron transport. Cellular and molecular life sciences : CMLS *66*, 3241–3261.

Aubry, L., Guetta, D. and Klein, G. (2009). The arrestin fold: variations on a theme. Current genomics *10*, 133–142.

Balk, J. and Schaedler, T. A. (2014). Iron cofactor assembly in plants. Annu Rev Plant Biol *65*, 125–153.

Banbury, D. N., Oakley, J. D., Sessions, R. B. and Banting, G. (2003). Tyrphostin A23 inhibits internalization of the transferrin receptor by perturbing the interaction between tyrosine motifs and the medium chain subunit of the AP-2 adaptor complex. J Biol Chem *278*, 12022–12028.

Bar, M. and Avni, A. (2009). EHD2 inhibits ligand-induced endocytosis and signaling of the leucine-rich repeat receptor-like protein LeEix2. Plant J *59*, 600–611.

Bibliography

Barberon, M., Dubeaux, G., Kolb, C., Isono, E., Zelazny, E. and Vert, G. (2014). Polarization of IRON-REGULATED TRANSPORTER 1 (IRT1) to the plant-soil interface plays crucial role in metal homeostasis. Proc Natl Acad Sci U S A *111*, 8293–8298.

Barberon, M. and Geldner, N. (2014). Radial transport of nutrients: the plant root as a polarized epithelium. Plant Physiology *166*, 528–537.

Barberon, M., Vermeer, J. E. M., De Bellis, D., Wang, P., Naseer, S., Andersen, T. G., Humbel, B. M., Nawrath, C., Takano, J., Salt, D. E. and Geldner, N. (2016). Adaptation of Root Function by Nutrient-Induced Plasticity of Endodermal Differentiation. Cell *164*, 447–459.

Barberon, M., Zelazny, E., Robert, S., Conejero, G., Curie, C., Friml, J. and Vert, G. (2011). Monoubiquitin-dependent endocytosis of the iron-regulated transporter 1 (IRT1) transporter controls iron uptake in plants. Proc Natl Acad Sci U S A *108*, E450–8.

Barbosa, I. C. R., Zourelidou, M., Willige, B. C., Weller, B. and Schwechheimer, C. (2014). D6 PROTEIN KINASE activates auxin transport-dependent growth and PIN-FORMED phosphorylation at the plasma membrane. Dev Cell *29*, 674–685.

Barriere, H., Nemes, C., Lechardeur, D., Khan-Mohammad, M., Fruh, K. and Lukacs, G. L. (2006). Molecular basis of oligoubiquitin-dependent internalization of membrane proteins in Mammalian cells. Traffic *7*, 282–297.

Bauer, M. and Pelkmans, L. (2006). A new paradigm for membrane-organizing and -shaping scaffolds. FEBS Lett *580*, 5559–5564.

Bays, N. W., Gardner, R. G., Seelig, L. P., Joazeiro, C. A. and Hampton, R. Y. (2001). Hrd1p/Der3p is a membrane-anchored ubiquitin ligase required for ER-associated degradation. Nat Cell Biol *3*, 24–29.

Becuwe, M. and Léon, S. (2014). Integrated control of transporter endocytosis and recycling by the arrestin-related protein Rod1 and the ubiquitin ligase Rsp5. eLife *3*.

Belgareh-Touzé, N., Léon, S., Erpapazoglou, Z., Stawiecka-Mirota, M., Urban-Grimal, D. and Haguenauer-Tsapis, R. (2008). Versatile role of the yeast ubiquitin ligase Rsp5p in intracellular trafficking. Biochem Soc Trans *36*, 791–796.

Ben-Saadon, R., Zaaroor, D., Ziv, T. and Ciechanover, A. (2006). The polycomb protein Ring1B generates self atypical mixed ubiquitin chains required for its in vitro histone H2A ligase activity. Molecular Cell *24*, 701–711.

Blondel, M.-O., Morvan, J., Dupré, S., Urban-Grimal, D., Haguenauer-Tsapis, R. and Volland, C. (2004). Direct sorting of the yeast uracil permease to the endosomal system is controlled by uracil binding and Rsp5p-dependent ubiquitylation. Mol Biol Cell *15*, 883–895.

Bolte, S. and Cordelières, F. P. (2006). A guided tour into subcellular colocalization analysis in light microscopy. Journal of Microscopy *224*, 213–232.

Bolte, S., Talbot, C., Boutte, Y., Catrice, O., Read, N. D. and Satiat-Jeunemaitre, B. (2004). FM-dyes as experimental probes for dissecting vesicle trafficking in living plant cells. Journal of Microscopy *214*, 159–173.

Bonifacino, J. S. and Glick, B. S. (2004). The mechanisms of vesicle budding and fusion. Cell *116*, 153–166.

Bonifacino, J. S., Suzuki, C. K., Lippincott-Schwartz, J., Weissman, A. M. and Klausner, R. D. (1989). Pre-Golgi degradation of newly synthesized T-cell antigen receptor chains: intrinsic sensitivity and the role of subunit assembly. J Cell Biol *109*, 73–83.

Bonifacino, J. S. and Traub, L. M. (2003). Signals for sorting of transmembrane proteins to endosomes and lysosomes. Annu Rev Biochem *72*, 395–447.

Borden, K. L. and Freemont, P. S. (1996). The RING finger domain: a recent example of a sequence-structure family. Current opinion in structural biology *6*, 395–401.

Boursiac, Y., Boudet, J., Postaire, O., Luu, D.-T., Tournaire-Roux, C. and Maurel, C. (2008). Stimulus-induced downregulation of root water transport involves reactive oxygen species-activated cell signalling and plasma membrane intrinsic protein internalization. Plant J *56*, 207–218.

Briat, J.-F., Dubos, C. and Gaymard, F. (2015). Iron nutrition, biomass production, and plant product quality. Trends Plant Sci *20*, 33–40.

Brumbarova, T., Brumbarova, T., Bauer, P., Bauer, P., Ivanov, R. and Ivanov, R. (2014). Molecular mechanisms governing Arabidopsis iron uptake. Trends Plant Sci *20*, 1–10.

Burd, C. G. and Emr, S. D. (1998). Phosphatidylinositol(3)-phosphate signaling mediated by specific binding to RING FYVE domains. Molecular Cell *2*, 157–162.

Callis, J. (2014). The Ubiquitination Machinery of the Ubiquitin System. The Arabidopsis Book *12*, e0174.

Carvalho, P., Stanley, A. M. and Rapoport, T. A. (2010). Retrotranslocation of a misfolded luminal ER protein by the ubiquitin-ligase Hrd1p. Cell *143*, 579–591.

Chaparro-Garcia, A., Schwizer, S., Sklenar, J., Yoshida, K., Petre, B., Bos, J. I. B., Schornack, S., Jones, A. M. E., Bozkurt, T. O. and Kamoun, S. (2015). Phytophthora infestans RXLR-WY Effector AVR3a Associates with Dynamin-Related Protein 2 Required for Endocytosis of the Plant Pattern Recognition Receptor FLS2. PLoS One *10*, e0137071.

Cheever, M. L., Sato, T. K., de Beer, T., Kutateladze, T. G., Emr, S. D. and Overduin, M. (2001). Phox domain interaction with PtdIns(3)P targets the Vam7 t-SNARE to vacuole membranes. Nat Cell Biol *3*, 613–618.

Chen, Q., Zhong, Y., Wu, Y., Liu, L., Wang, P., Liu, R., Cui, F., Li, Q., Yang, X., Fang, S. and Xie, Q. (2016). HRD1-mediated ERAD tuning of ER-bound E2 is conserved between plants and mammals. Nature plants *2*, 16094.

Bibliography

Chen, Y.-G. (2009). Endocytic regulation of TGF-beta signaling. Cell research *19*, 58–70.

Chen, Y.-Y., Wang, Y., Shin, L.-J., Wu, J.-F., Shanmugam, V., Tsednee, M., Lo, J.-C., Chen, C.-C., Wu, S.-H. and Yeh, K.-C. (2013). Iron is involved in the maintenance of circadian period length in Arabidopsis. Plant Physiology *161*, 1409–1420.

Cheng, S. H., Gregory, R. J., Marshall, J., Paul, S., Souza, D. W., White, G. A., O'Riordan, C. R. and Smith, A. E. (1990). Defective intracellular transport and processing of CFTR is the molecular basis of most cystic fibrosis. Cell *63*, 827–834.

Chinchilla, D., Zipfel, C., Robatzek, S., Kemmerling, B., Nürnberger, T., Jones, J. D. G., Felix, G. and Boller, T. (2007). A flagellin-induced complex of the receptor FLS2 and BAK1 initiates plant defence. Nature *448*, 497–500.

Chow, C.-M., Neto, H., Foucart, C. and Moore, I. (2008). Rab-A2 and Rab-A3 GTPases define a trans-golgi endosomal membrane domain in Arabidopsis that contributes substantially to the cell plate. The Plant Cell *20*, 101–123.

Clough, S. J. and Bent, A. F. (1998). Floral dip: a simplified method for Agrobacterium-mediated transformation of Arabidopsis thaliana. Plant J *16*, 735–743.

Colangelo, E. P. and Guerinot, M. L. (2004). The essential basic helix-loop-helix protein FIT1 is required for the iron deficiency response. The Plant Cell *16*, 3400–3412.

Colangelo, E. P. and Guerinot, M. L. (2006). Put the metal to the petal: metal uptake and transport throughout plants. Current Opinion in Plant Biology *9*, 322–330.

Collawn, J. F., Stangel, M., Kuhn, L. A., Esekogwu, V., Jing, S. Q., Trowbridge, I. S. and Tainer, J. A. (1990). Transferrin receptor internalization sequence YXRF implicates a tight turn as the structural recognition motif for endocytosis. Cell *63*, 1061–1072.

Connolly, E. L., Campbell, N. H., Grotz, N., Prichard, C. L. and Guerinot, M. L. (2003). Overexpression of the FRO2 ferric chelate reductase confers tolerance to growth on low iron and uncovers posttranscriptional control. Plant Physiol. *133*, 1102–1110.

Connolly, E. L., Fett, J. P. and Guerinot, M. L. (2002). Expression of the IRT1 metal transporter is controlled by metals at the levels of transcript and protein accumulation. The Plant Cell *14*, 1347–1357.

Cortese, K., Diaspro, A. and Tacchetti, C. (2009). Advanced correlative light/electron microscopy: current methods and new developments using Tokuyasu cryosections. The journal of histochemistry and cytochemistry : official journal of the Histochemistry Society *57*, 1103–1112.

Craig, A., Ewan, R., Mesmar, J., Gudipati, V. and Sadanandom, A. (2009). E3 ubiquitin ligases and plant innate immunity. J Exp Bot *60*, 1123–1132.

Crapeau, M., Merhi, A. and André, B. (2014). Stress conditions promote yeast Gap1 permease ubiquitylation and down-regulation via the arrestin-like Bul and Aly proteins. J Biol Chem *289*, 22103–22116.

Crump, C. M., Williams, J. L., Stephens, D. J. and Banting, G. (1998). Inhibition of the interaction between tyrosine-based motifs and the medium chain subunit of the AP-2 adaptor complex by specific tyrphostins. J Biol Chem *273*, 28073–28077.

Cui, F., Liu, L., Zhao, Q., Zhang, Z., Li, Q., Lin, B., Wu, Y., Tang, S. and Xie, Q. (2012). Arabidopsis ubiquitin conjugase UBC32 is an ERAD component that functions in brassinosteroid-mediated salt stress tolerance. Plant Cell *24*, 233–244.

Curie, C. and Briat, J.-F. (2003). Iron transport and signaling in plants. Annu Rev Plant Biol *54*, 183–206.

daSilva, L. L. P., Foresti, O. and Denecke, J. (2006). Targeting of the plant vacuolar sorting receptor BP80 is dependent on multiple sorting signals in the cytosolic tail. The Plant Cell *18*, 1477–1497.

David, Y., Ternette, N., Edelmann, M. J., Ziv, T., Gayer, B., Sertchook, R., Dadon, Y., Kessler, B. M. and Navon, A. (2011). E3 ligases determine ubiquitination site and conjugate type by enforcing specificity on E2 enzymes. J Biol Chem *286*, 44104–44115.

Dejonghe, W., Kuenen, S., Mylle, E., Vasileva, M., Keech, O., Viotti, C., Swerts, J., Fendrych, M., Ortiz-Morea, F. A., Mishev, K., Delang, S., Scholl, S., Zarza, X., Heilmann, M., Kourelis, J., Kasprowicz, J., Nguyen, L. S. L., Drozdzecki, A., Van Houtte, I., Szatmári, A.-M., Majda, M., Baisa, G., Bednarek, S. Y., Robert, S., Audenaert, D., Testerink, C., Munnik, T., Van Damme, D., Heilmann, I., Schumacher, K., Winne, J., Friml, J., Verstreken, P. and Russinova, E. (2016). Mitochondrial uncouplers inhibit clathrin-mediated endocytosis largely through cytoplasmic acidification. Nat Commun *7*, 11710.

Dettmer, J., Hong-Hermesdorf, A., Stierhof, Y.-D. and Schumacher, K. (2006). Vacuolar H+-ATPase activity is required for endocytic and secretory trafficking in Arabidopsis. The Plant Cell *18*, 715–730.

Dhonukshe, P., Aniento, F., Hwang, I., Robinson, D. G., Mravec, J., Stierhof, Y.-D. and Friml, J. (2007). Clathrin-mediated constitutive endocytosis of PIN auxin efflux carriers in Arabidopsis. Current Biology *17*, 520–527.

Di Rubbo, S., Irani, N. G., Kim, S. Y., Xu, Z.-Y., Gadeyne, A., Dejonghe, W., Vanhoutte, I., Persiau, G., Eeckhout, D., Simon, S., Song, K., Kleine-Vehn, J., Friml, J., De Jaeger, G., Van Damme, D., Hwang, I. and Russinova, E. (2013). The clathrin adaptor complex AP-2 mediates endocytosis of brassinosteroid insensitive1 in Arabidopsis. Plant Cell *25*, 2986–2997.

Doherty, G. J. and McMahon, H. T. (2009). Mechanisms of endocytosis. Annu Rev Biochem *78*, 857–902.

Donaldson, J. G. and Jackson, C. L. (2000). Regulators and effectors of the ARF GTPases. Curr Opin Cell Biol *12*, 475–482.

Donovan, A., Brownlie, A., Zhou, Y., Shepard, J., Pratt, S. J., Moynihan, J., Paw, B. H., Drejer, a., Barut, B., Zapata, a., Law, T. C., Brugnara, C., Lux, S. E., Pinkus, G. S., Pinkus, J. L., Kingsley, P. D., Palis, J., Fleming, M. D., Andrews, N. C. and Zon, L. I. (2000). Positional cloning of zebrafish ferroportin1 identifies a conserved vertebrate iron exporter. Nature *403*, 776–781.

Dores, M. R., Schnell, J. D., Maldonado-Baez, L., Wendland, B. and Hicke, L. (2010). The function of yeast epsin and Ede1 ubiquitin-binding domains during receptor internalization. Traffic *11*, 151–160.

Du, W., Tamura, K., Stefano, G. and Brandizzi, F. (2013). The integrity of the plant Golgi apparatus depends on cell growth-controlled activity of GNL1. Mol Plant *6*, 905–915.

Duckett, C., Oparka, K. J., Prior, D., Dolan, L. and Roberts, K. (1994). Dye-coupling in the root epidermis of Arabidopsis is progressively reduced during development. Development *120*, 3247–3255.

Dunn, R. and Hicke, L. (2001). Multiple roles for Rsp5p-dependent ubiquitination at the internalization step of endocytosis. J Biol Chem *276*, 25974–25981.

Dupre, S., Urban-Grimal, D. and Haguenauer-Tsapis, R. (2004). Ubiquitin and endocytic internalization in yeast and animal cells. Biochim Biophys Acta *1695*, 89–111.

Edelheit, O., Hanukoglu, A. and Hanukoglu, I. (2009). Simple and efficient site-directed mutagenesis using two single-primer reactions in parallel to generate mutants for protein structure-function studies. BMC Biotechnology *9*, 61.

Eide, D., Broderius, M., Fett, J. and Guerinot, M. L. (1996). A novel iron-regulated metal transporter from plants identified by functional expression in yeast. Proceedings of the National Academy of Sciences *93*, 5624–5628.

Ellson, C. D., Gobert-Gosse, S., Anderson, K. E., Davidson, K., Erdjument-Bromage, H., Tempst, P., Thuring, J. W., Cooper, M. A., Lim, Z. Y., Holmes, A. B., Gaffney, P. R., Coadwell, J., Chilvers, E. R., Hawkins, P. T. and Stephens, L. R. (2001). PtdIns(3)P regulates the neutrophil oxidase complex by binding to the PX domain of p40(phox). Nat Cell Biol *3*, 679–682.

Erpapazoglou, Z., Froissard, M., Nondier, I., Lesuisse, E., Haguenauer-Tsapis, R. and Belgareh-Touzé, N. (2008). Substrate- and ubiquitin-dependent trafficking of the yeast siderophore transporter Sit1. Traffic *9*, 1372–1391.

Erwee, M. G. and Goodwin, P. B. (1985). Symplast domains in extrastelar tissues of Egeria densa Planch. Planta *163*, 9–19.

Fan, L., Hao, H., Xue, Y., Zhang, L., Song, K., Ding, Z., Botella, M. A., Wang, H. and Lin, J. (2013). Dynamic analysis of Arabidopsis AP2 σ subunit reveals a key role in clathrin-mediated endocytosis and plant development. Development *140*, 3826–3837.

Bibliography

Fendrych, M., Synek, L., Pečenková, T., Drdová, E. J., Sekeres, J., De Rycke, R., Nowack, M. K. and Zárský, V. (2013). Visualization of the exocyst complex dynamics at the plasma membrane of Arabidopsis thaliana. Mol Biol Cell *24*, 510–520.

Foot, N. J., Dalton, H. E., Dorstyn, L., Shearwin-Whyatt, L. M., Tan, S.-S., Yang, B. and Kumar, S. (2008). Regulation of the divalent metal ion transporter DMT1 and iron homeostasis by a ubiquitin-dependent mechanism involving Ndfips and WWP2. Blood *112*, 4268–4275.

Foresti, O. and Denecke, J. (2008). Intermediate organelles of the plant secretory pathway: identity and function. Traffic *9*, 1599–1612.

Fortian, A., Dionne, L. K., Hong, S. H., Kim, W., Gygi, S. P., Watkins, S. C. and Sorkin, A. (2015). Endocytosis of Ubiquitylation-Deficient EGFR Mutants via Clathrin-Coated Pits is Mediated by Ubiquitylation. Traffic *16*, 1137–1154.

Friml, J., Yang, X., Michniewicz, M., Weijers, D., Quint, A., Tietz, O., Benjamins, R., Ouwerkerk, P. B. F., Ljung, K., Sandberg, G., Hooykaas, P. J. J., Palme, K. and Offringa, R. (2004). A PINOID-dependent binary switch in apical-basal PIN polar targeting directs auxin efflux. Science *306*, 862–865.

Fujimoto, M., Arimura, S.-i., Ueda, T., Takanashi, H., Hayashi, Y., Nakano, A. and Tsutsumi, N. (2010). Arabidopsis dynamin-related proteins DRP2B and DRP1A participate together in clathrin-coated vesicle formation during endocytosis. Proc Natl Acad Sci U S A *107*, 6094–6099.

Gadeyne, A., Sánchez-Rodríguez, C., Vanneste, S., Di Rubbo, S., Zauber, H., Vanneste, K., Van Leene, J., De Winne, N., Eeckhout, D., Persiau, G., Van De Slijke, E., Cannoot, B., Vercruysse, L., Mayers, J. R., Adamowski, M., Kania, U., Ehrlich, M., Schweighofer, A., Ketelaar, T., Maere, S., Bednarek, S. Y., Friml, J., Gevaert, K., Witters, E., Russinova, E., Persson, S., De Jaeger, G. and Van Damme, D. (2014). The TPLATE adaptor complex drives clathrin-mediated endocytosis in plants. Cell *156*, 691–704.

Galan, J. M. and Haguenauer-Tsapis, R. (1997). Ubiquitin lys63 is involved in ubiquitination of a yeast plasma membrane protein. EMBO J *16*, 5847–5854.

Galan, J. M., Moreau, V., Andre, B., Volland, C. and Haguenauer-Tsapis, R. (1996). Ubiquitination mediated by the Npi1p/Rsp5p ubiquitin-protein ligase is required for endocytosis of the yeast uracil permease. J Biol Chem *271*, 10946–10952.

Galcheva-Gargova, Z., Theroux, S. J. and Davis, R. J. (1995). The epidermal growth factor receptor is covalently linked to ubiquitin. Oncogene *11*, 2649–2655.

Gao, C., Luo, M., Zhao, Q., Yang, R., Cui, Y., Zeng, Y., Xia, J. and Jiang, L. (2014). A Unique Plant ESCRT Component, FREE1, Regulates Multivesicular Body Protein Sorting and Plant Growth. Curr Biol *24*, 2556–2563.

Gao, C., Zhuang, X., Cui, Y., Fu, X., He, Y., Zhao, Q., Zeng, Y., Shen, J., Luo, M. and Jiang, L. (2015). Dual roles of an Arabidopsis ESCRT component FREE1 in regulating vacuolar protein transport and autophagic degradation. Proc Natl Acad Sci U S A *112*, 1886–1891.

Gardner, R. G., Swarbrick, G. M., Bays, N. W., Cronin, S. R., Wilhovsky, S., Seelig, L., Kim, C. and Hampton, R. Y. (2000). Endoplasmic reticulum degradation requires lumen to cytosol signaling. Transmembrane control of Hrd1p by Hrd3p. J Cell Biol *151*, 69–82.

Gaullier, J. M., Ronning, E., Gillooly, D. J. and Stenmark, H. (2000). Interaction of the EEA1 FYVE finger with phosphatidylinositol 3-phosphate and early endosomes. Role of conserved residues. J Biol Chem *275*, 24595–24600.

Gaullier, J. M., Simonsen, A., D'Arrigo, A., Bremnes, B., Stenmark, H. and Aasland, R. (1998). FYVE fingers bind PtdIns(3)P. Nature *394*, 432–433.

Geldner, N., Anders, N., Wolters, H., Keicher, J., Kornberger, W., Muller, P., Delbarre, A., Ueda, T., Nakano, A. and Jurgens, G. (2003). The Arabidopsis GNOM ARF-GEF mediates endosomal recycling, auxin transport, and auxin-dependent plant growth. Cell *112*, 219–230.

Geldner, N., Dénervaud-Tendon, V., Hyman, D. L., Mayer, U., Stierhof, Y.-D. and Chory, J. (2009). Rapid, combinatorial analysis of membrane compartments in intact plants with a multicolor marker set. Plant J *59*, 169–178.

Geldner, N., Friml, J., Stierhof, Y. D., Jurgens, G. and Palme, K. (2001). Auxin transport inhibitors block PIN1 cycling and vesicle trafficking. Nature *413*, 425–428.

Geldner, N., Hyman, D. L., Wang, X., Schumacher, K. and Chory, J. (2007). Endosomal signaling of plant steroid receptor kinase BRI1. Genes Dev *21*, 1598–1602.

Geldner, N. and Robatzek, S. (2008). Plant receptors go endosomal: a moving view on signal transduction. Plant Physiol. *147*, 1565–1574.

Gershlick, D. C., Lousa, C. d. M., Foresti, O., Lee, A. J., Pereira, E. A., daSilva, L. L. P., Bottanelli, F. and Denecke, J. (2014). Golgi-dependent transport of vacuolar sorting receptors is regulated by COPII, AP1, and AP4 protein complexes in tobacco. Plant Cell *26*, 1308–1329.

Ghaddar, K., Merhi, A., Saliba, E., Krammer, E.-M., Prévost, M. and André, B. (2014). Substrate-induced ubiquitylation and endocytosis of yeast amino acid permeases. Mol. Cell Biol. *34*, 4447–4463.

Gietz, D., St Jean, A., Woods, R. A. and Schiestl, R. H. (1992). Improved method for high efficiency transformation of intact yeast cells. Nucleic Acids Res *20*, 1425.

Gillooly, D. J., Simonsen, A. and Stenmark, H. (2001). Cellular functions of phosphatidylinositol 3-phosphate and FYVE domain proteins. Biochem J *355*, 249–258.

Gitan, R. S. and Eide, D. J. (2000). Zinc-regulated ubiquitin conjugation signals endocytosis of the yeast ZRT1 zinc transporter. Biochem J *346 Pt 2*, 329–336.

Glebov, O. O., Bright, N. A. and Nichols, B. J. (2006). Flotillin-1 defines a clathrin-independent endocytic pathway in mammalian cells. Nat Cell Biol *8*, 46–54.

Bibliography

Goh, L. K., Huang, F., Kim, W., Gygi, S. and Sorkin, A. (2010). Multiple mechanisms collectively regulate clathrin-mediated endocytosis of the epidermal growth factor receptor. J Cell Biol *189*, 871–883.

Göhre, V., Spallek, T., Häweker, H., Mersmann, S., Mentzel, T., Boller, T., de Torres, M., Mansfield, J. W. and Robatzek, S. (2008). Plant pattern-recognition receptor FLS2 is directed for degradation by the bacterial ubiquitin ligase AvrPtoB. Curr Biol *18*, 1824–1832.

Goodman, O. B., Krupnick, J. G., Gurevich, V. V., Benovic, J. L. and Keen, J. H. (1997). Arrestin/clathrin interaction. Localization of the arrestin binding locus to the clathrin terminal domain. J Biol Chem *272*, 15017–15022.

Goodman, O. B., Krupnick, J. G., Santini, F., Gurevich, V. V., Penn, R. B., Gagnon, A. W., Keen, J. H. and Benovic, J. L. (1996). Beta-arrestin acts as a clathrin adaptor in endocytosis of the beta2-adrenergic receptor. Nature *383*, 447–450.

Green, L. S. and Rogers, E. E. (2004). FRD3 controls iron localization in Arabidopsis. Plant Physiol. *136*, 2523–2531.

Grossoehme, N. E., Akilesh, S., Guerinot, M. L. and Wilcox, D. E. (2006). Metal-binding thermodynamics of the histidine-rich sequence from the metal-transport protein IRT1 of Arabidopsis thaliana. Inorganic chemistry *45*, 8500–8508.

Guerinot, M. L. (2000). The ZIP family of metal transporters. Biochim Biophys Acta *1465*, 190–198.

Haas, T. J., Sliwinski, M. K., Martínez, D. E., Preuss, M., Ebine, K., Ueda, T., Nielsen, E., Odorizzi, G. and Otegui, M. S. (2007). The Arabidopsis AAA ATPase SKD1 is involved in multivesicular endosome function and interacts with its positive regulator LYST-INTERACTING PROTEIN5. The Plant Cell *19*, 1295–1312.

Hachez, C., Veljanovski, V., Reinhardt, H., Guillaumot, D., Vanhee, C., Chaumont, F. and Batoko, H. (2014). The Arabidopsis abiotic stress-induced TSPO-related protein reduces cell-surface expression of the aquaporin PIP2;7 through protein-protein interactions and autophagic degradation. Plant Cell *26*, 4974–4990.

Haglund, K., Sigismund, S., Polo, S., Szymkiewicz, I., Di Fiore, P. P. and Dikic, I. (2003). Multiple monoubiquitination of RTKs is sufficient for their endocytosis and degradation. Nat Cell Biol *5*, 461–466.

Hampton, R. Y. and Sommer, T. (2012). Finding the will and the way of ERAD substrate retrotranslocation. Curr Opin Cell Biol *24*, 460–466.

Haney, C. H. and Long, S. R. (2010). Plant flotillins are required for infection by nitrogen-fixing bacteria. Proc Natl Acad Sci U S A *107*, 478–483.

Hao, H., Fan, L., Chen, T., Li, R., Li, X., He, Q., Botella, M. A. and Lin, J. (2014). Clathrin and Membrane Microdomains Cooperatively Regulate RbohD Dynamics and Activity in Arabidopsis. Plant Cell *26*, 1729–1745.

Happel, N., Höning, S., Neuhaus, J.-M., Paris, N., Robinson, D. G. and Holstein, S. E. H. (2004). Arabidopsis mu A-adaptin interacts with the tyrosine motif of the vacuolar sorting receptor VSR-PS1. Plant J *37*, 678–693.

Hawryluk, M. J., Keyel, P. A., Mishra, S. K., Watkins, S. C., Heuser, J. E. and Traub, L. M. (2006). Epsin 1 is a polyubiquitin-selective clathrin-associated sorting protein. Traffic *7*, 262–281.

Hein, C., Springael, J. Y., Volland, C., Haguenauer-Tsapis, R. and Andre, B. (1995). NPl1, an essential yeast gene involved in induced degradation of Gap1 and Fur4 permeases, encodes the Rsp5 ubiquitin-protein ligase. Mol Microbiol *18*, 77–87.

Hendriks, I. A., D'Souza, R. C. J., Yang, B., Verlaan-de Vries, M., Mann, M. and Vertegaal, A. C. O. (2014). Uncovering global SUMOylation signaling networks in a site-specific manner. Nat Struct Mol Biol *21*, 927–936.

Herman, E. K., Walker, G., van der Giezen, M. and Dacks, J. B. (2011). Multivesicular bodies in the enigmatic amoeboflagellate Breviata anathema and the evolution of ESCRT 0. J Cell Sci *124*, 613–621.

Hicke, L. (2001). A new ticket for entry into budding vesicles-ubiquitin. Cell *106*, 527–530.

Hicke, L. and Dunn, R. (2003). Regulation of membrane protein transport by ubiquitin and ubiquitin-binding proteins. Annu Rev Cell Dev Biol *19*, 141–172.

Hicke, L. and Riezman, H. (1996). Ubiquitination of a yeast plasma membrane receptor signals its ligand-stimulated endocytosis. Cell *84*, 277–287.

Ho, C.-H., Lin, S.-H., Hu, H.-C. and Tsay, Y.-F. (2009). CHL1 functions as a nitrate sensor in plants. Cell *138*, 1184–1194.

Hofmann, R. M. and Pickart, C. M. (1999). Noncanonical MMS2-encoded ubiquitin-conjugating enzyme functions in assembly of novel polyubiquitin chains for DNA repair. Cell *96*, 645–653.

Holstein, S. E. H. (2002). Clathrin and plant endocytosis. Traffic *3*, 614–620.

Hong, S., Kim, S. A., Guerinot, M. L. and McClung, C. R. (2013). Reciprocal interaction of the circadian clock with the iron homeostasis network in Arabidopsis. Plant Physiology *161*, 893–903.

Hospenthal, M. K., Mevissen, T. E. T. and Komander, D. (2015). Deubiquitinase-based analysis of ubiquitin chain architecture using Ubiquitin Chain Restriction (UbiCRest). Nat Protoc *10*, 349–361.

Howitt, J., Putz, U., Lackovic, J., Doan, A., Dorstyn, L., Cheng, H., Yang, B., Chan-Ling, T., Silke, J., Kumar, S. and Tan, S.-S. (2009). Divalent metal transporter 1 (DMT1) regulation by Ndfip1 prevents metal toxicity in human neurons. Proc Natl Acad Sci U S A *106*, 15489–15494.

Huang, F., Goh, L. K. and Sorkin, A. (2007). EGF receptor ubiquitination is not necessary for its internalization. Proceedings of the National Academy of Sciences *104*, 16904–16909.

Huang, F., Kirkpatrick, D., Jiang, X., Gygi, S. and Sorkin, A. (2006). Differential regulation of EGF receptor internalization and degradation by multiubiquitination within the kinase domain. Molecular Cell *21*, 737–748.

Huang, F. and Sorkin, A. (2005). Growth factor receptor binding protein 2-mediated recruitment of the RING domain of Cbl to the epidermal growth factor receptor is essential and sufficient to support receptor endocytosis. Mol Biol Cell *16*, 1268–1281.

Huang, F., Zeng, X., Kim, W., Balasubramani, M., Fortian, A., Gygi, S. P., Yates, N. A. and Sorkin, A. (2013). Lysine 63-linked polyubiquitination is required for EGF receptor degradation. Proc Natl Acad Sci U S A *110*, 15722–15727.

Hurley, J. H. (2008). ESCRT complexes and the biogenesis of multivesicular bodies. Curr Opin Cell Biol *20*, 4–11.

Hwang, I. and Robinson, D. G. (2009). Transport vesicle formation in plant cells. Curr Opin Plant Biol *12*, 660–669.

Ichimura, Y., Kumanomidou, T., Sou, Y.-s., Mizushima, T., Ezaki, J., Ueno, T., Kominami, E., Yamane, T., Tanaka, K. and Komatsu, M. (2008). Structural basis for sorting mechanism of p62 in selective autophagy. J Biol Chem *283*, 22847–22857.

Irani, N. G., Di Rubbo, S., Mylle, E., Van den Begin, J., Schneider-Pizoń, J., Hniliková, J., Šíša, M., Buyst, D., Vilarrasa-Blasi, J., Szatmári, A.-M., Van Damme, D., Mishev, K., Codreanu, M.-C., Kohout, L., Strnad, M., Caño-Delgado, A. I., Friml, J., Madder, A. and Russinova, E. (2012). Fluorescent castasterone reveals BRI1 signaling from the plasma membrane. Nature chemical biology *8*, 583–589.

Isono, E., Katsiarimpa, A., Müller, I. K., Anzenberger, F., Stierhof, Y.-D., Geldner, N., Chory, J. and Schwechheimer, C. (2010). The deubiquitinating enzyme AMSH3 is required for intracellular trafficking and vacuole biogenesis in Arabidopsis thaliana. Plant Cell *22*, 1826–1837.

Ivanov, R., Brumbarova, T., Blum, A., Jantke, A.-M., Fink-Straube, C. and Bauer, P. (2014). SORTING NEXIN1 is required for modulating the trafficking and stability of the Arabidopsis IRON-REGULATED TRANSPORTER1. Plant Cell *26*, 1294–1307.

Jaillais, Y., Fobis-Loisy, I., Miege, C. and Gaude, T. (2008). Evidence for a sorting endosome in Arabidopsis root cells. Plant J *53*, 237–247.

Jaillais, Y., Fobis-Loisy, I., Miege, C., Rollin, C. and Gaude, T. (2006). AtSNX1 defines an endosome for auxin-carrier trafficking in Arabidopsis. Nature *443*, 106–109.

Jaillais, Y. and Gaude, T. (2007). Sorting out the sorting functions of endosomes in Arabidopsis. Plant Signaling & Behavior *2*, 556–558.

Jaillais, Y., Hothorn, M., Belkhadir, Y., Dabi, T., Nimchuk, Z. L., Meyerowitz, E. M. and Chory, J. (2011). Tyrosine phosphorylation controls brassinosteroid receptor activation by triggering membrane release of its kinase inhibitor. Genes Dev *25*, 232–237.

Jakoby, M., Wang, H.-Y., Reidt, W., Weisshaar, B. and Bauer, P. (2004). FRU (BHLH029) is required for induction of iron mobilization genes in Arabidopsis thaliana. FEBS Lett *577*, 528–534.

Jentsch, S. and Rumpf, S. (2007). Cdc48 (p97): a "molecular gearbox" in the ubiquitin pathway? Trends Biochem Sci *32*, 6–11.

Jiang, X. and Sorkin, A. (2003). Epidermal growth factor receptor internalization through clathrin-coated pits requires Cbl RING finger and proline-rich domains but not receptor polyubiquitylation. Traffic *4*, 529–543.

Jin, C. W., You, G. Y., He, Y. F., Tang, C., Wu, P. and Zheng, S. J. (2007a). Iron deficiency-induced secretion of phenolics facilitates the reutilization of root apoplastic iron in red clover. Plant Physiol. *144*, 278–285.

Jin, H., Yan, Z., Nam, K. H. and Li, J. (2007b). Allele-specific suppression of a defective brassinosteroid receptor reveals a physiological role of UGGT in ER quality control. Molecular Cell *26*, 821–830.

Johnson, A. and Vert, G. (2016). Unraveling K63 Polyubiquitination Networks by Sensor-Based Proteomics. Plant Physiology *171*, 1808–1820.

Kalinowska, K., Nagel, M.-K., Goodman, K., Cuyas, L., Anzenberger, F., Alkofer, A., Paz-Ares, J., Braun, P., Rubio, V., Otegui, M. S. and Isono, E. (2015). Arabidopsis ALIX is required for the endosomal localization of the deubiquitinating enzyme AMSH3. Proc Natl Acad Sci U S A *112*, E5543–51.

Kaminska, J., Gajewska, B., Hopper, A. K. and Zoładek, T. (2002). Rsp5p, a new link between the actin cytoskeleton and endocytosis in the yeast Saccharomyces cerevisiae. Mol. Cell Biol. *22*, 6946–6948.

Karahara, I., Suda, J., Tahara, H., Yokota, E., Shimmen, T., Misaki, K., Yonemura, S., Staehelin, L. A. and Mineyuki, Y. (2009). The preprophase band is a localized center of clathrin-mediated endocytosis in late prophase cells of the onion cotyledon epidermis. Plant J *57*, 819–831.

Kasai, K., Takano, J., Miwa, K., Toyoda, A. and Fujiwara, T. (2011). High boron-induced ubiquitination regulates vacuolar sorting of the BOR1 borate transporter in Arabidopsis thaliana. J Biol Chem *286*, 6175–6183.

Katsiarimpa, A., Anzenberger, F., Schlager, N., Neubert, S., Hauser, M.-T., Schwechheimer, C. and Isono, E. (2011). The Arabidopsis deubiquitinating enzyme AMSH3 interacts with ESCRT-III subunits and regulates their localization. Plant Cell *23*, 3026–3040.

Katsiarimpa, A., Kalinowska, K., Anzenberger, F., Weis, C., Ostertag, M., Tsutsumi, C., Schwechheimer, C., Brunner, F., Hückelhoven, R. and Isono, E. (2013). The deubiquitinating enzyme AMSH1 and the ESCRT-III subunit VPS2.1 are required for autophagic degradation in Arabidopsis. Plant Cell *25*, 2236–2252.

Katzmann, D. J., Babst, M. and Emr, S. D. (2001). Ubiquitin-Dependent Sorting into the Multivesicular Body Pathway Requires the Function of a Conserved Endosomal Protein Sorting Complex, ESCRT-I. Cell *106*, 145–155.

Kazazic, M., Bertelsen, V., Pedersen, K. W., Vuong, T. T., Grandal, M. V., Rødland, M. S., Traub, L. M., Stang, E. and Madshus, I. H. (2009). Epsin 1 is involved in recruitment of ubiquitinated EGF receptors into clathrin-coated pits. Traffic *10*, 235–245.

Kelly, B. T., McCoy, A. J., Späte, K., Miller, S. E., Evans, P. R., Höning, S. and Owen, D. J. (2008). A structural explanation for the binding of endocytic dileucine motifs by the AP2 complex. Nature *456*, 976–979.

Kelm, K. B., Huyer, G., Huang, J. C. and Michaelis, S. (2004). The internalization of yeast Ste6p follows an ordered series of events involving phosphorylation, ubiquitination, recognition and endocytosis. Traffic *5*, 165–180.

Kerk, D., Bulgrien, J., Smith, D. W., Barsam, B., Veretnik, S. and Gribskov, M. (2002). The complement of protein phosphatase catalytic subunits encoded in the genome of Arabidopsis. Plant Physiol. *129*, 908–925.

Kerkeb, L., Mukherjee, I., Chatterjee, I., Lahner, B., Salt, D. E. and Connolly, E. L. (2008). Iron-induced turnover of the Arabidopsis IRON-REGULATED TRANSPORTER1 metal transporter requires lysine residues. Plant Physiol. *146*, 1964–1973.

Kiba, T., Feria-Bourrellier, A.-B., Lafouge, F., Lezhneva, L., Boutet-Mercey, S., Orsel, M., Brehaut, V., Miller, A., Daniel-Vedele, F., Sakakibara, H. and Krapp, A. (2012). The Arabidopsis nitrate transporter NRT2.4 plays a double role in roots and shoots of nitrogen-starved plants. Plant Cell *24*, 245–258.

Kim, D.-Y., Scalf, M., Smith, L. M. and Vierstra, R. D. (2013). Advanced proteomic analyses yield a deep catalog of ubiquitylation targets in Arabidopsis. Plant Cell *25*, 1523–1540.

Kim, H. C. and Huibregtse, J. M. (2009). Polyubiquitination by HECT E3s and the determinants of chain type specificity. Mol. Cell Biol. *29*, 3307–3318.

Kim, H. T., Kim, K. P., Lledias, F., Kisselev, A. F., Scaglione, K. M., Skowyra, D., Gygi, S. P. and Goldberg, A. L. (2007). Certain pairs of ubiquitin-conjugating enzymes (E2s) and ubiquitin-protein ligases (E3s) synthesize nondegradable forked ubiquitin chains containing all possible isopeptide linkages. J Biol Chem *282*, 17375–17386.

Kim, S. Y., Xu, Z.-Y., Song, K., Kim, D. H., Kang, H., Reichardt, I., Sohn, E. J., Friml, J., Juergens, G. and Hwang, I. (2013). Adaptor protein complex 2-mediated endocytosis is crucial for male reproductive organ development in Arabidopsis. Plant Cell *25*, 2970–2985.

Kirchhausen, T. (2000). Clathrin. Annu Rev Biochem *69*, 699–727.

Kirchhausen, T. and Harrison, S. C. (1981). Protein organization in clathrin trimers. Cell *23*, 755–761.

Kirkin, V., Lamark, T., Sou, Y.-s., Bjørkøy, G., Nunn, J. L., Bruun, J.-A., Shvets, E., McEwan, D. G., Clausen, T. H., Wild, P., Bilusic, I., Theurillat, J.-P., Øvervatn, A., Ishii, T., Elazar, Z., Komatsu, M., Dikic, I. and Johansen, T. (2009). A role for NBR1 in autophagosomal degradation of ubiquitinated substrates. Mol Cell *33*, 505–516.

Kirst, M. E., Meyer, D. J., Gibbon, B. C., Jung, R. and Boston, R. S. (2005). Identification and characterization of endoplasmic reticulum-associated degradation proteins differentially affected by endoplasmic reticulum stress. Plant Physiol. *138*, 218–231.

Kitakura, S., Vanneste, S., Robert, S., Lofke, C., Teichmann, T., Tanaka, H. and Friml, J. (2011). Clathrin mediates endocytosis and polar distribution of PIN auxin transporters in Arabidopsis. Plant Cell *23*, 1920–1931.

Kleine-Vehn, J., Dhonukshe, P., Swarup, R., Bennett, M. and Friml, J. (2006). Subcellular trafficking of the Arabidopsis auxin influx carrier AUX1 uses a novel pathway distinct from PIN1. The Plant Cell *18*, 3171–3181.

Kleine-Vehn, J. and Friml, J. (2008). Polar targeting and endocytic recycling in auxin-dependent plant development. Annu Rev Cell Dev Biol *24*, 447–473.

Kleine-Vehn, J., Huang, F., Naramoto, S., Zhang, J., Michniewicz, M., Offringa, R. and Friml, J. (2009). PIN auxin efflux carrier polarity is regulated by PINOID kinase-mediated recruitment into GNOM-independent trafficking in Arabidopsis. Plant Cell *21*, 3839–3849.

Kleine-Vehn, J., Leitner, J., Zwiewka, M., Sauer, M., Abas, L., Luschnig, C. and Friml, J. (2008). Differential degradation of PIN2 auxin efflux carrier by retromer-dependent vacuolar targeting. Proc Natl Acad Sci U S A *105*, 17812–17817.

Kleine-Vehn, J., Wabnik, K., Martiniere, A., Langowski, L., Willig, K., Naramoto, S., Leitner, J., Tanaka, H., Jakobs, S., Robert, S., Luschnig, C., Govaerts, W., W Hell, S., Runions, J. and Friml, J. (2011). Recycling, clustering, and endocytosis jointly maintain PIN auxin carrier polarity at the plasma membrane. Mol Syst Biol *7*.

Kobayashi, T. and Nishizawa, N. K. (2012). Iron uptake, translocation, and regulation in higher plants. Annu Rev Plant Biol *63*, 131–152.

Kölling, R. and Hollenberg, C. P. (1994). The ABC-transporter Ste6 accumulates in the plasma membrane in a ubiquitinated form in endocytosis mutants. EMBO J *13*, 3261–3271.

Kolter, T. and Sandhoff, K. (2009). Lysosomal degradation of membrane lipids. FEBS Letters *584*, 1700–1712.

Komander, D. (2009). The emerging complexity of protein ubiquitination. Biochem Soc Trans *37*, 937–953.

König, S., Ischebeck, T., Lerche, J., Stenzel, I. and Heilmann, I. (2008). Salt-stress-induced association of phosphatidylinositol 4,5-bisphosphate with clathrin-coated vesicles in plants. Biochem J *415*, 387–399.

Korbei, B., Moulinier-Anzola, J., De-Araujo, L., Lucyshyn, D., Retzer, K., Khan, M. A. and Luschnig, C. (2013). Arabidopsis TOL proteins act as gatekeepers for vacuolar sorting of PIN2 plasma membrane protein. Curr Biol *23*, 2500–2505.

Korshunova, Y. O., Eide, D., Clark, W. G., Guerinot, M. L. and Pakrasi, H. B. (1999). The IRT1 protein from Arabidopsis thaliana is a metal transporter with a broad substrate range. Plant Mol. Biol. *40*, 37–44.

Koyano, F., Okatsu, K., Kosako, H., Tamura, Y., Go, E., Kimura, M., Kimura, Y., Tsuchiya, H., Yoshihara, H., Hirokawa, T., Endo, T., Fon, E. A., Trempe, J.-F., Saeki, Y., Tanaka, K. and Matsuda, N. (2014). Ubiquitin is phosphorylated by PINK1 to activate parkin. Nature *510*, 162–166.

Kozik, P., Francis, R. W., Seaman, M. N. J. and Robinson, M. S. (2010). A screen for endocytic motifs. Traffic *11*, 843–855.

Kraft, C., Peter, M. and Hofmann, K. (2010). Selective autophagy: ubiquitin-mediated recognition and beyond. Nat Cell Biol *12*, 836–841.

Kriegel, A., Andrés, Z., Medzihradszky, A., Krüger, F., Scholl, S., Delang, S., Patir-Nebioglu, M. G., Gute, G., Yang, H., Murphy, A. S., Peer, W. A., Pfeiffer, A., Krebs, M., Lohmann, J. U. and Schumacher, K. (2015). Job Sharing in the Endomembrane System: Vacuolar Acidification Requires the Combined Activity of V-ATPase and V-PPase. Plant Cell *27*, 3383–3396.

Krupnick, J. G., Goodman, O. B., Keen, J. H. and Benovic, J. L. (1997). Arrestin/clathrin interaction. Localization of the clathrin binding domain of nonvisual arrestins to the carboxy terminus. J Biol Chem *272*, 15011–15016.

Kuang, E., Qi, J. and Ronai, Z. (2013). Emerging roles of E3 ubiquitin ligases in autophagy. Trends Biochem Sci *38*, 453–460.

Kumar, K. G. S., Krolewski, J. J. and Fuchs, S. Y. (2004). Phosphorylation and specific ubiquitin acceptor sites are required for ubiquitination and degradation of the IFNAR1 subunit of type I interferon receptor. J Biol Chem *279*, 46614–46620.

Kurzchalia, T. V. and Parton, R. G. (1999). Membrane microdomains and caveolae. Curr Opin Cell Biol *11*, 424–431.

Lai, K., Bolognese, C. P., Swift, S. and McGraw, P. (1995). Regulation of inositol transport in Saccharomyces cerevisiae involves inositol-induced changes in permease stability and endocytic degradation in the vacuole. J Biol Chem *270*, 2525–2534.

Lam, B. C., Sage, T. L., Bianchi, F. and Blumwald, E. (2001). Role of SH3 domain-containing proteins in clathrin-mediated vesicle trafficking in Arabidopsis. The Plant Cell *13*, 2499–2512.

Langowski, L., Růzicka, K., Naramoto, S., Kleine-Vehn, J. and Friml, J. (2010). Trafficking to the outer polar domain defines the root-soil interface. Curr Biol *20*, 904–908.

Lauwers, E., Erpapazoglou, Z., Haguenauer-Tsapis, R. and André, B. (2010). The ubiquitin code of yeast permease trafficking. Trends Cell Biol *20*, 196–204.

Lauwers, E., Jacob, C. and André, B. (2009). K63-linked ubiquitin chains as a specific signal for protein sorting into the multivesicular body pathway. J Cell Biol *185*, 493–502.

Laxmi, A., Pan, J., Morsy, M. and Chen, R. (2008). Light plays an essential role in intracellular distribution of auxin efflux carrier PIN2 in Arabidopsis thaliana. PLoS One *3*, e1510.

Lazarovits, J. and Roth, M. (1988). A single amino acid change in the cytoplasmic domain allows the influenza virus hemagglutinin to be endocytosed through coated pits. Cell *53*, 743–752.

Le Bars, R., Marion, J., Le Borgne, R., Satiat-Jeunemaître, B. and Bianchi, M. W. (2014). ATG5 defines a phagophore domain connected to the endoplasmic reticulum during autophagosome formation in plants. Nat Commun *5*, 4121.

Lee, S.-C., Lan, W.-Z., Kim, B.-G., Li, L., Cheong, Y. H., Pandey, G. K., Lu, G., Buchanan, B. B. and Luan, S. (2007). A protein phosphorylation/dephosphorylation network regulates a plant potassium channel. Proceedings of the National Academy of Sciences *104*, 15959–15964.

Leitner, J., Petrášek, J., Tomanov, K., Retzer, K., Pařezová, M., Korbei, B., Bachmair, A., Zažímalová, E. and Luschnig, C. (2012). Lysine63-linked ubiquitylation of PIN2 auxin carrier protein governs hormonally controlled adaptation of Arabidopsis root growth. Proc Natl Acad Sci U S A *109*, 8322–8327.

Léon, S. and Haguenauer-Tsapis, R. (2009). Ubiquitin ligase adaptors: regulators of ubiquitylation and endocytosis of plasma membrane proteins. Experimental Cell Research *315*, 1574–1583.

Leshem, Y., Seri, L. and Levine, A. (2007). Induction of phosphatidylinositol 3-kinase-mediated endocytosis by salt stress leads to intracellular production of reactive oxygen species and salt tolerance. Plant J *51*, 185–197.

Letourneur, F. and Klausner, R. D. (1992). A novel di-leucine motif and a tyrosine-based motif independently mediate lysosomal targeting and endocytosis of CD3 chains. Cell *69*, 1143–1157.

Levkowitz, G., Waterman, H., Ettenberg, S. A., Katz, M., Tsygankov, A. Y., Alroy, I., Lavi, S., Iwai, K., Reiss, Y., Ciechanover, A., Lipkowitz, S. and Yarden, Y. (1999). Ubiquitin ligase activity and tyrosine phosphorylation underlie suppression of growth factor signaling by c-Cbl/Sli-1. Molecular Cell *4*, 1029–1040.

Levkowitz, G., Waterman, H., Zamir, E., Kam, Z., Oved, S., Langdon, W. Y., Beguinot, L., Geiger, B. and Yarden, Y. (1998). c-Cbl/Sli-1 regulates endocytic sorting and ubiquitination of the epidermal growth factor receptor. Genes Dev *12*, 3663–3674.

Li, J., Wen, J., Lease, K. A., Doke, J. T., Tax, F. E. and Walker, J. C. (2002). BAK1, an Arabidopsis LRR receptor-like protein kinase, interacts with BRI1 and modulates brassinosteroid signaling. Cell *110*, 213–222.

Li, J., Zhao-Hui, C., Batoux, M., Nekrasov, V., Roux, M., Chinchilla, D., Zipfel, C. and Jones, J. D. G. (2009). Specific ER quality control components required for biogenesis of the plant innate immune receptor EFR. Proc Natl Acad Sci U S A *106*, 15973–15978.

Li, M., Koshi, T. and Emr, S. D. (2015a). Membrane-anchored ubiquitin ligase complex is required for the turnover of lysosomal membrane proteins. J Cell Biol *25*, 3389.

Li, M., Rong, Y., Chuang, Y.-S., Peng, D. and Emr, S. D. (2015b). Ubiquitin-Dependent Lysosomal Membrane Protein Sorting and Degradation. Mol Cell *57*, 467–478.

Li, X., Wang, X., Yang, Y., Li, R., He, Q., Fang, X., Luu, D. T., Maurel, C. and Lin, J. (2011). Single-Molecule Analysis of PIP2;1 Dynamics and Partitioning Reveals Multiple Modes of Arabidopsis Plasma Membrane Aquaporin Regulation. The Plant Cell *23*, 3780–3797.

Lilley, B. N. and Ploegh, H. L. (2004). A membrane protein required for dislocation of misfolded proteins from the ER. Nature *429*, 834–840.

Lin, C. H., MacGurn, J. A., Chu, T., Stefan, C. J. and Emr, S. D. (2008). Arrestin-related ubiquitin-ligase adaptors regulate endocytosis and protein turnover at the cell surface. Cell *135*, 714–725.

Lingam, S., Mohrbacher, J., Brumbarova, T., Potuschak, T., Fink-Straube, C., Blondet, E., Genschik, P. and Bauer, P. (2011). Interaction between the bHLH transcription factor FIT and ETHYLENE INSENSITIVE3/ETHYLENE INSENSITIVE3-LIKE1 reveals molecular linkage between the regulation of iron acquisition and ethylene signaling in Arabidopsis. Plant Cell *23*, 1815–1829.

Liu, K. H., Huang, C. Y. and Tsay, Y. F. (1999). CHL1 is a dual-affinity nitrate transporter of Arabidopsis involved in multiple phases of nitrate uptake. The Plant Cell *11*, 865–874.

Liu, K.-H. and Tsay, Y.-F. (2003). Switching between the two action modes of the dual-affinity nitrate transporter CHL1 by phosphorylation. EMBO J *22*, 1005–1013.

Liu, Y. and Li, J. (2014). Endoplasmic reticulum-mediated protein quality control in Arabidopsis. Front Plant Sci *5*, 162.

Loerke, D., Mettlen, M., Yarar, D., Jaqaman, K., Jaqaman, H., Danuser, G. and Schmid, S. L. (2009). Cargo and dynamin regulate clathrin-coated pit maturation. PLoS Biol *7*, e57.

Lu, D., Lin, W., Gao, X., Wu, S., Cheng, C., Avila, J., Heese, A., Devarenne, T. P., He, P. and Shan, L. (2011). Direct ubiquitination of pattern recognition receptor FLS2 attenuates plant innate immunity. Science *332*, 1439–1442.

Luhtala, N. and Odorizzi, G. (2004). Bro1 coordinates deubiquitination in the multivesicular body pathway by recruiting Doa4 to endosomes. J Cell Biol *166*, 717–729.

Luschnig, C. and Vert, G. (2014). The dynamics of plant plasma membrane proteins: PINs and beyond. Development *141*, 2924–2938.

<center>*Bibliography*</center>

Luu, D.-T., Maurel, C., Martiniere, A., Sorieul, M. and Runions, J. (2011). Fluorescence recovery after photobleaching reveals high cycling dynamics of plasma membrane aquaporins in Arabidopsis roots under salt stress. The Plant Journal *69*, 894–905.

Ma, J. F., Tamai, K., Yamaji, N., Mitani, N., Konishi, S., Katsuhara, M., Ishiguro, M., Murata, Y. and Yano, M. (2006). A silicon transporter in rice. Nature *440*, 688–691.

Ma, J. F., Yamaji, N., Mitani, N., Tamai, K., Konishi, S., Fujiwara, T., Katsuhara, M. and Yano, M. (2007). An efflux transporter of silicon in rice. Nature *448*, 209–212.

Macia, E., Ehrlich, M., Massol, R., Boucrot, E., Brunner, C. and Kirchhausen, T. (2006). Dynasore, a cell-permeable inhibitor of dynamin. Dev Cell *10*, 839–850.

Madshus, I. H. and Stang, E. (2009). Internalization and intracellular sorting of the EGF receptor: a model for understanding the mechanisms of receptor trafficking. J Cell Sci *122*, 3433–3439.

Maierhofer, T., Diekmann, M., Offenborn, J. N., Lind, C., Bauer, H., Hashimoto, K., S Al-Rasheid, K. A., Luan, S., Kudla, J., Geiger, D. and Hedrich, R. (2014). Site- and kinase-specific phosphorylation-mediated activation of SLAC1, a guard cell anion channel stimulated by abscisic acid. Science signaling *7*, ra86–ra86.

Manning, G., Whyte, D. B., Martinez, R., Hunter, T. and Sudarsanam, S. (2002). The protein kinase complement of the human genome. Science *298*, 1912–1934.

Marchal, C., Haguenauer-Tsapis, R. and Urban-Grimal, D. (1998). A PEST-like sequence mediates phosphorylation and efficient ubiquitination of yeast uracil permease. Mol. Cell Biol. *18*, 314–321.

Marchal, C., Haguenauer-Tsapis, R. and Urban-Grimal, D. (2000). Casein kinase I-dependent phosphorylation within a PEST sequence and ubiquitination at nearby lysines signal endocytosis of yeast uracil permease. J Biol Chem *275*, 23608–23614.

Marquès-Bueno, M. M., Morao, A. K., Cayrel, A., Platre, M. P., Barberon, M., Caillieux, E., Colot, V., Jaillais, Y., Roudier, F. and Vert, G. (2016). A versatile Multisite Gateway-compatible promoter and transgenic line collection for cell type-specific functional genomics in Arabidopsis. Plant J *85*, 320–333.

Marshall, R. S., Li, F., Gemperline, D. C., Book, A. J. and Vierstra, R. D. (2015). Autophagic Degradation of the 26S Proteasome Is Mediated by the Dual ATG8/Ubiquitin Receptor RPN10 in Arabidopsis. Mol Cell *58*, 1053–1066.

Martiniere, A., Li, X., Runions, J., Lin, J., Maurel, C. and Luu, D.-T. (2012). Salt stress triggers enhanced cycling of Arabidopsis root plasma-membrane aquaporins. Plant Signal Behav *7*, 529–532.

Martins, S., Dohmann, E. M. N., Cayrel, A., Johnson, A., Fischer, W., Pojer, F., Satiat-Jeunemaître, B., Jaillais, Y., Chory, J., Geldner, N. and Vert, G. (2015). Internalization and vacuolar targeting of the brassinosteroid hormone receptor BRI1 are regulated by ubiquitination. Nat Commun *6*, 6151.

<center>140</center>

Matsuoka, K., Bassham, D. C., Raikhel, N. V. and Nakamura, K. (1995). Different sensitivity to wortmannin of two vacuolar sorting signals indicates the presence of distinct sorting machineries in tobacco cells. J Cell Biol *130*, 1307–1318.

Mbengue, M., Bourdais, G., Gervasi, F., Beck, M., Zhou, J., Spallek, T., Bartels, S., Boller, T., Ueda, T., Kuhn, H. and Robatzek, S. (2016). Clathrin-dependent endocytosis is required for immunity mediated by pattern recognition receptor kinases. Proc Natl Acad Sci U S A *113*, 11034–11039.

McGough, I. J. and Cullen, P. J. (2011). Recent advances in retromer biology. Traffic *12*, 963–971.

McMahon, H. T. and Boucrot, E. (2011). Molecular mechanism and physiological functions of clathrin-mediated endocytosis. Nat Rev Mol Cell Biol *12*, 517–533.

Melikova, M. S., Kondratov, K. A. and Kornilova, E. S. (2006). Two different stages of epidermal growth factor (EGF) receptor endocytosis are sensitive to free ubiquitin depletion produced by proteasome inhibitor MG132. Cell biology international *30*, 31–43.

Merhi, A. and André, B. (2012). Internal amino acids promote Gap1 permease ubiquitylation via TORC1/Npr1/14-3-3-dependent control of the Bul arrestin-like adaptors. Mol. Cell Biol. *32*, 4510–4522.

Meusser, B., Hirsch, C., Jarosch, E. and Sommer, T. (2005). ERAD: the long road to destruction. Nat Cell Biol *7*, 766–772.

Mevissen, T. E. T., Hospenthal, M. K., Geurink, P. P., Elliott, P. R., Akutsu, M., Arnaudo, N., Ekkebus, R., Kulathu, Y., Wauer, T., El Oualid, F., Freund, S. M. V., Ovaa, H. and Komander, D. (2013). OTU deubiquitinases reveal mechanisms of linkage specificity and enable ubiquitin chain restriction analysis. Cell *154*, 169–184.

Michaeli, S., Galili, G., Genschik, P., Fernie, A. R. and Avin-Wittenberg, T. (2016). Autophagy in Plants–What's New on the Menu? Trends Plant Sci *21*, 134–144.

Michniewicz, M., Zago, M. K., Abas, L., Weijers, D., Schweighofer, A., Meskiene, I., Heisler, M. G., Ohno, C., Zhang, J., Huang, F., Schwab, R., Weigel, D., Meyerowitz, E. M., Luschnig, C., Offringa, R. and Friml, J. (2007). Antagonistic regulation of PIN phosphorylation by PP2A and PINOID directs auxin flux. Cell *130*, 1044–1056.

Miwa, K., Takano, J., Omori, H., Seki, M., Shinozaki, K. and Fujiwara, T. (2007). Plants tolerant of high boron levels. Science *318*, 1417–1417.

Miyauchi, K., Kim, Y., Latinovic, O., Morozov, V. and Melikyan, G. B. (2009). HIV enters cells via endocytosis and dynamin-dependent fusion with endosomes. Cell *137*, 433–444.

Mizushima, N. and Komatsu, M. (2011). Autophagy: renovation of cells and tissues. Cell *147*, 728–741.

Mizushima, N., Yoshimori, T. and Ohsumi, Y. (2011). The role of Atg proteins in autophagosome formation. Annu Rev Cell Dev Biol *27*, 107–132.

Morrissey, J., Baxter, I. R., Lee, J., Li, L., Lahner, B., Grotz, N., Kaplan, J., Salt, D. E. and Guerinot, M. L. (2009). The ferroportin metal efflux proteins function in iron and cobalt homeostasis in Arabidopsis. Plant Cell *21*, 3326–3338.

Murashige, T. and Skoog, F. (1962). A Revised Medium for Rapid Growth and Bio Assays with Tobacco Tissue Cultures. Physiologia Plantarum *15*, 473–497.

Nam, K. H. and Li, J. (2002). BRI1/BAK1, a receptor kinase pair mediating brassinosteroid signaling. Cell *110*, 203–212.

Naramoto, S., Kleine-Vehn, J., Robert, S., Fujimoto, M., Dainobu, T., Paciorek, T., Ueda, T., Nakano, A., Van Montagu, M. C. E., Fukuda, H. and Friml, J. (2010). ADP-ribosylation factor machinery mediates endocytosis in plant cells. Proc Natl Acad Sci U S A *107*, 21890–21895.

Naramoto, S., Otegui, M. S., Kutsuna, N., De Rycke, R., Dainobu, T., Karampelias, M., Fujimoto, M., Feraru, E., Miki, D., Fukuda, H., Nakano, A. and Friml, J. (2014). Insights into the localization and function of the membrane trafficking regulator GNOM ARF-GEF at the Golgi apparatus in Arabidopsis. Plant Cell *26*, 3062–3076.

Nielsen, E., Cheung, A. Y. and Ueda, T. (2008). The regulatory RAB and ARF GTPases for vesicular trafficking. Plant Physiol. *147*, 1516–1526.

Nielsen, M., Albrethsen, J., Larsen, F. H. and Skriver, K. (2006). The Arabidopsis ADP-ribosylation factor (ARF) and ARF-like (ARL) system and its regulation by BIG2, a large ARF–GEF. Plant Science *171*, 707–717.

Niemes, S., Langhans, M., Viotti, C., Scheuring, D., San Wan Yan, M., Jiang, L., Hillmer, S., Robinson, D. G. and Pimpl, P. (2010). Retromer recycles vacuolar sorting receptors from the trans-Golgi network. Plant J *61*, 107–121.

Nies, D. H. (2003). Efflux-mediated heavy metal resistance in prokaryotes. FEMS microbiology reviews *27*, 313–339.

Nikko, E. and André, B. (2007). Evidence for a direct role of the Doa4 deubiquitinating enzyme in protein sorting into the MVB pathway. Traffic *8*, 566–581.

Nikko, E., Marini, A.-M. and André, B. (2003). Permease recycling and ubiquitination status reveal a particular role for Bro1 in the multivesicular body pathway. J Biol Chem *278*, 50732–50743.

Nikko, E., Sullivan, J. A. and Pelham, H. R. B. (2008). Arrestin-like proteins mediate ubiquitination and endocytosis of the yeast metal transporter Smf1. EMBO Rep *9*, 1216–1221.

Nishida, S., Tsuzuki, C., Kato, A., Aisu, A., Yoshida, J. and Mizuno, T. (2011). AtIRT1, the primary iron uptake transporter in the root, mediates excess nickel accumulation in Arabidopsis thaliana. Plant & Cell Physiology *52*, 1433–1442.

Nito, K., Wong, C. C. L., Yates, J. R. and Chory, J. (2013). Tyrosine phosphorylation regulates the activity of phytochrome photoreceptors. Cell reports *3*, 1970–1979.

Nozoye, T., Nagasaka, S., Bashir, K., Takahashi, M., Kobayashi, T., Nakanishi, H. and Nishizawa, N. K. (2014). Nicotianamine synthase 2 localizes to the vesicles of iron-deficient rice roots, and its mutation in the YXXφ or LL motif causes the disruption of vesicle formation or movement in rice. Plant J *77*, 246–260.

Obita, T., Saksena, S., Ghazi-Tabatabai, S., Gill, D. J., Perisic, O., Emr, S. D. and Williams, R. L. (2007). Structural basis for selective recognition of ESCRT-III by the AAA ATPase Vps4. Nature *449*, 735–739.

Odorizzi, G., Babst, M. and Emr, S. D. (1998). Fab1p PtdIns(3)P 5-kinase function essential for protein sorting in the multivesicular body. Cell *95*, 847–858.

Ohno, H., Stewart, J., Fournier, M. C., Bosshart, H., Rhee, I., Miyatake, S., Saito, T., Gallusser, A., Kirchhausen, T. and Bonifacino, J. S. (1995). Interaction of tyrosine-based sorting signals with clathrin-associated proteins. Science *269*, 1872–1875.

Oliviusson, P., Heinzerling, O., Hillmer, S., Hinz, G., Tse, Y. C., Jiang, L. and Robinson, D. G. (2006). Plant retromer, localized to the prevacuolar compartment and microvesicles in Arabidopsis, may interact with vacuolar sorting receptors. The Plant Cell *18*, 1239–1252.

Olsen, J. V., Blagoev, B., Gnad, F., Macek, B., Kumar, C., Mortensen, P. and Mann, M. (2006). Global, in vivo, and site-specific phosphorylation dynamics in signaling networks. Cell *127*, 635–648.

Olusanya, O., Andrews, P. D., Swedlow, J. R. and Smythe, E. (2001). Phosphorylation of threonine 156 of the mu2 subunit of the AP2 complex is essential for endocytosis in vitro and in vivo. Current Biology *11*, 896–900.

Olzmann, J. A. and Chin, L.-S. (2008). Parkin-mediated K63-linked polyubiquitination: a signal for targeting misfolded proteins to the aggresome-autophagy pathway. Autophagy *4*, 85–87.

Onelli, E., Prescianotto-Baschong, C., Caccianiga, M. and Moscatelli, A. (2008). Clathrin-dependent and independent endocytic pathways in tobacco protoplasts revealed by labelling with charged nanogold. J Exp Bot *59*, 3051–3068.

Oorschot, V. M. J., Sztal, T. E., Bryson-Richardson, R. J. and Ramm, G. (2014). Immuno correlative light and electron microscopy on Tokuyasu cryosections. Methods in cell biology *124*, 241–258.

Ortiz-Morea, F. A., Savatin, D. V., Dejonghe, W., Kumar, R., Luo, Y., Adamowski, M., Van den Begin, J., Dressano, K., Pereira de Oliveira, G., Zhao, X., Lu, Q., Madder, A., Friml, J., Scherer de Moura, D. and Russinova, E. (2016). Danger-associated peptide signaling in Arabidopsis requires clathrin. Proc Natl Acad Sci U S A *113*, 11028–11033.

Ortiz-Zapater, E., Soriano-Ortega, E., Marcote, M. J., Ortiz-Masiá, D. and Aniento, F. (2006). Trafficking of the human transferrin receptor in plant cells: effects of tyrphostin A23 and brefeldin A. Plant J *48*, 757–770.

Otegui, M. S. and Spitzer, C. (2008). Endosomal functions in plants. Traffic *9*, 1589–1598.

Owen, D. J. and Evans, P. R. (1998). A structural explanation for the recognition of tyrosine-based endocytotic signals. Science *282*, 1327–1332.

Paez Valencia, J., Goodman, K. and Otegui, M. S. (2016). Endocytosis and Endosomal Trafficking in Plants. Annu Rev Plant Biol *67*, 309–335.

Paiva, S., Vieira, N., Nondier, I., Haguenauer-Tsapis, R., Casal, M. and Urban-Grimal, D. (2009). Glucose-induced ubiquitylation and endocytosis of the yeast Jen1 transporter: role of lysine 63-linked ubiquitin chains. J Biol Chem *284*, 19228–19236.

Pankiv, S., Clausen, T. H., Lamark, T., Brech, A., Bruun, J.-A., Outzen, H., Øvervatn, A., Bjørkøy, G. and Johansen, T. (2007). p62/SQSTM1 binds directly to Atg8/LC3 to facilitate degradation of ubiquitinated protein aggregates by autophagy. J Biol Chem *282*, 24131–24145.

Park, M., Song, K., Reichardt, I., Kim, H., Mayer, U., Stierhof, Y.-D., Hwang, I. and Jurgens, G. (2013). Arabidopsis μ-adaptin subunit AP1M of adaptor protein complex 1 mediates late secretory and vacuolar traffic and is required for growth. Proc Natl Acad Sci U S A *110*, 10318–10323.

Paul, M. J. and Frigerio, L. (2007). Coated vesicles in plant cells. Seminars in cell & developmental biology *18*, 471–478.

Pawson, T. and Scott, J. D. (2005). Protein phosphorylation in signaling–50 years and counting. Trends Biochem Sci *30*, 286–290.

Peng, J., Schwartz, D., Elias, J. E., Thoreen, C. C., Cheng, D., Marsischky, G., Roelofs, J., Finley, D. and Gygi, S. P. (2003). A proteomics approach to understanding protein ubiquitination. Nat Biotechnol *21*, 921–926.

Pérez-Gómez, J. and Moore, I. (2007). Plant endocytosis: it is clathrin after all. Current Biology *17*, R217–9.

Perret, E., Lakkaraju, A., Deborde, S., Schreiner, R. and Rodriguez-Boulan, E. (2005). Evolving endosomes: how many varieties and why? Curr Opin Cell Biol *17*, 423–434.

Pfister, A., Barberon, M., Alassimone, J., Kalmbach, L., Lee, Y., Vermeer, J. E. M., Yamazaki, M., Li, G., Maurel, C., Takano, J., Kamiya, T., Salt, D. E., Roppolo, D. and Geldner, N. (2014). A receptor-like kinase mutant with absent endodermal diffusion barrier displays selective nutrient homeostasis defects. eLife *3*, e03115.

Pickart, C. M. and Fushman, D. (2004). Polyubiquitin chains: polymeric protein signals. Curr Opin Chem Biol *8*, 610–616.

Pilon, M., Schekman, R. and Römisch, K. (1997). Sec61p mediates export of a misfolded secretory protein from the endoplasmic reticulum to the cytosol for degradation. EMBO J *16*, 4540–4548.

Pinheiro, H., Samalova, M., Geldner, N., Chory, J., Martinez, A. and Moore, I. (2009). Genetic evidence that the higher plant Rab-D1 and Rab-D2 GTPases exhibit distinct but overlapping interactions in the early secretory pathway. J Cell Sci *122*, 3749–3758.

Pourcher, M., Santambrogio, M., Thazar, N., Thierry, A.-M., Fobis-Loisy, I., Miege, C., Jaillais, Y. and Gaude, T. (2010). Analyses of sorting nexins reveal distinct retromer-subcomplex functions in development and protein sorting in Arabidopsis thaliana. Plant Cell *22*, 3980–3991.

Puig, S. and Peñarrubia, L. (2009). Placing metal micronutrients in context: transport and distribution in plants. Curr Opin Plant Biol *12*, 299–306.

Raiborg, C. and Stenmark, H. (2009). The ESCRT machinery in endosomal sorting of ubiquitylated membrane proteins. Nature *458*, 445–452.

Rancour, D. M., Dickey, C. E., Park, S. and Bednarek, S. Y. (2002). Characterization of AtCDC48. Evidence for multiple membrane fusion mechanisms at the plane of cell division in plants. Plant Physiol. *130*, 1241–1253.

Raths, S., Rohrer, J., Crausaz, F. and Riezman, H. (1993). end3 and end4: two mutants defective in receptor-mediated and fluid-phase endocytosis in Saccharomyces cerevisiae. J Cell Biol *120*, 55–65.

Reggiori, F. and Klionsky, D. J. (2013). Autophagic processes in yeast: mechanism, machinery and regulation. Genetics *194*, 341–361.

Reggiori, F. and Pelham, H. R. (2001). Sorting of proteins into multivesicular bodies: ubiquitin-dependent and -independent targeting. EMBO J *20*, 5176–5186.

Reichardt, I., Stierhof, Y.-D., Mayer, U., Richter, S., Schwarz, H., Schumacher, K. and Jurgens, G. (2007). Plant cytokinesis requires de novo secretory trafficking but not endocytosis. Current Biology *17*, 2047–2053.

Reiter, E. and Lefkowitz, R. J. (2006). GRKs and beta-arrestins: roles in receptor silencing, trafficking and signaling. Trends in endocrinology and metabolism: TEM *17*, 159–165.

Richter, C. M., West, M. and Odorizzi, G. (2013). Doa4 function in ILV budding is restricted through its interaction with the Vps20 subunit of ESCRT-III. J Cell Sci *126*, 1881–1890.

Richter, S., Geldner, N., Schrader, J., Wolters, H., Stierhof, Y.-D., Rios, G., Koncz, C., Robinson, D. G. and Jurgens, G. (2007). Functional diversification of closely related ARF-GEFs in protein secretion and recycling. Nature *448*, 488–492.

Ricotta, D., Conner, S. D., Schmid, S. L., von Figura, K. and Höning, S. (2002). Phosphorylation of the AP2 mu subunit by AAK1 mediates high affinity binding to membrane protein sorting signals. J Cell Biol *156*, 791–795.

Robatzek, S., Chinchilla, D. and Boller, T. (2006). Ligand-induced endocytosis of the pattern recognition receptor FLS2 in Arabidopsis. Genes Dev *20*, 537–542.

Robinson, D. G. (2015). Endocytosis: Is There Really a Recycling from Late Endosomes? Mol Plant *8*, 1554–1556.

Robinson, D. G., Jiang, L. and Schumacher, K. (2008). The endosomal system of plants: charting new and familiar territories. Plant Physiol. *147*, 1482–1492.

Robinson, N. J., Procter, C. M., Connolly, E. L. and Guerinot, M. L. (1999). A ferric-chelate reductase for iron uptake from soils. Nature *397*, 694–697.

Rogers, E. E., Eide, D. J. and Guerinot, M. L. (2000). Altered selectivity in an Arabidopsis metal transporter. Proceedings of the National Academy of Sciences *97*, 12356–12360.

Ron, M. and Avni, A. (2004). The receptor for the fungal elicitor ethylene-inducing xylanase is a member of a resistance-like gene family in tomato. The Plant Cell *16*, 1604–1615.

Roppolo, D., De Rybel, B., Dénervaud-Tendon, V., Pfister, A., Alassimone, J., Vermeer, J. E. M., Yamazaki, M., Stierhof, Y.-D., Beeckman, T. and Geldner, N. (2011). A novel protein family mediates Casparian strip formation in the endodermis. Nature *473*, 380–383.

Russinova, E., Borst, J. W., Kwaaitaal, M., Caño-Delgado, A., Yin, Y., Chory, J. and de Vries, S. C. (2004). Heterodimerization and endocytosis of Arabidopsis brassinosteroid receptors BRI1 and AtSERK3 (BAK1). The Plant Cell *16*, 3216–3229.

Salomé, P. A., Oliva, M., Weigel, D. and Krämer, U. (2013). Circadian clock adjustment to plant iron status depends on chloroplast and phytochrome function. EMBO J *32*, 511–523.

Santi, S. and Schmidt, W. (2009). Dissecting iron deficiency-induced proton extrusion in Arabidopsis roots. New Phytol *183*, 1072–1084.

Saslowsky, D. E., Cho, J. A., Chinnapen, H., Massol, R. H., Chinnapen, D. J.-F., Wagner, J. S., De Luca, H. E., Kam, W., Paw, B. H. and Lencer, W. I. (2010). Intoxication of zebrafish and mammalian cells by cholera toxin depends on the flotillin/reggie proteins but not Derlin-1 or -2. The Journal of clinical investigation *120*, 4399–4409.

Schaaf, G., Honsbein, A., Meda, A. R., Kirchner, S., Wipf, D. and von Wirén, N. (2006). AtIREG2 encodes a tonoplast transport protein involved in iron-dependent nickel detoxification in Arabidopsis thaliana roots. J Biol Chem *281*, 25532–25540.

Schellmann, S. and Pimpl, P. (2009). Coats of endosomal protein sorting: retromer and ESCRT. Curr Opin Plant Biol *12*, 670–676.

Scheuring, D., Viotti, C., Krüger, F., Künzl, F., Sturm, S., Bubeck, J., Hillmer, S., Frigerio, L., Robinson, D. G., Pimpl, P. and Schumacher, K. (2011). Multivesicular bodies mature from the trans-Golgi network/early endosome in Arabidopsis. Plant Cell *23*, 3463–3481.

Schlossman, D. M., Schmid, S. L., Braell, W. A. and Rothman, J. E. (1984). An enzyme that removes clathrin coats: purification of an uncoating ATPase. J Cell Biol *99*, 723–733.

Schmid, N. B., Giehl, R. F. H., Doll, S., Mock, H. P., Strehmel, N., Scheel, D., Kong, X., Hider, R. C. and von Wiren, N. (2014). Feruloyl-CoA 6'-Hydroxylase1-Dependent Coumarins Mediate Iron Acquisition from Alkaline Substrates in Arabidopsis. Plant Physiol. *164*, 160–172.

Schmidt, O. and Teis, D. (2012). The ESCRT machinery. Curr Biol *22*, R116–20.

Schroeder, B., Srivatsan, S., Shaw, A., Billadeau, D. and McNiven, M. A. (2012). CIN85 phosphorylation is essential for EGFR ubiquitination and sorting into multivesicular bodies. Mol Biol Cell *23*, 3602–3611.

Séguéla, M., Briat, J.-F., Vert, G. and Curie, C. (2008). Cytokinins negatively regulate the root iron uptake machinery in Arabidopsis through a growth-dependent pathway. Plant J *55*, 289–300.

Semerdjieva, S., Shortt, B., Maxwell, E., Singh, S., Fonarev, P., Hansen, J., Schiavo, G., Grant, B. D. and Smythe, E. (2008). Coordinated regulation of AP2 uncoating from clathrin-coated vesicles by rab5 and hRME-6. J Cell Biol *183*, 499–511.

Sette, P., Jadwin, J. A., Dussupt, V., Bello, N. F. and Bouamr, F. (2010). The ESCRT-associated protein Alix recruits the ubiquitin ligase Nedd4-1 to facilitate HIV-1 release through the LYPXnL L domain motif. Journal of virology *84*, 8181–8192.

Sharfman, M., Bar, M., Ehrlich, M., Schuster, S., Melech-Bonfil, S., Ezer, R., Sessa, G. and Avni, A. (2011). Endosomal signaling of the tomato leucine-rich repeat receptor-like protein LeEix2. Plant J *68*, 413–423.

Shenoy, S. K., McDonald, P. H., Kohout, T. A. and Lefkowitz, R. J. (2001). Regulation of receptor fate by ubiquitination of activated beta 2-adrenergic receptor and beta-arrestin. Science *294*, 1307–1313.

Shenoy, S. K., Xiao, K., Venkataramanan, V., Snyder, P. M., Freedman, N. J. and Weissman, A. M. (2008). Nedd4 mediates agonist-dependent ubiquitination, lysosomal targeting, and degradation of the beta2-adrenergic receptor. J Biol Chem *283*, 22166–22176.

Shin, L.-J., Lo, J.-C., Chen, G.-H., Callis, J., Fu, H. and Yeh, K.-C. (2013). IRT1 degradation factor1, a ring E3 ubiquitin ligase, regulates the degradation of iron-regulated transporter1 in Arabidopsis. Plant Cell *25*, 3039–3051.

Sieben, C., Mikosch, M., Brandizzi, F. and Homann, U. (2008). Interaction of the K(+)-channel KAT1 with the coat protein complex II coat component Sec24 depends on a di-acidic endoplasmic reticulum export motif. Plant J *56*, 997–1006.

Sigismund, S., Woelk, T., Puri, C., Maspero, E., Tacchetti, C., Transidico, P., Di Fiore, P. P. and Polo, S. (2005). Clathrin-independent endocytosis of ubiquitinated cargos. Proceedings of the National Academy of Sciences *102*, 2760–2765.

Simon, M. L. A., Platre, M. P., Assil, S., van Wijk, R., Chen, W. Y., Chory, J., Dreux, M., Munnik, T. and Jaillais, Y. (2014). A multi-colour/multi-affinity marker set to visualize phosphoinositide dynamics in Arabidopsis. Plant J *77*, 322–337.

Singh, R. K., Zerath, S., Kleifeld, O., Scheffner, M., Glickman, M. H. and Fushman, D. (2012). Recognition and cleavage of related to ubiquitin 1 (Rub1) and Rub1-ubiquitin chains by components of the ubiquitin-proteasome system. Molecular & cellular proteomics : MCP *11*, 1595–1611.

Sivitz, A., Grinvalds, C., Barberon, M., Curie, C. and Vert, G. (2011). Proteasome-mediated turnover of the transcriptional activator FIT is required for plant iron-deficiency responses. Plant J *66*, 1044–1052.

Sivitz, A. B., Hermand, V., Curie, C. and Vert, G. (2012). Arabidopsis bHLH100 and bHLH101 control iron homeostasis via a FIT-independent pathway. PLoS One *7*, e44843.

Smalle, J., Vierstra, R. D., Smalle, J. and Vierstra, R. D. (2004). The ubiquitin 26S proteasome proteolytic pathway. Annu Rev Plant Biol *55*, 555–590.

Smith, J. M., Leslie, M. E., Robinson, S. J., Korasick, D. A., Zhang, T., Backues, S. K., Cornish, P. V., Koo, A. J., Bednarek, S. Y. and Heese, A. (2014a). Loss of Arabidopsis thaliana Dynamin-Related Protein 2B reveals separation of innate immune signaling pathways. PLoS pathogens *10*, e1004578.

Smith, J. M., Salamango, D. J., Leslie, M. E., Collins, C. A. and Heese, A. (2014b). Sensitivity to Flg22 is modulated by ligand-induced degradation and de novo synthesis of the endogenous flagellin-receptor FLAGELLIN-SENSING2. Plant Physiology *164*, 440–454.

Socha, A. L. and Guerinot, M. L. (2014). Mn-euvering manganese: the role of transporter gene family members in manganese uptake and mobilization in plants. Front Plant Sci *5*, 106.

Soetens, O., De Craene, J. O. and Andre, B. (2001). Ubiquitin is required for sorting to the vacuole of the yeast general amino acid permease, Gap1. J Biol Chem *276*, 43949–43957.

Sorieul, M., Santoni, V., Maurel, C. and Luu, D.-T. (2011). Mechanisms and effects of retention of over-expressed aquaporin AtPIP2;1 in the endoplasmic reticulum. Traffic *12*, 473–482.

Sorkin, A. and Goh, L. K. (2009). Endocytosis and intracellular trafficking of ErbBs. Experimental Cell Research *315*, 683–696.

Soubeyran, P., Kowanetz, K., Szymkiewicz, I., Langdon, W. Y. and Dikic, I. (2002). Cbl-CIN85-endophilin complex mediates ligand-induced downregulation of EGF receptors. Nature *416*, 183–187.

Spence, J., Sadis, S., Haas, A. L. and Finley, D. (1995). A ubiquitin mutant with specific defects in DNA repair and multiubiquitination. Mol. Cell Biol. *15*, 1265–1273.

Spitzer, C., Reyes, F. C., Buono, R., Sliwinski, M. K., Haas, T. J. and Otegui, M. S. (2009). The ESCRT-related CHMP1A and B proteins mediate multivesicular body sorting of auxin carriers in Arabidopsis and are required for plant development. The Plant Cell *21*, 749–766.

Spitzer, C., Schellmann, S., Sabovljevic, A., Shahriari, M., Keshavaiah, C., Bechtold, N., Herzog, M., Müller, S., Hanisch, F.-G. and Hülskamp, M. (2006). The Arabidopsis elch mutant reveals functions of an ESCRT component in cytokinesis. Development *133*, 4679–4689.

Springael, J. Y. and Andre, B. (1998). Nitrogen-regulated ubiquitination of the Gap1 permease of Saccharomyces cerevisiae. Mol Biol Cell *9*, 1253–1263.

Stanley, R. E., Ragusa, M. J. and Hurley, J. H. (2014). The beginning of the end: how scaffolds nucleate autophagosome biogenesis. Trends Cell Biol *24*, 73–81.

Staub, O., Gautschi, I., Ishikawa, T., Breitschopf, K., Ciechanover, A., Schild, L. and Rotin, D. (1997). Regulation of stability and function of the epithelial Na+ channel (ENaC) by ubiquitination. EMBO J *16*, 6325–6336.

Strader, L. C. and Bartel, B. (2009). The Arabidopsis PLEIOTROPIC DRUG RESIS-TANCE8/ABCG36 ATP binding cassette transporter modulates sensitivity to the auxin precursor indole-3-butyric acid. The Plant Cell *21*, 1992–2007.

Su, W., Liu, Y., Xia, Y., Hong, Z. and Li, J. (2011). Conserved endoplasmic reticulum-associated degradation system to eliminate mutated receptor-like kinases in Arabidopsis. Proc Natl Acad Sci U S A *108*, 870–875.

Sutter, J.-U., Sieben, C., Hartel, A., Eisenach, C., Thiel, G. and Blatt, M. R. (2007). Abscisic acid triggers the endocytosis of the arabidopsis KAT1 K+ channel and its recycling to the plasma membrane. Current Biology *17*, 1396–1402.

Suzuki, K., Kubota, Y., Sekito, T. and Ohsumi, Y. (2007). Hierarchy of Atg proteins in pre-autophagosomal structure organization. Genes to Cells *12*, 209–218.

Swatek, K. N. and Komander, D. (2016). Ubiquitin modifications. Nature Publishing Group *26*, 399–422.

Takano, J., Miwa, K., Yuan, L., von Wirén, N. and Fujiwara, T. (2005). Endocytosis and degradation of BOR1, a boron transporter of Arabidopsis thaliana, regulated by boron availability. Proceedings of the National Academy of Sciences *102*, 12276–12281.

Takano, J., Noguchi, K., Yasumori, M., Kobayashi, M., Gajdos, Z., Miwa, K., Hayashi, H., Yoneyama, T. and Fujiwara, T. (2002). Arabidopsis boron transporter for xylem loading. Nature *420*, 337–340.

Takano, J., Tanaka, M., Toyoda, A., Miwa, K., Kasai, K., Fuji, K., Onouchi, H., Naito, S. and Fujiwara, T. (2010). Polar localization and degradation of Arabidopsis boron transporters through distinct trafficking pathways. Proc Natl Acad Sci U S A *107*, 5220–5225.

Tamura, K., Shimada, T., Ono, E., Tanaka, Y., Nagatani, A., Higashi, S.-I., Watanabe, M., Nishimura, M. and Hara-Nishimura, I. (2003). Why green fluorescent fusion proteins have not been observed in the vacuoles of higher plants. Plant J *35*, 545–555.

Tan, J. M. M., Wong, E. S. P., Kirkpatrick, D. S., Pletnikova, O., Ko, H. S., Tay, S.-P., Ho, M. W. L., Troncoso, J., Gygi, S. P., Lee, M. K., Dawson, V. L., Dawson, T. M. and Lim, K.-L. (2008). Lysine 63-linked ubiquitination promotes the formation and autophagic clearance of protein inclusions associated with neurodegenerative diseases. Human molecular genetics *17*, 431–439.

Tanaka, H., Kitakura, S., De Rycke, R., De Groodt, R. and Friml, J. (2009). Fluorescence imaging-based screen identifies ARF GEF component of early endosomal trafficking. Curr Biol *19*, 391–397.

Tang, D. and Zhou, J.-M. (2016). PEPRs spice up plant immunity. EMBO J *35*, 4–5.

Tang, R.-J., Zhao, F.-G., Garcia, V. J., Kleist, T. J., Yang, L., Zhang, H.-X. and Luan, S. (2015). Tonoplast CBL-CIPK calcium signaling network regulates magnesium homeostasis in Arabidopsis. Proc Natl Acad Sci U S A *112*, 3134–3139.

Teh, O.-K. and Moore, I. (2007). An ARF-GEF acting at the Golgi and in selective endocytosis in polarized plant cells. Nature *448*, 493–496.

TerBush, D. R., Maurice, T., Roth, D. and Novick, P. (1996). The Exocyst is a multiprotein complex required for exocytosis in Saccharomyces cerevisiae. EMBO J *15*, 6483–6494.

Terrell, J., Shih, S., Dunn, R. and Hicke, L. (1998). A function for monoubiquitination in the internalization of a G protein-coupled receptor. Molecular Cell *1*, 193–202.

Thomine, S. and Vert, G. (2013). Iron transport in plants: better be safe than sorry. Curr Opin Plant Biol *16*, 322–327.

Tian, Q., Zhang, X., Yang, A., Wang, T. and Zhang, W.-H. (2016). CIPK23 is involved in iron acquisition of Arabidopsis by affecting ferric chelate reductase activity. Plant science : an international journal of experimental plant biology *246*, 70–79.

Traub, L. M. (2009). Tickets to ride: selecting cargo for clathrin-regulated internalization. Nat Rev Mol Cell Biol *10*, 583–596.

Tse, Y. C., Lo, S. W., Hillmer, S., Dupree, P. and Jiang, L. (2006). Dynamic response of prevacuolar compartments to brefeldin a in plant cells. Plant Physiol. *142*, 1442–1459.

Tse, Y. C., Mo, B., Hillmer, S., Zhao, M., Lo, S. W., Robinson, D. G. and Jiang, L. (2004). Identification of multivesicular bodies as prevacuolar compartments in Nicotiana tabacum BY-2 cells. The Plant Cell *16*, 672–693.

Ungewickell, E. and Branton, D. (1981). Assembly units of clathrin coats. Nature *289*, 420–422.

Ungewickell, E., Ungewickell, H., Holstein, S. E., Lindner, R., Prasad, K., Barouch, W., Martin, B., Greene, L. E. and Eisenberg, E. (1995). Role of auxilin in uncoating clathrin-coated vesicles. Nature *378*, 632–635.

Van Damme, D., Gadeyne, A., Vanstraelen, M., Inzé, D., Van Montagu, M. C. E., De Jaeger, G., Russinova, E. and Geelen, D. (2011). Adaptin-like protein TPLATE and clathrin recruitment during plant somatic cytokinesis occurs via two distinct pathways. Proc Natl Acad Sci U S A *108*, 615–620.

van Leeuwen, W., Ökrész, L., Bögre, L. and Munnik, T. (2004). Learning the lipid language of plant signalling. Trends Plant Sci *9*, 378–384.

Vanhee, C., Zapotoczny, G., Masquelier, D., Ghislain, M. and Batoko, H. (2011). The Arabidopsis multistress regulator TSPO is a heme binding membrane protein and a potential scavenger of porphyrins via an autophagy-dependent degradation mechanism. Plant Cell *23*, 785–805.

Vermeer, J. E. M., van Leeuwen, W., Tobena-Santamaria, R., Laxalt, A. M., Jones, D. R., Divecha, N., Gadella, T. W. J. and Munnik, T. (2006). Visualization of PtdIns3P dynamics in living plant cells. The Plant Journal *47*, 687–700.

Verstreken, P., Kjaerulff, O., Lloyd, T. E., Atkinson, R., Zhou, Y., Meinertzhagen, I. A. and Bellen, H. J. (2002). Endophilin mutations block clathrin-mediated endocytosis but not neurotransmitter release. Cell *109*, 101–112.

Vert, G., Briat, J. F. and Curie, C. (2001). Arabidopsis IRT2 gene encodes a root-periphery iron transporter. Plant J *26*, 181–189.

Vert, G. and Chory, J. (2011). Crosstalk in cellular signaling: background noise or the real thing? Dev Cell *21*, 985–991.

Vert, G., Grotz, N., Dédaldéchamp, F., Gaymard, F., Guerinot, M. L., Briat, J.-F. and Curie, C. (2002). IRT1, an Arabidopsis transporter essential for iron uptake from the soil and for plant growth. The Plant Cell *14*, 1223–1233.

Vert, G. A., Briat, J.-F. and Curie, C. (2003). Dual regulation of the Arabidopsis high-affinity root iron uptake system by local and long-distance signals. Plant Physiol. *132*, 796–804.

Vierstra, R. D. (2009). The ubiquitin-26S proteasome system at the nexus of plant biology. Nat Rev Mol Cell Biol *10*, 385–397.

Viotti, C., Bubeck, J., Stierhof, Y.-D., Krebs, M., Langhans, M., van den Berg, W., van Dongen, W., Richter, S., Geldner, N., Takano, J., Jurgens, G., de Vries, S. C., Robinson, D. G. and Schumacher, K. (2010). Endocytic and secretory traffic in Arabidopsis merge in the trans-Golgi network/early endosome, an independent and highly dynamic organelle. Plant Cell *22*, 1344–1357.

Viotti, C., Krüger, F., Krebs, M., Neubert, C., Fink, F., Lupanga, U., Scheuring, D., Boutté, Y., Frescatada-Rosa, M., Wolfenstetter, S., Sauer, N., Hillmer, S., Grebe, M. and Schumacher, K. (2013). The endoplasmic reticulum is the main membrane source for biogenesis of the lytic vacuole in Arabidopsis. Plant Cell *25*, 3434–3449.

Wang, C., Yan, X., Chen, Q., Jiang, N., Fu, W., Ma, B., Liu, J., Li, C., Bednarek, S. Y. and Pan, J. (2013). Clathrin light chains regulate clathrin-mediated trafficking, auxin signaling, and development in Arabidopsis. Plant Cell *25*, 499–516.

Wang, D., Harper, J. F. and Gribskov, M. (2003). Systematic trans-genomic comparison of protein kinases between Arabidopsis and Saccharomyces cerevisiae. Plant Physiol. *132*, 2152–2165.

Wang, L., Li, H., Lv, X., Chen, T., Li, R., Xue, Y., Jiang, J., Jin, B., Baluška, F., Šamaj, J., Wang, X. and Lin, J. (2015). Spatiotemporal Dynamics of the BRI1 Receptor and its Regulation by Membrane Microdomains in Living Arabidopsis Cells. Mol Plant *8*, 1334–1349.

Wang, N., Cui, Y., Liu, Y., Fan, H., Du, J., Huang, Z., Yuan, Y., Wu, H. and Ling, H.-Q. (2013). Requirement and functional redundancy of Ib subgroup bHLH proteins for iron deficiency responses and uptake in Arabidopsis thaliana. Mol Plant *6*, 503–513.

Wang, R., Liu, D. and Crawford, N. M. (1998). The Arabidopsis CHL1 protein plays a major role in high-affinity nitrate uptake. Proceedings of the National Academy of Sciences *95*, 15134–15139.

Wang, X. and Chory, J. (2006). Brassinosteroids regulate dissociation of BKI1, a negative regulator of BRI1 signaling, from the plasma membrane. Science *313*, 1118–1122.

Ward, D. M. and Kaplan, J. (2012). Ferroportin-mediated iron transport: expression and regulation. Biochim Biophys Acta *1823*, 1426–1433.

Waterman, H., Katz, M., Rubin, C., Shtiegman, K., Lavi, S., Elson, A., Jovin, T. and Yarden, Y. (2002). A mutant EGF-receptor defective in ubiquitylation and endocytosis unveils a role for Grb2 in negative signaling. EMBO J *21*, 303–313.

Weinberg, J. S. and Drubin, D. G. (2014). Regulation of clathrin-mediated endocytosis by dynamic ubiquitination and deubiquitination. Curr Biol *24*, 951–959.

Weissman, A. M. (2001). Themes and variations on ubiquitylation. Nat Rev Mol Cell Biol *2*, 169–178.

Wendland, B. (2002). Epsins: adaptors in endocytosis? Nat Rev Mol Cell Biol *3*, 971–977.

Williams, R. L. and Urbé, S. (2007). The emerging shape of the ESCRT machinery. Nat Rev Mol Cell Biol *8*, 355–368.

Winter, V. and Hauser, M.-T. (2006). Exploring the ESCRTing machinery in eukaryotes. Trends Plant Sci *11*, 115–123.

Xie, Z., Nair, U. and Klionsky, D. J. (2008). Atg8 controls phagophore expansion during autophagosome formation. Mol Biol Cell *19*, 3290–3298.

Xu, J., Li, H.-D., Chen, L.-Q., Wang, Y., Liu, L.-L., He, L. and Wu, W.-H. (2006). A protein kinase, interacting with two calcineurin B-like proteins, regulates K+ transporter AKT1 in Arabidopsis. Cell *125*, 1347–1360.

Xu, P., Duong, D. M., Seyfried, N. T., Cheng, D., Xie, Y., Robert, J., Rush, J., Hochstrasser, M., Finley, D. and Peng, J. (2009). Quantitative proteomics reveals the function of unconventional ubiquitin chains in proteasomal degradation. Cell *137*, 133–145.

Yamaoka, S., Shimono, Y., Shirakawa, M., Fukao, Y., Kawase, T., Hatsugai, N., Tamura, K., Shimada, T. and Hara-Nishimura, I. (2013). Identification and dynamics of Arabidopsis adaptor protein-2 complex and its involvement in floral organ development. Plant Cell *25*, 2958–2969.

Ye, Y., Meyer, H. H. and Rapoport, T. A. (2001). The AAA ATPase Cdc48/p97 and its partners transport proteins from the ER into the cytosol. Nature *414*, 652–656.

Ye, Y., Shibata, Y., Yun, C., Ron, D. and Rapoport, T. A. (2004). A membrane protein complex mediates retro-translocation from the ER lumen into the cytosol. Nature *429*, 841–847.

Yoshinari, A., Fujimoto, M., Ueda, T., Inada, N., Naito, S. and Takano, J. (2016). DRP1-Dependent Endocytosis is Essential for Polar Localization and Boron-Induced Degradation of the Borate Transporter BOR1 in Arabidopsis thaliana. Plant & Cell Physiology *57*, 1985–2000.

Yuan, Y., Wu, H., Wang, N., Li, J., Zhao, W., Du, J., Wang, D. and Ling, H.-Q. (2008). FIT interacts with AtbHLH38 and AtbHLH39 in regulating iron uptake gene expression for iron homeostasis in Arabidopsis. Cell Res *18*, 385–397.

Yuan, Y. X., Zhang, J., Wang, D. W. and Ling, H.-Q. (2005). AtbHLH29 of Arabidopsis thaliana is a functional ortholog of tomato FER involved in controlling iron acquisition in strategy I plants. Cell Res *15*, 613–621.

Zárský, V., Kulich, I., Fendrych, M. and Pečenková, T. (2013). Exocyst complexes multiple functions in plant cells secretory pathways. Curr Opin Plant Biol *16*, 726–733.

Zelazny, E., Barberon, M., Curie, C. and Vert, G. (2011). Ubiquitination of transporters at the forefront of plant nutrition. Plant Signal Behav *6*, 1597–1599.

Zelazny, E., Miecielica, U., Borst, J. W., Hemminga, M. A. and Chaumont, F. (2009). An N-terminal diacidic motif is required for the trafficking of maize aquaporins ZmPIP2;4 and ZmPIP2;5 to the plasma membrane. Plant J *57*, 346–355.

Zelazny, E., Santambrogio, M., Pourcher, M., Chambrier, P., Berne-Dedieu, A., Fobis-Loisy, I., Miege, C., Jaillais, Y. and Gaude, T. (2013). Mechanisms governing the endosomal membrane recruitment of the core retromer in Arabidopsis. J Biol Chem *288*, 8815–8825.

Zhang, J., Nodzyński, T., Pěnčík, A., Rolčík, J. and Friml, J. (2010). PIN phosphorylation is sufficient to mediate PIN polarity and direct auxin transport. Proc Natl Acad Sci U S A *107*, 918–922.

Zhang, Y., Persson, S., Hirst, J., Robinson, M. S., Van Damme, D. and Sánchez-Rodríguez, C. (2015). Change your TPLATE, change your fate: plant CME and beyond. Trends Plant Sci *20*, 41–48.

Zhuang, X., Wang, H., Lam, S. K., Gao, C., Wang, X., Cai, Y. and Jiang, L. (2013). A BAR-domain protein SH3P2, which binds to phosphatidylinositol 3-phosphate and ATG8, regulates autophagosome formation in Arabidopsis. Plant Cell *25*, 4596–4615.

Zourelidou, M., Absmanner, B., Weller, B., Barbosa, I. C. R., Willige, B. C., Fastner, A., Streit, V., Port, S. A., Colcombet, J., de la Fuente van Bentem, S., Hirt, H., Kuster, B., Schulze, W. X., Hammes, U. Z. and Schwechheimer, C. (2014). Auxin efflux by PIN-FORMED proteins is activated by two different protein kinases, D6 PROTEIN KINASE and PINOID. eLife *3*, 810.

Titre : Mécanismes moléculaires contrôlant l'ubiquitination et l'endocytose du transporteur de fer IRON-REGULATED TRANSPORTER 1 d'*Arabidopsis thaliana*

Mots-clés : Nutrition métallique, Ubiquitination, Endocytose, Phosphorylation, Trafic, Polarité

Résumé : L'ubiquitination est une modification post-traductionnelle qui joue un rôle majeur chez les organismes vivants. Chez *Arabidopsis thaliana*, le transporteur de fer racinaire IRT1 est endocyté à la suite de la monoubiquitination de deux résidus lysine situés au niveau de sa grande boucle cytosolique. Cependant, les mécanismes régissant l'endocytose médiée par l'ubiquitine ainsi que son rôle biologique restent flous. Au cours de ma Thèse, j'ai mis en évidence que la dynamique d'IRT1 était contrôlée par les métaux substrats secondaires du transporteur (à savoir le zinc, le manganèse et le cobalt). En l'absence de ces métaux, IRT1 est localisé à la membrane plasmique avec une polarité latérale le positionnant sur la face externe des cellules de l'épiderme racinaire. La présence de ces mêmes métaux à un niveau physiologique entraîne la monoubiquitination d'IRT1 et son internalisation vers les endosomes précoces. J'ai démontré que lorsque les métaux substrats secondaires d'IRT1 sont présents en excès, les modifications monoubiquitine sont alors allongées en chaînes de polyubiquitines liées par le résidu lysine-63, entrainant ainsi son adressage vers la vacuole et sa dégradation. Mes travaux ont par ailleurs permis d'élucider les mécanismes moléculaires impliquées dans la réponse des plantes à l'excès de métaux substrats d'IRT1. J'ai notamment montré que l'endocytose d'IRT1 était dépendante i) d'un motif riche en résidus histidine dans la séquence d'IRT1 qui est capable de fixer ces métaux autres que le fer, ii) de la phosphorylation d'IRT1 au niveau d'un résidu thréonine par une protéine kinase en cours d'investigation, et iii) de l'E3 ligase à domaine RING IDF1. D'un point de vue physiologique, l'endocytose d'IRT1 médiée par l'ubiquitine et dépendante des métaux protège la plante d'une suraccumulation de ces métaux autres que le fer qui sont hautement réactifs.

Title : Molecular mechanisms driving the ubiquitination and endocytosis of the *Arabidopsis* iron transporter IRON-REGULATED TRANSPORTER 1

Keywords : Metal nutrition, Ubiquitination, Endocytosis, Phosphorylation, Trafficking, Polarity

Abstract : Ubiquitination is a post-translational modification playing a major role in living organisms. In *Arabidopsis thaliana*, the root iron transporter IRT1 is endocytosed following the monoubiquitination of two lysine residues located in its large cytosolic loop. However, the mechanisms driving IRT1 ubiquitin-mediated endocytosis and its biological relevance remains unclear. During my PhD, I uncovered that IRT1 dynamics is controlled by its secondary metal substrates (i.e. zinc, manganese and cobalt). In the absence of these non-iron metals, IRT1 is found at the cell-surface of root epidermal cells with an outer lateral polarity, while their presence at physiological levels triggers IRT1 monoubiquitination, internalization and accumulation in early endosomes. However, upon non-iron metal excess, monoubiquitin modifications are extended into K63 polyubiquitin chains to promote the vacuolar targeting of IRT1 and its degradation. I investigated further the molecular mechanisms driving plant responses to non-iron metal excess. I notably showed that this regulation by non-iron metals is dependent on i) a histidine-rich stretch in IRT1 that is able to directly bind to non-iron metals, ii) the subsequent recruitment of a kinase currently under investigation which phosphorylates IRT1 at a threonine residue, and iii) the RING E3 ligase IDF1. Altogether, the metal-dependent ubiquitin-mediated endocytosis of IRT1 protects the plant from overaccumulation of highly reactive non-iron metals.